Università degli studi di Padova
Facoltà di Scienze MM.FF.NN.
Dipartimento di Fisica "G. Galilei"

SCUOLA DI DOTTORATO DI RICERCA IN FISICA

CICLO XXIII

Phenomenology of Discrete Groups in Flavor Symmetries

Coordinatore: Ch.mo Prof. ATTILIO STELLA

Supervisore: Ch.mo Prof. FERRUCCIO FERUGLIO

Dottorando: Dott. ALESSIO PARIS

January 31, 2011

Abstract

The experimental determination of flavor parameters (mass values, mixing angles and phases) suffer, in the lepton sector, from large uncertainties. Moreover, the ground on which theoretical models are built is not firm and although we have several clues to guide us toward the solution of the puzzle, no approach can be considered conclusive up to now. The situation gets more complicated by the fact that many theoretical constructions predict correctly many features of neutrino oscillation, but we still lack enough experimental sensitivity to discriminate among them, to refute the wrong and identify the best candidates to describe how nature works. Some of the most useful and popular tools to try to solve the flavor puzzle are the discrete symmetry groups. In this thesis we will deal with three distinct aspects of the current theoretical research on neutrino physics and discrete flavor symmetries. We will explicitly construct a model based on the discrete group A_5 in order to explain neutrino mixing. Phenomenological consequences will be discussed at the Leading and Next-to- Leading order, while special emphasis will be put on the naturalness of the vacuum alignment that spontaneously breaks the symmetry.

We will analyze the phenomenology of flavor models beyond the neutrino sector: in particular, rare decays of the muon and the tau will be discussed in models based on the symmetry group $A_4 \times Z_3 \times U(1)$ and realized at a high-energy scale, both in a frame-independent way and in a particular supersymmetric realization. Moreover, we will consider models in which the flavor scale coincides with the electroweak scale and more than one Higgs fields are present and charged under a generic discrete flavor group. In this case, the constraints come from the Higgs phenomenology and the search for flavor violation.

Finally, we will consider the effects of including a model for neutrinos in a larger and more realistic framework, adding Supersymmetry and the Seesaw mechanism. One of the key test is to check if the high-energy predictions of a given flavor model are stable against quantum corrections of the renormalization group. We will show general results applying to a broad class of textures called mass-independent; as an explicit example of this class, we will pick the Tribimaximal realization of the Altarelli-Feruglio model.

Riassunto della Tesi

Da un punto di vista sperimentale i parametri della fisica del sapore (valori delle masse, angoli di mescolamento e fasi) mostrano ancora larghe bande di incertezza, specialmente nel settore dei leptoni. Inoltre, la base sulla quale i modelli teorici vengono costruiti non ancora solida e nessun approccio puó dichiararsi definitivo nonostante i numerosi indizi che ci possono guidare verso la soluzione del problema. La situazione é resa piú complicata dal fatto che molti modelli riproducono correttamente l'oscillazione dei neutrini, ma non si possiede ancora sufficiente sensitivitá sperimentale per separare quelli sbagliati dai candidati piú plausibili per descrivere il meccanismo che la natura ha adottato. I gruppi di simmetria discreti sono fra gli strumenti pi utili e popolari nel tentativo di risolvere il problema del sapore. In questa tesi ci occuperemo di tre distinti aspetti appartenenti alla ricerca teorica sulla fisica dei neutrini e sui gruppi di sapore discreti. Costruiremo esplicitamente un modello basato sul gruppo di simmetria discreto A_5 che spieghi il mescolamento dei neutrini. Si studieranno le conseguenze fenomenologiche per i due ordini perturbativi piú bassi, sottolineando in particolare come i valori di aspettazione sul vuoto che rompono spontaneamnete la simmetria compaiono in modo naturale.

Analizzeremo poi alcuni modelli di sapore al di fuori dell'oscillazione dei neutrini: in particolare discuteremo decadimenti rari delle particelle μ e τ in modelli di sapore basati sul gruppo di simmetria $A_4 \times Z_3 \times U(1)$. I decadimenti verranno discussi sia senza specificare una teoria generale che in un contesto supersimmetrico. Passeremo poi ad esempi in cui la scala della fisica del sapore é fatta coincidere con la scala elettrodebole ed in cui piú campi di Higgs, carichi essi stessi sotto il gruppo di sapore, sono presenti. In questo caso Per concludere, verranno studiati gli effetti nell'incluedere un modello di sapore all'interno di una teoria piú ampia e realistica, ovvero aggiungendo la Supersimmetria e il cosiddetto meccanismo di Seesaw. Uno dei punti chiave é la verifica che le predizioni di un dato modello, valide ad alte energie, non vengano rovinate dalle correzioni quantistiche causate dal gruppo di rinormalizzazione. Mostreremo dei risultati generali che si applicano ad un'ampia classe di schemi detti indipendenti dalle masse (mass-independant): come esempio esplicito sceglieremo lo schema tribimassimale implementato nel modello di Altarelli e Feruglio.

Contents

Introduction and Outline

Despite the amazing experimental effort that has confirmed its many features and predictions, it is a spread belief that the Standard Model is somehow incomplete, or even a simple effective theory of a more general physical framework. There are many theoretical reasons that seem to support this view, but before the discovery of neutrino oscillations there were no serious experimental argument to confirm it.

Neutrino oscillation requires that neutrinos have mass, and this requirement obliges us to modify, even only in a minimal way, the particle content of the SM and the corresponding Lagrangian. Although the excitement about opening a windows to new physics, the discovery of oscillating neutrinos made the flavor sector of the SM even more complicated than before: it added to the ten parameters of quark mixing (six mass eigenvalues, three angles and a CP phase) ten or twelve parameters describing the lepton mixing, depending on the Dirac or Majorana nature of neutrinos. But the biggest surprise was that leptons mix in a very different way with respect to quarks. In fact, the former show two large angles and one angle which, given our current knowledge, could be vanishing or is, in any case, very small; the latter show instead three small angles, whose order of magnitude can be express as powers of the Cabibbo angle $\lambda \sim 0.22$.

After a decade of efforts, we know now that the angle that measure the atmospheric oscillations is large, possibly maximal. The solar angle has the smallest uncertainties, it is not maximal, and its particular value is a fundamental hint, as we will see many times in this work, for model-building. Finally, the reactor angle is bounded by an upper limit, while its value is still compatible with zero [1–3].

What we do not know about neutrinos is maybe more than what we learned. The reactor angle is still unmeasured; due to the smallness of θ_{13} we have no clue on the size of CP violation in the lepton sector; we ignore the absolute value of neutrino mass, although beta-decay experiments and cosmology bound it from above, and the hierarchy of the spectrum; we can not answer the fundamental question whether neutrinos are Dirac or Majorana particles. However, this lack of data did not prevent physicists to build models able to fit the empirical evidences. In particular, symmetry is a powerful tool to explore the flavor problem from a theoretical point of view. Of course, the field of symmetries is ample: they can be global or local, Abelian or non-Abelian, discrete or continuous. In this work we will focus on the class of discrete non-Abelian theories, which is a very popular setup to describe neutrino mixing. The original reason of this popularity is the fact that large mixing angles point directly toward discrete rotations, as exemplified by the symmetry of solids.

The differences among quarks and leptons suggest that different symmetries may act on different particles. It is a common prejudice, however, that at some high scale their description is unified. As a consequence, many efforts have been put to find a symmetry that fits both sectors. In this work, we forget about this issue and focus mainly on models and phenomenologies of leptons.

Before moving on to concrete realization of these ideas, it is important to stress that a maximal atmospheric angle is unachievable with an exact symmetry. Then one is forced to study models where the symmetry is broken either explicitly or spontaneously. The task of model-building should then consist in discovering a natural way to explain neutrino mixing and to produce the desired breaking. There are two main paths to implement a discrete symmetry with a correct breaking in the flavor sector: the first, which is the most explored, is to build a model where the symmetry is realized at a very high energy (possibly a scale of Grand Unification) and a completely new set of scalar degrees of freedom, called flavons, acquires vacuum expectation values (VEVs). The mixing texture is then realized by a hidden sector, whose consequences can be discovered in some related low-energy observables; in the second, the flavor scale coincides with the Electroweak scale, more than one Higgs are present and they usually belong to a non-trivial representation of the symmetry. This second approach has the advantage to need less new degrees of freedom, and to offer, perhaps, the chance of observing some direct evidences at LHC; on the other hand, it is in general less predictive and need a good dose of fine-tuning of the parameters, while the Higgs phenomenology has to be analyzed carefully not to find it theoretically and empirically inconsistent. Moreover, it is easier to find a correct vacuum alignment in the latter case, because usually it is sufficient to break the symmetry in one direction only to accommodate both charged leptons and neutrinos, while the flavon case usually needs two different vacuum breaking directions and the task to obtain them in a natural way is more difficult.

Regarding the last point, working in the Minimal Supersymmetric Standard Model (MSSM) helps to reach the goal. Due to the holonomicity of the superpotential it is possible to break the symmetry into two subgroups, denoted as G_l and G_ν, which rule charged leptons and neutrinos, respectively. We must stress, however, that in most cases the chosen discrete symmetry is not enough: additional constraints coming from Z_n or $U(1)$ groups are necessary and implemented in most of the models. Their function is to forbid operators that, if included in the Lagrangian, would spoil the desired predictions, or to give some extra-details of the model, as the hierarchy among charged lepton masses, that can not be obtained through the starting symmetry alone.

After showing three textures for neutrino oscillations that fall in the broader class satisfying $\mu - \tau$ symmetry (namely Tribimaximal, Bimaximal and Golden Ratio textures) we focus on the Golden Ratio prediction for the solar angle and build a complete model to obtain it [4]. Our setup is based on the group $A_5 \times Z_5 \times Z_3$. We discuss at the Leading Order the vacuum alignment derived by the minimization of the most general superpotential built out of the flavon fields and invariant under our symmetry. There are a finite number of solutions: one of them lead straightforwardly to the Golden Ratio pattern. We discuss the spectrum of neutrinos and deduce that it is compatible with both

normal and inverted hierarchy. We discuss the Next-to-Leading-Order corrections, find them to be under control and plot the corrected values of the solar and reactor angles. Our results show that even in the presence of higher-order corrections the predicted reactor angle remains far below the current and future experimental sensitivity.

Since many models correctly reproduce the features of neutrino oscillations, there must be an alternative way to distinguish among them and to rule out those that are incorrect. For this reason it is important to draw the effects of one's model beyond the neutrino sector and to verify if it remains viable even if included in a larger and more realistic theoretical frame, like adding the Seesaw mechanism or Supersymmetry. The flavon realizations, in fact, lay at high-energy, while the low-energy observables are at the electroweak scale: the picture obtained by imposing a flavor symmetry is then modified by the renormalization group equations. The running between the two scales is different if you consider an effective theory for neutrino mass or if we include Seesaw, if we work in the Standard Model or in the MSSM. We chose to discuss the evolution of flavor models with the type I Seesaw, both in the SM and in the MSSM [5]. We find some general results valid for the so-called mass-independent textures, to which the Tribimaximal, Bimaximal and Golden Ratio textures belong. As an example, we analyze in details the effects on the Altarelli-Feruglio model [6], a Tribimaximal realization based on the symmetry group $A_4 \times Z_3 \times U(1)$.

The same group is the topic of another part of this thesis, in which lepton flavor violating processes are discussed [9]. First, we organize the operators that cause flavor violation according to their particle content, in an effective, model-independent frame. We demonstrate that the allowed processes satisfy a selection rule, that excludes, in particular, radiative decays. After that, the Altarelli-Feruglio model is considered. The fact that this model is supersymmetric changes in a drastic way the predictions of the effective case, allows to avoid the aforementioned selection rule and modifies the branching ratios of the decays.

Finally, we will deal with models in which the flavor symmetry is realized at the electroweak energy scale [10, 11]. In this class of models, there are usually more copies of the Higgs field and they are charged under a symmetry group. The connection between the electroweak and the flavor symmetry breaking opens the door to new effects that provide constraints to the theoretical building. They come in particular from Higgs phenomenology (perturbative unitarity, Z and W decays etc.) and from flavor violation processes. After developing a general formalism to constrain, we will apply it to three distinct models present in literature.

The thesis is organized as follows. In the first chapter we fix the notation and review some aspects of the Standard model and its possible extensions. The mechanism to give mass to neutrinos is discussed, along with a brief report of the experimental data on flavor physics and neutrino oscillation in particular. The chapter also includes a summary of the features of Supersymmetry and of the MSSM. Chapter 2 presents the flavor puzzle and suggests non-Abelian discrete symmetries as an useful tool to investigate it. After a list of three mass-independent textures for neutrino oscillation, Tribimaximal, Bimaximal and Golden Ratio, the Altarelli-Feruglio model is reported in full detail. In Chapter 3

we show a natural model for the Golden Ratio prediction based on the discrete group A_5. In the fourth chapter, renormalization group equations are reported and applied to Seesaw models based on discrete-symmetries. The general case of mass-independent textures is analyzed, while a concrete example of the effects of running is given by the Altarelli-Feruglio model. In Chapter 5 we discuss rare decays of muon and tau particles in models based on $A_4 \times Z_3 \times U(1)$. Again, the Altarelli-Feruglio paper provides us a concrete realization. Finally, in Chapter 6 we deal with a multi-Higgs flavor symmetry based on A_4. After a general discussion on the different sources of constraints, we apply it to three model by Ma, Morisi-Peinado and Lavoura-Kuhbock.

Chapter 1

The Standard Model and Beyond

1.1 The Standard Model and the Neutrino Masses

The interactions of what we call fundamental particles are described by the Standard Model of particle physics [12]. In its mathematical form, the Standard Model is a quantum field theory in a four-dimensional Minkowski space, whose Lagrangian is invariant under the gauge group $SU(3)_c \times SU(2)_L \times U(1)_Y$. The first group, $SU(3)_c$, describes quantum chromodynamics, the theory of strong interactions of colored particles, such as gluons and quarks. The $SU(2)_L \times U(1)_Y$ term is the group of the electroweak force, which describes the behavior of the weak gauge bosons, W^+, W^- and Z^0, as well as the electromagnetic one, the photon γ, in their mutual interactions and in the presence of fermions.

The constituents of matter are leptons and quarks, which transform as four-component Dirac spinors under the Lorentz group. Using the Weyl or chiral representation of the Lorentz group, in which the γ^μ have vanishing 2×2 block diagonal components, it is possible to define Dirac spinors Ψ as the sum of two two-components Weyl spinors with opposite chirality

$$\Psi = \begin{pmatrix} \Psi_L \\ \Psi_R \end{pmatrix} . \tag{1.1}$$

Each of these new spinors belongs to a different representation of the Standard Model. If the left- and right-handed Weyl spinors of a Dirac spinor satisfy $\Psi_L = i\sigma^{2*}\Psi_R^*$, then the four-component spinor is called Majorana spinor and the two parts are equivalent.

In this work we will mainly adopt another notation: we consider a basis in which all the fields are left-handed and therefore Ψ refers to the true left-handed component and Ψ^c to the charge conjugate of the right-handed part. Using this convention, we clarify the equivalence between the two- and the four-component notations. For example e (e^c) denotes the left-handed (right-handed) component of the electron field. In terms of the four-component spinor $\psi_e^T = (e, \overline{e}^c)$, the bilinears $\overline{e}\,\overline{\sigma}^\nu e$ and $e^c\sigma^\nu\overline{e}^c$ correspond to $\overline{\psi}_e\gamma^\nu P_L\psi_e$ and $\overline{\psi}_e\gamma^\nu P_R\psi_e$ (where $P_{L,R} = \frac{1}{2}(1\mp\gamma^5)$) respectively. We take $\sigma^\mu \equiv (1, \vec{\sigma})$, $\overline{\sigma}^\mu \equiv (1, -\vec{\sigma})$, $\sigma^{\mu\nu} \equiv \frac{1}{4}(\sigma^\mu\overline{\sigma}^\nu - \sigma^\nu\overline{\sigma}^\mu)$, $\overline{\sigma}^{\mu\nu} \equiv \frac{1}{4}(\overline{\sigma}^\mu\sigma^\nu - \overline{\sigma}^\nu\sigma^\mu)$ and $g_{\mu\nu} = \mathrm{diag}(+1, -1, -1, -1)$, where $\vec{\sigma} = (\sigma^1, \sigma^2, \sigma^3)$ are the 2×2 Pauli matrices:

$$\sigma^1 = \begin{pmatrix} 0 & 1 \\ 1 & 0 \end{pmatrix} \qquad \sigma^2 = \begin{pmatrix} 0 & -i \\ i & 0 \end{pmatrix} \qquad \sigma^3 = \begin{pmatrix} 1 & 0 \\ 0 & -1 \end{pmatrix} . \tag{1.2}$$

Leptons and quarks are present in three generations or families and each of them includes four left-handed $SU(2)_L$-doublets, one in the lepton sector, $\ell = (\nu,\, e)$, and three in the quark sector, $q = (u,\, d)$, and seven right-handed $SU(2)_L$-singlets, the charged lepton e^c and the up- and down-quarks u^c and d^c. The symmetry charge assignments of one such family under the Standard Model gauge group are displayed in Table 1.1, along with the symmetry assignments of the Higgs boson $H = (H^+,\, H^0)$. The electric charge is given by $Q_{\rm em} = T_{3L} + Y$, where T_{3L} is the weak isospin and Y the hypercharge.

	ℓ	e^c	q	u^c	d^c	H
$SU(3)_c$	**1**	**1**	**3**	$\overline{\mathbf{3}}$	$\overline{\mathbf{3}}$	**1**
$SU(2)_L$	**2**	**1**	**2**	**1**	**1**	**2**
$U(1)_Y$	$-1/2$	$+1$	$+1/6$	$-2/3$	$+1/3$	$+1/2$

Table 1.1: *Charge assignments of leptons, quarks and the Higgs field under the Standard Model gauge group.*

The fermion assignments are such that the SM results anomaly-free and the gauge group symmetry of the Lagrangian is preserved at the quantum level. The most general $SU(3)_c \times SU(2)_L \times U(1)_Y$ gauge invariant renormalizable Lagrangian density can be written as follows:

$$\mathscr{L}_{\rm SM} = \mathscr{L}_K + \mathscr{L}_Y + V \ , \tag{1.3}$$

where $\mathscr{L}_K$ contains the kinetic terms and the gauge interactions for fermions and bosons, while $\mathscr{L}_Y$ referees to the fermion Yukawa terms and V is the scalar potential. The Yukawa Lagrangian can be written as

$$\mathscr{L}_Y = (Y_e)_{ij}\, e^c_i H^\dagger \ell_j + (Y_d)_{ij}\, d^c_i H^\dagger q_j + (Y_u)_{ij}\, u^c_i \widetilde{H}^\dagger q_j + \text{h.c.} \tag{1.4}$$

where $\widetilde{H} \equiv i\sigma^2 H^*$. The Standard Model gauge group prevents direct fermion mass terms in the Lagrangian. However, it is customary to account for the mass of fermions and of the gauge bosons $W^\pm$ and Z to a unique mechanism, the Higgs spontaneous symmetry breaking. When the neutral component of the Higgs field acquires a non-vanishing vacuum expectation value (VEV), $\langle H^0 \rangle = v/\sqrt{2}$ with $v \simeq 246$ GeV, the electroweak symmetry is spontaneously broken,

$$SU(2)_L \times U(1)_Y \longrightarrow U(1)_{em} \ , \tag{1.5}$$

and as a result all the fermions, apart from neutrinos, acquire non-vanishing masses:

$$\mathscr{L}_Y = (M_u)\, u^c_i u_j + (M_d)_{ij}\, d^c_i d_j + (M_e)_{ij}\, e^c_i e_j \qquad \text{where} \qquad M_i = Y_i \frac{v}{\sqrt{2}} \ . \tag{1.6}$$

However, the experimental observation of the past two decades have undoubtedly confirmed the oscillation of neutrinos among different families [1]. From the point of view

of quantum theory, this phenomenon is possible if neutrinos have non-vanishing masses. However, the SM lacks the mechanism to give mass to neutrinos and this fact suggest the need to extend it. The minimal variation consists in the introduction of a set of right-handed neutrinos, ν^c, which transform under the gauge group of the Standard Model as ($\mathbf{1}$, $\mathbf{1}$, 0), i.e. they do not have any interactions with the vector bosons. In this way, it is possible to construct a Yukawa term for neutrinos similar to the up-quark Yukawa:

$$(Y_\nu)_{ij}\, \nu_i^c \widetilde{H}^\dagger \ell_j + \text{h.c.} \tag{1.7}$$

which in the electroweak symmetry broken phase becomes a neutrino Dirac mass term

$$(m_\nu)_{ij}\, \nu_i^c \nu_j \qquad \text{where} \qquad m_\nu = Y_\nu \frac{v}{\sqrt{2}}\,. \tag{1.8}$$

According to the observations, $m_\nu \sim 0.1$ eV and as a consequence it requires that $Y_\nu \sim 10^{-12}$, which does not find any natural explanation.

An alternative minimal extension of the Standard Model consists in assuming the explicit violation of the accidental global symmetry L, the lepton number, at a very high energy scale, Λ_L. It is then possible to write the Weinberg operator [13], a five-dimensional non-renormalizable term suppressed by Λ_L:

$$\mathcal{O}_5 = \frac{1}{2}(Y_\nu)_{ij} \frac{(\ell_i \widetilde{H}^*)\,(\widetilde{H}^\dagger \ell_j)}{\Lambda_L}\,. \tag{1.9}$$

When the Higgs field develops the VEV, this produces a neutrino Majorana mass term

$$(m_\nu)_{ij} \nu_i \nu_j \qquad \text{where} \qquad m_\nu = Y_\nu \frac{v^2}{4\Lambda_L}\,. \tag{1.10}$$

Considering again an average value for the neutrino masses of the order of 0.1 eV, it implies that Λ_L can reach $10^{14\div 15}$ GeV, for $(Y_\nu)_{ij} = \mathcal{O}(1)$. Once we accept explicit lepton number violation, we gain an elegant explanation for the lightness of neutrinos as they turn out to be inversely proportional to the large scale where lepton number is violated.

1.1.1 The See-Saw Mechanism

Three different high scale renormalizable interactions have been proposed to account for the violation of the lepton number and the smallness of neutrino masses. They are known as the See-saw mechanisms, because the heaviest the new degrees of freedom are, the lightest the left-handed neutrinos become. Neutrino mass is generated by the tree-level exchange of three different types of new particles: right-handed neutrinos, fermion $SU(2)_L$-triplets and scalar $SU(2)_L$-triplets. We explain in the following how Type I See-saw [14], based on the introduction of right-handed neutrinos, works.

The presence of new fermions with no gauge interactions, which play the role of right-handed neutrinos, is quite plausible because any grand unified theory (GUT) group larger than $SU(5)$ requires them: for example, ν^c complete the representation $\mathbf{16}$ of $SO(10)$.

As already anticipated they have a Dirac Yukawa interaction Y_ν with the left-handed neutrinos. Assuming explicit lepton number violation a second term appears, a Majorana mass M_R: the Lagrangian can then be written as

$$\mathscr{L}_{\text{type I}} = (Y_\nu)_{ij}\nu_i^c \widetilde{H}^\dagger \ell_j + \frac{1}{2}(M_R)_{ij}\nu_i^c \nu_j^c + \text{h.c.} \,. \tag{1.11}$$

Y_ν and M_R are 3×3 matrices in the flavor space: M_R is symmetric and is usually associated with a high-energy scale Λ, while Y_ν is in general non hermitian and non symmetric. The Dirac mass term originates through the Higgs mechanism as in eq. (1.8). On the other hand, the Majorana mass term is $SU(3) \times SU(2)_L \times U(1)_Y$ invariant and therefore the Majorana masses are unprotected and naturally of the order of the cutoff of the low-energy theory. The full neutrino mass matrix is a 6×6 mass matrix in the flavor space and can be written as

$$M_\nu = \begin{array}{c} \\ \nu \\ \nu^c \end{array} \begin{array}{c} \begin{array}{cc} \nu & \nu^c \end{array} \\ \begin{pmatrix} 0 & m_D^T \\ m_D & M_R \end{pmatrix} \end{array} , \tag{1.12}$$

where $m_D = Y_\nu\, v/\sqrt{2}$. By block-diagonalizing M_ν, the light neutrino mass matrix is obtained as

$$m_\nu = -m_D^T M_R^{-1} m_D \,. \tag{1.13}$$

This is the well known type I See-Saw Mechanism: the light neutrino masses are quadratic in the Dirac masses and inversely proportional to the large Majorana ones, justifying the lightness of the left-handed neutrinos.

This construction holds true for any number of heavy ν^c coupled to the three known light neutrinos. In the case of only two ν^c, one light neutrino remains massless, which is a possibility not excluded by the present data.

1.2 The Physical Basis and the Mixing Matrices

If we simply assume that the lepton number is explicitly violated, when the electroweak symmetry is broken all fermions develop a mass term:

$$\mathscr{L}_{\text{mass}} = (M_u)\, u_i^c u_j + (M_d)_{ij}\, d_i^c d_j + (M_e)_{ij}\, e_i^c e_j + \frac{1}{2}(m_\nu)_{ij}\nu_i\nu_j \,, \tag{1.14}$$

where M_i and m_ν are 3×3 mass matrices in the flavor space. Counting the number of free parameters, there are nine complex entries for each mass matrix, apart for m_ν which is symmetric and owns only six. To reduce this amount, we can move to the physical basis in which the kinetic terms are canonical and all the mass matrices are diagonal. In this basis also the Yukawa coupling matrices are diagonal and therefore there is no tree-level flavor changing currents mediated by the neutral Higgs boson. This feature is in general lost extending the Standard Model by introducing multiple Higgs doublets or extra fermions.

We make unitary transformations on the fermions in the family space in order to move to the physical basis. Unitarity of these matrices ensures that the kinetic terms remain canonical. Specifically, we define $V_{u,\,u^c,\,d,\,d^c}$ and $U_{e,\,e^c,\,\nu}$ such that the transformations produce the following diagonal matrices:

$$\begin{aligned} V_{u^c}^\dagger\, M_u\, V_u &= \mathrm{diag}(m_u,\, m_c,\, m_t)\ , \qquad & V_{d^c}^\dagger\, M_d\, V_d &= \mathrm{diag}(m_d,\, m_s,\, m_b)\ , \\ U_{e^c}^\dagger\, M_e\, U_e &= \mathrm{diag}(m_e,\, m_\mu,\, m_\tau)\ , \qquad & U_\nu^T\, m_\nu\, U_\nu &= \mathrm{diag}(m_1,\, m_2,\, m_3)\ . \end{aligned} \tag{1.15}$$

Moving to the physical basis, the unitary matrices V_i and U_i should enter into all the fermion interactions. As already noted, the associated transformations bring the Yukawa couplings of fermions with the Higgs boson in the diagonal form. After these rotations the couplings of fermions to the Z^0 boson and to the photon remain diagonal, as well. It follows that in the Standard Model flavor is conserved by the tree-level exchange of neutral bosons. The charged current interactions are brought in a non-diagonal form: considering for simplicity only the negative charged current J_μ^-, we see that

$$J_\mu^- = \overline{\nu}\gamma_\mu e + \overline{u}\gamma_\mu d \longrightarrow \overline{\nu}\gamma_\mu U_\nu^\dagger U_e e + \overline{u}\gamma_\mu V_u^\dagger V_d d\ . \tag{1.16}$$

The products of the diagonalizing unitary matrices are defined as the mixing matrices for leptons, the Pontecorvo-Maki-Nakagawa-Sakata (PMNS) matrix [15], and for quarks, the Cabibbo-Kobayashi-Maskawa (CKM) matrix [16, 17], respectively:

$$U = U_e^\dagger U_\nu \qquad \text{and} \qquad V = V_u^\dagger V_d\ . \tag{1.17}$$

As the product of two unitary matrices, U and V are unitary as well. As said, before, a 3×3 unitary matrix has nine complex independent parameters. It is possible to absorb some of them through a redefinition of the fermion fields such that only three angles and one phase are left (1+2 phases if neutrinos are Majorana particles). The angles rule the mixing between the flavor eigenstates and the phases are responsible for CP violation. The standard parametrization of the CKM and PMNS matrices are in terms of the angles θ_{12}, θ_{13} and θ_{23} and of the phase δ:

$$\begin{aligned} V &= \begin{pmatrix} 1 & 0 & 0 \\ 0 & c_{23} & s_{23} \\ 0 & -s_{23} & c_{23} \end{pmatrix} \cdot \begin{pmatrix} c_{13} & 0 & s_{13}e^{-i\delta} \\ 0 & 1 & 0 \\ -s_{13}e^{i\delta} & 0 & c_{13} \end{pmatrix} \cdot \begin{pmatrix} c_{12} & s_{12} & 0 \\ -s_{12} & c_{12} & 0 \\ 0 & 0 & 1 \end{pmatrix} \\ &= \begin{pmatrix} c_{12}c_{13} & c_{13}s_{12} & s_{13}e^{-i\delta} \\ -c_{23}s_{12} - c_{12}s_{13}s_{23}e^{i\delta} & c_{12}c_{23} - s_{12}s_{13}s_{23}e^{i\delta} & c_{13}s_{23} \\ s_{12}s_{23} - c_{12}c_{23}s_{13}e^{i\delta} & -c_{12}s_{23} - c_{23}s_{12}s_{13}e^{i\delta} & c_{13}c_{23} \end{pmatrix}\ , \end{aligned} \tag{1.18}$$

where c_{ij} and s_{ij} stand for $\cos\theta_{ij}$ and $\sin\theta_{ij}$ (with $0 \le \theta_{ij} \le \pi/2$), respectively, and the Dirac CP-violating phase lies in the range $0 \le \delta < 2\pi$. This notation has various advantages: the rotation angles are defined and labeled in a way which is related to the mixing of two specific generations; as a result if one of these angles vanishes, so does the

mixing between the two respective generations. Moreover in the limit $\theta_{23} = \theta_{13} = 0$ the third generation decouples and the situation reduces to the usual Cabibbo mixing of the first two generations with $\sin\theta_{12}$ identified to the Cabibbo angle [16].

The standard parametrization of the lepton mixing is similar to eq. (1.18): we can write the PMNS matrix as the product of four parts

$$\begin{aligned} U = & \; R_{23}(\theta_{23}) \cdot R_{13}(\theta_{13},\, \delta) \cdot R_{12}(\theta_{12}) \cdot P \\ = & \begin{pmatrix} c_{12}c_{13} & c_{13}s_{12} & s_{13}e^{-i\delta} \\ -c_{23}s_{12} - c_{12}s_{13}s_{23}e^{i\delta} & c_{12}c_{23} - s_{12}s_{13}s_{23}e^{i\delta} & c_{13}s_{23} \\ s_{12}s_{23} - c_{12}c_{23}s_{13}e^{i\delta} & -c_{12}s_{23} - c_{23}s_{12}s_{13}e^{i\delta} & c_{13}c_{23} \end{pmatrix} \cdot P \,, \end{aligned} \tag{1.19}$$

where P is the matrix of the Majorana phases $P = \mathrm{diag}(e^{i\varphi_1/2},\, e^{i\varphi_2/2},\, 1)$, c_{ij} and s_{ij} represent $\cos\theta_{ij}$ and $\sin\theta_{ij}$, respectively, and δ is the Dirac CP-violating phase. Angles and phases have well defined ranges: $0 \leq \theta_{12},\, \theta_{23},\, \theta_{13} \leq \dfrac{\pi}{2}$ and $0 \leq \delta,\, \varphi_1,\, \varphi_2 < 2\pi$. Majorana phases are not present in eq. (1.19) if total lepton number is conserved.

In analytical and numerical analysis, quark and lepton mixing matrices are not in the standard form as in eqs. (1.18, 1.19) but it is possible to recover the mixing angles θ_{ij} and the phases δ, φ_1 and φ_2 through the following procedure. Denoting the generic mixing matrix as W, the mixing angles are given by

$$\sin\theta_{13} = |W_{13}| \,, \qquad \tan\theta_{12} = \left(\frac{|W_{12}|}{|W_{11}|}\right) \,, \qquad \tan\theta_{23} = \left(\frac{|W_{23}|}{|W_{33}|}\right) \,, \tag{1.20}$$

if $|W_{11}|$ ($|W_{33}|$) is non-vanishing, otherwise θ_{12} (θ_{23}) is equal to $\pi/2$. For the Dirac CP-violating phase we use the relation

$$W_{ii}^* W_{ij} W_{ji} W_{jj}^* = c_{12}\, c_{13}^2\, c_{23}\, s_{13} \left(e^{-i\delta}\, s_{12}\, s_{23} - c_{12}\, c_{23}\, s_{13}\right) \tag{1.21}$$

which holds for $i, j \in \{1, 2, 3\}$ and $i \neq j$. Then the phase δ is given by

$$\delta = -\arg\left(\frac{\dfrac{W_{ii}^* W_{ij} W_{ji} W_{jj}^*}{c_{12}\, c_{13}^2\, c_{23}\, s_{13}} + c_{12}\, c_{23}\, s_{13}}{s_{12}\, s_{23}}\right) \tag{1.22}$$

where $i, j \in \{1, 2, 3\}$ and $i \neq j$. An additional parameter, the Jarlskog invariant [18] which measures the amount of the CP violation is defined as:

$$\begin{aligned} J_{\mathrm{CP}} = & \frac{1}{2}\left|\mathrm{Im}(W_{11}^* W_{12} W_{21} W_{22}^*)\right| \,=\, \frac{1}{2}\left|\mathrm{Im}(W_{11}^* W_{13} W_{31} W_{33}^*)\right| \\ = & \frac{1}{2}\left|\mathrm{Im}(W_{22}^* W_{23} W_{32} W_{33}^*)\right| \,=\, \frac{1}{2}\left|c_{12}\, c_{13}^2\, c_{23}\, \sin\delta\, s_{12}\, s_{13}\, s_{23}\right| \,. \end{aligned} \tag{1.23}$$

To conclude the Majorana phases, that are present only in the lepton mixing matrix, are given by

$$\varphi_1 = 2\arg(e^{i\delta_e}\, U_{11}^*) \,, \qquad \varphi_2 = 2\arg(e^{i\delta_e}\, U_{12}^*) \,, \tag{1.24}$$

where $\delta_e = \arg(e^{i\delta}\, W_{13})$.

1.2.1 Experimental Data and Prospects

Experimentally, the CKM matrix has well defined entries [19]: a fit on the data, considering the unitary conditions, gives the following results,

$$
\begin{aligned}
|V| &= \begin{pmatrix} V_{ud} & V_{us} & V_{ub} \\ V_{cd} & V_{cs} & V_{cb} \\ V_{td} & V_{ts} & V_{tb} \end{pmatrix} \\
&= \begin{pmatrix} 0.97428 \pm 0.00015 & 0.2253 \pm 0.0007 & 0.00347^{+0.00016}_{-0.00012} \\ 0.2252 \pm 0.0007 & 0.97345^{+0.00015}_{-0.00016} & 0.0410^{+0.0011}_{-0.0007} \\ 0.00862^{+0.00026}_{-0.00020} & 0.0403^{+0.0011}_{-0.0007} & 0.999152^{+0.000030}_{-0.000045} \end{pmatrix} .
\end{aligned}
\tag{1.25}
$$

Making use of the standard parametrization, it is possible to extract the values of the quark mixing angles: in terms of $\sin\theta_{ij}$ we naively have

$$
\sin\theta_{12} \simeq 0.2253 , \qquad \sin\theta_{23} \simeq 0.0410 , \qquad \sin\theta_{13} \simeq 0.0035 . \tag{1.26}
$$

In the same way it is possible to recover the phase-convention-independent J_{CP} and the result of the data fit is

$$
J_{CP} = (2.91^{+0.19}_{-0.11}) \times 10^{-5} . \tag{1.27}
$$

A convenient summary of the neutrino oscillation data is given in Table 1.2. The pattern of the mixing is characterized by two large angles and a small one: θ_{23} is compatible with a maximal value, but the accuracy admits relatively large deviations; θ_{12} is large, but about 5σ far from the maximal value; θ_{13} has only an upper bound. According to the type of the experiments which measured them, the mixing angle θ_{23} is called atmospheric, θ_{12} solar and θ_{13} reactor. We underline that there is a tension among the two global fits presented in Table 1.2 on the central value of the reactor angle: in [2] we can read a suggestion for a positive value of $\sin^2\theta_{13} \simeq 0.016 \pm 0.010$ [1.6σ], while in [3] a best fit value consistent with zero within less than 1σ is found.

It is interesting to note that the large lepton mixing angles contrast with the small angles of the CKM matrix. Furthermore, to compare with eq. (1.25), we display the allowed ranges of the entries of the PMNS matrix [20]:

$$
|U| = \begin{pmatrix} U_{e1} & U_{e2} & U_{e3} \\ U_{\mu 1} & U_{\mu 2} & U_{\mu 3} \\ U_{\tau 1} & U_{\tau 2} & U_{\tau 3} \end{pmatrix} = \begin{pmatrix} 0.79 - 0.88 & 0.47 - 0.61 & < 0.20 \\ 0.19 - 0.52 & 0.42 - 0.73 & 0.58 - 0.82 \\ 0.20 - 0.53 & 0.44 - 0.74 & 0.56 - 0.81 \end{pmatrix} . \tag{1.28}
$$

Experiments showed that quarks and charged leptons have strongly hierarchical masses: the mass of the first families are smaller than those of the second families and the third

parameter	Ref. [2] best fit (1σ)	Ref. [2] 3σ-interval	Ref. [3] best fit (1σ)	Ref. [3] 3σ-interval
Δm^2_{sol} [$\times 10^{-5}\text{eV}^2$]	$7.67^{+0.16}_{-0.19}$	$7.14 - 8.19$	$7.65^{+0.23}_{-0.20}$	$7.05 - 8.34$
Δm^2_{atm} [$\times 10^{-3}\text{eV}^2$]	$2.39^{+0.11}_{-0.08}$	$2.06 - 2.81$	$2.40^{+0.12}_{-0.11}$	$2.07 - 2.75$
$\sin^2\theta_{12}$	$0.312^{+0.019}_{-0.018}$	$0.26 - 0.37$	$0.304^{+0.022}_{-0.016}$	$0.25 - 0.37$
$\sin^2\theta_{23}$	$0.466^{+0.073}_{-0.058}$	$0.331 - 0.644$	$0.50^{+0.07}_{-0.06}$	$0.36 - 0.67$
$\sin^2\theta_{13}$	$0.016^{+0.010}_{-0.010}$	≤ 0.046	$0.010^{+0.016}_{-0.011}$	≤ 0.056

Table 1.2: *Neutrino oscillation parameters from two independent global fits [2, 3].*

families are the heaviest. The quark masses are given by [19][§]

$$\begin{aligned} &m_u = 1.7 \div 3.3 \text{ MeV} , && m_c = 1.27^{+0.07}_{-0.09} \text{ GeV} , && m_t = 172.0 \pm 0.9 \pm 1.3 \text{ GeV} , \\ &m_d = 4.1 \div 5.8 \text{ MeV} , && m_s = 101^{+29}_{-21} \text{ MeV} , && m_b = 4.19^{+0.18}_{-0.06} \text{ GeV} . \end{aligned} \tag{1.29}$$

The charged lepton masses are very precisely known and they read [19]

$$\begin{aligned} m_e &= 0.510998910 \pm 0.000000023 \text{ MeV} , \\ m_\mu &= 105.658367 \pm 0.000004 \text{ MeV} , \\ m_\tau &= 1776.82 \pm 0.16 \text{ MeV} . \end{aligned} \tag{1.30}$$

In the neutrino sector the mass hierarchy is much milder and only two mass squared differences have been measured in oscillation experiments.[¶] The mass squared differences are defined as

$$\begin{aligned} \Delta m^2_{21} &= m^2_2 - m^2_1 \equiv \Delta m^2_{sol} = (7.59 \pm 0.20) \times 10^{-5} \text{ eV}^2 , \\ \Delta m^2_{31} &= m^2_3 - m^2_1 \equiv \pm \Delta m^2_{atm} = (2.43 \pm 0.13) \times 10^{-3} \text{ eV}^2 \end{aligned} \tag{1.31}$$

and in Table 1.2 we can read the results of two independent global fits on neutrino oscillation data from [2] and [3]. It is interesting to report also the ratio between the two

[§]The u-, d-, and s-quark masses are estimates of so-called "current-quark masses", in a mass-independent subtraction scheme such as $\overline{\text{MS}}$ at a scale $\mu \approx 2$ GeV. The c- and b-quark masses are the "running" masses, $m(\mu = m)$, in the $\overline{\text{MS}}$ scheme. Only the mass of the t-quark is a result of direct observation of top events.

[¶]There is an indication for the existence of a third independent mass squared difference from the LSND experiment [21], which could be explained only if an additional (sterile) neutrino is considered. The MiniBooNE collaboration [22] did not confirm the LSND result with neutrinos, but seems to support it for antineutrinos [23]. Results from MINOS [24] point toward a neutrino/antineutrino anomaly, too. The existence of a sterile neutrino and a third mass squared difference is still controversial.

mass squared differences [3]:

$$r = \frac{\Delta m^2_{sol}}{\Delta m^2_{atm}} = 0.032^{+0.006}_{-0.005} \, . \tag{1.32}$$

Due to the ambiguity in the sign of the atmospheric mass squared difference, neutrinos can have two mass hierarchies: they can be normally hierarchical (NH) if $m_1 < m_2 < m_3$ or inversely hierarchical (IH) if $m_3 < m_1 < m_2$. Furthermore, if the absolute mass scale is much larger than the mass squared differences then we cannot speak about hierarchy: in this case the neutrino spectrum is quasi degenerate (QD) and we speak about mass ordering. It is common to redefine the atmospheric mass squared difference to account for the type of the hierarchy: indeed Δm^2_{atm} is taken to be the mass squared difference between the heaviest and the lightest mass eigenstates and therefore

$$|m_3^2 - m_1^2(m_2^2)| \equiv \Delta m^2_{atm} \tag{1.33}$$

for the normal (inverse) hierarchy.

Regarding the experimental prospects on neutrino mass and mixing there are several future experiments that will provide information. They are:

- many reactor and accelerator experiments are devoted to improve the sensitivity on the reactor angle θ_{13}. The combined limit of DOUBLE CHOOZ [25], Daya Bay [26], MINOS [27], RENO [28], T2K [29] and NOvA [30] should reach $\sin^2 2\theta_{13} \lesssim 10^{-2}$ [31]. The results of these experiments will also set the schedule of CP violation searches;

- β-decay experiments which measure the endpoint of the tritium decay and to good approximation probe $m^2_{\nu_e} = \sum_i |U^2_{ei}| m_i^2$ and consequently the absolute scale of neutrino mass. The most recent experiment is Mainz [32] and it puts an upper bound at 99% of CL of $m_{\nu_e} < 2.1$ eV. The Katrin experiment will improve the sensitivity to m_{ν_e} by one order of magnitude down to ~ 0.2 eV [33]. Cosmology can also set an upper bound on the sum of the neutrino masses. As a result [34] $\sum_i m_i < 0.19 \div 2.6$ eV;

- the neutrinoless-double-beta ($0\nu 2\beta$) decay is a viable decay for a little class of nuclei only in the hypothesis of Majorana nature for neutrinos. Dedicated experiments could probe the ee element of the neutrino Majorana mass:

$$m_{ee} = \sum_i U^2_{ei} m_i = \cos\theta^2_{13}(m_1 \cos\theta^2_{12} e^{i\varphi_1} + m_2 \sin\theta^2_{12} e^{i\varphi_2}) + m_3 \sin\theta^2_{13} \, , \tag{1.34}$$

  where φ_i are the Majorana phases. Nowadays only an upper bound of 0.35 eV on this quantity has been put by the Heidelberg-Moscow collaboration [35], but the future experiments are expected to reach better sensitivities: 90 meV [36] (GERDA), 20 meV [37] (Majorana), 50 meV [38] (SuperNEMO), 15 meV [39] (CUORE) and 24 meV [40] (EXO).

1.3 Supersymmetry

In the Standard Model two Higgs parameters appear in the scalar potential: m_H and λ_H, which are the mass and the quartic coupling of the Higgs boson, respectively. The Higgs VEV is linked to these parameter as

$$\langle H \rangle \equiv \frac{v}{\sqrt{2}} = \sqrt{-\frac{m_H^2}{2\lambda_H}} \,. \tag{1.35}$$

Since λ_H is bounded from above by various consistency conditions (such as perturbative unitarity), and given the measured value $v \simeq 246$ GeV, it follows that it should be roughly $-m_H^2 \sim (100 \text{ GeV})^2$. The parameter m_H receives corrections from the virtual effects of every particle that couples to the Higgs field. These corrections depend quadratically on the high-energy cut-off scale; the Higgs mass is unprotected against them and this fact is called the hierarchy problem. If the cutoff scale is taken to be close to the Planck scale $M_P \approx 10^{19}$ GeV, the corrections due to the fermion loops are much larger than the weak scale. Supersymmetry (SUSY) was rapidly recognized as an elegant solution to this problem [§]. The introduction of supermultiplets composed of the known SM particles and of yet-to-be-discovered, heavy partners allows to mitigate the corrections to a logarithmic term. SUSY can be considered an extension of the usual 4-dimensional space-time Poincaré symmetry, in which new fermionic operators, that transform a boson field into a fermion field and vice versa, are introduced. The generators of the Poincaré algebra and the new spin 1/2 operators form a superalgebra, whose irreducible representations, called supermultiplets or superfields, contain both fermionic and bosonic degrees of freedom. The squared-mass operator $P_\mu P^\mu$ commutes with every single operators of the superalgebra, so it follows that particles belonging to the same supermultiplet should have the same mass. Since this feature has never been observed, we must conclude that somehow SUSY is a spontaneously broken symmetry. As a consequence the Lagrangian is the sum of two terms,

$$\mathscr{L} = \mathscr{L}_{SUSY} + \mathscr{L}_{soft}, \tag{1.36}$$

where $\mathscr{L}_{SUSY}$ is the supersymmetric preserving part, while $\mathscr{L}_{soft}$ breaks SUSY softly, in order to preserve the relations that solve the hierarchy problem. In the minimal supersymmetric extension of the Standard Model (MSSM), SM fermions and their superpartners belong to so-called chiral supermultiplets. The superpartners are spinless bosons and their names are built placing a s- before the partner's name (as an example, the partner of the electron is the selectron). The gauge bosons, along with their 1/2-spin partners called gauginos, belong to gauge multiplets. Finally, there are two additional chiral supermultiplets to which two independent Higgs fields and two Higgsinos are assigned. The usual Standard Model Higgs H, defined in Table 1.1, is renamed to H_d and it is responsible for giving mass to the down quarks and to the charged leptons. The extra Higgs, H_u, is required to generate the Dirac mass of the up quarks (and of neutrinos if ν^c are included),

[§]For a detailed introduction to Supersymmetry, see [41]

as a requirement of the theory prevents the charge conjugate of H_d from playing that role (in contrast to what happens with H in the Standard Model). After electroweak symmetry breaking the neutral components of the Higgs fields acquire VEVs:

$$\langle H_u^0 \rangle = v_u \ , \quad \langle H_d^0 \rangle = v_d. \tag{1.37}$$

They are related to the mass of the Z^0 boson by

$$v_u^2 + v_d^2 = \frac{v^2}{2} = \frac{2m_Z}{g^2 + g'^2} \approx (174 \text{ GeV})^2, \tag{1.38}$$

and the ratio of the VEVs is a free parameter of the theory and is traditionally written as

$$\tan\beta = \frac{v_u}{v_d}. \tag{1.39}$$

It is not difficult to generalize the Standard Model description of Section 1.1 to the supersymmetric context: each Standard Model field is considered to be a part of a superfield, z, and the Lagrangian of the model can be written as a sum of different terms in the following way

$$\mathscr{L} \ = \ \int d^2\theta d^2\overline{\theta} \mathcal{K}(\overline{z}, e^{2V} z) + \left[\int d^2\theta w(z) + \text{h.c.} \right] + \frac{1}{4} \left[\int d^2\theta f(z) \mathcal{W}\mathcal{W} + \text{h.c.} \right] \ , \tag{1.40}$$

where $\mathcal{K}(\overline{z}, z)$ is the Kähler potential, a real gauge-invariant function of the chiral superfields z and their conjugates, of dimensionality (mass)^2; $w(z)$ is the superpotential, an analytic gauge-invariant function of the chiral superfields, of dimensionality (mass)^3; $f(z)$ is the gauge kinetic function, a dimensionless analytic gauge-invariant function; V is the Lie-algebra valued vector supermultiplet, describing the gauge fields and their superpartners. Finally $\mathcal{W}$ is the chiral superfield describing, together with the function $f(z)$, the kinetic terms of gauge bosons and their superpartners. θ and $\overline{\theta}$ are spinor degrees of freedom and correspond to transformations in the superspace, defined by the union of the usual space-time and of the space on which the superymmetric operators act.

The scalar potential $V \equiv V(\tilde{z}, \tilde{z}^\dagger)$ is composed of two contributions. One is usually called the F-term, obtained from the superpotential as $F_i \equiv \partial w(\tilde{z})/\partial \tilde{z}_i$, where i is an index labeling the components of whatever representation the field has under the gauge group (for example, two components if the chiral superfield containing $\tilde{z}_i$ is a doublet of $SU(2)$). The other contribution is usually called the D-term, and is associated with the gauge group: $D^a \equiv g_a (M_{FI}^a)^2 - g_a \tilde{z}^\dagger T^a \tilde{z}$, where a labels the generators T^a of the group and $(M_{FI}^a)^2$ denotes the contribution of the Fayet-Iliopoulos (FI) term, which may be non-zero only for Abelian $U(1)$ factors of the group. Assuming a canonical Kähler potential, $\mathcal{K} = \overline{z}_i z_i$ and summarizing the two contributions we have

$$V = F^\dagger F + \frac{1}{2} D^2 = \sum_i \left| \frac{dw(z)}{d\tilde{z}_i} \right|^2 + \frac{1}{2} \sum_a \left(g_a (M_{FI}^a)^2 - g_a \tilde{z}^\dagger T^a \tilde{z} \right)^2 \ . \tag{1.41}$$

In terms of the hierarchy problem, m_H receives new contributions from the Standard Model superpartners in such a way that the loop diagrams with superparticles in the loop

have exactly the same value as those ones with Standard Model particles in the loop, but with opposite sign (due to the minus sign coming from the fermion loop): Supersymmetry enables the exact cancellation of the quadratic divergence, leaving only milder logarithmic divergences.

If from one side in supersymmetric theories there is a natural explanation of the hierarchy problem, dangerous gauge-invariant, renormalizable operators appear: the most general super potential would include also terms which violate either the baryon number (B) or the total lepton number (L). The existence of these terms corresponds to B- and L-violating processes, which however have not been observed: a strong constraint comes from the non-observation of the proton decay. A possible way out to this problem is represented by the introduction of a new symmetry in MSSM, which allows the Yukawa terms, but suppresses B- and L-violating terms in the renormalizable superpotential. This new symmetry is called "matter parity" or equivalently "R-parity". The matter parity is a multiplicative conserved quantum number defined as

$$P_M = (-1)^{3(B-L)} \tag{1.42}$$

for each particle in the theory. It is easy to check that quark and lepton supermultiplets have $P_M = -1$, while Higgs supermultiplets, gauge bosons and gauginos have $P_M = +1$. In the superpotential only terms for which $P_M = +1$ are allowed. The advantage of such a solution is that B and L are violated only due to non-renormalizable terms in the Lagrangian and therefore in tiny amounts.

It is common to use also a second definition of this symmetry: the R-parity refers to

$$P_R = (-1)^{3(B-L)+2s} , \tag{1.43}$$

where s is the spin of the particle. The two definitions are precisely equivalent, since the product of $(-1)^{2s}$ is always equal to $+1$ for the particles in a vertex that conserves angular moment. Under this symmetry all the Standard Model particles and the Higgs bosons have even R-parity ($P_R = +1$), while all their superpartners have odd R-parity ($P_R = -1$).

The phenomenological consequences of an R-parity conservation in a theory are extremely important: the lightest sparticle with odd R-parity is called lightest supersymmetric particle (LSP) and is absolutely stable; each sparticle, other then the LSP, must eventually decay in a state with an odd number of LSPs; sparticles can only be produced in even numbers, at colliders.

Chapter 2

Discrete Flavor Symmetries and the Flavor Problem

Most of the free parameters of the Standard Model are inherent to the flavor sector. The mass values of quarks and leptons, their mixing angles and phases remain without a definitive theoretical explanation although experimental data have been accumulated for decades. Neutrino mixing could turn to be fundamental to solve the flavor problem, since it is very different from the quark mixing, for which the angles are small. To build up theoretical models of neutrino mixing one must guess which features of the data are relevant in order to identify the basic principles for the formulation of the model. Of course, one can assume that the particular pattern of the PMNS matrix (1.28) is accidental and has no deep physical meaning. The experimental data could then be fitted varying the parameters of a chosen framework. On the other hand, if we assume that neutrino mixing hides a specific physical pattern, then we are led to consider models that naturally produce that pattern as a first approximation and only a very special dynamics can lead to this peculiar mixing matrix. Discrete non Abelian groups (for a review see [42]) naturally emerge as suitable flavor symmetries, because they immediately suggest rotations by fixed, discrete and possibly large angles. In the following I will discuss three cases of a broader class of neutrino mixing patterns based on $\mu - \tau$ symmetry. Through a general argument it is shown that specific predictions on the values of the mixing angles can be naturally related to the property of some discrete groups.

2.1 Lepton Mixing Angles and Platonic Solids

On a pure phenomenological basis there are attractive patterns that could provide a good LO approximation for the lepton mixing. In particular the data are firmly indicating that the atmospheric mixing angle is close to maximal and that the reactor angle is the smallest one so that, in a crude approximation, we can take $\sin^2\theta_{23} = 1/2$ and $\sin^2\theta_{13} = 0$. In the same approximation, several choices have been suggested for the solar angle, such as $\sin^2\theta_{12} = 1/2$ (Bimaximal pattern), $\sin^2\theta_{12} = 1/3$ (Tri-Bimaximal) and $\tan\theta_{12} = 1/\phi$

(Golden Ratio). Clearly, depending on the pattern chosen as first approximation to the data, appropriate sub leading corrections are needed, smaller for the TB and GR mixing patterns and larger for the BM one. In the basis where the charged leptons are diagonal the most general neutrino mass matrices corresponding to the considered LO approximations are given by

$$m_\nu = U^*_{PMNS}\ \mathtt{diag}(m_1, m_2, m_3)\ U^\dagger_{PMNS} \quad . \tag{2.1}$$

with a mixing matrix

$$U_{PMNS} = \begin{pmatrix} c_{12} & s_{12} & 0 \\ -\frac{s_{12}}{\sqrt{2}} & \frac{c_{12}}{\sqrt{2}} & -\frac{1}{\sqrt{2}} \\ -\frac{s_{12}}{\sqrt{2}} & \frac{c_{12}}{\sqrt{2}} & \frac{1}{\sqrt{2}} \end{pmatrix} \quad , \tag{2.2}$$

where $c_{12} \equiv \cos\theta_{12}$ and $s_{12} \equiv \sin\theta_{12}$. The three cases we are interested in are obtained by specializing the value of θ_{12}. By applying eq. (2.1) we find a matrix of the form:

$$m_\nu = \begin{pmatrix} x & y & y \\ y & z & w \\ y & w & z \end{pmatrix} \quad , \tag{2.3}$$

with coefficients x, y, z and w satisfying the following relations:

$$\begin{array}{lcll} z+w & = & x & \mathtt{BM} \\ z+w & = & x+y & \mathtt{TB} \\ z+w & = & x-\sqrt{2}y & \mathtt{GR} \quad . \end{array} \tag{2.4}$$

Thus we have three textures each depending on three independent complex parameters. Each of them can be completely characterized by a simple symmetry requirement, that of being invariant under two independent commuting parity transformations, U and S:

$$S^2 = U^2 = 1 \quad , \qquad [S, U] = 0 \quad . \tag{2.5}$$

Indeed the mass matrix of eq. (2.3) is the most general one invariant under the so-called $\mu - \tau$ exchange symmetry, generated by:

$$U = \begin{pmatrix} 1 & 0 & 0 \\ 0 & 0 & 1 \\ 0 & 1 & 0 \end{pmatrix} \quad . \tag{2.6}$$

Moreover, depending on the particular chosen texture, we have another generator S, which can be found by using the constraints in eq. (2.4). We list the solutions in Table 2.1. The

requirement of invariance under U and S completely determine the mass textures listed above. Namely, given a generic neutrino mass matrix m_ν the most general solutions to the equations:

$$U^T\ m_\nu\ U = m_\nu \quad , \qquad S^T\ m_\nu\ S = m_\nu \quad , \tag{2.7}$$

with U and S given in eq. (2.6) and in Table 2.1, are the mass matrices defined by eqs. (2.3) and (2.4).

At the same time the requirement that the combination $m_l^\dagger m_l$ is diagonal can be fulfilled by asking that the charged lepton sector is invariant under the action of a cyclic symmetry of Z_n type. Calling T the corresponding generator, with $T^n = 1$, we can choose T so that the solution of

$$T^\dagger\ (m_l^\dagger m_l)\ T = (m_l^\dagger m_l) \tag{2.8}$$

is a diagonal matrix. In minimal constructions realizing BM, TB and GR mixings the generator T can be chosen as in Table 2.1. With this choice T has the additional property:

$$(ST)^3 = 1 \quad . \tag{2.9}$$

	BM	**TB**	**GR**
S	$\frac{1}{\sqrt{2}}\begin{pmatrix} 0 & -1 & -1 \\ -1 & 1/\sqrt{2} & -1/\sqrt{2} \\ -1 & -1/\sqrt{2} & 1/\sqrt{2} \end{pmatrix}$	$\frac{1}{3}\begin{pmatrix} -1 & 2 & 2 \\ 2 & -1 & 2 \\ 2 & 2 & -1 \end{pmatrix}$	$\frac{1}{\sqrt{5}}\begin{pmatrix} 1 & \sqrt{2} & \sqrt{2} \\ \sqrt{2} & -\phi & 1/\phi \\ \sqrt{2} & 1/\phi & -\phi \end{pmatrix}$
T	$\begin{pmatrix} -1 & 0 & 0 \\ 0 & -i & 0 \\ 0 & 0 & i \end{pmatrix}$	$\begin{pmatrix} 1 & 0 & 0 \\ 0 & \omega & 0 \\ 0 & 0 & \omega^2 \end{pmatrix}$	$\begin{pmatrix} 1 & 0 & 0 \\ 0 & e^{i\frac{2\pi}{5}} & 0 \\ 0 & 0 & e^{i\frac{8\pi}{5}} \end{pmatrix}$

Table 2.1: Generators S and T for the different mixing patterns ($\phi = (1+\sqrt{5})/2$ and $\omega = -1/2 + i\sqrt{3}/2$).

A model giving rise to the desired lepton mixing matrix U_{PMNS} can be obtained starting from the family group G_f generated by S, T and U. The family symmetry should be spontaneously broken by a set of scalar fields in such a way that, at the LO, the charged lepton sector has a residual invariance under the group generated by T, whereas the neutrino sector has a residual invariance under the group generated by S and U. The desired lepton mixing U_{PNMS} arises by construction, independently from the base choice. In existing models the $\mu - \tau$ exchange symmetry generated by U arises at the LO as an accidental symmetry. In this case the family symmetry G_f is generated by S and T satisfying:

$$S^2 = (ST)^3 = 1 \qquad \text{and} \qquad T^n = 1 \quad , \tag{2.10}$$

with $n = 4$ for BM, $n = 3$ for TB and $n = 5$ for GR. These are the defining relations of S_4 (BM) [43], A_4 (TB) [44] and A_5 (GR) [4,45–47], which are the proper symmetry group of the cube/octahedron, tetrahedron and dodecahedron/icosahedron, respectively. We find rather intriguing that Platonic solids and their symmetries are in a natural correspondence with the most popular lepton mixing patterns. Notice that these groups are all subgroups of the modular group, defined by the presentation $S^2 = (ST)^3 = 1$.

2.1.1 The Bimaximal Mixing Pattern

The Bimaximal mixing [48] predicts $\sin^2\theta_{12} = 1/2$, to which corresponds a well defined relation between the mass parameters: $w = x - z$ (2.4). The most general mass matrix of the BM-type can be written as

$$m_\nu = \begin{pmatrix} x & y & y \\ y & z & x-z \\ y & x-z & z \end{pmatrix} \tag{2.11}$$

and satisfies an additional symmetry for which $(m_\nu)_{1,1} = (m_\nu)_{2,2} + (m_\nu)_{2,3}$. Apart from the Majorana phases, eq. (2.11) depends on only three real parameters, the masses, which can be written in terms of the mass parameters x, y and z:

$$m_1 = x + \sqrt{2}y\ , \qquad m_2 = x - \sqrt{2}y\ , \qquad m_3 = 2z - x\ . \tag{2.12}$$

These masses are the eigenvalues of eq. (2.11), while the eigenstates define the unitary transformation which diagonalizes the mass matrix in such a way that $m_\nu^{\rm diag} = U_{BM}^T m_\nu U_{BM}$, where the unitary matrix is given by

$$U_{BM} = \begin{pmatrix} 1/\sqrt{2} & -1/\sqrt{2} & 0 \\ 1/2 & 1/2 & -1/\sqrt{2} \\ 1/2 & 1/2 & +1/\sqrt{2} \end{pmatrix}\ . \tag{2.13}$$

Notice that this matrix is mass-independent. It is useful to express eq. (2.11) in terms of m_i instead of x, y and z:

$$\begin{aligned} m_\nu &= U_{BM}\,\mathrm{diag}(m_1,\, m_2,\, m_3)\, U_{BM}^T \\ &= \frac{m_3}{2}\begin{pmatrix} 0 & 0 & 0 \\ 0 & 1 & -1 \\ 0 & -1 & 1 \end{pmatrix} + \frac{m_2}{4}\begin{pmatrix} 2 & -\sqrt{2} & -\sqrt{2} \\ -\sqrt{2} & 1 & 1 \\ -\sqrt{2} & 1 & 1 \end{pmatrix} + \frac{m_1}{4}\begin{pmatrix} 2 & \sqrt{2} & \sqrt{2} \\ \sqrt{2} & 1 & 1 \\ \sqrt{2} & 1 & 1 \end{pmatrix}\ . \end{aligned} \tag{2.14}$$

Clearly, all type of hierarchies among neutrino masses can be accommodated. The smallness of the ratio $r = \Delta m^2_{sun}/\Delta m^2_{atm}$ requires either $|xy| \ll |z^2|$ (normal hierarchy) or $|x| \sim |z| \ll |y|$ (inverse hierarchy) or $|y| \ll |x| \sim |z|$ (approximate degeneracy except for $x \sim 2z$).

A final comment on the agreement of this scheme with the experimental data is worth. In the bimaximal pattern the solar angle is assumed maximal, $\sin^2\theta_{12} = 1/2$, to be compared with the latest experimental determination: at 3σ error level, $\sin^2\theta_{12} = 0.26 - 0.37$ from [2] or $\sin^2\theta_{12} = 0.25 - 0.37$ from [3], and the Bimaximal pattern can be considered at most as a zeroth order approximation that needs large corrections.

2.1.2 The Tribimaximal Mixing Pattern

In the so-called Tribimaximal or Harrison-Perkins-Scott pattern [49] a vanishing reactor angle, a maximal atmospheric angle and $\sin^2\theta_{12} = 1/3$ are assumed. From eq. (2.4) it results $w = x + y - z$ and therefore the most generic mass matrix of the TB-type is given by

$$m_\nu = \begin{pmatrix} x & y & y \\ y & z & x+y-z \\ y & x+y-z & z \end{pmatrix} . \tag{2.15}$$

This matrix satisfies the so-called magic symmetry, for which the sum of the entries of each row and columns are equal, or $(m_\nu)_{1,1} = (m_\nu)_{2,2} + (m_\nu)_{2,3} - (m_\nu)_{1,3}$. The mass eigenvalues can be written in terms of the parameters x, y and z:

$$m_1 = x - y \, , \qquad m_2 = x + 2y \, , \qquad m_3 = 2z - x - y \, . \tag{2.16}$$

These eigenvalues come from the diagonalisation of eq. (2.15) by the use of a unitary transformation in such a way that $m_\nu^{\rm diag} = U_{TB}^T m_\nu U_{TB}$, where the unitary matrix is given by

$$U_{TB} = \begin{pmatrix} \sqrt{2/3} & 1/\sqrt{3} & 0 \\ -1/\sqrt{6} & 1/\sqrt{3} & -1/\sqrt{2} \\ -1/\sqrt{6} & 1/\sqrt{3} & +1/\sqrt{2} \end{pmatrix} . \tag{2.17}$$

Notice again that U_{TB} does not depend on the mass eigenvalues, in complete analogy to the Bimaximal pattern of eq. (2.13).

It is useful to write eq. (2.15) in terms of m_i instead of x, y and z:

$$\begin{aligned} m_\nu &= U_{TB}\, {\rm diag}(m_1,\, m_2,\, m_3)\, U_{TB}^T \\ &= \frac{m_3}{2}\begin{pmatrix} 0 & 0 & 0 \\ 0 & 1 & -1 \\ 0 & -1 & 1 \end{pmatrix} + \frac{m_2}{3}\begin{pmatrix} 1 & 1 & 1 \\ 1 & 1 & 1 \\ 1 & 1 & 1 \end{pmatrix} + \frac{m_1}{6}\begin{pmatrix} 4 & -2 & -2 \\ -2 & 1 & 1 \\ -2 & 1 & 1 \end{pmatrix} . \end{aligned} \tag{2.18}$$

All the type of neutrino spectra can be accommodated: $m_3 >> m_2 >> m_1$ defines a normal hierarchy; a degenerate model is given by choosing $m_3 \approx -m_2 \approx m_1$; for $m_1 \approx -m_2$ and $m_3 \approx 0$ the inverse hierarchy case is achieved. However, stability under renormalization group running strongly prefers opposite signs for the first and the second eigenvalue which are related to solar oscillations and have the smallest mass squared splitting (see Chapter 4 for details).

Finally we underline that this mixing pattern is a very good approximation of the experimental data: the Tribimaximal values for the atmospheric and the reactor angles are inside the 1σ error level, while that one for the solar angle is very close to the upper 1σ value.

2.1.3 The Golden Ratio Prediction

In the Golden Ratio prediction [51, 52] a maximal atmospheric angle and $\theta_{13} = 0$ are assumed. It receives the name from the relation $\tan\theta_{12} = 1/\varphi$, where if φ is the irrational number known as Golden Ratio, defined as $\varphi = \frac{1+\sqrt{5}}{2}$. From eq. (2.4) it results $w = x - \sqrt{2}y - z$ and therefore the most generic mass matrix of the TB-type is given by

$$m_\nu = \begin{pmatrix} x & y & y \\ y & z & x-\sqrt{2}y-z \\ y & x-\sqrt{2}y-z & z \end{pmatrix} . \tag{2.19}$$

As in the previous cases, the mass eigenvalues are functions of the three parameters of the matrix (2.19).

$$m_1 = \frac{5}{3}(x - \frac{2\sqrt{2}}{3+\sqrt{5}}y) , \qquad m_2 = \frac{5}{3}(x + \frac{3+\sqrt{5}}{\sqrt{2}}y) , \qquad m_3 = -x - \sqrt{10}y + 2z . \tag{2.20}$$

These eigenvalues come from the diagonalization of eq. (2.19) by the use of a unitary transformation in such a way that $m_\nu^{\rm diag} = U_{GR}^T m_\nu U_{GR}$, where the unitary matrix is given by

$$U_{GR} = \begin{pmatrix} \sqrt{\frac{\phi}{\sqrt{5}}} & \sqrt{\frac{1}{\sqrt{5}\phi}} & 0 \\ -\sqrt{\frac{1}{2\sqrt{5}\phi}} & \sqrt{\frac{\phi}{2\sqrt{5}}} & -1/\sqrt{2} \\ -\sqrt{\frac{1}{2\sqrt{5}\phi}} & \sqrt{\frac{\phi}{2\sqrt{5}}} & +1/\sqrt{2} \end{pmatrix} . \tag{2.21}$$

As the two previous cases U_{GR} does not depend on the mass eigenvalues and therefore it belongs to the class of mass-independent textures.

It is useful to write eq. (2.19) in terms of m_i instead of x, y and z:

$$\begin{aligned} m_\nu &= U_{GR}\,\mathrm{diag}(m_1,\, m_2,\, m_3)\, U_{GR}^T \\ &= \frac{m_3}{2}\begin{pmatrix} 0 & 0 & 0 \\ 0 & 1 & -1 \\ 0 & -1 & 1 \end{pmatrix} + \frac{m_2}{10}\begin{pmatrix} \frac{2}{\varphi^2} & \sqrt{2} & \sqrt{2} \\ \sqrt{2} & \varphi^2 & \varphi^2 \\ \sqrt{2} & \varphi^2 & \varphi^2 \end{pmatrix} + \frac{m_1}{10}\begin{pmatrix} 2\varphi^2 & -\sqrt{2} & -\sqrt{2} \\ -\sqrt{2} & \frac{1}{\varphi^2} & \frac{1}{\varphi^2} \\ -\sqrt{2} & \frac{1}{\varphi^2} & \frac{1}{\varphi^2} \end{pmatrix} . \end{aligned} \tag{2.22}$$

All the type of neutrino spectra can be accommodated. We underline that this mixing pattern is a good approximation of the experimental data: the values for the atmospheric and the reactor angles are inside the 1σ error level, while that one for the solar angle is

close to the lower border of the 2σ range. A small correction could shift it toward the best experimental value.

2.2 Overview of Flavor Symmetries

In the previous section we discussed how the particular structure of U_{PMNS} lead to adopt particular non-Abelian discrete symmetry groups. In the following, we describe in a general way the advantages and disadvantages of this choice.

There is a large variety of symmetries which can be used: they can be either Abelian or non-Abelian, either local or global (or even a combination of them) and finally either discrete or continuous. Historically, flavor symmetries were first used to describe the quark sector and the Abelian $U(1)$ symmetry has been shown to be able to explain the observed quark mass hierarchies and mixing. In this approach developed by Froggatt and Nielsen in 1979 [53], there is a flavon field S, a gauge-invariant scalar, which acquires a vacuum expectation value (VEV) and breaks the $U(1)$ symmetry. It is possible to define a small parameter $\epsilon = \langle S \rangle / \Lambda_f$, where the cutoff Λ_f is the scale of flavor dynamics usually associated with some heavy fermions which are integrated out. This symmetry breaking is then communicated to fermions with a non-universal mechanism, in such a way that different fermions receive different powers of ϵ. The advantage of this mechanism is that the Yukawas can be of $\mathcal{O}(1)$ and the fermion masses and mixing are explained as powers of the expansion parameter ϵ. On the other hand, the main disadvantage consists in the lack of well-defined predictions: masses and mixing angles are only predicted up to unknown $\mathcal{O}(1)$ coefficients. Furthermore, certain mixing patterns such as the Bimaximal and the Tribimaximal schemes cannot be achieved with an Abelian symmetry. Therefore we can conclude that the predictive power of a non-Abelian symmetry is in general larger than that of an Abelian one.

Concerning the local or the global attribute of a flavor symmetry, we have to remember that the requirement of anomaly freedom for a local symmetry can put strong constraints on the charge assignment of the fermions. Furthermore, locality preserves the symmetry from being broken by quantum gravity effects at the Planck scale.

We now discuss the advantages and disadvantages of using a continuous or a discrete group. In the case of a spontaneously broken symmetry a continuous one leads to the appearance of Goldstone or gauge bosons. On the other hand, the breaking of a discrete group is safe from such a consequence. Furthermore, using the continuous groups such as $SO(3)$ or $SU(3)$, we have only a single non-trivial possibility to describe the three fermion families and the type of contractions is also strongly limited. On the contrary, adopting a discrete symmetry, there are several small representations which can be fairly used.

After this brief summary, we restrict to the context of non-Abelian discrete flavor symmetries which are in general more predictive than Abelian ones and that are safe from dangerous effects such as the appearance of Goldstone or gauge bosons. Furthermore, the

particular mixing pattern in the lepton sector can be very well explained by the use of certain discrete symmetries, which are all subgroups of $SU(3)$. In the rest of this section we do not enter in the details of each group, referring to [50] for the general group theory and to the following chapters where some of these group are treated in detail.

In general, groups containing a three-dimensional representation are chosen, because it is possible to collect all the fermion families in a unique representation, such as with $SO(3)$ or $SU(3)$, but with more freedom in the type of couplings. However, this is not a rule, since it is possible to organize the three families in a $2 + 1$ representation, for example in S_4 given that the third family is usually heavier than the other.

Although discrete flavor symmetry were introduced in the lepton sector to study the related neutrino phenomenology, efforts have been made in order to find a common symmetry behind quarks and leptons. For example, the tetrahedral group A_4, which was first used to obtain the Tribimaximal mixing, was then extended to quarks. However, when the quark sector is considered, it results a highly non-trivial task to get a (even non grand) unified description of fermions. A possible strategy to overcome the problem is to enlarge the symmetry: th group T', the double coverage of A_4, or S_4, which contains the tetrahedral group as a subgroup, are good choices.

A general feature of models based on (discrete) groups is that, unfortunately, the symmetry alone is not sufficient to fully account for the fermion mass hierarchies and mixing in the majority of the cases. A first problem concerns the differences between leptons and quarks: two (of three) large lepton mixing angles with respect to three small and hierarchical quark ones; neutrinos with a much milder mass hierarchy with respect to the charged fermions. A viable solution consists in avoiding interferences among the two sectors, at least in first approximation, and to keep them separated additional groups, such as the Abelian factors Z_n, are implemented in the complete flavor symmetry group. A second problem refers to the use of the three-dimensional representation, which is usually adopted to describe leptons: the components of a triplet show degenerate masses, unless some breaking parameter is introduced. From this the problem of how to describe the charged lepton mass hierarchy follows and two kind of solutions have been proposed: the Froggatt-Nielsen (FN) mechanism, which consists in introducing an additional (global or local) $U(1)_{FN}$ factor under which right-handed fermions transform, is the most used.

The gauge group of the Standard Model prevents direct fermion mass terms and the Higgs mechanism is addressed to be responsible for them, but it leaves the measured flavor structure unexplained. When a flavor symmetry is implemented in a model, new fields are needed: it is necessary that they acquire VEVs, that communicated to the fermions accounts for masses and mixing. People usually refer to this kind of new degrees of freedom with the name of "flavons". They usually are invariant under the gauge group of the Standard Model and transform only under the flavor symmetry; their masses are typically much larger then the electroweak scale, introducing an additional energy scale in the model.

In order not to introduce further scales into the theory, an alternative approach has been pursued: the flavor and the electroweak symmetries are broken together due to

the introduction of several copies of the Standard Model Higgs doublet which transform non-trivially under the flavor group. It is well-known that such multi-Higgs models find strong constraints by direct searches for Higgs bosons and by indirect bounds from flavor changing neutral current and lepton flavor violating processes.

The requirement of a broken flavor symmetry is also the result of a well-known no-go theorem [54, 55], which affirms that the atmospheric mixing angle is always undetermined in the limit of the exact symmetry and in particular $\theta_{12} = \pi/4$ can not be obtained. Only when small breaking parameters are considered in the mass matrices, it is possible to recover this result. This goal is achieved if the breaking terms have suitable orientations in the flavor space; this is connected to the VEV (mis)alignment of the flavons: if the breaking terms are produced by a spontaneous symmetry breaking, in general two independent sectors of flavons are needed, indeed one of them communicates the breaking to charged fermions and the other one to neutrinos. It is worth to underline that the VEV (mis)alignment of the flavons is an highly non-trivial problem to solve, which could put severe constraints on the choice of the group representations and on the minimal number of new degrees of freedom. Usually, working in a supersymmetric environment or adding extra dimensions helps, but apart from expanding the mathematical apparatus of a model, it forces us to introduce additional degrees of freedom. In particular, in the MSSM it is often necessary to add driving fields, charged under R-symmetry, to the superpotential. Minimizing it with respect to these new scalars provides the desired vacuum alignment. We stress here that in some case this is not an unavoidable feature, as we will show explicitly in the next chapter.

2.3 A Concrete Example: the Altarelli-Feruglio Model

We recall here the main features of the Altarelli-Feruglio (AF) model [6–8], which is based on the flavor group $G_f = A_4 \times Z_3 \times U(1)_{FN}$: the spontaneous breaking of A_4 is responsible for the Tribimaximal mixing; the cyclic symmetry Z_3 prevents the appearance of dangerous couplings and helps keeping separated the charged lepton sector and the neutrino one; the $U(1)_{FN}$ provides a natural hierarchy among the charged lepton masses.

A_4 is the group of the even permutations of 4 objects, isomorphic to the group of discrete rotations in the three-dimensional space that leave invariant a regular tetrahedron. It is generated by two elements S and T obeying the relations [50]:

$$S^2 = (ST)^3 = T^3 = 1 \, . \tag{2.23}$$

It has three independent one-dimensional representations, $\mathbf{1}$, $\mathbf{1}'$ and $\mathbf{1}''$ and one three-dimensional representation $\mathbf{3}$. We present a set of generators S and T for the various representations, and the relevant multiplication rules in appendix A.1. The group A_4 has two obvious subgroups: G_S, which is a reflection subgroup generated by S, and G_T, which is the group generated by T, isomorphic to Z_3. These subgroups are of interest for us because G_S and G_T are the relevant low-energy symmetries of the neutrino and

the charged-lepton sectors at the leading order, respectively. The Tribimaximal mixing is then a direct consequence of this special symmetry breaking pattern, which is achieved via the vacuum misalignment of triplet scalar fields. If $\Phi = (\Phi_1, \Phi_2, \Phi_3)$ denotes the generic scalar triplet, the VEV

$$\langle \Phi \rangle \propto (1, 1, 1) \tag{2.24}$$

breaks A_4 down to G_S, while

$$\langle \Phi \rangle \propto (1, 0, 0) \tag{2.25}$$

breaks A_4 down to G_T. The flavor symmetry breaking sector of the model includes the scalar fields φ_T, φ_S, ξ and θ. In Table 2.2, we can see the fermion and the scalar content of the model and their transformation properties under G_f.

	ℓ	e^c	μ^c	τ^c	H	θ	φ_T	φ_S	ξ
A_4	**3**	**1**	**1″**	**1′**	**1**	**1**	**3**	**3**	**1**
Z_3	ω	ω^2	ω^2	ω^2	1	1	1	ω	ω
$U(1)_{FN}$	0	2	1	0	0	-1	0	0	0

Table 2.2: *The transformation properties of the fields under A_4, Z_3 and $U(1)_{FN}$.*

As anticipated above, the specific breaking patter of the symmetry which leads to the Tribimaximal scheme and to hierarchical masses for leptons requires that ξ and θ develop a non vanishing VEV and that the following specific vacuum misalignment for the triplets occurs:

$$\langle \varphi_T \rangle = (v_T,\, 0,\, 0)\ , \qquad \langle \varphi_S \rangle = (v_S,\, v_S,\, v_S)\ . \tag{2.26}$$

In [6, 7] it has been shown a natural explanation of this misalignment. These VEVs can be very large, much larger than the electroweak scale. From the analysis in [6, 7], it is reasonable to choose:

$$\frac{VEV}{\Lambda_f} \approx \lambda^2\ , \tag{2.27}$$

where VEV stands for the generic non-vanishing VEV of the flavons, Λ_f the cutoff of the theory and λ the Cabibbo angle. Since the ratio in eq. (2.27) represents the typical expansion parameter when including higher dimensional operators, it keeps all the leading order results stable, up to correction of relative order λ^2. A very useful parametrization of VEV/Λ_f is the following:

$$\frac{\langle \varphi_T \rangle}{\Lambda_f} = (u,\, 0,\, 0)\ , \quad \frac{\langle \varphi_S \rangle}{\Lambda_f} = c_b(u,\, u,\, u)\ , \quad \frac{\langle \xi \rangle}{\Lambda_f} = c_a\, u, \quad \frac{\langle \theta \rangle}{\Lambda_f} = t\ , \tag{2.28}$$

where $c_{a,b}$ are complex numbers with absolute value of order one, while u and t are the small symmetry breaking parameters of the theory (they can be taken real through field redefinitions).

Once defined the transformations of all the fields under G_f, it is possible to write down the Yukawa interactions: at the leading order they read

$$\mathscr{L}_e = \frac{y_e}{\Lambda_f^3}\theta^2 e^c H^\dagger (\varphi_T \ell) + \frac{y_\mu}{\Lambda_f^2}\theta\mu^c H^\dagger (\varphi_T \ell)' + \frac{y_\tau}{\Lambda_f}\tau^c H^\dagger (\varphi_T \ell)'' + h.c. \tag{2.29}$$

$$\mathscr{L}_\nu = \frac{x_a}{\Lambda_f \Lambda_L}\xi(\tilde{H}^\dagger \ell \tilde{H}^\dagger \ell) + \frac{x_b}{\Lambda_f \Lambda_L}(\varphi_S \tilde{H}^\dagger \ell \tilde{H}^\dagger \ell) + h.c.\ , \tag{2.30}$$

where y_i and x_i are complex numbers with absolute value of order one. The contractions under $SU(2)_L$ are understood and the notation $(\ldots)$, $(\ldots)'$ and $(\ldots)''$ refers to the contractions in $\mathbf{1}$, $\mathbf{1'}$ and $\mathbf{1''}$, respectively. We distinguish two different energy scales: Λ_f refers to the energy scale of the flavor dynamics while Λ_L to the scale at which the lepton number is violated. We assume here that $\Lambda_f \sim \Lambda_L$.

When the flavons develop VEVs in agreement with eq. (2.28) and after the electroweak symmetry breaking, the leading order mass matrix of charged leptons takes the following form: in the basis of canonical kinetic terms,

$$M_e = \begin{pmatrix} y_e t^2 & 0 & 0 \\ 0 & y_\mu t & 0 \\ 0 & 0 & y_\tau \end{pmatrix} \frac{v\, u}{\sqrt{2}}\ . \tag{2.31}$$

Once in the physical basis, the entries on the diagonal are identified to the masses of the charged leptons and the relative hierarchy among them is given by the parameter t: when

$$t \approx 0.05 \tag{2.32}$$

then the mass hierarchy is in agreement with the experimental measurements. As we will see in the following sections, the model admits a well defined range for the parameter u which can approximatively be set to

$$0.003 \lesssim u \lesssim 0.05\ . \tag{2.33}$$

In the neutrino sector, the leading order Majorana mass matrix is given by

$$m_\nu = \begin{pmatrix} a + 2b/3 & -b/3 & -b/3 \\ -b/3 & 2b/3 & a - b/3 \\ -b/3 & a - b/3 & 2b/3 \end{pmatrix} \frac{v^2}{\Lambda_L}\ , \tag{2.34}$$

where $a \equiv x_a\, c_a\, u$ and $b \equiv x_b\, c_b\, u$. At this order the mass matrix is diagonalized by

$$U_\nu^T m_\nu U_\nu = \frac{v^2}{\Lambda_L}\mathrm{diag}(|a+b|,\, |a|,\, |-a+b|)\ , \tag{2.35}$$

where $U_\nu = U_{TB} P$. The matrix U_{TB} is the Tribimaximal transformation of eq. (2.17), while P is the matrix of the Majorana phases,

$$P = \mathrm{diag}(e^{i\alpha_1/2},\, e^{i\alpha_2/2},\, e^{i\alpha_3/2})\ , \tag{2.36}$$

with $\alpha_1 = -\arg(a+b)$, $\alpha_2 = -\arg(a)$ and $\alpha_3 = -\arg(-a+b)$.

It is possible to generalize this description also to the supersymmetric context. In this case G_f accounts for an additional term, a continuous R-symmetry $U(1)_R$, that contains the usual R-parity as a subgroup and simplifies the constructions of the scalar potential: under this symmetry, the matter superfields transform as $U(1)_R = 1$, while the scalar ones are neutral.

It is easy to extend eqs. (2.29, 2.30) in the supersymmetric case: two Higgs doublets $H_{(d,u)}$, invariant under A_4, substitute H and $\widetilde{H}$, respectively; the Lagrangian $\mathscr{L}_e$ is identified to the leading order charge lepton superpotential w_e and $\mathscr{L}_\nu$ is identified to the leading order neutrino superpotential w_ν. Moreover, it is necessary to introduce a further flavon $\tilde{\xi}$, which exactly transforms as ξ but does not acquire any VEV. As a result it does not have any impact on the previous discussion and its relevance is only linked to the way in which the VEV misalignment is recovered (see [7] for further details).

While t is still equal to 0.05 in order to have a correct charged lepton mass hierarchy, the range for u slightly changes:

$$0.007 \lesssim u \lesssim 0.05 \; . \tag{2.37}$$

2.3.1 The Neutrino Mass Spectrum

We now summarize the results for the neutrino mass spectrum. Notice that the following analysis is valid in the Standard Model as well as in its supersymmetric extension, by substituting v with v_u when necessary. The neutrino masses are given by

$$m_1 = |a+b|\frac{v^2}{\Lambda_L} \; , \qquad m_2 = |a|\frac{v^2}{\Lambda_L} \; , \qquad m_3 = |-a+b|\frac{v^2}{\Lambda_L} \; . \tag{2.38}$$

They can be expressed in terms of only three independent parameters: a possible choice that simplifies the analysis consists in taking $|a|$, ρ and Δ, where ρ and Δ are defined as

$$\frac{b}{a} = \rho\, e^{i\Delta} \; , \tag{2.39}$$

with Δ in the range $[0,\, 2\pi]$. From the experimental side only the squared mass differences have been measured and as a result the spectrum is not fully determined and indeed Δ is still a free parameter: we can, however, bound Δ requiring that $|\cos\Delta| \leq 1$. Before proceeding it is useful to express ρ and $\cos\Delta$ as functions of some physical observables. To this purpose we calculate the following mass ratios: for both the hierarchies we have

$$\frac{m_{1(3)}^2}{m_2^2} = 1 \pm 2\rho\cos\Delta + \rho^2 \; . \tag{2.40}$$

It is then easy to express ρ and $\cos\Delta$ as a function of the neutrino masses:

$$\rho = \sqrt{\frac{m_1^2 - 2m_2^2 + m_3^2}{2m_2^2}} \; , \qquad \cos\Delta = \frac{m_1^2 - m_3^2}{2\sqrt{2}m_2\sqrt{m_1^2 - 2m_2^2 + m_3^2}} \; . \tag{2.41}$$

Using now the definitions of the mass squared differences,

$$\Delta m^2_{sol} \equiv m_2^2 - m_1^2 \,, \qquad \Delta m^2_{atm} \equiv |m_3^2 - m_1^2(m_2^2)| \,, \tag{2.42}$$

it is possible to express $\cos\Delta$ as a function of only the lightest neutrino mass. Imposing the constraint $|\cos\Delta| \leq 1$, it results that only the normal hierarchy is allowed and taking the most conservative case (the 3σ upper value for $\Delta m^2_{\rm sol}$ and the 3σ lower value for $\Delta m^2_{\rm atm}$ as in [2]) we have

$$m_1 > 14.1 \ \text{meV} \,. \tag{2.43}$$

This value corresponds to $\cos\Delta = -1$ and it is the value for which the spectrum presents the strongest hierarchy: the values of the masses of the other two neutrinos are given by

$$m_2 = 16.7 \ \text{meV} \qquad \text{and} \qquad m_3 = 47.5 \ \text{meV} \,. \tag{2.44}$$

Furthermore the sum of the neutrino masses in this case is about 78.3 meV. When $\cos\Delta$ approached the zero, the neutrino spectrum becomes quasi degenerate.

Not only the neutrino masses can be written as a function of the lightest neutrino mass, but also the phases: since in the Tribimaximal mixing the reactor angle is vanishing, the Dirac CP phase is undetermined at the leading order; on the contrary the Majorana phases are well defined and they can be expressed through ρ and Δ. Since we are interested in physical observables, we report only phase differences, $\alpha_{ij} \equiv (\alpha_i - \alpha_j)/2$: in terms of ρ and Δ in order to keep compact the expressions,

$$\sin(2\alpha_{13}) = \frac{2\rho\sin\Delta}{\sqrt{(\rho^2-1)^2 + 4\rho^2\sin^2\Delta}} \,, \qquad \sin(2\alpha_{23}) = \frac{\rho\sin\Delta}{\sqrt{1 - 2\rho\cos\Delta + \rho^2}} \,. \tag{2.45}$$

It will be useful to report also $\sin(2\alpha_{12})$:

$$\sin(2\alpha_{12}) = -\frac{\rho\sin\Delta}{\sqrt{1 + 2\rho\cos\Delta + \rho^2}} \,. \tag{2.46}$$

These results are valid only at the leading order and some deviations are expected with the introduction of the higher-order terms, that is illustrated in the following section. The corrections are expected to be of relative order u, whose allowed range is defined in eqs. (2.33, 2.37). However, close to $\cos\Delta = -1$, where the bounds are saturated, the corrections to both the numerator and the denominator of eq. (2.41) remain of relative order u and as a result the lower bound on m_1 of eq. (2.43) is not significantly affected. Major effects could appear when the spectrum is quasi degenerate, $\cos\Delta \approx 0$.

2.3.2 The Next-To-Leading Order Contributions

Another important implication of the spontaneously broken flavor symmetry is that the leading order predictions are always subjected to corrections due to higher-dimensional operators. The latter are suppressed by additional powers of the cutoff Λ_f and can be organized in a suitable double power expansion in u and t.

At the NLO there are may additional terms which can be added to the Lagrangian. Since φ_T is the only scalar field which is neutral under the Abelian part of the flavor symmetry, all the NLO terms contain the terms already present in the leading order Lagrangian with an additional insertion of φ_T/Λ_f. In addition to these terms, there are also corrections to the leading vacuum alignment in eq. (2.28):

$$\begin{aligned} \frac{\langle\varphi_T\rangle}{\Lambda_f} &= (u,0,0) + (c_1 u^2,\, c_2 u^2,\, c_3 u^2) \\ \frac{\langle\varphi_S\rangle}{\Lambda_f} &= c_b(u,u,u) + (c_4 u^2,\, c_5 u^2,\, c_6 u^2) \\ \frac{\langle\xi\rangle}{\Lambda_f} &= c_a u + c_7 u^2 \ , \end{aligned} \tag{2.47}$$

where c_i are complex numbers with absolute value of order one. Note that in the supersymmetric version, the model predicts $c_2 = c_3$. Here we will not perform a detailed analysis for NLO operators and the origin of eq. (2.47) (see [6, 7] for a detailed study). As a result of these NLO contributions, the quantities generally deviate from their initial values for terms of relative order u:

$$Y_e + \delta Y_e \ , \qquad m_\nu + \delta m_\nu \ . \tag{2.48}$$

These corrections affect also the mixing angles and it is not difficult to see that deviations from Tribimaximal are also of relative order u with respect to their leading order values [6, 7]:

$$\sin^2\theta_{23} = \frac{1}{2} + \mathcal{O}(u), \qquad \sin^2\theta_{12} = \frac{1}{3} + \mathcal{O}(u), \qquad \sin\theta_{13} = \mathcal{O}(u). \tag{2.49}$$

Since the solar mixing angle is, at present, the most precisely known, we require that its value remains inside the 3σ range [1]. This requirement results in an upper bound on u of about 0.05. On the other hand, from eq. (2.31), we have the following relations:

$$\begin{aligned} u &= \frac{1}{|y_\tau|}\frac{\sqrt{2}m_\tau}{v} \approx 0.01\frac{1}{|y_\tau|} && \text{in the SM} \\ u &\simeq \frac{\tan\beta}{|y_\tau|}\frac{\sqrt{2}m_\tau}{v} \approx 0.01\frac{\tan\beta}{|y_\tau|} && \text{in the MSSM} \end{aligned} \tag{2.50}$$

where for the τ lepton we have used its pole mass $m_\tau = (1776.84 \pm 0.17)$ MeV [19]. Requesting $|y_\tau| < 3$ we find a lower limit for u of about 0.003 in the Standard Model case; in the supersymmetric context, the same requirements provides a lower bound close to the upper bound 0.05 for $\tan\beta = 15$, whereas for $\tan\beta = 2$ it is $u > 0.007$. From now on, we will choose the maximal range of u as

$$0.003 \lesssim u \lesssim 0.05 \tag{2.51}$$

for the Standard Model context, while for the supersymmetric case we take

$$0.007 \lesssim u \lesssim 0.05 \ , \tag{2.52}$$

which shrinks when $\tan\beta$ is increased from 2 to 15.

The NLO terms affect also the previous results for the neutrino phases. All the new parameters which perturb the leading order results are complex and therefore they introduce corrections to the phases of the PMNS matrix. Due to the large amount of such a parameters, we expect non-negligible deviations from the leading order values.

2.3.3 Type I See-Saw Realization

It is possible to easily modify the previous model to accommodate the (type I) See-Saw mechanism. In this part we do such an extension and analyze the differences with the effective model. Notice that this part is written considering an underlying Standard Model context, but the extension to the supersymmetric one is trivial, following the same strategy as in the effective model.

We introduce conjugate right-handed neutrino fields ν^c transforming as a triplet of A_4 and we modify the transformation properties of some other fields according to Table 2.3.

	ν^c	φ_S	ξ	$\tilde{\xi}$
A_4	**3**	**3**	**1**	**1**
Z_3	ω^2	ω^2	ω^2	ω^2
$U(1)_{FN}$	0	0	0	0

Table 2.3: *The transformation properties of ν^c, φ_S, ξ and $\tilde{\xi}$ under $A_4 \times Z_3 \times U(1)_{FN}$. The rest of the fields still transform as in Table 2.2. Notice that $\tilde{\xi}$ is present only in the supersymmetric context.*

The Lagrangian changes only in the neutrino sector and it is given by

$$\mathscr{L}_\nu = y(\nu^c \widetilde{H}^\dagger \ell) + x_a \xi(\nu^c \nu^c) + x_b(\varphi_S \nu^c \nu^c) + h.c. + \dots \ , \tag{2.53}$$

where dots stand for higher-order contributions.

The vacuum alignment of the flavons is exactly the one described in eqs. (2.28, 2.47). When the flavons develop VEVs in agreement with eq. (2.28) and after the electroweak symmetry breaking, the Dirac and the Majorana mass matrices, at the leading order, are given by

$$m_D = \frac{y\,v}{\sqrt{2}} \begin{pmatrix} 1 & 0 & 0 \\ 0 & 0 & 1 \\ 0 & 1 & 0 \end{pmatrix} \ , \qquad M_R = \begin{pmatrix} a+2b/3 & -b/3 & -b/3 \\ -b/3 & 2b/3 & a-b/3 \\ -b/3 & a-b/3 & 2b/3 \end{pmatrix} \ , \tag{2.54}$$

where $a \equiv 2x_a c_a u$ and $b \equiv 2x_b c_b u$. The complex symmetric matrix M_R is diagonalized by the transformation

$$\hat{M}_R = U_R^T M_R U_R \ , \tag{2.55}$$

where $\hat{M}_R$ is a diagonal matrix with real and positive entries, given by

$$\hat{M}_R \equiv \text{diag}(M_1,\, M_2,\, M_3) = \text{diag}(|a+b|, |a|, |-a+b|)\ , \tag{2.56}$$

while the unitary matrix U_R can be written as $U_R = U_{TB}P$, where P is the diagonal matrix of the Majorana phases already defined in eq. (2.36). After the electroweak symmetry breaking, the mass matrix for the light neutrinos is recovered from the well known type I See-Saw formula

$$m_\nu = -m_D^T M_R^{-1} m_D = -\frac{y^2\, v^2}{2} M_R^{-1} \tag{2.57}$$

where the last passage is possible considering that $M_R^{-1} m_D = m_D M_R^{-1}$. From eq. (2.55), $U_R^\dagger M_R^{-1} U_R^* = \text{diag}(M_1^{-1},\, M_2^{-1},\, M_3^{-1})$ and as a result the light neutrino mass matrix can be diagonalized by

$$\hat{m}_\nu = U_\nu^T m_\nu U_\nu\ , \tag{2.58}$$

where $U_\nu = iU_R^* = iU_{TB}P^*$. The diagonal matrix $\hat{m}_\nu$ has real and positive entries written as

$$m_i = \frac{v^2}{2}\frac{y^2}{M_i}\ , \tag{2.59}$$

which explicitly give the following values

$$m_1 = \frac{v^2}{2}\frac{y^2}{|a+b|}\ , \qquad m_2 = \frac{v^2}{2}\frac{y^2}{|a|}\ , \qquad m_3 = \frac{v^2}{2}\frac{y^2}{|-a+b|}\ . \tag{2.60}$$

In these expressions we have absorbed the possible phase of y inside the matrix P: this phase however is not observable and thus we could have assumed a positive y from the beginning without loss of generality. We can repeat the analysis presented in Section 2.3.1 to study the light neutrino spectrum in this case. Taking $|a| = M_2 = v^2y^2/(2m_2)$, we find that both the orderings can be described and that the lightest neutrino masses span the following ranges: for the most conservative case,

$$\begin{aligned} &\text{normal hierarchy:} && 4.3\ \text{meV} < m_1 < 6.2\ \text{meV} \\ &\text{inverse hierarchy:} && m_3 > 15.8\ \text{meV}\ . \end{aligned} \tag{2.61}$$

For the normal hierarchy, m_1 spans a narrow range of values, which corresponds to values of Δ close to zero. This completely determines the neutrino masses inside a very small range and represents a prediction of the model. On the other hand, for the inverse hierarchy, m_3 is bounded only from below and the minimum is achieved when Δ is close to $\pm\pi$. In Figure 2.1 we can read off the light neutrino spectrum and its dependence with the lightest neutrino mass.

From eq. (2.59) it is possible to describe the leading order spectrum of the right-handed neutrinos as a function of a unique parameter, which is the lightest left-handed neutrino mass. In all the allowed range for $m_{1,3}$, the order of magnitude of the right-handed neutrino masses falls between 10^{14} GeV and 10^{15} GeV. In fig. (2.1) we show explicitly the right-handed neutrino masses for normal hierarchy and inverse hierarchy,

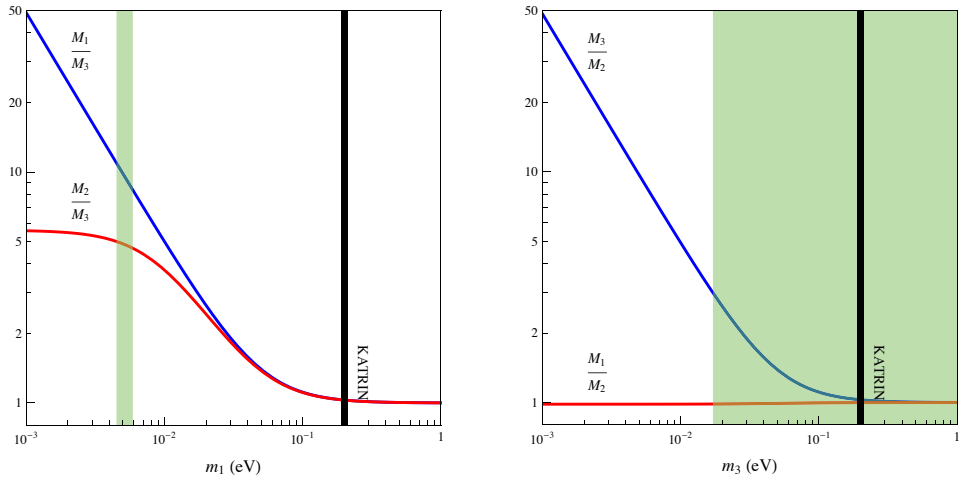

Figure 2.1: *Plots of the heavy neutrino masses, as a function of the lightest left-handed neutrino mass. On the left the normal hierarchy and on the right the inverse hierarchy. The green areas refer to the allowed range for $m_{1(3)}$ as in eq. (2.61). The vertical black lines correspond to the future sensitivity of KATRIN experiment.*

on the left and on the right respectively. The ratios among the masses are well defined for the NH, thanks to the narrow allowed range for m_1: $M_1/M_3 \sim 11$ and $M_2/M_3 \sim 5$. In the case of the IH, the ratio M_1/M_2 is fixed at 1 while M_3/M_2 varies from about 3 to 1, going from the lower bound of m_3 up to the KATRIN sensitivity. The analysis done for the Majorana phases in eqs. (2.45, 2.46) is still valid here.

Chapter 3

The Golden Ratio Pattern from the Symmetry Group A_5

Neutrino oscillation and the lepton mixing matrix U_{PMNS} still suffer from large uncertainties. As seen in Chapter 1, the parameters related to CP violations are totally unknown at present. The reactor angle θ_{13} is the smallest mixing angle, but there is only an upper bound on it and its value can range from zero to about 0.2. The atmospheric mixing angle θ_{23} is compatible with being maximal, but deviations from maximality are still allowed to some extent. The most precisely measured angle is the solar angle θ_{12}, which is large but not maximal, with a 1σ uncertainty of less than 2 degrees:

$$\sin^2\theta_{12} = 0.304^{+0.022}_{-0.016}, \sin^2\theta_{12} = 0.321^{+0.023}_{-0.022}. \tag{3.1}$$

Despite the lack of a precise knowledge of U_{PMNS}, the present data guide us while searching for a first-order approximation providing the basis of a theoretical description. Some of them, based on a $\mu-\tau$ symmetry and predicting the values $\sin^2\theta_{23} = 1/2$ and $\theta_{13} = 0$ have been described in Chapter 2. Tri-bimaximal mixing (TB) is perhaps the most studied pattern [49]. It predicts $\sin^2\theta_{12} = 1/3$, which is within two standard deviations from the current best value. TB mixing can be reproduced at the LO in many models based on discrete and continuous flavor symmetries [42]. A minimal construction is based on A_4. In Bimaximal mixing (BM) the solar angle is maximal, $\sin^2\theta_{12} = 1/2$, outside the presently allowed range [48]. To reconcile the LO approximation with the data, the expansion parameter should be not-too-small, of the order of the Cabibbo angle. Sub-leading corrections of this size are expected to affect also other parameters, such as θ_{13}, which is thus predicted close to the present experimental upper bound.

Another plausible mixing pattern is the one where $\sin^2\theta_{23} = 1/2$, $\theta_{13} = 0$ and $\tan\theta_{12} = 1/\phi$ where $\phi = (1+\sqrt{5})/2$ is the Golden Ratio (GR) [51,52]. This pattern, called GR the hereafter, is the focus of the present part of our work. We have

$$\sin^2\theta_{12} = \frac{1}{\sqrt{5}\phi} = \frac{2}{5+\sqrt{5}} \approx 0.276 \quad . \tag{3.2}$$

This value is about two standard deviations below the experimental range and can be

brought inside the allowed interval by a small NLO correction, of order 0.05 radiants. [§] The GR characterizes several properties of the icosahedron and a natural candidate for the flavor symmetry giving rise to (3.2) is the icosahedral one, related to the group A_5. This relation was pointed out for the first time while trying to connect the value of the solar angle to the Golden Ratio [51]. Indeed there have been attempts to construct a model based on the A_5 symmetry [45] to the purpose of reproducing the GR mixing pattern, but a complete model does not exist to date. Recently, the group A_5 was also applied to a scenario with a fourth lepton family [46], while the double cover of the icosahedral group was used to reproduce the quark mixing [47]. In models based on spontaneously broken flavor symmetries a crucial feature is the discussion of the vacuum alignment. The family symmetry is broken by the Vevs of flavon fields and the desired mixing pattern is intimately related to the directions of these VEVs in flavor space. In a complete model the VEV alignment should occur naturally, as the outcome of the minimization of the energy density of the theory. To our knowledge none of the existing proposals of what we called the GR pattern have solved the vacuum alignment problem.

Aim of the present chapter is to build a complete model based on the family group A_5 and reproducing the GR mixing pattern in a natural way. We will discuss how the symmetry group A_5 can be used to generate the GR mixing pattern. We will show that the invariance of a general neutrino mass matrix under a parity transformation S guide us in a straightforward way to the icosahedral symmetry. We will also specify the field content of the model, develop a natural way of symmetry breaking and discuss the phenomenological consequences at the LO and NLO.

3.1 A Family Symmetry for the Golden Ratio

We start by analyzing the property of the most general neutrino mass matrix leading to the Golden Ratio (GR) prediction for the solar mixing angle. We chose a basis where the mass matrix for the charged leptons m_l is diagonal. More precisely, it is sufficient that the combination $m_l^\dagger m_l$ is diagonal, so that there is no contribution to the lepton mixing from the charged lepton sector. We should also make a choice for θ_{23} and θ_{13}. To begin with we assume a leading order approximation where $\sin^2\theta_{23} = 1/2$, $\sin^2\theta_{13} = 0$ and $\tan\theta_{12} = 1/\phi$ where $\phi = (1+\sqrt{5})/2$ is the GR. We look for the most general neutrino mass matrix m_ν leading to this mixing pattern. Such a matrix can be constructed by acting with the corresponding mixing matrix U_{GR} on a generic diagonal neutrino mass matrix:

$$m_\nu = U_{GR}^* \, \mathtt{diag}(m_1, m_2, m_3) \, U_{GR}^\dagger \quad . \tag{3.3}$$

In a particular phase convention, the matrix U_{GR} representing our mixing pattern is given by:

[§] An alternative proposal [56] relating the Golden Ratio to the lepton mixing assumes $\cos\theta_{12} = \phi/2$. Consequently we have $\sin^2\theta_{12} = \frac{1}{4}(3-\phi) \approx 0.345$, about two standard deviations above the experimental value. In [57] this prediction was deduced from the symmetry of the dihedral group D_{10}.

$$U_{GR} = \begin{pmatrix} \cos\theta_{12} & \sin\theta_{12} & 0 \\ \dfrac{\sin\theta_{12}}{\sqrt{2}} & -\dfrac{\cos\theta_{12}}{\sqrt{2}} & \dfrac{1}{\sqrt{2}} \\ \dfrac{\sin\theta_{12}}{\sqrt{2}} & -\dfrac{\cos\theta_{12}}{\sqrt{2}} & -\dfrac{1}{\sqrt{2}} \end{pmatrix} \quad , \tag{3.4}$$

with $\tan\theta_{12} = 1/\phi$. By applying eq. (3.3) we find a matrix of the form:

$$m_\nu = \begin{pmatrix} x & y & y \\ y & z & w \\ y & w & z \end{pmatrix} \quad , \tag{3.5}$$

with coefficients x, y, z and w satisfying the following relation:

$$z + w = x - \sqrt{2}y \quad . \tag{3.6}$$

The matrix in eq. (3.5) is the most general one giving rise to $\theta_{13} = 0$ and θ_{23} maximal. The constraint of eq. (3.6) arises from further specifying the solar mixing angle.

The matrix in eqs. (3.5-3.6) can be completely characterized by a simple symmetry requirement. Indeed, it is invariant under the action of the two unitary transformations:

$$U = \begin{pmatrix} 1 & 0 & 0 \\ 0 & 0 & 1 \\ 0 & 1 & 0 \end{pmatrix} \qquad S = \frac{1}{\sqrt{5}} \begin{pmatrix} 1 & \sqrt{2} & \sqrt{2} \\ \sqrt{2} & -\phi & 1/\phi \\ \sqrt{2} & 1/\phi & -\phi \end{pmatrix} \quad , \tag{3.7}$$

which satisfy

$$S^2 = U^2 = 1 \quad , \qquad [S, U] = 0 \quad , \tag{3.8}$$

and generate a group $G_\nu = Z_2 \times Z_2$. Conversely, the requirement of invariance under U and S completely characterize m_ν in eqs. (3.5-3.6). Namely, given a generic neutrino mass matrix m_ν the most general solution to the equations:

$$U^T \, m_\nu \, U = m_\nu \quad , \qquad S^T \, m_\nu \, S = m_\nu \quad , \tag{3.9}$$

with U and S given in eq. (3.7), is the mass matrix defined by eqs. (3.5) and (3.6).

In the chosen basis, where $m_l^\dagger m_l$ is diagonal, there is no contribution to the lepton mixing from the charged lepton sector and the mixing matrix U_{GR} originates only from the diagonalization of m_ν. To construct a model for the desired mixing pattern, we should require that a diagonal $m_l^\dagger m_l$ arises naturally, as the general solution of a symmetry or dynamical requirement. For instance, we can require that the charged lepton sector is invariant under a family group G_l enforcing a diagonal $m_l^\dagger m_l$. In our LO approximation the groups G_ν and G_l should be seen as the residual vacuum symmetries characterizing the neutrino sector and the charged lepton sector, respectively. Such a configuration can be

induced by the spontaneous breaking of some family symmetry G_f, through the vacuum expectation values of two different sets of flavons that selectively couple to neutrinos and to charged leptons. It is not strictly necessary that G_f entirely contains G_l and G_ν as subgroups, since a part of the residual symmetries can arise accidentally, due to the specific field content of the model, as the baryon and the lepton numbers arise as accidental classical symmetries in the standard model. A natural candidate for the family symmetry G_f giving rise to the GR prediction for the solar mixing angle is the proper symmetry group of the icosahedral, the alternating group A_5 [58]. One of the possible presentations of A_5 is in term of two generators S and T satisfying:

$$S^2 = (ST)^3 = 1 \qquad \text{and} \qquad T^5 = 1 \quad . \tag{3.10}$$

We make the following ansatz: we assume that the $\mu-\tau$ exchange symmetry generated by U arises as an accidental symmetry of the neutrino mass matrix, at the LO in the allowed lepton coupling constants. We then identify the matrix S in eq. (3.7) with the generator S of A_5. Given the explicit form of the generator S, the algebraic relation (3.10) allows to determine the matrix corresponding to the generator T. We find:

$$T = \begin{pmatrix} 1 & 0 & 0 \\ 0 & e^{\frac{2\pi i}{5}} & 0 \\ 0 & 0 & e^{\frac{8\pi i}{5}} \end{pmatrix} \quad . \tag{3.11}$$

This is an encouraging result. Indeed the condition

$$T^\dagger \, (m_l^\dagger m_l) \, T = (m_l^\dagger m_l) \tag{3.12}$$

requires $m_l^\dagger m_l$ to be a diagonal matrix and the natural candidate for the subgroup G_l is the group Z_5 generated by T. We look for a model invariant under the family symmetry A_5, where, after spontaneous breaking, the residual symmetries of the neutrino sector and of the charged lepton sector are those generated by (S, U) and T, respectively. The $\mu - \tau$ symmetry is accidental and is slightly broken by higher order corrections, resulting in deviations from the LO predictions $\theta_{13} = 0$ and $\theta_{23} = \pi/4$. By construction the model predicts GR for the solar mixing angle.

Notice that this approach automatically guarantees the independence of the mixing matrix U_{GR} and the other physical results from the base choice. Indeed, in a generic basis where the generators are $X_\Omega = \Omega \; X \; \Omega^\dagger$ $(X = S, T, U)$, Ω denoting a unitary 3×3 matrix, in general the combination $m_l^\dagger m_l$ is no more diagonal and the neutrino mass matrix m_ν have a texture different from the one in eqs. (3.5-3.6). However, as a result of the residual symmetries, $m_l^\dagger m_l$ is diagonalized by Ω, whereas m_ν is diagonalized by $(\Omega \; U_{GR})$, the physical mixing matrix remaining U_{GR}.

3.2 The Group A_5

The group A_5 is the group of the even permutations of five objects. It is the proper symmetry group of two of the five Platonic solids, the icosahedron and the dodecahedron. It has 60 elements that can be grouped into five conjugacy classes with 1, 12, 12, 15 and 20 elements. The five irreducible representations are the invariant singlet, two inequivalent triplets, a tetraplet and a pentaplet. The characters of A_5 are collected in Table 3.1. The

A_5	C_1	$12C_2^{[5]}$	$12C_3^{[5]}$	$15C_4^{[2]}$	$20C_5^{[3]}$
$\chi^{[\mathbf{1}]}$	1	1	1	1	1
$\chi^{[\mathbf{3}]}$	3	ϕ	$(1-\phi)$	-1	0
$\chi^{[\mathbf{3'}]}$	3	$(1-\phi)$	ϕ	-1	0
$\chi^{[\mathbf{4}]}$	4	-1	-1	0	1
$\chi^{[\mathbf{5}]}$	5	0	0	1	-1

Table 3.1: Characters of the A_5 group.

products of two A_5 representations can be decomposed according to the following rules

$$\begin{aligned}
3 \otimes 3 &= (1+5)_S + 3_A \\
3' \otimes 3' &= (1+5)_S + 3'_A \\
3 \otimes 3' &= 4+5 \\
3 \otimes 4 &= 3'+4+5 \\
3' \otimes 4 &= 3+4+5 \\
3 \otimes 5 &= 3+3'+4+5 \\
3' \otimes 5 &= 3+3'+4+5 \\
4 \otimes 4 &= (1+4+5)_S + (3+3')_A \\
4 \otimes 5 &= 3+3'+4+5+5 \\
5 \otimes 5 &= (1+4+5+5)_S + (3+3'+4)_A
\end{aligned} \tag{3.13}$$

where the suffices $S(A)$ denote the symmetric(antisymmetric) property of the corresponding representation. The product between the singlet and any representation r gives r. As recalled in the previous section, A_5 is generated by two elements S and T, with the

presentation

$$S^2 = (ST)^3 = 1 \qquad \text{and} \qquad T^5 = 1 \quad . \tag{3.14}$$

The element S belongs to the class $C_4^{[2]}$ and the element T to the class $C_2^{[5]}$. We find useful to work in a basis where the T generator for the various representations is always diagonal. Since this choice is unconventional we list in Table 3.2 the matrices associated to S and T in our basis. In Appendix A we made connection with other basis used in the literature.

	S	$\frac{5}{2\pi i}\log(T)$
3	$\frac{1}{\sqrt{5}}\begin{pmatrix} 1 & \sqrt{2} & \sqrt{2} \\ \sqrt{2} & -\phi & \frac{1}{\phi} \\ \sqrt{2} & \frac{1}{\phi} & -\phi \end{pmatrix}$	$\mathtt{diag}(0,1,4)$
$3'$	$-\frac{1}{\sqrt{5}}\begin{pmatrix} 1 & \sqrt{2} & \sqrt{2} \\ \sqrt{2} & \frac{1}{\phi} & -\phi \\ \sqrt{2} & -\phi & \frac{1}{\phi} \end{pmatrix}$	$\mathtt{diag}(0,2,3)$
4	$-\frac{1}{5}\begin{pmatrix} -\sqrt{5} & (\phi-3) & (\phi+2) & -\sqrt{5} \\ (\phi-3) & \sqrt{5} & \sqrt{5} & (\phi+2) \\ (\phi+2) & \sqrt{5} & \sqrt{5} & (\phi-3) \\ -\sqrt{5} & (\phi+2) & (\phi-3) & -\sqrt{5} \end{pmatrix}$	$\mathtt{diag}(1,2,3,4)$
5	$\frac{1}{5}\begin{pmatrix} -1 & \sqrt{6} & -\sqrt{6} & -\sqrt{6} & -\sqrt{6} \\ \sqrt{6} & 2-\phi & 2\phi & 2(1-\phi) & -1-\phi \\ -\sqrt{6} & 2\phi & 1+\phi & 2-\phi & 2(-1+\phi) \\ -\sqrt{6} & 2(1-\phi) & 2-\phi & 1+\phi & -2\phi \\ -\sqrt{6} & -1-\phi & -2(1-\phi) & -2\phi & 2-\phi \end{pmatrix}$	$\mathtt{diag}(0,1,2,3,4)$

Table 3.2: S and T generators of A_5 in the basis where T is diagonal.

Notice that the matrices S and T of the previous section coincide with those of the A_5 generators in the representation 3. We have derived the Clebsh-Gordan coefficients entering the decomposition of the representation products. They are given in Appendix A.

3.3 A Model with A_5 Family Symmetry

In this section we define our model. We focus on the lepton sector and, to facilitate the task related to the vacuum alignment, we consider a supersymmetric model in the limit of exact supersymmetry (SUSY). SUSY breaking effects do not affect lepton masses and mixing angles. Among the fields in the lepton sector we include three gauge singlets ν_i^c and the neutrino masses will be dominated by the contribution of a type I see-saw mechanism [14]. A version of the model without see-saw, where the neutrino masses are described by effective higher-dimensional operators, is equally possible. It would lead to the same predictions for the lepton mixing angles.

To start with we assign both the SU(2) lepton doublets l and the right-handed neutrinos ν^c to the representation 3 of A_5. We take the SU(2) singlets e^c, μ^c and τ^c as invariant A_5 singlets. Higgs doublets $H_{u,d}$ are also singlets of A_5. In the neutrino sector we can write a renormalizable Yukawa coupling of the type $(\nu^c l)H_u$, the notation (...) standing for the combination of the fields in parenthesis giving an A_5 singlet. The product $\nu^c\nu^c$ is symmetric and contains a singlet and a pentaplet of A_5 and, to discuss the most general case, we introduce two flavon chiral multiplets ξ and φ_S transforming as 1 and 5 of A_5, respectively. They are completely neutral under the gauge interactions. In the charged lepton sector renormalizable Yukawa interactions are not allowed and we need additional flavons transforming as 3 under A_5. To solve the vacuum alignment problem a minimum of three triplets is needed, since trilinear interaction terms depending on less than three triplets vanish by the A_5 symmetry. We include three triplets φ, φ' and φ'', neutral under the gauge interactions. An additional flavon ξ', singlet of A_5, is also introduced to implement the desired vacuum alignment. To avoid couplings of the flavon multiplets to the wrong sector we also need to enlarge the flavor symmetry. This is done by considering the group $G_f = A_5 \times Z_5 \times Z_3$. In Table 3.3 we collect the chiral supermultiplets and their transformation properties under G_f. Notice that, at variance with other constructions based on flavor symmetries, we do not introduce the so-called driving fields.

	e^c	μ^c	τ^c	l	ν^c	$H_{u,d}$	φ	φ'	φ''	φ_S	ξ	ξ'
$\mathbf{A_5}$	1	1	1	3	3	1	3	3	3	5	1	1
Z_5	0	4	1	0	0	0	0	4	1	0	0	0
Z_3	1	1	1	2	1	0	0	0	0	1	1	2

Table 3.3: Chiral multiplets and their transformation properties.

The additional symmetry Z_3 is a discrete version of the total lepton number and is broken by the VEVs of the flavons of the neutrino sector, φ_S, ξ and ξ'. This symmetry prevents a direct mass term for ν^c. The presence of the new Z_5 factor forces each of the lepton multiplets e^c, μ^c and τ^c to couple to only one of the triplets φ, φ' and φ'', at the LO. The additional factors Z_3 and Z_5 play also an important role both in the

construction of the flavon scalar potential and in the classification of NLO corrections. The superpotential for the lepton multiplets reads:

$$\begin{aligned} w &= y(\nu^c l)H_u + \sqrt{\frac{3}{2}} y_1 \xi(\nu^c \nu^c) + y_5(\varphi_S \nu^c \nu^c) \\ &+ y_e e^c(\frac{\varphi}{\Lambda} l)H_d + y_\mu \mu^c(\frac{\varphi''}{\Lambda} l)H_d + y_\tau \tau^c(\frac{\varphi'}{\Lambda} l)H_d + ... \end{aligned} \tag{3.15}$$

where dots stand for higher order operators and Λ denotes the cut-off scale. Notice that the LO Yukawa couplings of the charged fermions are described by non-renormalizable operators. As we will see in section 5, where we will discuss the vacuum alignment, at the LO the flavons φ_S, ξ, φ, φ' and φ'' acquire VEVs of the type:

$$\begin{aligned} \langle \varphi_S \rangle &= (-\sqrt{\frac{2}{3}}(p+q), -p, q, q, p)\ \Lambda \\ \langle \xi \rangle &= s\ \Lambda \\ \langle \varphi \rangle &= (u, 0, 0)\ \Lambda \\ \langle \varphi' \rangle &= (0, u', 0)\ \Lambda \\ \langle \varphi'' \rangle &= (0, 0, u'')\ \Lambda \quad . \end{aligned} \tag{3.16}$$

where p, q, s, u, u', u'' are dimensionless coefficients. Such a pattern completely specifies lepton masses and mixing angles, at the LO. Plugging the VEVs of φ_S, ξ, φ, φ' and φ'' into the superpotential w and working out the A_5 invariant combinations, with the help of the results of the previous section and those of the Appendix A, we can find the LO mass matrices m_l and m_ν.

In the charged lepton sector, after breaking of A_5, the relevant part of the superpotential becomes

$$y_e u\ e^c l_e H_d + y_\mu u''\ \mu^c l_\mu H_d + y_\tau u'\ \tau^c l_\tau H_d \quad . \tag{3.17}$$

There is no contribution to the lepton mixing from this sector and charged lepton masses are

$$m_e = y_e u v_d \quad , \qquad m_\mu = y_\mu u'' v_d \quad , \qquad m_\tau = y_\tau u' v_d \quad , \tag{3.18}$$

v_d being the VEV of the neutral component of H_d. We might be surprised by the fact that m_l is diagonal, since only the VEV of φ leaves the Z_5^T subgroup generated by T invariant, while the VEVs of φ' and φ'' break Z_5^T. We can understand this result by recalling that the flavor symmetry G_f contains a factor Z_5, distinct from Z_5^T. The VEVs of φ, φ' and φ'' break $A_5 \times Z_5$ down to the diagonal subgroup Z_5^D contained in the product $Z_5^T \times Z_5$. It is this residual group that guarantees a diagonal m_l in our construction.

Similarly, in the neutrino sector we read from eq. (3.15) the mass matrices M for the

right-handed neutrinos and m_D, the Dirac one:

$$M = \sqrt{6} \begin{pmatrix} y_1 s + \frac{2}{3} y_5 (p+q) & y_5 \frac{p}{\sqrt{2}} & y_5 \frac{p}{\sqrt{2}} \\ y_5 \frac{p}{\sqrt{2}} & y_5 q & y_1 s - \frac{1}{3} y_5 (p+q) \\ y_5 \frac{p}{\sqrt{2}} & y_1 s - \frac{1}{3} y_5 (p+q) & y_5 q \end{pmatrix} \Lambda \quad . \tag{3.19}$$

$$m_D = y \begin{pmatrix} 1 & 0 & 0 \\ 0 & 0 & 1 \\ 0 & 1 & 0 \end{pmatrix} v_u \quad , \tag{3.20}$$

where v_u is the VEV of the Higgs doublet H_u. Since M is $\mu - \tau$ symmetric and m_D is proportional to the matrix U in eq. (3.7), from the see-saw formula we have

$$m_\nu = m_D^T M^{-1} m_D = y^2 v_u^2 M^{-1} \tag{3.21}$$

We notice that M has precisely the structure given in eqs. (3.5) and (3.6) and therefore both M and its inverse are diagonalized by the mixing matrix in eq. (3.4) with $\tan\theta_{12} = 1/\phi$:

$$U_{GR}^T \, m_\nu \, U_{GR} = \texttt{diag}(m_1, m_2, m_3) \quad . \tag{3.22}$$

Therefore U_{GR} represents the contribution to the lepton mixing coming from the neutrino sector, as desired. This result crucially depends on the VEV of the flavon pentaplet φ_S, which will be derived from the minimization of the scalar potential in Section 3.4. We observe that such a VEV is left invariant by the action of the generator S, as can be immediately checked by multiplying the 5×5 matrix S of Table 3.2 and the vector $(-\sqrt{2/3}(p+q), -p, q, q, p)$. This is the reason why the residual symmetry of the neutrino sector contains the parity subgroup generated by S. The presence of the $\mu - \tau$ symmetry is more subtle. Indeed the generator S of the 5 representation has three eigenvalues equal to one and the corresponding eigenvector can be parametrized as

$$(-\sqrt{2/3}(p+q+r\phi), -p+r, q+2r\phi, q, p+r) \quad . \tag{3.23}$$

This is the most general VEV of φ_S that leaves S unbroken. It is easy to construct the corresponding neutrino mass matrix m_ν and check that in the general case, with $r \neq 0$, m_ν is not $\mu - \tau$ symmetric. In our model it is the minimization of the scalar potential that selects the vacuum with $r = 0$, thus enforcing the $\mu - \tau$ symmetry. We will demonstrate this result in Section 3.4.

The charged fermion masses depend on three sets of independent parameters, which do not display a manifest relative hierarchy. It is easy to induce the correct hierarchy by assigning Froggatt-Nielsen $\mathrm{U}(1)_F$ charges $2q$ and q to e^c, and μ^c, respectively [53]. The spontaneous breaking of such $\mathrm{U}(1)_F$ by the VEV of a scalar fields carrying a negative units of F explains why $y_e << y_\mu << y_\tau$. In the LO approximation the spectrum of the

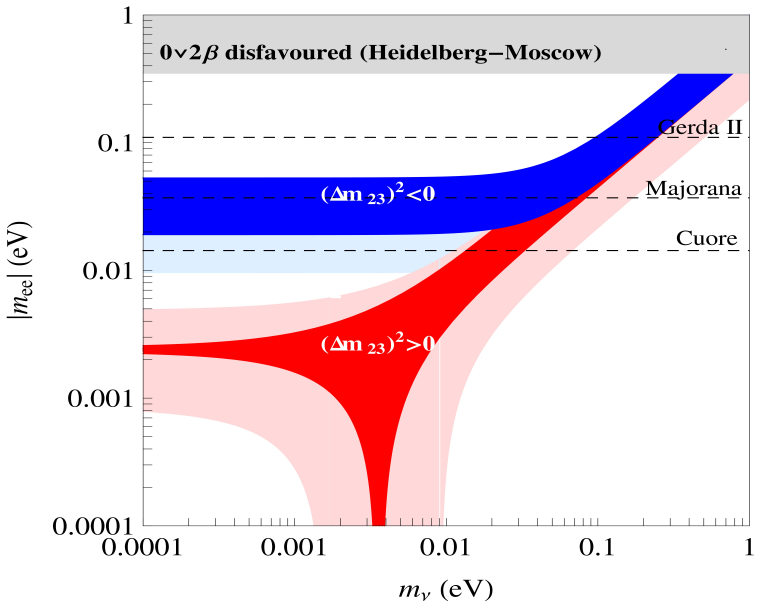

Figure 3.1: Predictions for $|m_{ee}|$ versus the lightest neutrino mass, for normal (red) and inverted (blue) mass ordering. In lighter regions the mass parameters are completely free. In darker regions they are correlated as prescribed by the LO approximation of our model.

light neutrinos is

$$m_1 = \frac{1}{A+B+C}, \quad m_2 = \frac{1}{A+B-C}, \quad m_3 = \frac{1}{-A+2B}. \tag{3.24}$$

where A, B and C are complex parameters defined as

$$A = 6y_1 q \frac{\Lambda}{\sqrt{6}y^2 v_u^2}, \quad B = y_5(p+4q)\frac{\Lambda}{\sqrt{6}y^2 v_u^2}, \quad C = 3\sqrt{5}y_5 p \frac{\Lambda}{\sqrt{6}y^2 v_u^2}. \tag{3.25}$$

There are no special relations between the three complex parameter and thus we have no prediction on the neutrino spectrum, that can have both normal and inverted ordering. A moderate tuning among the parameters is needed in order to reproduce the ratio between solar and atmospheric squared mass differences. The mass combination entering neutrinoless double-beta decay, m_{ee}, is given by $y^2 v_u^2 (M^{-1})_{11}$ and depends on the same parameters A, B and C. By expressing the absolute values of A, B and C in terms of Δm^2_{sol}, Δm^2_{atm}, the smallest neutrino mass and the phases of A, B and C, we can derive a range for $|m_{ee}|$ as a function of the smallest neutrino mass by varying the available phases. We plot the result in Figure 3.1, where the lighter region refer to the unconstrained case (see the first reference in [1]), and the darker one corresponds to the present model, in the LO approximation.

The dominant contribution from local effective operators to the light neutrino masses is $(llh_u h_u \xi')$. This operator is suppressed compared to the see-saw contribution, since the former is of order VEV/Λ^2, while the latter is of order $1/VEV$. Moreover, it is easy

to see that the new effective term preserves the $\mu - \tau$ symmetry and the Golden Ratio prediction.

3.4 Vacuum Alignment

The results of the previous section crucially depend on the assumed set of VEVs, eq. (3.16), and the purpose of this section is to show that they derive from the minimization of the scalar potential of the theory, without ad-hoc tuning of the parameters involved. The transformation properties of the flavon fields allow to write the following contribution to the superpotential

$$\begin{aligned} w_f &= M_0\xi\xi' + g_1\xi(\varphi_S^2) + g_2(\varphi_S^3)_1 + g_3(\varphi_S^3)_2 + \frac{g_4}{3}\xi^3 + \frac{g_5}{3}\xi'^3 \\ &+ M_1(\varphi^2) + M_2(\varphi'\varphi'') + g(\varphi\varphi'\varphi'') + ... \end{aligned} \tag{3.26}$$

where dots stand for higher dimensional terms, which will contribute at the NLO. There are two independent cubic invariants that can be built from a pentaplet and they are denoted by the suffices 1 and 2 in w_f. There are no driving fields in our construction and the minima are derived by analyzing the F-terms of the flavons themselves. At the LO there is no mixing between ξ, ξ', φ_S, that control the neutrino mass terms and φ, φ' and φ'', that give rise to the charged lepton Yukawas. We can separately discuss the two sets of minima. We start from the neutrino sector. The condition

$$\frac{\partial w_f}{\partial \xi'} = M_0\xi + g_5\xi'^2 = 0 \tag{3.27}$$

is solved by

$$\xi = -\frac{g_5}{M_0}\xi'^2 \quad . \tag{3.28}$$

Another set of conditions is given by

$$\frac{\partial w_f}{\partial \varphi_{Si}} = 0 \quad . \tag{3.29}$$

To solve these equations it is convenient to move to the so-called Cummins-Patera basis [59, 60] for the generators S and T. In this basis the generator S for the five-dimensional representation is diagonal, $S_{CP} = \texttt{diag}(+1, -1, -1, +1, +1)$. The explicit form of T for the 5 representation in the Cummins-Patera basis as well as the unitary matrix relating the two basis is given in Appendix B. We denote the components of φ_S in the Cummins-Patera basis by

$$\varphi_S = (X_1, X_2, X_3, Z, \bar{Z}) \quad , \tag{3.30}$$

where X_i $(i = 1, 2, 3)$, Z and $\bar{Z}$ should be seen as independent complex quantities. The terms of the superpotential w_f that depend on φ_S are explicitly given by:

$$\begin{aligned} w_f &= g_1\xi(X_1^2 + X_2^2 + X_3^2 + 2Z\bar{Z}) \\ &+ g_2\left(Z^3 - \bar{Z}^3 - 3(X_1^2 + \omega^2 X_2^2 + \omega X_3^2)Z + 3(X_1^2 + \omega X_2^2 + \omega^2 X_3^2)\bar{Z}\right) \\ &+ g_3\left(Z^3 + \bar{Z}^3 + (X_1^2 + \omega^2 X_2^2 + \omega X_3^2)Z + (X_1^2 + \omega X_2^2 + \omega^2 X_3^2)\bar{Z}\right. \\ &- \left. 4X_1X_2X_3\right) + ... \end{aligned} \tag{3.31}$$

where

$$\omega = e^{\frac{2\pi i}{3}} \quad . \tag{3.32}$$

We have explicitly solved the equations (3.29) in this basis. We found no non-trivial solutions invariant under T and seven independent solutions invariant under S. They can be grouped in two pairs and a triplet. Each of these sets is closed under the action of the generator T. One of the triplet of solutions is given by:

$$X_1 = X_2 = X_3 = 0 \quad , \tag{3.33}$$

$$\begin{aligned} Z &= -\frac{2g_1g_5}{3M_0}\frac{1}{(g_2-g_3)^{1/3}(g_2+g_3)^{2/3}}\xi'^2 \quad , \\ \bar{Z} &= +\frac{2g_1g_5}{3M_0}\frac{1}{(g_2-g_3)^{2/3}(g_2+g_3)^{1/3}}\xi'^2 \quad , \end{aligned} \tag{3.34}$$

where we have also made use of eq. (3.28). The other two solutions belonging to the triplet are obtained by multiplying Z by $\omega(\omega^2)$ and $\bar{Z}$ by $\omega^2(\omega)$. The condition $X_2 = X_3 = 0$ correspond to the invariance under S, whereas $X_1 = 0$ is an additional specific feature of this set of solutions.

In each of these minima we have the basis independent result:

$$(\varphi_S^2) = -\frac{8g_1^2g_5^2}{9M_0^2}\frac{1}{(g_2-g_3)(g_2+g_3)}\xi'^4 \quad . \tag{3.35}$$

We have a finite multiplicity of minima and we chose the minimum in eqs. (3.33,3.34). Before coming back to our basis, we analyze the equation

$$\frac{\partial w_f}{\partial \xi} = M_0\xi' + g_1(\varphi_S^2) + g_4\xi^2 = 0 \quad , \tag{3.36}$$

which, by making use of (3.28) and (3.35), becomes

$$\frac{\xi'}{M_0} - \left[\frac{8g_1^3g_5^2}{9(g_2-g_3)(g_2+g_3)} - g_4g_5^2\right]\frac{\xi'^4}{M_0^4} = 0 \quad . \tag{3.37}$$

This equation has non-vanishing solutions for ξ', which make non-trivial the solutions (3.28) and (3.33, 3.34). With the help of the unitary transformation relating the Cummins-Patera basis to ours we find that in our basis the minimum (3.33, 3.34) translates into

$$\langle\varphi_S\rangle = (-\sqrt{\frac{2}{3}}(p+q), -p, q, q, p)\ \Lambda \tag{3.38}$$

with

$$\begin{aligned} p &= \frac{1}{2\sqrt{2}\Lambda}\left[\omega\left(\sqrt{\frac{3}{5}}-i\right)Z - \left(\sqrt{\frac{3}{5}}+i\right)\bar{Z}\right] \\ q &= \frac{1}{2\sqrt{2}\Lambda}\left[\omega\left(\sqrt{\frac{3}{5}}+i\right)Z - \left(\sqrt{\frac{3}{5}}-i\right)\bar{Z}\right] \quad , \end{aligned} \tag{3.39}$$

with Z and $\bar{Z}$ given by eq. (3.34). We have recovered the pattern displayed in Section 3.3. Notice that this result does not depend on the specific value of the Z and $\bar{Z}$ components, but rather on the conditions $X_i = 0$. In particular, the $\mu - \tau$ parity symmetry is related to the vanishing of the X_1 component.

Moving to the flavons φ, φ' and φ'', the relevant part of the superpotential is given by

$$\begin{aligned} w_f &= M_1(\varphi^2) + M_2(\varphi'\varphi'') + g(\varphi\varphi'\varphi'') + ... \\ &= M_1(\varphi_1^2 + 2\varphi_2\varphi_3) + M_2(\varphi_1'\varphi_1'' + \varphi_2'\varphi_3'' + \varphi_3'\varphi_2'') \\ &+ g(\varphi_1\varphi_2'\varphi_3'' + \varphi_2\varphi_3'\varphi_1'' + \varphi_3\varphi_1'\varphi_2'' - \varphi_1\varphi_3'\varphi_2'' - \varphi_2\varphi_1'\varphi_3'' - \varphi_3\varphi_2'\varphi_1'') + ... \end{aligned} \quad (3.40)$$

The minima in the φ, φ' and φ'' can be found by solving the system of equations:

$$\frac{\partial w_f}{\partial \varphi_i} = 0 \quad , \qquad \frac{\partial w_f}{\partial \varphi_i'} = 0 \quad , \qquad \frac{\partial w_f}{\partial \varphi_i''} = 0 \quad , \quad (3.41)$$

which, using a vectorial notation, can be written as

$$2M_1\ \hat{\varphi} + g\ \varphi' \times \varphi'' = 0 \quad , \quad 2M_2\ \hat{\varphi}'' - g\ \varphi \times \varphi'' = 0 \quad , \quad 2M_2\ \hat{\varphi}' + g\ \varphi \times \varphi' = 0 \quad , \quad (3.42)$$

where $\times$ denotes the external product and, for any vector $v = (v_1, v_2, v_3)$, we set $\hat{v} = (v_1, v_3, v_2)$. To solve this system it is useful to recognize that the LO part of the superpotential that depends only on the fields φ, φ' and φ'' is invariant under the linear transformation

$$\varphi \to \Omega R\ \Omega^{-1}\varphi \quad , \qquad \varphi' \to y\ \Omega R\ \Omega^{-1}\varphi' \quad , \qquad \varphi'' \to \frac{1}{y}\ \Omega R\ \Omega^{-1}\varphi'' \quad , \quad (3.43)$$

where y is a complex dimensionless parameter,

$$\Omega = \begin{pmatrix} 1 & 0 & 0 \\ 0 & \frac{1}{\sqrt{2}} & \frac{-i}{\sqrt{2}} \\ 0 & \frac{1}{\sqrt{2}} & \frac{+i}{\sqrt{2}} \end{pmatrix} \quad (3.44)$$

and R is a general complex orthogonal matrix, $R^T R = 1$, depending on three complex parameters. As we shall see this invariance is accidental and is broken by the NLO contributions to the superpotential. By exploiting such an invariance we can always reach the particular minimum with $\varphi_2 = \varphi_3 = 0$. It is easy to see that one such solution is given by[¶]

$$\begin{aligned} \varphi_0 &= -\frac{M_2}{g}\,(1,0,0) \\ \varphi_0' &= \frac{\sqrt{2M_1M_2}}{g}\,(0,1,0) \\ \varphi_0'' &= \frac{\sqrt{2M_1M_2}}{g}\,(0,0,1) \quad , \end{aligned} \quad (3.45)$$

[¶]There is also another solution where the entries of φ' and φ'' are exchanged.

The general solution of the system (3.42) is given by

$$\varphi = \Omega R\, \Omega^{-1}\varphi_0 \quad , \qquad \varphi' = y\, \Omega R\, \Omega^{-1}\varphi'_0 \quad , \qquad \varphi'' = \frac{1}{y}\, \Omega R\, \Omega^{-1}\varphi'_0 \quad , \tag{3.46}$$

The degeneracies related to R and y are accidental. Indeed the transformations of eq. (3.43) are not symmetries of our system, but rather accidental symmetries of the LO approximation. It is easy to see that the symmetry related to the rotation R is removed at the NLO, by including operators of dimension four in w_f. As we will discuss in the next section, the inclusion of the most general set of operators of dimension four in the flavon fields, leads to the result $R = 1$, thus justifying the choice of the previous section. The symmetry under the rescaling y is removed by adding invariant operators of dimension five.

3.5 Higher-order Corrections

3.5.1 Vacuum Alignment

The vacuum alignment discussed in the previous section is modified by the contribution to the superpotential from higher dimensional operators. If we denote by VEV the typical vacuum expectation value of the flavon fields, we expect corrections to the LO minima of order VEV/Λ. These corrections can be kept small by asking $VEV/\Lambda \ll 1$. Nevertheless they play an important role in removing some of the degeneracy that affect the LO result. In the following discussion we include all NLO operators, that is operators of dimension four depending on the flavon fields. A complete set of invariants under the flavor group is given by

$$\begin{array}{ll}
Q_1 = (\varphi\varphi)(\varphi\varphi) & Q_{11} = ((\varphi\varphi)_5(\varphi'\varphi'')_5) \\
Q_2 = (\varphi\varphi')(\varphi\varphi'') & Q_{12} = ((\varphi'\varphi')_5(\varphi''\varphi'')_5) \\
Q_3 = (\varphi'\varphi'')(\varphi'\varphi'') & Q_{13} = (((\varphi_S\varphi_S)_{5_1}\varphi_S)_3\varphi) \\
Q_4 = (\varphi'\varphi')(\varphi''\varphi'') & Q_{14} = (((\varphi_S\varphi_S)_{5_2}\varphi_S)_3\varphi) \\
Q_5 = (\varphi\varphi)(\varphi'\varphi'') & Q_{15} = (((\varphi_S\varphi_S)_4\varphi_S)_3\varphi) \\
Q_6 = ((\varphi\varphi')_3(\varphi\varphi'')_3) & Q_{16} = \xi'(\varphi_S(\varphi\varphi)_5) \\
Q_7 = ((\varphi'\varphi'')_3(\varphi'\varphi'')_3) & Q_{17} = \xi'(\varphi_S(\varphi'\varphi'')_5) \\
Q_8 = ((\varphi\varphi')_5(\varphi\varphi'')_5) & Q_{18} = \xi\xi'(\varphi\varphi) \\
Q_9 = ((\varphi'\varphi'')_5(\varphi'\varphi'')_5) & Q_{19} = \xi\xi'(\varphi'\varphi'') \\
Q_{10} = ((\varphi\varphi)_5(\varphi\varphi)_5) & Q_{20} = \xi'^2(\varphi_S\varphi_S) \quad .
\end{array} \tag{3.47}$$

the NLO contribution to the flavon superpotential is

$$\delta w_1 + \delta w_2 + \delta w_3 \tag{3.48}$$

where

$$\delta w_1 = \sum_{i=1}^{12} x_i \frac{Q_i}{\Lambda} \quad , \qquad \delta w_2 = \sum_{i=13}^{19} x_i \frac{Q_i}{\Lambda} \quad , \qquad \delta w_3 = x_{20}\frac{Q_{20}}{\Lambda} \tag{3.49}$$

It is useful to deal with the contribution $w_f + \delta w_1$ first. This includes all quartic operators that depend on the fields φ, φ' and φ'' only. In this case the minima of φ, φ' and φ'' can be analyzed in a analytic form. This part of the superpotential breaks the invariance of eq. (3.43), but is still invariant under the linear transformation

$$\varphi \to \Omega R_{23}\, \Omega^{-1} \varphi \quad , \qquad \varphi' \to y\, \Omega R_{23}\, \Omega^{-1} \varphi' \quad , \qquad \varphi'' \to \frac{1}{y}\, \Omega R_{23}\, \Omega^{-1} \varphi'' \quad , \tag{3.50}$$

with Ω given in eq. (3.44) and

$$R_{23} = \begin{pmatrix} 1 & 0 & 0 \\ 0 & \cos\alpha & \sin\alpha \\ 0 & -\sin\alpha & \cos\alpha \end{pmatrix} \tag{3.51}$$

with α complex. We start by looking for a minimum for φ, φ' and φ'' with the same orientation of the one in eq. (3.45)

$$\begin{aligned} \varphi_0 &= (u, 0, 0)\, \Lambda \\ \varphi_0' &= (0, u', 0)\, \Lambda \\ \varphi_0'' &= (0, 0, u'')\, \Lambda \quad , \end{aligned} \tag{3.52}$$

Along this direction the minimum conditions reduce to

$$\begin{aligned} & g u' u'' + 2\frac{M_1}{\Lambda} u + 4(x_2 + x_{11}) u^3 + \frac{1}{2}(4x_6 - 4x_7 + 3x_9 + 2x_{12}) u u' u'' = 0 \\ & g u + \frac{M_2}{\Lambda} + \frac{1}{4}(4x_6 - 4x_7 + 3x_9 + 2x_{12}) u^2 + \frac{1}{2}(4x_4 + 4x_8 + x_{10} + 6x_{13}) u' u'' = 0 \quad . \end{aligned}$$

We find that the values of the u, u' and u'' components are the ones given in eq. (3.45) plus small perturbations of order VEV/Λ. The solution (3.52) is not isolated. It is continuously connected to an infinite set of solutions given by

$$\varphi = \Omega R_{23}\, \Omega^{-1} \varphi_0 \quad , \qquad \varphi' = y\, \Omega R_{23}\, \Omega^{-1} \varphi_0' \quad , \qquad \varphi'' = \frac{1}{y} \Omega R_{23}\, \Omega^{-1} \varphi_0' \quad . \tag{3.53}$$

Thus the degeneracy present at the LO has been only partially removed by the NLO contribution δw_1. The remaining degeneracy is removed by the contribution δw_2. We have analyzed the full NLO superpotential $w_f + \delta w_1 + \delta w_2 + \delta w_3$ by looking for numerical solution to the minimum equations. Looking for minima for the fields φ, φ' and φ'' we have frozen the value of φ_S to its LO minimum, eq. (3.16). Under this condition it is easy to see that the operators Q_{13}, Q_{14} and Q_{15} vanish. Moreover the operator Q_{20} does not influence the minima of φ, φ' and φ'' and the effect of the operators Q_{18} and Q_{19} can be absorbed in a redefinition of the parameters M_1 and M_2 of the LO superpotential. In our numerical simulation g, x_{1-12} and $x_{16,17}$ are complex random numbers generated with a flat distribution in the square defined by the corners $[-(1+i)/\sqrt{2}, (1+i)/\sqrt{2}]$. To get an expansion parameter VEV/Λ of order 0.01, we have taken values of $M_{1,2}/\Lambda$, $\langle\varphi_S\rangle/\Lambda$ and ξ'/Λ in the square defined by the corners $[-(1+i)/\sqrt{2}, (1+i)/\sqrt{2}] \times 10^{-2}$. We have

performed 50.000 independent minimizations of the scalar potential. We find that the mean values of the VEVs, normalized to one up to terms of order $(VEV/\Lambda)^2$, are

$$\begin{aligned} \langle\varphi\rangle &= (100, 0.35+0.17i, 0.35+0.17i)\times 10^{-2} \\ \langle\varphi'\rangle &= (-0.51-0.03i, 100, -0.53-0.05i)\times 10^{-2} \\ \langle\varphi''\rangle &= (-0.51-0.03i, -0.53-0.05i, 100)\times 10^{-2} \quad . \end{aligned} \tag{3.54}$$

Notice that the induced perturbations are not independent. We have $\langle\varphi_2\rangle = \langle\varphi_3\rangle$, $\langle\varphi_1'\rangle = \langle\varphi_1''\rangle$ and $\langle\varphi_3'\rangle = \langle\varphi_2''\rangle$. This is true not only on average, but also separately for each individual minimization. The direction of the minima in flavor space is now completely determined and coincides, up to corrections of relative order VEV/Λ with the alignment (5.2) needed to enforce the desired mixing pattern. The only remaining flat direction is that related to the overall scale of φ' and φ'' (the parameter y in eq. (3.43)), since also the NLO superpotential only depends on the combination $\varphi'\varphi''$. This last flat direction is removed at NNLO order where terms depending separately on φ' and φ'' first occur in the superpotential. Finally the contribution δw_2 also modifies the VEVs of ξ, ξ' and φ_S compared to their LO values. Also these corrections are of relative order VEV/Λ.

In summary the analysis of the scalar potential of the model in the SUSY limit shows that the minima of the flavon fields are given by

$$\begin{aligned} \langle\varphi_S\rangle &= (-\sqrt{\frac{2}{3}}(p+q), -p, q, q, p)\ \Lambda + O(\frac{VEV^2}{\Lambda}) \\ \langle\xi\rangle &= s\ \Lambda + O(\frac{VEV^2}{\Lambda}) \\ \langle\varphi\rangle &= (u, 0, 0)\ \Lambda + O(\frac{VEV^2}{\Lambda}) \\ \langle\varphi'\rangle &= (0, u', 0)\ \Lambda + O(\frac{VEV^2}{\Lambda}) \\ \langle\varphi''\rangle &= (0, 0, u'')\ \Lambda + O(\frac{VEV^2}{\Lambda}) \quad . \end{aligned} \tag{3.55}$$

This proves that the lepton mixing pattern originates from the dynamics of our model and not from an ad hoc choice of the underlying parameters.

3.5.2 Other Higher-order Operators

Beyond the operators (3.47), that correct the lepton mass spectrum through the flavon VEVs, there are other higher-dimensional operators contributing directly to lepton masses. We only consider NLO contributions. At this order the charged lepton mass matrix m_l is not affected. At LO m_l is dominated by operators of order $1/\Lambda$. At NLO we

find the following three invariant operators:

$$\begin{aligned}&\frac{1}{\Lambda^2}e^c(\varphi'\varphi''l)H_d,\\&\frac{1}{\Lambda^2}\mu^c(\varphi''\varphi l)H_d,\\&\frac{1}{\Lambda^2}\tau^c(\varphi\varphi' l)H_d.\end{aligned}\tag{3.56}$$

From the multiplication rules reported in the Appendix and the alignment shown in the previous sections it is easy to show that the NLO VEVs of the new triplets are

$$\begin{aligned}(\varphi'\varphi'')_3 &= (u'\ u'', 0, 0)\Lambda^2,\\(\varphi\varphi')_3 &= (0, u\ u', 0)\Lambda^2,\\(\varphi''\varphi)_3 &= (0, 0, u''\ u)\Lambda^2\end{aligned}\tag{3.57}$$

and that they exactly align in the same direction as φ, φ' and φ'', respectively. Thus these operators do not modify the LO structure of m_l. We conclude that, at NLO, the charged lepton mass matrix is only modified by the corrections to vacuum alignment analyzed in Section 3.5.1.

The neutrino sector receives corrections from the operators:

$$\begin{aligned}&(\nu^c l\varphi)H_u\\&\xi'^2(\nu^c\nu^c)\\&(\varphi\varphi_S\nu^c\nu^c).\end{aligned}\tag{3.58}$$

The first one modifies non-trivially the Dirac neutrino mass matrix m_D. The second one, after the breaking of the flavor symmetry, can be absorbed by redefining the coupling constant y_1. The third one changes the Majorana mass matrix M for the heavy neutrinos. The neutrino mass matrix m_ν receives two type of corrections at the NLO. One coming from the modified vacuum for the flavon φ_S and another one from the operators (3.58). The corrections to the entries of φ_S are unrelated to each other and consequently slightly modify the vacuum alignment shown in eq. (3.38). Neutrino masses and mixing angles are modified by terms of relative order VEV/Λ. The size of this correction is constrained by the agreement between the predicted and observed value of θ_{12}. Not to spoil the successful prediction of θ_{12}, the ratio VEV/Λ should not exceed a few percent. In Figure 3.2 we show the relation between $\sin^2\theta_{12}$ and $\sin^2\theta_{13}$ at the NLO order as a result of a numerical simulation with random parameters. The simulation takes into account all the corrections coming from eqs. (3.55) and (3.58).

We recognize a possible correlation: in general either θ_{12} or θ_{13} can deviate significantly from the LO prediction, but not both at the same time. When VEV/Λ is of order 0.01, the maximal correction to the reactor angle remains far below the sensitivity of future experiments [31] and the result from the global fit on neutrino oscillation given in [2], where a value not too far from the current limit is reported. On the other hand, θ_{12} could be shifted toward the experimental value shown in (3.1).

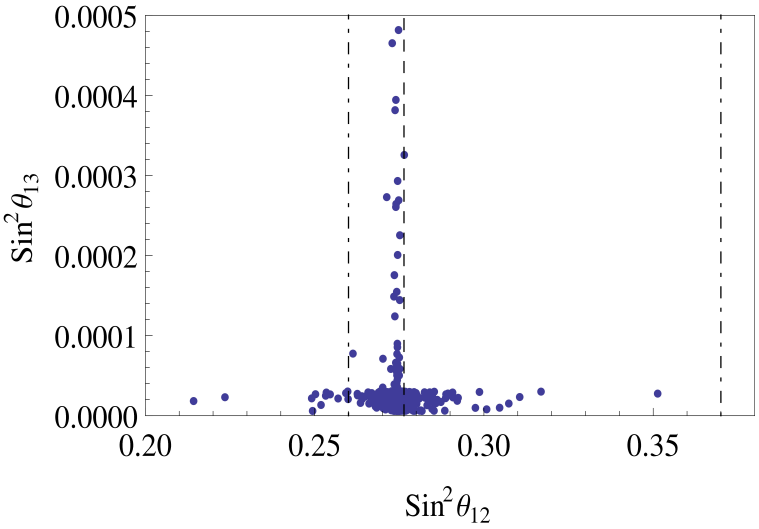

Figure 3.2: Correlation between $\sin^2\theta_{12}$ and $\sin^2\theta_{13}$ at the NLO. For the triplets φ, φ' and φ'' the mean values in (3.54) were chosen. $\langle\varphi_S\rangle/\Lambda$, $\langle\xi\rangle/\Lambda$ and $\langle\xi'\rangle/\Lambda$ have values in the square defined by the corners $[-(1+i)10^{-2}/\sqrt{2}, (1+i)10^{-2}/\sqrt{2}]$. Similarly the other parameters are complex random numbers generated with a flat distribution in the square defined by the corners $[-(1+i)/\sqrt{2}, (1+i)/\sqrt{2}]$. The LO prediction for the solar angle is also shown (dashed line), along with the extremes of the 3σ experimental range (dot-dashed lines).

3.6 Conclusion of the Chapter

We think that the GR mixing pattern, where $\sin^2\theta_{23} = 1/2$, $\theta_{13} = 0$ and $\tan\theta_{12} = 1/\phi$, should be considered on the same foot as other more popular schemes, such as the TB and the BM ones, in our attempts to construct a model of lepton masses and mixing angles. Indeed the GR scheme is compatible with the experimental data. The largest deviation is for the solar angle, where the predicted value is about two standard deviations below the present experimental central value. In this work we have built a supersymmetric model reproducing the GR pattern in the LO approximation. In the limit of exact GR mixing we have identified two transformations S and T, leaving invariant the neutrino mass matrix and the charged lepton mass matrix respectively, and generating the discrete group A_5. Following this hint, we have chosen as the family symmetry of our model $A_5 \times Z_5 \times Z_3$ where the $Z_5 \times Z_3$ factor forbids unwanted couplings between the flavon fields and the matter fields. In the supersymmetric limit we have analyzed the most general scalar potential for the flavon fields up to terms suppressed by one power of the cutoff Λ. In a finite portion of the parameter space, without any fine-tuning of the parameters, we find an isolated minimum of the scalar potential where the flavon VEVs give rise to the GR mixing pattern, up to terms of order VEV/Λ. Choosing VEV/Λ of order few percent we can have an excellent agreement between theory and data for both the solar and the atmospheric mixing angles. The mixing angle θ_{13} is expected to be of order few degrees.

The neutrino masses depend on three complex parameters so that both types of ordering can be accommodated. Neutrino masses and squared mass differences can be fitted but not predicted. At the LO we find restrictions on the allowed value of m_{ee}, once the mass ordering and the smallest neutrino mass have been fixed.

To achieve the desired vacuum alignment there is no need of driving fields, a tool often used in this type of constructions. Neglecting matter multiplets, the energy density of the theory only depends on the flavon fields, that are self-aligned at the minimum. To our best knowledge our model is the first example where the GR mixing pattern is derived from a full minimization of the energy density.

We think that our model provides a valuable alternative to other existing proposals. There are not sufficient hints in the data to prefer other mixing patterns, such as the TB one, to the GR one. Indeed in most of the existing models, including the present one, TB, BM, GR or other mixing patterns are only lowest order approximations, unavoidably corrected by powers of the symmetry breaking parameters. From this point of view, TB and GR mixing patterns can be both considered excellent first order approximations to the existing data. It is remarkable that the TB, BM and GR mixing patterns can be obtained from minimal constructions based on the symmetry groups A_4, S_4 and A_5, which are the proper symmetry groups of the Platonic solids. To make a comparative experimental test of these constructions other observable quantities should be considered, such as for instance the rates of lepton flavor violating processes, which, depending on the assumed supersymmetry breaking scale, could be within the reach of the presently running or planned experiments.

Chapter 4

Running Effects on Flavour Models

In many flavor models mass matrices and mixing are generated at a very high energy scale. In order to compare the high-energy predictions with the experimental results, it is necessary to evolve the observables to low energies through the renormalization group (RG) running.

In general the deviations from high energy values due to the running consist in minor corrections which cannot be measured in the future neutrino experiments, but in some special case these deviations undergo a large enhancement and may cause a conflict between the original setup and data.

In the present chapter we will discuss the effects of the renormalization group running on the lepton sector when masses and mixing are the result of an underlying flavor symmetry, both in the Standard Model and in the MSSM.

When the lightness of the neutrino masses is explained through the five-dimensional Weinberg operator, it is a general result [61] that the running corrections become relevant only when the neutrino spectrum is almost degenerate or inversely hierarchical (and only for particular values of the Majorana phases) or when in the supersymmetric context $\tan\beta$ is large. Similar results have been found when particular flavor structures for the neutrino masses are invoked, such as the Tribimaximal [62] and the Bimaximal [63] patterns.

When we consider models in which the type I See-Saw mechanism in implemented, few studies have been proposed in literature [64] and only regarding general, in particular non-flavor, models. For this reason we focus [5] our attention only on flavor models in which the type I See-Saw is responsible for the light neutrino masses.

We first describe, in a very general context, two kinds of interesting constraints on the Dirac neutrino Yukawa Y_ν from flavor symmetries and then analyze their impact on running effects. We start considering flavor models in which Y_ν is proportional to a unitary matrix as it is the case, for example, when the right-handed singlet neutrinos or the charged leptons are in an irreducible representation of the flavor group G_f. Then we extend this constraint to a more general class of flavor models in which the mixing textures are independent from the mass eigenstates: examples are the Tribimaximal, Bimaximal and Golden Ratio textures presented in the previous chapter.

As a general result, we find that in this class of models, the effect of the running

through the See-Saw thresholds can always be absorbed by a small shift on neutrino mass eigenvalues and the mixing angles remain unchanged. This conclusion is, in particular, independent both from the specific mixing pattern implied by the flavor symmetry and from the basis in which we are working.

In a second moment, as an explicit example, we describe in detail the running effects on the Tribimaximal mixing texture in the Altarelli-Feruglio model described in Section 2.3.

4.1 Running Effects on Neutrino Mass Operator m_ν

In this section we begin to analyze, in a general context, the renormalization group equations (RGEs) for neutrino masses below and above the See-Saw threshold, both in the Standard Model and in the MSSM extended with three right-handed neutrinos. We consider the Lagrangian in the lepton sector of the type I See-Saw already defined in eqs. (1.4, 1.11):

$$\mathscr{L} = e^c Y_e H^\dagger \ell + \nu^c Y_\nu \widetilde{H}^\dagger \ell + \nu^c M_R \nu^c + h.c. \tag{4.1}$$

where the supersymmetric case is easily derived considering two Higgs doublets, all the fields as supermultiplets and identifying the homomorphic part of $\mathscr{L}$ with a superpotential. In what follows we concentrate only on the Standard Model particles and for this reason in our notation a chiral superfield and its R-parity even component are denoted by the same letter.

Given the heavy Majorana and the Dirac neutrino mass matrices, M_R and $m_D = Y_\nu v/\sqrt{2}$ respectively, the light m_ν is obtained from block-diagonalizing the complete 6×6 neutrino mass matrix,

$$m_\nu = -\frac{v^2}{2} Y_\nu^T M_R^{-1} Y_\nu \ , \tag{4.2}$$

The matrix m_ν is modified by quantum corrections according to the RGEs widely studied in the literature [64]. For completeness, in Appendix B, we report the full RGEs for all the interested quantities in the running. In order to analytically study the change of $m_\nu(\mu)$ from high to low-energy, it is useful to work in the basis in which the Majorana neutrino mass is diagonal and real, $\hat{M}_R = \mathrm{diag}(M_S, M_M, M_L)$. The mass eigenvalues can be ordered as $M_S < M_M < M_L$. Furthermore, we can divide the running effects in three distinct energy ranges: from the cutoff Λ of the theory down to M_L, the mass of the heaviest right-handed neutrino; from M_L down to M_S, the mass of the lightest right-handed neutrino; below M_S down to ϱ, which can be either m_Z, considered as the electroweak scale, or m_{SUSY}, the average energy scale for the supersymmetric particles.

$\Lambda_f \longrightarrow M_L$. Above the highest See-Saw scale the three right-handed neutrinos are all active and the dependence of the effective light neutrino mass matrix from the renormalization scale μ is given by mean of the $\mu-$dependence of Y_ν and M_R:

$$m_\nu(\mu) \ = \ -\frac{v^2}{2}\, Y_\nu^T(\mu)\, M_R^{-1}(\mu)\, Y_\nu(\mu) \ . \tag{4.3}$$

Then from the RGEs in eqs. (B. 1, B. 2), it is not difficult to see that the evolution of the effective mass matrix m_ν is given by:

$$16\pi^2 \frac{\mathrm{d}m_\nu}{\mathrm{d}t} = \left(C_e Y_e^\dagger Y_e + C_\nu Y_\nu^\dagger Y_\nu\right)^T m_\nu + m_\nu \left(C_e Y_e^\dagger Y_e + C_\nu Y_\nu^\dagger Y_\nu\right) + \bar{\alpha}\, m_\nu \tag{4.4}$$

with

$$\begin{aligned} C_e &= -\frac{3}{2}\,, \qquad C_\nu = \frac{1}{2} && \text{in the SM} \\ C_e &= C_\nu = 1 && \text{in the MSSM} \end{aligned} \tag{4.5}$$

and

$$\begin{aligned} \bar{\alpha}_{SM} &= 2\,\mathrm{Tr}\left[3Y_u^\dagger Y_u + 3Y_d^\dagger Y_d + Y_\nu^\dagger Y_\nu + Y_e^\dagger Y_e\right] - \frac{9}{10}g_1^2 - \frac{9}{2}g_2^2 \\ \bar{\alpha}_{MSSM} &= 2\,\mathrm{Tr}\left[3Y_u^\dagger Y_u + Y_\nu^\dagger Y_\nu\right] - \frac{6}{5}g_1^2 - 6g_2^2\,. \end{aligned} \tag{4.6}$$

$\mathbf{M_L \longrightarrow M_S}$. The effective neutrino mass matrix m_ν below the highest See-Saw scale can be obtained by sequentially integrating out ν_n^c with $n = L, M, S$:

$$m_\nu = -\frac{v^2}{4}\left(\overset{(n)}{\kappa} + 2\overset{(n)}{Y_\nu}{}^T \overset{(n)}{M_R}{}^{-1} \overset{(n)}{Y_\nu}\right) \tag{4.7}$$

where $\overset{(n)}{\kappa}$ is the coefficient of the effective neutrino mass operator $(\widetilde{H}^\dagger \ell)^T (\widetilde{H}^\dagger \ell)$. From the (tree-level) matching condition, it is given by

$$\overset{(n)}{\kappa}_{ij} = 2(Y_\nu^T)_{in}\, M_n^{-1}\, (Y_\nu)_{nj}\,, \tag{4.8}$$

which is imposed at $\mu = M_n$. At M_L, the 2×3 Yukawa matrix $\overset{(L)}{Y_\nu}$ is obtained by simply removing the L-th row of Y_ν and the 2×2 mass matrix $\overset{(L)}{M_R}$ is found from M_R by removing the L-th row and L-th column. Further decreasing the energy scale down to M_M, $\overset{(M)}{Y_\nu}$ is a single-row matrix, obtained by removing the M-th row from $\overset{(L)}{Y_\nu}$, and $\overset{(M)}{M_R}$ consists of a single parameter, found by removing the M-th row and M-th column from $\overset{(L)}{M_R}$. Finally at M_S, $\overset{(S)}{Y_\nu}$ and $\overset{(S)}{M_R}$ are vanishing.

In the Standard Model, the two parts which define m_ν in eq. (4.7) evolve in different ways. We can summarize the corresponding RGEs as follows:

$$16\pi^2 \frac{\mathrm{d}\overset{(n)}{X}}{\mathrm{d}t} = \left(\frac{1}{2}\overset{(n)}{Y_\nu}{}^\dagger \overset{(n)}{Y_\nu} - \frac{3}{2}Y_e^\dagger Y_e\right)^T \overset{(n)}{X} + \overset{(n)}{X}\left(\frac{1}{2}\overset{(n)}{Y_\nu}{}^\dagger \overset{(n)}{Y_\nu} - \frac{3}{2}Y_e^\dagger Y_e\right) + \overset{(n)}{\bar{\alpha}}_X \overset{(n)}{X} \tag{4.9}$$

where

$$\begin{aligned} \overset{(n)}{\bar{\alpha}}_\kappa &= 2\,\mathrm{Tr}\left[3Y_u^\dagger Y_u + 3Y_d^\dagger Y_d + \overset{(n)}{Y_\nu}{}^\dagger \overset{(n)}{Y_\nu} + Y_e^\dagger Y_e\right] - 3g_2^2 + \lambda_H \\ \overset{(n)}{\bar{\alpha}}_{Y_\nu^T M_R^{-1} Y_\nu} &= 2\,\mathrm{Tr}\left[3Y_u^\dagger Y_u + 3Y_d^\dagger Y_d + \overset{(n)}{Y_\nu}{}^\dagger \overset{(n)}{Y_\nu} + Y_e^\dagger Y_e\right] - \frac{9}{10}g_1^2 - \frac{9}{2}g_2^2\,, \end{aligned} \tag{4.10}$$

with λ_H the Higgs self-coupling.[§]

In MSSM the running of $\overset{(n)}{\kappa}$ and of $\overset{(n)}{Y_\nu}^T \overset{(n)}{M_R}^{-1} \overset{(n)}{Y_\nu}$ is the same and therefore we can write

$$16\pi^2 \frac{\mathrm{d}m_\nu}{\mathrm{d}t} = \left(Y_e^\dagger Y_e + \overset{(n)}{Y_\nu}^\dagger \overset{(n)}{Y_\nu}\right)^T m_\nu + m_\nu \left(Y_e^\dagger Y_e + \overset{(n)}{Y_\nu}^\dagger \overset{(n)}{Y_\nu}\right) + \overset{(n)}{\bar{\alpha}} m_\nu \,, \tag{4.11}$$

where

$$\overset{(n)}{\bar{\alpha}} = 2\,\mathrm{Tr}\left[3Y_u^\dagger Y_u + \overset{(n)}{Y_\nu}^\dagger \overset{(n)}{Y_\nu}\right] - \frac{6}{5}g_1^2 - 6g_2^2 \,. \tag{4.12}$$

$M_S \longrightarrow \lambda$. For energy range below the mass scale of the lightest right-handed neutrino, all the ν_n^c are integrated out and $\overset{(S)}{Y_\nu}$ and $\overset{(S)}{M_R}$ vanish. In the right-hand side of eq. (4.7) only the term $\overset{(S)}{\kappa}$ is not vanishing and in this case the effective mass matrix m_ν evolves as:

$$16\pi^2 \frac{\mathrm{d}m_\nu}{\mathrm{d}t} = \left(C_e Y_e^\dagger Y_e\right)^T m_\nu + m_\nu \left(C_e Y_e^\dagger Y_e\right) + \overset{(S)}{\bar{\alpha}}\, m_\nu \tag{4.13}$$

with

$$\begin{aligned} \overset{(S)}{\bar{\alpha}}_{SM} &= 2\,\mathrm{Tr}\left[3Y_u^\dagger Y_u + 3Y_d^\dagger Y_d + Y_e^\dagger Y_e\right] - 3g_2^2 + \lambda_H \\ \overset{(S)}{\bar{\alpha}}_{MSSM} &= 6\,\mathrm{Tr}\left[Y_u^\dagger Y_u\right] - \frac{6}{5}g_1^2 - 6g_2^2 \,. \end{aligned} \tag{4.14}$$

4.1.1 Analytical Approximation to the Running Evolution of m_ν

Now we analytically solve the RGEs for m_ν in the leading Log approximation. All the Yukawa couplings $Y_i^\dagger Y_i$ for $i = \nu, e, u, d$ are evaluated at their initial value at the cutoff Λ. Furthermore we will keep only the leading contributions from each $Y_i^\dagger Y_i$ term, for $i = e, u, d$, i.e. $|y_\tau|^2$, $|y_t|^2$ and $|y_b|^2$ respectively. The corrections to the leading order $Y_i^\dagger Y_i$ come from their running evolution as well as from their sub leading terms and they contribute to the final result as sub leading effects and we can safely neglect them in our analytical estimate.

In the MSSM context, the general solution to eqs. (4.4, 4.11, 4.13) have all the same structure, which is approximately given by

$$m_{\nu\,(\text{lower Energy})} \approx I_U J_e^T J_\nu^T m_{\nu\,(\text{higher Energy})} J_\nu J_e \tag{4.15}$$

where I_U, J_e and J_ν are all exponentials of integrals containing loop suppressing factors and as a result they are close to 1. Note that I_U is a universal contribution defined as

$$I_U = \exp\left[-\frac{1}{16\pi^2}\int \overset{(n)}{\bar{\alpha}}\,\mathrm{d}t\right] \tag{4.16}$$

where the integral runs between two subsequent energy scales and we have extended the definition of $\overset{(n)}{\bar{\alpha}}$ by identifying $\overset{(\Lambda)}{\bar{\alpha}} \equiv \bar{\alpha}$ in order to include the range from Λ down to M_L. J_e is

[§]We use the convention that the Higgs self-interaction term in the Lagrangian is $-\lambda_H (H^\dagger H)^2/4$.

the contribution from charged lepton Yukawa couplings which is always flavor-dependent, while J_ν is the contribution from the neutrino Yukawa coupling: they are given by

$$J_e = \exp\left[-\frac{1}{16\pi^2}\int Y_e^\dagger Y_e \,\mathrm{d}t\right] , \qquad J_\nu = \exp\left[-\frac{1}{16\pi^2}\int \overset{(n)}{Y}{}_\nu^\dagger \overset{(n)}{Y}_\nu \,\mathrm{d}t\right] , \tag{4.17}$$

where also here we have extended the definition of $\overset{(n)}{Y}_\nu$ by identifying $\overset{(\Lambda)}{Y}_\nu$ with Y_ν in order to include the range between Λ and M_L. [§] Differently from J_e, J_ν can be flavor-dependent or not.

In the Standard Model context, the running effects do not factorize, due to the different evolution of $\overset{(n)}{\kappa}$ and $\overset{(n)}{Y}{}_\nu^T \overset{(n)}{M}{}_R^{-1} \overset{(n)}{Y}_\nu$ between the See-Saw mass thresholds. However eq. (4.15) applies also to the Standard Model context when m_ν is a result of a flavor symmetry: in this case, by a suitable redefinition of the parameters which define the mass eigenvalues, the sum $\overset{(n)}{\kappa} + \overset{(n)}{Y}{}_\nu^T \overset{(n)}{M}{}_R^{-1} \overset{(n)}{Y}_\nu$ after the running evolution has exactly the same flavor structure of $m_{\nu\,(\text{higher Energy})}$. For the purposes of the present discussion we simply assume that eq. (4.15) is valid also in the Standard Model context and an explicit example will be proposed in Section 4.2.3.

Expanding J_e and J_ν in Taylor series and summing up eq. (4.15) on several energy ranges one can approximately calculate the neutrino mass at low-energy as

$$m_{\nu(\varrho)} \simeq I_U \left(m_{\nu(\Lambda)} + \Delta m_\nu^{(J_e)} + \Delta m_\nu^{(J_\nu)}\right) , \tag{4.18}$$

where the low-energy scale ϱ is m_Z in the case of Standard Model and m_{SUSY} for MSSM. The explicit form of the universal part I_U is given by:

$$\begin{aligned} I_U^{\text{SM}} = 1 \times \exp\Bigg[-\frac{1}{16\pi^2}\Bigg[&\left(-\frac{9}{10}g_1^2 - \frac{9}{2}g_2^2 + 6|y_t|^2\right)\ln\frac{\Lambda_f}{m_Z} + \left(\frac{9}{10}g_1^2 + \frac{3}{2}g_2^2 + \lambda_H\right)\ln\frac{M_S}{m_Z} + \\ &+ y^2\left(2\ln\frac{M_M}{M_S} + 4\ln\frac{M_L}{M_M} + 7\ln\frac{\Lambda_f}{M_L}\right)\Bigg]\Bigg] , \end{aligned} \tag{4.19}$$

$$\begin{aligned} I_U^{\text{MSSM}} = 1 \times \exp\Bigg[-\frac{1}{16\pi^2}\Bigg[&\left(-\frac{6}{5}g_1^2 - 6g_2^2 + 6|y_t|^2\right)\ln\frac{\Lambda_f}{m_{SUSY}} + \\ &+ y^2\left(2\ln\frac{M_M}{M_S} + 4\ln\frac{M_L}{M_M} + 8\ln\frac{\Lambda_f}{M_L}\right)\Bigg]\Bigg] . \end{aligned} \tag{4.20}$$

$\Delta m_\nu^{(J_e)}$ is the the contribution from J_e and can easily be calculated as:

$$\Delta m_\nu^{(J_e)} = m_{\nu(\Lambda)}\ \mathrm{diag}(0,0,\Delta_\tau) + \mathrm{diag}(0,0,\Delta_\tau) m_{\nu(\Lambda)} \tag{4.21}$$

[§] In eq. (4.17), the combination $Y_e^\dagger Y_e$ should enter with $\overset{(n)}{Y}_e$ instead of Y_e, as one can see from the RGEs in Appendix B. In our approximation, however, they coincide.

where the small parameter Δ_τ is given by

$$\begin{aligned} \Delta_\tau &\equiv -\frac{3m_\tau^2}{16\pi^2 v^2}\ln\frac{\Lambda}{m_Z} && \text{in the SM} \\ \Delta_\tau &\equiv \frac{m_\tau^2}{8\pi^2 v^2}(1+\tan^2\beta)\ln\frac{\Lambda}{m_{SUSY}} && \text{in the MSSM} \end{aligned} \tag{4.22}$$

with $\tan\beta$ the usual ratio between the VEVs of the neutral spin zero components of H_u and H_d, the two doublets responsible for electroweak symmetry breaking in the MSSM. On the other hand, the contribution from J_ν, $\Delta m_\nu^{(J_\nu)}$, non trivially depends on the neutrino Yukawa coupling Y_ν which cannot be determined by low-energy observables without additional ingredients. In Section 4.2, we will analyze strong impacts of the flavor symmetries on J_ν, but before proceeding, we comment on the hierarchy among the various running contributions to the neutrino mass. Indeed, assuming that the flavor symmetries have no effects on Y_ν, we expect that

$$Y_\nu^\dagger Y_\nu \sim \overset{(n)}{Y}{}_\nu^\dagger \overset{(n)}{Y}_\nu = \mathcal{O}(1) \tag{4.23}$$

and therefore we conclude that the contribution from J_ν always dominates. In [5] we explicitly show that this conclusion holds both in the Standard Model and in the MSSM even for large $\tan\beta$ (we consider $\tan\beta = 60$ as the maximal value). One should expect that a similar observation holds also for the lepton mixing angles, but quite frequently flavor symmetries imply a J_ν which is flavor-independent or has no effects on mixing angles, as we will see in a moment.

4.2 Flavor Symmetries and Running Effects

In the present section, we will apply the general results of the running evolution of the neutrino mass operator m_ν to models beyond the Standard Model, where a flavor symmetry is added to the gauge group of the Standard Model. The main task is to track some interesting connections between the running effects and the realization of the flavor symmetry.

In a given basis, $Y_e^\dagger Y_e$ and m_ν can be diagonalized by unitary matrices, U_e and U_ν, respectively. The lepton mixing matrix is given by $U = U_e^\dagger U_\nu$. In a flavor model, the charged lepton Yukawa, the neutrino mass matrix and therefore the PMNS matrix are dictated by the flavor symmetry G_f. We have already discussed in Section 2.2 that G_f must be spontaneously broken in order to naturally describe fermion masses and mixing: here, we simply assume that G_f is spontaneously broken by a set of flavon fields Φ at a very high scale. Suppose that, at the leading order, the neutrino mixing matrix is given by U_0 which differs from U by sub leading contributions $\sim \langle\Phi\rangle/\Lambda_f$ where Λ_f is the cutoff scale of the flavor symmetry G_f. We will begin with some general assumptions on U_0 without however specifying its form. Then we will move to specialize in a concrete case in which U_0 is given by the Tribimaximal mixing pattern. Similar studies can be done

considering other mass-independent textures, such as the Bimaximal, the golden-ratio and (sometimes) the Trimaximal schemes.

4.2.1 Running Effects on Neutrino Mixing Patterns

As described in Section 4.1 the relevant running effects on m_ν are encoded in the combinations $Y_e^\dagger Y_e$ and $Y_\nu^\dagger Y_\nu$. Furthermore, we observe that a relevant contribution to the running of $Y_e^\dagger Y_e$ is encoded by $Y_\nu^\dagger Y_\nu$.

We perform the analysis in the basis in which the charged leptons are diagonal, then at high energy we have

$$Y_e^\dagger Y_e = \mathrm{diag}(m_e^2, m_\mu^2, m_\tau^2)\frac{2}{v^2}\ . \tag{4.24}$$

From now on, we will use v in the notation of the Standard Model and in order to convert similar expressions to the MSSM, it is sufficient to substitute v with $v_{u,d}$, when dealing with neutrinos or charged leptons, respectively. This simple form changes when evolving down to low energies. This running effect of $Y_e^\dagger Y_e$ on m_ν is of second order and we can safely forget it. However it can generate a non trivial U_e and consequently introduces additional corrections to the PMNS matrix U. We will return to this effect in Section 4.2.2.

Since flavor symmetries impose constraints on Y_ν, they should have some impacts also on running effects. In this section we are interested in two classes of constraints. The first class is characterized by Y_ν proportional to a unitary matrix: $Y_\nu^\dagger Y_\nu \sim 1$ or $Y_\nu Y_\nu^\dagger \sim 1$ is frequent in the presence of a flavor symmetry, since it is, for example, a consequence of the first Schur's lemma when ℓ or ν^c transforms in a irreducible representation of the group G_f [65]. In the second class, we assume that m_ν can be exactly diagonalized by U_0 according to

$$\hat{m}_\nu = U_0^T m_\nu U_0 \tag{4.25}$$

where $\hat{m}_\nu = \mathrm{diag}(m_1, m_2, m_3)$ with m_i positive and U_0 is a mass-independent mixing pattern enforced by the flavor symmetry G_f. Independently from the way in which G_f is broken, it is straightforward to see that the neutrino Yukawa coupling in the basis of diagonal right-handed Majorana neutrinos, which we indicate as $\hat{Y}_\nu$, has the following simple form

$$\hat{Y}_\nu = iD\,U_0^\dagger \tag{4.26}$$

where $D = \mathrm{diag}(\pm\sqrt{2m_1M_1}, \pm\sqrt{2m_2M_2}, \pm\sqrt{2m_3M_3})/v$. Notice that $\hat{Y}_\nu$ becomes unitary if $D \sim 1$. However, the present case is not strictly a generalization of the previous one since a unitary Y_ν does not necessarily imply a mass-independent mixing pattern.

In [5] we show that m_ν does not change its flavor structure under J_ν if Y_ν belongs to one of these classes: the running effects from J_ν correct only the neutrino mass eigenvalues but not the mixing angles. Therefore, the only flavor-dependent running contribution to m_ν is encoded in J_e.

A Special Case $U_0 = iU_{\rm TB}P^*$ and $D \propto \mathbf{diag}(1,1,-1)$

In this part we consider a special case of $\hat{Y}_\nu = iD\,U_0^\dagger$ in which the expression of U_0 is enforced by the flavor symmetry group A_4 in the context of the Altarelli-Feruglio model described in Section 2.3. A more detailed analysis of the running effects will be discussed in the next section. Here we only comment on the constraints on the mixing matrix $U_0 = iU_{\rm TB}P^*$ and the neutrino Yukawa coupling in the hatted basis:

$$\hat{Y}_\nu \equiv yPU_{TB}^T O_{23} = yP \begin{pmatrix} \sqrt{2/3} & -1/\sqrt{6} & -1/\sqrt{6} \\ 1/\sqrt{3} & +1/\sqrt{3} & +1/\sqrt{3} \\ 0 & +1/\sqrt{2} & -1/\sqrt{2} \end{pmatrix} \tag{4.27}$$

where y is a positive parameter of order $\mathcal{O}(1)$, P is the usual diagonal matrix of the Majorana phases and O_{23} is defined as

$$O_{23} = \begin{pmatrix} 1 & 0 & 0 \\ 0 & 0 & 1 \\ 0 & 1 & 0 \end{pmatrix} . \tag{4.28}$$

In order to confront eq. (4.27) with the general expression $\hat{Y}_\nu = iD\,U_0^\dagger$ we observe that

$$\hat{Y}_\nu = yPU_{TB}^T O_{23} U_{TB} U_{TB}^T = \mathrm{diag}(y,y,-y)PU_{TB}^T . \tag{4.29}$$

Then we conclude that (4.27) corresponds to the special case in which $D = \mathrm{diag}(y,y,-y)$. Furthermore, in the Altarelli-Feruglio model considered in this section, there is a very simple relation between m_i and M_i given by $m_i = v_u^2 y^2/2M_i$.

Now we explicitly calculate the renormalization group running from Λ_f down to ϱ for this special case using the approximate analytical expressions given in Section 4.1.1. In the physical basis, it is useful to define the light neutrino mass matrix eq. (4.2) at the initial energy scale Λ_f: by imposing the condition $m_{\nu(\Lambda)} = U_0^* \hat{m}_\nu U_0^\dagger$, we have

$$\begin{aligned} m_\nu^{TB} &= -U_{TB}\,P\,\hat{m}_\nu\,P\,U_{TB}^T \\ &= -\left[\frac{\tilde{m}_3}{2}\begin{pmatrix} 0 & 0 & 0 \\ 0 & 1 & -1 \\ 0 & -1 & 1 \end{pmatrix} + \frac{\tilde{m}_2}{3}\begin{pmatrix} 1 & 1 & 1 \\ 1 & 1 & 1 \\ 1 & 1 & 1 \end{pmatrix} + \frac{\tilde{m}_1}{6}\begin{pmatrix} 4 & -2 & -2 \\ -2 & 1 & 1 \\ -2 & 1 & 1 \end{pmatrix}\right] , \end{aligned} \tag{4.30}$$

where $\tilde{m}_i = m_i e^{i\alpha_i}$. It is necessary to specify the kind of neutrino mass spectrum: in the normal hierarchy the light neutrinos are ordered as $m_1 < m_2 < m_3$ and the heavy ones as $M_3 < M_2 < M_1$; while in the inverse hierarchy they are arranged as $m_3 < m_1 \lesssim m_2$ and $M_2 \lesssim M_1 < M_3$.

The general result of the running effects on m_ν is given by eq. (4.18) which in our case becomes

$$m_{\nu(\varrho)} = I_U \left(m_\nu^{TB} + \Delta m_\nu^{(J_e)} + \Delta m_\nu^{(J_\nu)}\right) . \tag{4.31}$$

The analytical result for both I_U and $\Delta m_\nu^{(J_e)}$ (see Section 4.1) does not depend on the type of the neutrino spectrum, it is sufficient to identify M_S, M_M, M_L with the correct hierarchy between M_1, M_2, M_3 . In particular, for the Tribimaximal mixing pattern, the contribution from J_e is given by

$$\begin{aligned}\Delta m_\nu^{(J_e)} &= m_\nu^{TB}\ \mathrm{diag}(0,\,0,\,\Delta_\tau) + \mathrm{diag}(0,\,0,\,\Delta_\tau) m_\nu^{TB} \\ &= -\begin{pmatrix} 0 & 0 & \frac{\tilde{m}_1}{3} - \frac{\tilde{m}_2}{3} \\ 0 & 0 & -\frac{\tilde{m}_1}{6} - \frac{\tilde{m}_2}{3} + \frac{\tilde{m}_3}{2} \\ \frac{\tilde{m}_1}{3} - \frac{\tilde{m}_2}{3} & -\frac{\tilde{m}_1}{6} - \frac{\tilde{m}_2}{3} + \frac{\tilde{m}_3}{2} & -\frac{\tilde{m}_1}{3} - \frac{2\tilde{m}_2}{3} - \tilde{m}_3 \end{pmatrix} \Delta_\tau \ .\end{aligned} \tag{4.32}$$

Naturally, the contribution from J_ν depends on the type of the neutrino spectrum, however it can be written in the same form for both the spectra:

$$\Delta m_\nu^{(J_\nu)} = -\left[\frac{\tilde{m}'_1}{6} \begin{pmatrix} 4 & -2 & -2 \\ -2 & 1 & 1 \\ -2 & 1 & 1 \end{pmatrix} + \frac{2\tilde{m}'_2}{3} \begin{pmatrix} 1 & 1 & 1 \\ 1 & 1 & 1 \\ 1 & 1 & 1 \end{pmatrix} + \tilde{m}'_3 \begin{pmatrix} 0 & 0 & 0 \\ 0 & 1 & -1 \\ 0 & -1 & 1 \end{pmatrix} \right] \tag{4.33}$$

where $\tilde{m}'_i$ are redefinitions of the light neutrino masses:

Normal Hierarchy:

$$\begin{aligned} &\tilde{m}'_1 = \tilde{m}_1(p+q)\ , \quad \tilde{m}'_2 = \tilde{m}_2(x+q)\ , \quad \tilde{m}'_3 = \tilde{m}_3(x+z) \quad \text{in the SM} \\ &\tilde{m}'_1 = 0\ , \qquad\quad \tilde{m}'_2 = 2\tilde{m}_2 x\ , \qquad\quad \tilde{m}'_3 = 2\tilde{m}_3(x+z) \quad \text{in the MSSM} \end{aligned} \tag{4.34}$$

with

$$\begin{aligned} p &= -\frac{1}{16\pi^2}(-3g_2^2 + \lambda + \frac{9}{10}g_1^2 + \frac{9}{2}g_2^2) \ln\frac{M_1}{M_2} \\ q &= -\frac{1}{16\pi^2}(-3g_2^2 + \lambda + \frac{9}{10}g_1^2 + \frac{9}{2}g_2^2) \ln\frac{M_2}{M_3} \\ x &= -\frac{y^2}{32\pi^2} \ln\frac{M_1}{M_2} \\ z &= -\frac{y^2}{32\pi^2} \ln\frac{M_2}{M_3}\ ; \end{aligned} \tag{4.35}$$

Inverse Hierarchy:

$$\begin{aligned} &\tilde{m}'_1 = \tilde{m}_1(x+q)\ , \quad \tilde{m}'_2 = \tilde{m}_2(x+z)\ , \quad \tilde{m}'_3 = \tilde{m}_3(p+q) \quad \text{in the SM} \\ &\tilde{m}'_1 = 2\tilde{m}_1 x\ , \qquad\quad \tilde{m}'_2 = 2\tilde{m}_2(x+z)\ , \quad \tilde{m}'_3 = 0 \qquad\quad \text{in the MSSM} \end{aligned} \tag{4.36}$$

with

$$\begin{aligned} p &= -\frac{1}{16\pi^2}(-3g_2^2+\lambda+\frac{9}{10}g_1^2+\frac{9}{2}g_2^2)\ln\frac{M_3}{M_1} \\ q &= -\frac{1}{16\pi^2}(-3g_2^2+\lambda+\frac{9}{10}g_1^2+\frac{9}{2}g_2^2)\ln\frac{M_1}{M_2} \\ x &= -\frac{y^2}{32\pi^2}\ln\frac{M_3}{M_1} \\ z &= -\frac{y^2}{32\pi^2}\ln\frac{M_1}{M_2}\,. \end{aligned} \tag{4.37}$$

Comparing m_ν^{TB} of eq. (4.30) with the perturbations Δm_ν of eqs. (4.33), we note the presence of the same flavor structure for several matrices and in particular, by redefining $\tilde{m}_i$ to absorb the terms $\tilde{m}_i'$ it is possible to account for the See-Saw contributions from the renormalization group running into m_ν^{TB}. As a consequence the leading order predictions for the Tribimaximal angles receive corrections only from the terms proportional to Δ_τ. This result explicitly confirms what we outlined in the previous section.

4.2.2 Running Effects in the Charged Lepton Sector

The presence of a term proportional to $\hat{Y}_\nu^\dagger\hat{Y}_\nu$ in the RG equation for Y_e can switch on off-diagonal entries in the charged lepton Yukawa matrix Y_e. When rotated away, this additional contribution introduces a non-trivial U_e and consequently corrects the lepton mixing matrix U. For a unitary $\hat{Y}_\nu$, this correction appears only between the See-Saw mass scales while in the general case it appears already from the cutoff Λ_f.

In close analogy with the running effects on neutrino mass matrix in eq. (4.31), the full result of the running for charged lepton mass matrix can conventionally be written as

$$(Y_e^\dagger Y_e)_{(\varrho)} = I_e\left[(Y_e^\dagger Y_e)_{(\Lambda_f)} + \Delta(Y_e^\dagger Y_e)\right]\,, \tag{4.38}$$

where I_e is an irrelevant global coefficient which can be absorbed by, for example, y_τ. Now we move to the case of Tribimaximal mixing pattern. In this case, the flavor-dependent corrections can be explicitly calculated:

NH case:

$$\Delta(Y_e^\dagger Y_e) \simeq y_\tau^2\left[a_e\begin{pmatrix}0&0&1\\0&0&-1/2\\1&-1/2&5\end{pmatrix}+b_e\begin{pmatrix}0&0&0\\0&0&-1\\0&-1&2\end{pmatrix}+c_e\begin{pmatrix}0&0&0\\0&0&0\\0&0&2\end{pmatrix}\right]\,, \tag{4.39}$$

IH case:

$$\Delta(Y_e^\dagger Y_e) \simeq y_\tau^2\left[a_e'\begin{pmatrix}0&0&0\\0&0&1\\0&1&2\end{pmatrix}+b_e'\begin{pmatrix}0&0&1\\0&0&1\\1&1&2\end{pmatrix}+c_e'\begin{pmatrix}0&0&0\\0&0&0\\0&0&2\end{pmatrix}\right]\,, \tag{4.40}$$

where the coefficients are

$$\begin{aligned} a_e = b'_e &= -\frac{C'_\nu}{16\pi^2}\frac{y^2}{3}\ln\frac{M_1}{M_2}, & b_e &= -\frac{C'_\nu}{16\pi^2}\frac{y^2}{2}\ln\frac{M_2}{M_3}\,, \\ c_e = c'_e &= -\frac{3C'_e y_\tau^2}{16\pi^2}\ln\frac{\Lambda_f}{m_{SUSY}(m_Z)}\,, & a'_e &= -\frac{C'_\nu}{16\pi^2}\frac{y^2}{2}\ln\frac{M_3}{M_1}\,, \end{aligned} \tag{4.41}$$

and $C'_\nu = -3/2$ (1), $C'_e = 3/2$ (3) in the Standard Model (MSSM). Here we observe that the off-diagonal contributions to $Y_e^\dagger Y_e$ are encoded in a_e, b_e, a'_e and b'_e which depend only on the See-Saw scales M_i. As a result, as we will show in the next section, c_e and c'_e do not affect the lepton mixing angles.

4.2.3 Full Running Effects on the Tribimaximal Mixing Pattern

In this section, we combine various contributions discussed in previous sections into the observable matrix U from which we extract angles and phases at low-energy. Since we are interested in physical quantities, we eliminate one of the phases of P and in particular we express each result as a function of $\alpha_{ij} \equiv (\alpha_i - \alpha_j)/2$, removing α_3. The corrected mixing angles can be written as

$$\theta_{ij(\varrho)} = \theta_{ij}^{TB} + k_{ij} + \ldots \tag{4.42}$$

where $\theta_{13}^{TB} = 0$, $\theta_{12}^{TB} = \arcsin\sqrt{1/3}$, $\theta_{23}^{TB} = -\pi/4$, dots stand for sub leading corrections and k_{ij} are defined by

$$\begin{aligned} k_{12} &= \frac{1}{3\sqrt{2}}\left(\frac{|\tilde{m}_1+\tilde{m}_2|^2}{m_2^2-m_1^2}\Delta_\tau - 3a_e\right) \\ k_{23} &= \begin{cases} \dfrac{1}{6}\left[\left(\dfrac{|\tilde{m}_1+\tilde{m}_3|^2}{m_3^2-m_1^2} + 2\dfrac{|\tilde{m}_2+\tilde{m}_3|^2}{m_3^2-m_2^2}\right)\Delta_\tau - 3a_e - 6b_e\right] & \text{for NH} \\ \dfrac{1}{6}\left[\left(\dfrac{|\tilde{m}_1+\tilde{m}_3|^2}{m_3^2-m_1^2} + 2\dfrac{|\tilde{m}_2+\tilde{m}_3|^2}{m_3^2-m_2^2}\right)\Delta_\tau + 3a_e + 3a'_e\right] & \text{for IH} \end{cases} \end{aligned} \tag{4.43}$$

$$k_{13} = \frac{1}{3\sqrt{2}}\sqrt{4m_3^2\Delta_\tau^2\left(\frac{m_1\sin\alpha_{13}}{m_1^2-m_3^2} - \frac{m_2\sin\alpha_{23}}{m_2^2-m_3^2}\right)^2 + \left[\left(\frac{|\tilde{m}_1+\tilde{m}_3|^2}{m_1^2-m_3^2} - \frac{|\tilde{m}_2+\tilde{m}_3|^2}{\tilde{m}_2^2-\tilde{m}_3^2}\right)\Delta_\tau - 3a_e\right]^2}\,.$$

In the previous expressions we can clearly distinguish the contributions coming from the diagonalize of the corrected Tribimaximal neutrino mass matrix (4.31) and those from the diagonalize of (4.38). As it is clear from (4.41), the corrections to the Tribimaximal mixing from the charged lepton sector is important only for hierarchical right-handed neutrinos and will approach to zero as soon as the spectrum becomes degenerate. On the other hand, the corrections from the neutrino sector should be enhanced if the light neutrinos are quasi-degenerate and if the $\tan\beta$ is large, in the MSSM case.

The physical Majorana phases are also corrected due to the running and we found the following results:

$$\alpha_{ij(\varrho)} \simeq \alpha_{ij} + \delta\alpha_{ij}\Delta_\tau + \dots \tag{4.44}$$

where α_{ij} are the starting values at Λ_f and

$$\delta\alpha_{13} = \frac{2}{3}\frac{m_1 m_2 \sin(\alpha_{13}-\alpha_{23})}{m_2^2 - m_1^2}\,, \qquad \delta\alpha_{23} = \frac{4}{3}\frac{m_1 m_2 \sin(\alpha_{13}-\alpha_{23})}{m_2^2 - m_1^2}\,. \tag{4.45}$$

At Λ_f, $\sin\theta_{13}^{TB}$ is vanishing and as a result the Dirac CP-violating phase is undetermined. An alternative is to study the Jarlskog invariants which are well-defined at each energy scale. At Λ_f, J_{CP} is vanishing, while after the renormalization group running it is given by

$$J_{CP} = \frac{1}{18}\left| m_3 \left(\frac{m_1 \sin\alpha_{13}}{m_1^2 - m_3^2} - \frac{m_2 \sin\alpha_{23}}{m_2^2 - m_3^2} \right) \right| \Delta_\tau\,. \tag{4.46}$$

Two comments are worth. First of all, in the expression for k_{13}, it is easy to recover the resulting expression for J_{CP} as the first term under the square root, apart global coefficients. This means that the running procedure introduces a mixing between the expression of the reactor angle and of the Dirac CP-phase. Moreover we can recover the value of the Dirac CP-phase directly from eq. (4.46) and we get the following expression:

$$\begin{aligned}\cot\delta = &- \frac{m_1(m_2^2-m_3^2)\cos\alpha_{13} - m_2(m_1^2-m_3^2)\cos\alpha_{23} - m_3(m_1^2-m_2^2)}{m_1(m_2^2-m_3^2)\sin\alpha_{13} - m_2(m_1^2-m_3^2)\sin\alpha_{23}} + \\ &- \frac{3a_e(m_2^2-m_3^2)(m_1^2-m_3^2)}{2m_3\left[m_1(m_2^2-m_3^2)\sin\alpha_{13} - m_2(m_1^2-m_3^2)\sin\alpha_{23}\right]\Delta_\tau}\,.\end{aligned} \tag{4.47}$$

In the neutrino sector, the running contributions from the See-Saw terms are present only in the resulting mass eigenvalues:

$$m_{i(\lambda)} \simeq m_i(1+\delta m_i) + \dots \tag{4.48}$$

where m_i are the starting values at Λ_f and δm_i, in both the Standard Model and the MSSM and in both the normally and inversely hierarchical spectra, are given by

$$\delta m_1 = \frac{m_1'}{m_1} - \frac{\Delta_\tau}{3}\,, \qquad \delta m_2 = 2\frac{m_2'}{m_2} - \frac{2\Delta_\tau}{3}\,, \qquad \delta m_3 = 2\frac{m_3'}{m_3} - \Delta_\tau\,, \tag{4.49}$$

with $m_i' \equiv |\tilde{m}_i'|$, given as in eqs. (4.34, 4.36).

4.3 Running Effects in the Altarelli-Feruglio Model

In this section we will apply the analysis of renormalization group running effects on the lepton mixing angles to the Altarelli-Feruglio model, already introduced in Section 2.3. In order to perform such a study, it is important to verify the initial assumptions made in Section 4.2.3, in particular, we see that eq. (4.27) exactly corresponds to the one

implied by the Altarelli-Feruglio model, when moving to the physical basis (the phase of y can be absorbed in the definition of P). On the other side, the presence of flavon fields has a relevant impact on the results of the analysis. In the unbroken phase, flavons are active fields and should modify the RGEs. Since the only source of the A_4 breaking is the VEVs of the flavons, any flavor structure is preserved above the corresponding energy scale, whatever interactions are present. In particular, the Lagrangian (2.53) contains all possible leading order terms, given the group assignments, and its invariance under A_4 is maintained moving downward to the scale $\langle\varphi\rangle$, where significant changes in the flavor structure can appear. From eqs. (2.54) and (2.56), we deduce that $\langle\varphi\rangle \sim M_i$ and as a result in the Altarelli-Feruglio model Δ_τ must be proportional to $\ln(\langle\varphi\rangle/\varrho)$ and not to $\ln(\Lambda_f/\varrho)$. Furthermore, it is relevant for the subsequent discussion to recall the level of degeneracy of the neutrino masses in the allowed space of parameters. The ratios between the right-handed neutrinos are well defined for the normal hierarchy, $M_1/M_3 \sim 11$ and $M_2/M_3 \sim 5$, while in the case of the inverse hierarchy, the ratio M_1/M_2 is fixed at 1 while M_3/M_2 varies from about 3 to 1, going from the lower bound of m_3 up to the KATRIN sensitivity.

We will separately discuss the evolution of angles and phases for both type of hierarchy. In the following, the results will be shown for the Standard Model and for the MSSM with $\tan\beta = 15$ in the absence of other explicit indications. Without loss of generality, we choose $y = 1$ for our numerical analysis. We also set $\langle\varphi\rangle = 10^{15}$. The spectrum spans the range obtained in (2.61).

4.3.1 Running of the Angles

Since we are interested in deviations of the corrected mixing angles from the Tribimaximal predictions and in comparing them with experimental values, it is convenient to relate the coefficients k_{ij} defined in Section 4.2.3 with physical observables. Keeping in mind that $|k_{ij}| \ll 1$ and that we start from a Tribimaximal mixing matrix, it follows that

$$\sin\theta_{13} \simeq k_{13} \,, \qquad \cos 2\theta_{23} \simeq 2k_{23} \,, \qquad \sin^2\theta_{12} - \frac{1}{3} \simeq \frac{2\sqrt{2}}{3} k_{12} \,. \tag{4.50}$$

The corrections to the tribimaximal mixing angles as functions of $m_{1,3}$ in the normal and inverse hierarchies are shown in Figure 4.1.

We begin with the case of the normal hierarchy. Since the dependence of the corrected mixing angles from Δ_τ is the same, Standard Model corrections are generally expected to be smaller than those in MSSM. However, from Figure 4.1 we see that, in normal hierarchy, there is not a large split between the two curves for Standard Model and MSSM. This fact suggests a dominant contribution coming from the charged lepton sector as discussed in Section 4.2.3. For the atmospheric and reactor angles, the deviations from the Tribimaximal predictions lie roughly one order of magnitude below the 1σ limit. In particular, running effects on $\sin\theta_{13}$ are even smaller than the NLO contributions analyzed in Section 2.3.2 which are of $\mathcal{O}(u)$, without cancellations. On the other hand,

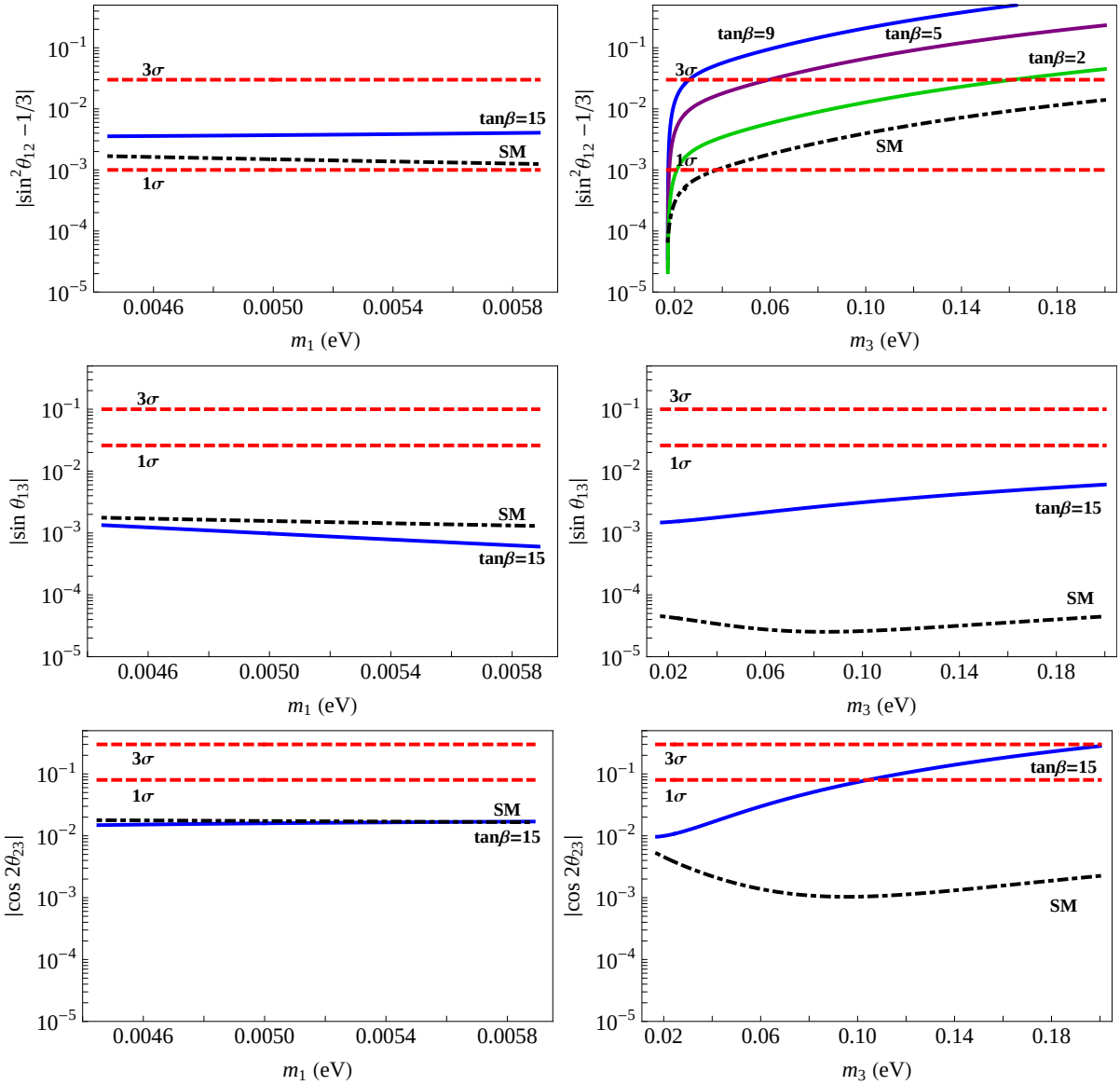

Figure 4.1: *Corrections to the Tribimaximal mixing angles as functions of the lightest neutrino masses, for the normal hierarchy on the left and for the inverse hierarchy on the right. The plots show the MSSM case with* $\tan\beta = 15$ *(solid blue) and the Standard Model case (black dashed), compared to the current* 1σ *and* 3σ *limits (dashed red).* $m_{1,3}$ *are restricted in a range which is given by eq. (2.61) or by the KATRIN bound.*

since the experimental value of the solar angle is better measured than the other two, the running effects become more important in this case. Indeed, the running corrections to the Tribimaximal solar angle evade the 1σ limit as it can be clearly seen in Figure 4.1. Anyway, we observe that for both the atmospheric and solar angles, the running contribution is of the same order as the contribution from NLO operators.

Now we move to analyze the case of the inverse hierarchy. In this case, since the neutrino spectrum predicted by the Altarelli-Feruglio model is almost degenerate and in particular $m_2/m_1 \sim 1$, the contribution from the charged lepton sector in eqs. (4.40) is sub dominant. As a consequence the information which distinguishes the Standard Model

case from the MSSM one is mainly dictated by Δ_τ defined in eq. (4.22). As a result the running effects in the MSSM are always larger than in the Standard Model and for large $\tan\beta$ they are potentially dangerous. The curves corresponding to the atmospheric and reactor angles do not go above the 3σ and 1σ windows respectively. However, the deviation from θ_{12}^{TB} presents a more interesting situation. For example, for $\tan\beta \gtrsim 10$, the running effects push the value of the solar angle beyond the 3σ limit for the entire spectrum. For lower values of $\tan\beta$, the model is within the 3σ limit only for a (small) part of the spectrum where the neutrinos are less degenerate. Comparing with the running effects, in the inverse hierarchy, the contribution from NLO operators in the Altarelli-Feruglio model is under control.

4.3.2 Running of the Phases

Majorana phases are affected by renormalization group running effects too. Since there is no experimental information on Majorana phases available at this moment we will simply show their values at low-energy, comparing them with the predictions in the Altarelli-Feruglio model. We stress again that they are completely determined by only one parameter, the mass of the lightest neutrino, m_1 for the normal hierarchy and m_3 for the inverse hierarchy.

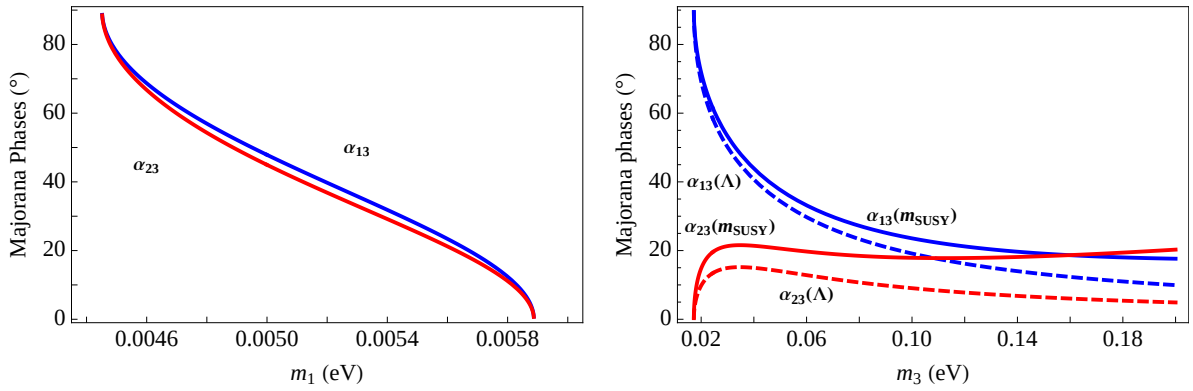

Figure 4.2: *Majorana phases α_{13} and α_{23} as functions of the lightest left-handed neutrino masses. For the normal hierarchy (left panel) the corresponding curves at low and high energies are indistinguishable. For the inverse hierarchy (right panel) the curves refer to low-energy values in MSSM with $\tan\beta = 15$ (solid blue or red) and the Altarelli-Feruglio predictions at Λ_f (dashed blue or red).*

In the case of normal hierarchy, Majorana phases are essentially not corrected by running effects. This feature is due to the fact that $\delta\alpha_{13}$ and $\delta\alpha_{23}$ of eqs. (4.45) are proportional to $\sin(\alpha_{13}-\alpha_{23})$ which is close to zero, as we can see looking at the left panel of Figure 4.2. In the case of inverse hierarchy, MSSM running effects always increase the values of phases when moving from high energy to low-energy and they are maximized for $\tan\beta = 15$, especially when the neutrino spectrum becomes degenerate. On the contrary,

in the Standard Model context, the low-energy curves cannot be distinguished from the high energy ones.

As described in Section 4.2.3, a definite Dirac CP violating phase δ arises from running effects even if, in the presence of a Tribimaximal mixing pattern, it is undetermined in the beginning. Although the final Dirac phase can be large, Jarlskog invariant, which measures an observable CP violation, remains small because of the smallness of θ_{13}. These results are valid both for the Standard Model and for MSSM.

4.4 Conclusion of the Chapter

In this chapter we have studied the running effects on neutrino mixing patterns when neutrino masses are generated by See-Saw I. The running contribution from the neutrino Yukawa coupling Y_ν, encoded in J_ν, is generally dominant at energies above the See-Saw threshold. However, this effect, which in general introduces appreciable deviations from the leading order mixing patterns, does not affect the mixing angles, under specific conditions: in the first part of the chapter, we have analyzed two classes of models in which this indeed happens. The first class is characterized by a Y_ν proportional to a unitary matrix. It is the case, for example, when the right-handed singlet neutrinos or the charged leptons belong to an irreducible representation of the flavor group. The second class is the mass-independent mixing pattern, in which, in particular, the effects of J_ν can be absorbed by a small shift of neutrino mass eigenvalues leaving mixing angles unchanged. The widely studied Tribimaximal mixing pattern belongs, for example, to this second class of models.

Subsequently, we focused on the Altarelli-Feruglio model. The aim was to analyze the running effects on the Tribimaximal mixing pattern in addition to the NLO corrections already present in this model due to the spontaneous breaking of the symmetry and to confront them with experimental values. The analysis has been performed both in the Standard Model and MSSM. We found that for the normal hierarchy light neutrinos, the dominant running contribution comes from the charged lepton sector which weakly depends on both $\tan\beta$ and mass degeneracy. As a result, for this type of spectrum, the Tribimaximal prediction is stable under running evolution. Moreover, the running contribution is of the same order or smaller with respect to the contribution from NLO operators. On the other hand, in the case of the inverse hierarchy, the deviation of the solar angle from its Tribimaximal value can be larger than the NLO contribution and, in particular in MSSM, for $\tan\beta \gtrsim 10$ an inversely hierarchical spectrum is strongly disfavored. In the end, we observe that for both spectra, the reactor angle θ_{13} does not receive appreciable deviations from zero.

Chapter 5

Rare Decays in A_4-Based Models

If we assume that the experimental values of mixing angles hint at a new physical framework beyond the Standard Model, as the one provided by discrete symmetries, we still face the task to discriminate among the possible choices of the underlying symmetry and model. In fact, as pointed out in Chapter 2, several theoretical textures are compatible with the current data on neutrino oscillation.As a consequence, we need to improve our knowledge of neutrino mixing or to test models beyond the neutrino sector.

The latter possibility can be offered by processes with lepton flavor violation (LFV) expected, at some level, for massive and non-trivially mixed neutrinos. At low-energy LFV is described by dimension six operators, suppressed by two powers of a new physics scale M, which could be much smaller than the fundamental scale Λ at which the flavor symmetry is generated, thus allowing observable effects. In models based on flavor symmetries rates of LFV transitions usually receive a double suppression: one from $1/M^4$ and one from the parameters that break the flavor symmetry. In a set of papers [66–68] radiative decays of the charged leptons have been analyzed in models invariant under $A_4 \times Z_3 \times U(1)_{FN}$, like the Altarelli-Feruglio model discussed in Chapter 2. Remembering that two breaking parameters $u \approx t \approx 0.01$ are present, a generic suppression u^2/M^4 for the rates was found, that can become more severe in a supersymmetric (SUSY) realization of $A_4 \times Z_3 \times U(1)_{FN}$. For instance, in this last case the decay rate of $\mu \to e\gamma$ can scale as t^2u^2/M^4, leaving room to a relatively light scale of new physics M.

In this chapter we complete the analysis of LFV in $A_4 \times Z_3 \times U(1)_{FN}$ symmetric models, by building the most general dimension six effective Lagrangian allowed by the symmetry. Contrary to the expectations of many models based on flavor symmetries, such effective Lagrangian contains four-lepton operators that break the conservation of the individual lepton numbers, while being fully invariant under the flavor symmetry [66]. These operators leads to LFV transitions whose rates are suppressed only by $1/M^4$, which can result in strong bounds on the scale M. We carefully analyze all such transitions, that satisfy the selection rule $\Delta L_e \Delta L_\mu \Delta L_\tau = \pm 2$. We separate our discussion according to the type of leptons involved in the transition: four neutrinos, two neutrinos plus two charged leptons, and four charged leptons. We find that the strength of the new LFV operators are most severely bound by the observed universality of leptonic muon and tau decays,

from the agreement between the Fermi constant measured in the muon decay and that extracted from the m_W/m_Z ratio, and from the limits on the rare decays $\tau^- \to \mu^+ e^- e^-$ and $\tau^- \to e^+ \mu^- \mu^-$. The present experimental limits on the branching ratios of these two tau decays push the scale M above 10 TeV.

We also analyze a specific SUSY realization of $A_4 \times Z_3 \times U(1)_{FN}$, motivated by several considerations: it offers a natural solution to the required vacuum alignment, it might be required to realize the embedding of the model in a grand unified theory and it provides a natural framework for a relatively small scale of new physics M, related to the SUSY breaking scale. In this SUSY model the four-lepton LFV operators arise from box diagrams, with neutralinos, charginos and sleptons circulating in the loop. For all processes that were allowed by the selection rule $\Delta L_e \Delta L_\mu \Delta L_\tau = \pm 2$, we find rates suppressed at least by eight powers of the symmetry breaking parameters t and/or u, at variance with the result of the model-independent analysis. We provide a detail explanation for this singular behavior and we reconsider all possible LFV transitions in the SUSY model, ending up with a complete picture of the most relevant LFV processes for the model at hand.

5.1 Classification of Four-lepton Operators

We will consider a model based on the flavor symmetry group

$$G_f = A_4 \times Z_3 \times U(1)_{FN}, \tag{5.1}$$

as described in details in Chapter 2. The flavor symmetry breaking sector of the model includes the scalar fields φ_T, φ_S, ξ and θ. The transformation properties of the lepton fields L, E_e, E_μ, E_τ, of the electroweak scalar doublet H and of the flavon fields have been recalled in Table 5.1. Notice that at variance with the notation introduced in Chapter 1, in the following we use the fields E_e, E_μ and E_τ instead of e^c, μ^c and τ^c. The different notations are connected by the equality $E_e = \overline{e}^c$ and the same for the muon and the tau. As a consequence, $L \equiv (L_e, L_\mu, L_\tau)$ are left-handed SU(2) doublets with hypercharge Y=-1/2, while E_e, E_μ and E_τ are right-handed SU(2) singlets with hypercharge $Y = -1$. Chirality projectors are understood. The following pattern of VEVs for the flavon fields

$$\begin{aligned} \frac{\langle \varphi_T \rangle}{\Lambda} &= (u, 0, 0) + O(u^2) \\ \frac{\langle \varphi_S \rangle}{\Lambda} &= c_b (u, u, u) + O(u^2) \\ \frac{\langle \xi \rangle}{\Lambda} &= c_a u + O(u^2) \\ \frac{\langle \theta \rangle}{\Lambda} &= t \end{aligned} \tag{5.2}$$

where u and t are the small, real, symmetry breaking parameters of the theory, guarantees that the lepton mixing is approximately TB. The parameters $c_{a,b}$ are pure numbers of order

one and Λ is the cutoff of the theory. It is possible to achieve this pattern of VEVs in a natural way, as the result of the minimization of the scalar potential of the theory [7, 69].

Field	L	E_e	E_μ	E_τ	H	φ_T	φ_S	ξ	θ
A_4	3	1	$1'$	$1''$	1	3	3	1	1
Z_3	ω	ω	ω	ω	1	1	ω	ω	1
$U(1)_{FN}$	0	-2	-1	0	0	0	0	0	-1

Table 5.1: The transformation rules of the fields under the symmetries associated with the groups A_4, Z_3 and $U(1)_{FN}$.

At the leading order, neglecting the $O(u^2)$ contributions, the mass matrix for the charged leptons is diagonal with the relative hierarchy described by the parameter t. To reproduce the correct hierarchy we need

$$t \approx 0.05 \quad . \tag{5.3}$$

In the same approximation, the neutrino mass matrix is diagonalized by the TB mixing matrix (2.17). The symmetry breaking parameter u should approximately lie in the range

$$0.005 < u < 0.05 \quad , \tag{5.4}$$

the lower bound coming from the requirement that the Yukawa coupling of the τ does not exceed 4π, and the upper bound coming from the requirement that the higher order corrections, so far neglected, do not modify too much the leading TB mixing. The inclusion of higher order corrections modifies all mixing angles by quantities of relative order u and in order to keep the agreement between the predicted and measured values of the solar angle within few degrees, u should not exceed approximately 0.05. The unknown angle θ_{13} is expected to be of order u, not far from the future aimed for experimental sensitivity [31]. Constraints from baryogenesis have been discussed in ref. [70].

The fields of Table 5.1 and their transformation properties are common to a generic class of models, differing from each other by the specific mechanism leading to the desired vacuum alignment, eq. (5.2), and by additional heavy degrees of freedom. One such model has been realized in the SUSY framework [6], where the special properties of the scalar potential in the SUSY limit are helpful in obtaining the correct vacuum structure. To construct a general low-energy effective Lagrangian depending on lepton fields we only need the information contained in Table 5.1 and we do not need to specify any particular model, but in the second part of the chapter we will make contact with the SUSY realization of ref. [6].

A complete basis of four-lepton operators, invariant under the SU(2)× U(1) gauge symmetry, have been introduced by Buchmüller and Wyler in [71]. Up to flavor combination, it consists of four independent dimension-six operators:

$$\begin{aligned}
(\mathcal{O}_{LE})^{\beta\delta}_{\alpha\gamma} &= (\bar{L}^{\beta}E_{\gamma})(\bar{E}^{\delta}L_{\alpha})\,, && (5.5)\\
(\mathcal{O}^{\mathbf{1}}_{LL})^{\beta\delta}_{\alpha\gamma} &= (\bar{L}^{\beta}\gamma^{\rho}L_{\alpha})(\bar{L}^{\delta}\gamma_{\rho}L_{\gamma})\,, && (5.6)\\
(\mathcal{O}^{\mathbf{3}}_{LL})^{\beta\delta}_{\alpha\gamma} &= (\bar{L}^{\beta}\gamma^{\rho}\vec{\tau}L_{\alpha})(\bar{L}^{\delta}\gamma_{\rho}\vec{\tau}L_{\gamma})\,, && (5.7)\\
(\mathcal{O}_{EE})^{\beta\delta}_{\alpha\gamma} &= (\bar{E}^{\beta}\gamma^{\rho}E_{\alpha})(\bar{E}^{\delta}\gamma_{\rho}E_{\gamma})\,. && (5.8)
\end{aligned}$$

We are using a four-component spinor notation and $\vec{\tau}$ denotes the Pauli matrices acting on SU(2) indices. Greek letters specify the flavor content. Their possible values are e, μ and τ. The effective Lagrangian, invariant under SU(2)× U(1) gauge transformations, and depending on L_α and E_β is given by:

$$\begin{aligned}
\mathcal{L}_{eff} = &- 2\sqrt{2}G_F\left[(\varepsilon_{LE})^{\alpha\gamma}_{\beta\delta}(\mathcal{O}_{LE})^{\beta\delta}_{\alpha\gamma} + (\varepsilon^{\mathbf{1}}_{LL})^{\alpha\gamma}_{\beta\delta}(\mathcal{O}^{\mathbf{1}}_{LL})^{\beta\delta}_{\alpha\gamma}\right.\\
&+ \left.(\varepsilon^{\mathbf{3}}_{LL})^{\alpha\gamma}_{\beta\delta}(\mathcal{O}^{\mathbf{3}}_{LL})^{\beta\delta}_{\alpha\gamma} + (\varepsilon_{EE})^{\alpha\gamma}_{\beta\delta}(\mathcal{O}_{EE})^{\beta\delta}_{\alpha\gamma}\right] + ... \qquad (5.9)
\end{aligned}$$

We have normalized the interaction strength to the Fermi constant G_F, which here we define by the relation [§]

$$R \equiv \frac{m_W^2}{m_Z^2} = \frac{1}{2} + \sqrt{\frac{1}{4} - \frac{\pi\alpha_{em}(m_Z^2)}{\sqrt{2}G_F m_Z^2(1-\Delta r)}} \qquad (5.10)$$

where $m_{W,Z}$ are the electroweak gauge boson masses, $\alpha_{em}(m_Z^2)$ is the running QED coupling constant evaluated at the m_Z scale, and Δr is the relevant SM radiative correction. This relation defines the constant G_F in terms of the experimental value of the W and Z boson masses. The Lagrangian $\mathcal{L}_{eff}$ is hermitian under the following conditions:

$$\begin{aligned}
(\varepsilon_{LE})^{\alpha\gamma}_{\beta\delta} &= (\varepsilon_{LE})^{\beta\delta}_{\alpha\gamma}\\
(\varepsilon^{\mathbf{1,3}}_{LL})^{\alpha\gamma}_{\beta\delta} &= (\varepsilon^{\mathbf{1,3}}_{LL})^{\beta\delta}_{\alpha\gamma}\\
(\varepsilon_{EE})^{\alpha\gamma}_{\beta\delta} &= (\varepsilon_{EE})^{\beta\delta}_{\alpha\gamma} \quad . \qquad (5.11)
\end{aligned}$$

Dots in (5.9) stand for higher order operators. The most general dimension-six effective Lagrangian depending on lepton fields also include other operators that we mention for completeness. They fall into two classes. The first one includes operators of dipole type, describing leptonic electric and magnetic dipole moments and flavor changing radiative transitions such as $\mu \to e\gamma$, $\tau \to \mu\gamma$ and $\tau \to e\gamma$:

$$\begin{aligned}
(\mathcal{O}^{B}_{dip})^{\beta}_{\alpha} &= \bar{E}^{\beta}\sigma^{\mu\nu}B_{\mu\nu}H^{\dagger}L_{\alpha}\\
(\mathcal{O}^{W}_{dip})^{\beta}_{\alpha} &= \bar{E}^{\beta}\sigma^{\mu\nu}\vec{\tau}\,\vec{W}_{\mu\nu}H^{\dagger}L_{\alpha} \quad . \qquad (5.12)
\end{aligned}$$

[§]It is useful to keep G_F distinguished from G_μ, the constant extracted from muon decay.

Their effect in the model under consideration has been analyzed in refs. [66]. The second class includes operators bilinear in the lepton fields containing a derivative and a double insertion of the Higgs multiplet H:

$$\begin{aligned}(\mathcal{O}^{\mathbf{1}}_{LH})^{\beta}_{\alpha} &= \left(\bar{L}^{\beta}H\right)\mathrm{i}\not{\partial}(H^{\dagger}L_{\alpha}) \\ (\mathcal{O}^{\mathbf{3}}_{LH})^{\beta}_{\alpha} &= \left(\bar{L}^{\beta}\vec{\tau}H\right)\mathrm{id}(H^{\dagger}\vec{\tau}L_{\alpha}) \\ (\mathcal{O}_{EH})^{\beta}_{\alpha} &= \left(H^{\dagger}\mathrm{i}D^{\rho}H\right)\left(\bar{E}^{\beta}\gamma_{\rho}E_{\alpha}\right) \quad ,\end{aligned} \tag{5.13}$$

where D denotes the SM covariant derivative. They modify kinetic terms of neutrinos and charged leptons and lead to deviations in the neutral and charged leptonic currents as well as to deviation from unitarity in the leptonic mixing matrix. Their effects have been discussed in general in refs. [72–74]. In the model under consideration the leading contribution to this second class of operators is flavor conserving and will not be further discussed here.

The operators $(\mathcal{O}^{\mathbf{1}}_{LL})^{\beta\delta}_{\alpha\gamma}$ and $(\mathcal{O}^{\mathbf{3}}_{LL})^{\beta\delta}_{\alpha\gamma}$ only differs by the contraction of the SU(2) indices. In terms of SU(2) components, they are given by:

$$(\mathcal{O}^{\mathbf{1}}_{LL})^{\beta\delta}_{\alpha\gamma} = \left(\bar{\nu}^{\beta}\gamma^{\rho}\nu_{\alpha} + \bar{e}^{\beta}\gamma^{\rho}e_{\alpha}\right)\left(\bar{\nu}^{\delta}\gamma_{\rho}\nu_{\gamma} + \bar{e}^{\delta}\gamma_{\rho}e_{\gamma}\right) \tag{5.14}$$

$$\begin{aligned}(\mathcal{O}^{\mathbf{3}}_{LL})^{\beta\delta}_{\alpha\gamma} &= \left(\bar{\nu}^{\beta}\gamma^{\rho}e_{\alpha} + \bar{e}^{\beta}\gamma^{\rho}\nu_{\alpha}\right)\left(\bar{\nu}^{\delta}\gamma_{\rho}e_{\gamma} + \bar{e}^{\delta}\gamma_{\rho}\nu_{\gamma}\right) \\ &- \left(\bar{\nu}^{\beta}\gamma^{\rho}e_{\alpha} - \bar{e}^{\beta}\gamma^{\rho}\nu_{\alpha}\right)\left(\bar{\nu}^{\delta}\gamma_{\rho}e_{\gamma} - \bar{e}^{\delta}\gamma_{\rho}\nu_{\gamma}\right) \\ &+ \left(\bar{\nu}^{\beta}\gamma^{\rho}\nu_{\alpha} - \bar{e}^{\beta}\gamma^{\rho}e_{\alpha}\right)\left(\bar{\nu}^{\delta}\gamma_{\rho}\nu_{\gamma} - \bar{e}^{\delta}\gamma_{\rho}e_{\gamma}\right) \quad .\end{aligned} \tag{5.15}$$

The flavor symmetry G_f imposes some restrictions on the coefficients of $\mathcal{L}_{eff}$. In a low-energy approximation, below the scale of flavor symmetry breaking, the four-lepton operators of the model originate either from genuine dimension-six operators invariant under G_f or from higher-dimensional G_f-invariant operators involving the insertions of the flavon multiplets. After the breaking of G_f by the VEVs in eq. (5.2), the latter become four-lepton operators proportional to some positive power of the symmetry breaking parameters t and/or u. As a consequence, the coefficients $\varepsilon^{\alpha\gamma}_{\beta\delta} \equiv \{(\varepsilon_{LE})^{\alpha\gamma}_{\beta\delta}, (\varepsilon^{\mathbf{1}}_{LL})^{\alpha\gamma}_{\beta\delta}, (\varepsilon^{\mathbf{1}}_{LL})^{\alpha\gamma}_{\beta\delta}, (\varepsilon_{EE})^{\alpha\gamma}_{\beta\delta}\}$ can be expanded in powers of the symmetry breaking parameters t and u.

$$\varepsilon^{\alpha\gamma}_{\beta\delta} = (\varepsilon^{(0)})^{\alpha\gamma}_{\beta\delta} + (\varepsilon^{(1,0)})^{\alpha\gamma}_{\beta\delta}\, t + (\varepsilon^{(0,1)})^{\alpha\gamma}_{\beta\delta}\, u + ... \tag{5.16}$$

Given the smallness of these parameters, here we will focus on the leading terms $(\varepsilon^{(0)})^{\alpha\gamma}_{\beta\delta}$, that is on the operators that do not vanish when the symmetry breaking effects are neglected. In particular, there are four-lepton operators that violate flavor while being invariant under G_f and not suppressed by powers of t and/or u. We will classify them

and we will study their effects. We find:

$$\begin{aligned}
\mathcal{L}_{eff} = \; & - \; 2\sqrt{2}G_F\alpha \left(\bar{E}^\tau\gamma^\rho E_\mu \; \bar{E}^e\gamma_\rho E_\mu + \bar{E}^\mu\gamma^\rho \; E_\tau\bar{E}^\mu\gamma_\rho E_e\right) \\
& - \; 2\sqrt{2}G_F\alpha_1 \left(\bar{L}^e\gamma^\rho L_e \; \bar{L}^e\gamma_\rho L_e + 4 \; \bar{L}^\mu\gamma^\rho L_\mu \; \bar{L}^\tau\gamma_\rho L_\tau + \right. \\
& \qquad \left. 2 \; \bar{L}^\mu\gamma^\rho L_e \; \bar{L}^\tau\gamma_\rho L_e + 2 \; \bar{L}^e\gamma^\rho L_\mu \; \bar{L}^e\gamma_\rho L_\tau\right) \\
& - \; 2\sqrt{2}G_F\beta_1 \left(\bar{L}^\mu\gamma^\rho L_\mu \; \bar{L}^\mu\gamma_\rho L_\mu + 4 \; \bar{L}^\tau\gamma^\rho L_\tau \; \bar{L}^e\gamma_\rho L_e + \right. \\
& \qquad \left. 2 \; \bar{L}^\tau\gamma^\rho L_\mu \; \bar{L}^e\gamma_\rho L_\mu + 2 \; \bar{L}^\mu\gamma^\rho L_\tau \; \bar{L}^\mu\gamma_\rho L_e\right) \\
& - \; 2\sqrt{2}G_F\gamma_1 \left(\bar{L}^\tau\gamma^\rho L_\tau \; \bar{L}^\tau\gamma_\rho L_\tau + 4 \; \bar{L}^e\gamma^\rho L_e \; \bar{L}^\mu\gamma_\rho L_\mu + \right. \\
& \qquad \left. 2 \; \bar{L}^e\gamma^\rho L_\tau \; \bar{L}^\mu\gamma_\rho L_\tau + 2 \; \bar{L}^\tau\gamma^\rho L_e \; \bar{L}^\tau\gamma_\rho L_\mu\right) \\
& - \; 2\sqrt{2}G_F\alpha_3 \left(\bar{L}^e\gamma^\rho\vec{\tau}L_e \; \bar{L}^e\gamma_\rho\vec{\tau}L_e + 4 \; \bar{L}^\mu\gamma^\rho\vec{\tau}L_\mu \; \bar{L}^\tau\gamma_\rho\vec{\tau}L_\tau + \right. \\
& \qquad \left. 2 \; \bar{L}^\mu\gamma^\rho\vec{\tau}L_e \; \bar{L}^\tau\gamma_\rho\vec{\tau}L_e + 2 \; \bar{L}^e\gamma^\rho\vec{\tau}L_\mu \; \bar{L}^e\gamma_\rho\vec{\tau}L_\tau\right) \\
& - \; 2\sqrt{2}G_F\beta_3 \left(\bar{L}^\mu\gamma^\rho\vec{\tau}L_\mu \; \bar{L}^\mu\gamma_\rho\vec{\tau}L_\mu + 4 \; \bar{L}^\tau\gamma^\rho\vec{\tau}L_\tau \; \bar{L}^e\gamma_\rho\vec{\tau}L_e + \right. \\
& \qquad \left. 2 \; \bar{L}^\tau\gamma^\rho\vec{\tau}L_\mu \; \bar{L}^e\gamma_\rho\vec{\tau}L_\mu + 2 \; \bar{L}^\mu\gamma^\rho\vec{\tau}L_\tau \; \bar{L}^\mu\gamma_\rho\vec{\tau}L_e\right) \\
& - \; 2\sqrt{2}G_F\gamma_3 \left(\bar{L}^\tau\gamma^\rho\vec{\tau}L_\tau \; \bar{L}^\tau\gamma_\rho\vec{\tau}L_\tau + 4 \; \bar{L}^e\gamma^\rho\vec{\tau}L_e \; \bar{L}^\mu\gamma_\rho\vec{\tau}L_\mu + \right. \\
& \qquad \left. 2 \; \bar{L}^e\gamma^\rho\vec{\tau}L_\tau \; \bar{L}^\mu\gamma_\rho\vec{\tau}L_\tau + 2 \; \bar{L}^\tau\gamma^\rho\vec{\tau}L_e \; \bar{L}^\tau\gamma_\rho\vec{\tau}L_\mu\right) + ... \qquad (5.17)
\end{aligned}$$

where dots stands for operators that do not violate lepton flavor. For instance, there are three independent operators of the type $(\mathcal{O}_{LE})^{\beta\delta}_{\alpha\gamma}$, but they are all flavor conserving. Notice that among the operators of the type $(\mathcal{O}_{EE})^{\beta\delta}_{\alpha\gamma}$ only one of them is flavor violating. We found three independent operators of the type $(\mathcal{O}^{\mathbf{1}}_{LL})^{\beta\delta}_{\alpha\gamma}$ that violate lepton flavor, and we call the corresponding coefficients α_1, β_1 and γ_1. Similarly, there are three independent flavor-violating operators of the type $(\mathcal{O}^{\mathbf{3}}_{LL})^{\beta\delta}_{\alpha\gamma}$, entering the Lagrangian with weights given by the coefficients α_3, β_3 and γ_3. All other operators in $\mathcal{L}_{eff}$ either conserve flavor or are suppressed by some power of the symmetry breaking parameters t and u. From the Lagrangian (5.17) it is clear that symmetry restricts the allowed operators to a class satisfying the selection rule $\Delta L_e\Delta L_\mu\Delta L_\tau = 0, \pm 2$. By expanding the Lagrangian (5.17) in neutrino and charged lepton components we get:

$$\mathcal{L}_{eff} = \mathcal{L}_{4\nu} + \mathcal{L}_{decay} + \mathcal{L}_{NSI} + \mathcal{L}_{ch} \qquad (5.18)$$

where

$$\begin{aligned}
\mathcal{L}_{4\nu} \; = \; & -2\sqrt{2}G_F \times \\
& \{(\alpha_1+\alpha_3) \; \bar{\nu}_e\gamma^\rho\nu_e \; \bar{\nu}_e\gamma_\rho\nu_e + (\beta_1+\beta_3) \; \bar{\nu}_\mu\gamma^\rho\nu_\mu \; \bar{\nu}_\mu\gamma_\rho\nu_\mu + (\gamma_1+\gamma_3)\bar{\nu}_\tau\gamma^\rho\nu_\tau \; \bar{\nu}_\tau\gamma_\rho\nu_\tau + \\
& 4\left[(\gamma_1+\gamma_3) \; \bar{\nu}_e\gamma^\rho\nu_e \; \bar{\nu}_\mu\gamma_\rho\nu_\mu + (\alpha_1+\alpha_3) \; \bar{\nu}_\mu\gamma^\rho\nu_\mu \; \bar{\nu}_\tau\gamma_\rho\nu_\tau + (\beta_1+\beta_3)\bar{\nu}_\tau\gamma^\rho\nu_\tau \; \bar{\nu}_e\gamma_\rho\nu_e\right] + \\
& 2\left[(\alpha_1+\alpha_3) \; \bar{\nu}_\mu\gamma^\rho\nu_e \; \bar{\nu}_\tau\gamma_\rho\nu_e + (\beta_1+\beta_3) \; \bar{\nu}_\tau\gamma^\rho\nu_\mu \; \bar{\nu}_e\gamma_\rho\nu_\mu + (\gamma_1+\gamma_3)\bar{\nu}_e\gamma^\rho\nu_\tau \; \bar{\nu}_\mu\gamma_\rho\nu_\tau \right. \\
& \left. + h.c.\right]\} \qquad (5.19)
\end{aligned}$$

$$\begin{aligned}\mathcal{L}_{decay} &= -2\sqrt{2}G_F \times \\ &[(1+8\gamma_3)\ \bar{e}\gamma^\rho\nu_e\ \bar{\nu}_\mu\gamma_\rho\mu + 2(\alpha_1+\alpha_3)\ \bar{e}\gamma^\rho\nu_\tau\ \bar{\nu}_e\gamma_\rho\mu + 2(\beta_1+\beta_3)\ \bar{e}\gamma^\rho\nu_\mu\ \bar{\nu}_\tau\gamma_\rho\mu + \\ &(1+8\alpha_3)\ \bar{\mu}\gamma^\rho\nu_\mu\ \bar{\nu}_\tau\gamma_\rho\tau + 2(\beta_1+\beta_3)\ \bar{\mu}\gamma^\rho\nu_e\ \bar{\nu}_\mu\gamma_\rho\tau + 2(\gamma_1+\gamma_3)\ \bar{\mu}\gamma^\rho\nu_\tau\ \bar{\nu}_e\gamma_\rho\tau + \\ &(1+8\beta_3)\ \bar{e}\gamma^\rho\nu_e\ \bar{\nu}_\tau\gamma_\rho\tau + 2(\alpha_1+\alpha_3)\ \bar{e}\gamma^\rho\nu_\mu\ \bar{\nu}_e\gamma_\rho\tau + 2(\gamma_1+\gamma_3)\ \bar{e}\gamma^\rho\nu_\tau\ \bar{\nu}_\mu\gamma_\rho\tau] \\ &+h.c. \end{aligned} \tag{5.20}$$

$$\begin{aligned}\mathcal{L}_{NSI} &= -2\sqrt{2}G_F \times \\ &\{[2(\alpha_1+\alpha_3)\ \bar{\nu}_e\gamma^\rho\nu_e + 4(\gamma_1-\gamma_3)\ \bar{\nu}_\mu\gamma^\rho\nu_\mu + 4(\beta_1-\beta_3)\ \bar{\nu}_\tau\gamma^\rho\nu_\tau]\ \bar{e}\gamma_\rho e + \\ &[4(\gamma_1-\gamma_3)\ \bar{\nu}_e\gamma^\rho\nu_e + 2(\beta_1+\beta_3)\ \bar{\nu}_\mu\gamma^\rho\nu_\mu + 4(\alpha_1-\alpha_3)\ \bar{\nu}_\tau\gamma^\rho\nu_\tau]\ \bar{\mu}\gamma_\rho\mu + \\ &[4(\beta_1-\beta_3)\ \bar{\nu}_e\gamma^\rho\nu_e + 4(\alpha_1-\alpha_3)\ \bar{\nu}_\mu\gamma^\rho\nu_\mu + 2(\gamma_1+\gamma_3)\ \bar{\nu}_\tau\gamma^\rho\nu_\tau]\ \bar{\tau}\gamma_\rho\tau\} \end{aligned} \tag{5.21}$$

$$\begin{aligned}\mathcal{L}_{ch} &= -2\sqrt{2}G_F \times \\ &\{(\alpha_1+\alpha_3)\ \bar{e}\gamma^\rho e\ \bar{e}\gamma_\rho e + (\beta_1+\beta_3)\ \bar{\mu}\gamma^\rho\mu\ \bar{\mu}\gamma_\rho\mu + (\gamma_1+\gamma_3)\bar{\tau}\gamma^\rho\tau\ \bar{\tau}\gamma_\rho\tau + \\ &4\left[(\gamma_1+\gamma_3)\ \bar{e}\gamma^\rho e\ \bar{\mu}\gamma_\rho\mu + (\alpha_1+\alpha_3)\ \bar{\mu}\gamma^\rho\mu\ \bar{\tau}\gamma_\rho\tau + (\beta_1+\beta_3)\bar{\tau}\gamma^\rho\tau\ \bar{e}\gamma_\rho e\right] + \\ &2\left[(\alpha_1+\alpha_3)\ \bar{\mu}\gamma^\rho e\ \bar{\tau}\gamma_\rho e + (\beta_1+\beta_3)\ \bar{\tau}\gamma^\rho\mu\ \bar{e}\gamma_\rho\mu + (\gamma_1+\gamma_3)\bar{e}\gamma^\rho\tau\ \bar{\mu}\gamma_\rho\tau + h.c.\right] + \\ &\alpha\left[\bar{E}^\tau\gamma^\rho E_\mu\ \bar{E}^e\gamma_\rho E_\mu + h.c.\right]\} \end{aligned} \tag{5.22}$$

In our notation all above fields are left-handed, except the charged leptons $E_{e,\mu,\tau}$ that are right-handed.

5.2 Bounds

We discuss the bounds on the parameters $\varepsilon = \{\alpha, \alpha_{1,3}, \beta_{1,3}, \gamma_{1,3}\}$, by distinguishing three types of operators: those involving neutrinos only, those involving both neutrinos and charged leptons and finally those depending on charged leptons only. For simplicity we assume that all the new parameters ε are real.

5.2.1 Neutrino Self-interactions

Neutrino self-interactions are poorly constrained by present data [75]. Extremely mild bounds come from astrophysics. For instance limits can be derived by requiring that the mean free path of neutrinos propagating in the medium between the supernova SN1987A and us is comparable to or larger than the distance to the supernova [76]. Such bounds would allow self-coupling of a four-fermion interaction larger than the Fermi coupling by many order of magnitudes. Stronger bounds can be derived from the agreement between the observed invisible decay width of the Z boson and the value predicted by the Standard

Model (SM). New neutrino self-interactions of the type considered here would contribute to both the decay width of the Z into four neutrinos at the tree level [77], and to the decay width of the Z into two neutrinos at the one-loop level [78]. These new contributions remain sufficiently small for values of the couplings $\alpha_{1,3}, \beta_{1,3}, \gamma_{1,3}$ smaller than approximately $1 \div 100$.

5.2.2 Neutrino-Charged Lepton Interactions

The new operators containing two neutrinos and two charged leptons lead to several effects. Some of them add to the SM Lagrangian to modify the prediction for the purely leptonic decays of the charged leptons μ and τ. The relevant Lagrangian for muon and tau decays is $\mathcal{L}_{decay}$, from which we can identify the "Fermi" constants extracted from the decays $\mu \to e\bar{\nu}\nu$, $\tau \to \mu\bar{\nu}\nu$, $\tau \to e\bar{\nu}\nu$, that we call G_μ, $G_{\tau\mu}$ and $G_{\tau e}$, respectively. By expanding the results in powers of the real parameters ε, we find:

$$\begin{aligned} G_\mu &= G_F\left(1 + 8\gamma_3 + 2(\alpha_1+\alpha_3)^2 + 2(\beta_1+\beta_3)^2 + ...\right) \\ G_{\tau\mu} &= G_F\left(1 + 8\alpha_3 + 2(\beta_1+\beta_3)^2 + 2(\gamma_1+\gamma_3)^2 + ...\right) \\ G_{\tau e} &= G_F\left(1 + 8\beta_3 + 2(\gamma_1+\gamma_3)^2 + 2(\alpha_1+\alpha_3)^2 + ...\right) \end{aligned} \tag{5.23}$$

where dots stand for higher powers of the parameters. We see that the operators $\mathcal{O}^{\mathbf{3}}_{LL}$ lead to amplitudes that interfere with the SM ones, so that the sensitivity to the corresponding parameters is higher, whereas the operators $\mathcal{O}^{\mathbf{1}}_{LL}$ contribute to the decays through non-interfering amplitudes. The presence of the new operators leads to deviations from universality in weak interactions. We have

$$\begin{aligned} \left(\frac{G_{\tau e}}{G_\mu}\right)^2 &= 1 + 16(\beta_3-\gamma_3) + 4(\gamma_1^2 + 49\gamma_3^2 - \beta_1^2 + 15\beta_3^2 + 2\gamma_1\gamma_3 - 2\beta_1\beta_3 - 64\gamma_3\beta_3) \\ \left(\frac{G_{\tau\mu}}{G_\mu}\right)^2 &= 1 + 16(\alpha_3-\gamma_3) + 4(\gamma_1^2 + 49\gamma_3^2 - \alpha_1^2 + 15\alpha_3^2 + 2\gamma_1\gamma_3 - 2\alpha_1\alpha_3 - 64\gamma_3\alpha_3) \\ \left(\frac{G_{\tau\mu}}{G_{\tau e}}\right)^2 &= 1 + 16(\alpha_3-\beta_3) + 4(\beta_1^2 + 49\beta_3^2 - \alpha_1^2 + 15\alpha_3^2 + 2\beta_1\beta_3 - 2\alpha_1\alpha_3 - 64\beta_3\alpha_3) \end{aligned} \tag{5.24}$$

These ratios can be directly compared with data using the following relations:

$$\begin{aligned} \left(\frac{G_{\tau e}}{G_\mu}\right)^2 &= \frac{\tau_\mu}{\tau_\tau} BR(\tau^- \to e^-\bar{\nu}_e\nu_\tau) \left(\frac{m_\mu}{m_\tau}\right)^5 \frac{f(m_e^2/m_\mu^2) r^\mu_{EW}}{f(m_e^2/m_\tau^2) r^\tau_{EW}} \\ \left(\frac{G_{\tau\mu}}{G_\mu}\right)^2 &= \frac{\tau_\mu}{\tau_\tau} BR(\tau^- \to \mu^-\bar{\nu}_\mu\nu_\tau) \left(\frac{m_\mu}{m_\tau}\right)^5 \frac{f(m_e^2/m_\mu^2) r^\mu_{EW}}{f(m_\mu^2/m_\tau^2) r^\tau_{EW}} \\ \left(\frac{G_{\tau\mu}}{G_{\tau e}}\right)^2 &= \frac{BR(\tau^- \to \mu^-\bar{\nu}_\mu\nu_\tau)}{BR(\tau^- \to e^-\bar{\nu}_e\nu_\tau)} \frac{f(m_e^2/m_\tau^2)}{f(m_\mu^2/m_\tau^2)} \end{aligned} \tag{5.25}$$

where $\tau_{\mu,\tau}$ are the muon and tau lifetimes, $f(x) = 1 - 8x + 8x^3 - x^4 - 12x^2 \log x$ and radiative corrections are those of the SM [79]

$$r_{EW}^l = \left(1 + \frac{3}{5}\frac{m_l^2}{m_W^2}\right)\left(1 + \frac{\alpha(m_l)}{2\pi}\left(\frac{25}{4} - \pi^2\right)\right) \quad , \tag{5.26}$$

$$\alpha^{-1}(m_l) = \alpha^{-1} - \frac{2}{3\pi}\log\frac{m_l}{m_e} + \frac{1}{6\pi} \quad . \tag{5.27}$$

From the measured values of τ_τ and of $BR(\tau^- \to \mu^-\bar{\nu}_\mu\nu_\tau)$, $BR(\tau^- \to e^-\bar{\nu}_e\nu_\tau)$ and their ratio [19, 80]

$$\tau_\tau = (290.6 \pm 1.1) \times 10^{-15} s \ , \tag{5.28}$$

$$\begin{aligned} BR(\tau^- \to e^-\bar{\nu}_\mu\nu_\tau) &= 0.1785 \pm 0.0005 \ , \\ BR(\tau^- \to \mu^-\bar{\nu}_\mu\nu_\tau) &= 0.1736 \pm 0.0005 \ , \\ \frac{BR(\tau^- \to \mu^-\bar{\nu}_\mu\nu_\tau)}{BR(\tau^- \to e^-\bar{\nu}_\mu\nu_\tau)} &= 0.9796 \pm 0.0040 \ , \end{aligned} \tag{5.29}$$

we get

$$\left(\frac{G_{\tau e}}{G_\mu}\right)^2 = 1.0025 \pm 0.0047 \ , \quad \left(\frac{G_{\tau\mu}}{G_\mu}\right)^2 = 1.0025 \pm 0.0048 \ , \quad \left(\frac{G_{\tau\mu}}{G_{\tau e}}\right)^2 = 1.0072 \pm 0.0041 \tag{5.30}$$

Assuming values of the parameters ε roughly of the same order, we see that the deviations from the SM prediction are dominated by the operators of type $\mathcal{O}^{\mathbf{3}}_{LL}$, and we obtain the bounds

$$\begin{aligned} -0.0007 &< \beta_3 - \gamma_3 < 0.0010 \quad [3\sigma] \\ -0.0007 &< \alpha_3 - \gamma_3 < 0.0010 \quad [3\sigma] \\ -0.0003 &< \alpha_3 - \beta_3 < 0.0012 \quad [3\sigma] \end{aligned} \tag{5.31}$$

When the operators $\mathcal{O}^{\mathbf{3}}_{LL}$ can be neglected, we get a milder bound on the new parameters. For instance, if $\beta_3 = \gamma_3 = 0$, we have

$$-0.0033 < \gamma_1^2 - \beta_1^2 < 0.0043 \quad [3\sigma] \tag{5.32}$$

If we parametrize the effective Lagrangian in terms of a new mass scale M, through the relation

$$2\sqrt{2}G_F\varepsilon = \frac{1}{M^2} \tag{5.33}$$

we see that an upper bound on $|\varepsilon|$ of order 0.001(0.06) corresponds to a lower bound on M of order 5.5(0.7) TeV.

The comparison between G_F in (5.10), extracted from the W mass, and G_μ in (5.23), obtained from the muon lifetime, leads to additional constraints on the parameters. It

is convenient to express the ratio $R = (m_W^2/m_Z^2)$ in terms of G_μ. By expanding up to second order in the new parameters, we get

$$R = R_{SM}\left[1 - \frac{(1-R_{SM})}{(2R_{SM}-1)}\left(8\gamma_3 + 2(\alpha_1+\alpha_3)^2 + 2(\beta_1+\beta_3)^2\right) - 64\frac{R_{SM}(1-R_{SM})^2}{(2R_{SM}-1)^3}\gamma_3^2\right] \tag{5.34}$$

where we have defined

$$R_{SM} \equiv \frac{1}{2} + \sqrt{\frac{1}{4} - \frac{\pi\alpha_{em}(m_Z^2)}{\sqrt{2}G_\mu m_Z^2(1-\Delta r)}} = 0.77680(0.77611) \tag{5.35}$$

The numerical values have been obtained from ref. [81] in the OSII scheme, by using as inputs $m_Z = 91.1875$ GeV, $\alpha_s(m_Z) = 0.118$, $\Delta\alpha_h^{(5)} = 0.02761$, $m_t = 173.1$ GeV and $m_H = 115(200)$ GeV. The experimental value of R, obtained by combining the PDG averages of the W and Z masses is

$$R_{\texttt{exp}} = 0.77735 \pm 0.00048 \tag{5.36}$$

We first compare (5.34) and (5.36) assuming dominance of the γ_3 parameter. We obtain

$$-0.0010 < \gamma_3 < 0.0004 \quad [3\sigma] \quad . \tag{5.37}$$

If γ_3 is negligible, we get

$$-0.0041 < (\alpha_1+\alpha_3)^2 + (\beta_1+\beta_3)^2 < 0.0014 \quad [3\sigma] \quad . \tag{5.38}$$

The bounds are approximately in the same range derived from the universality of the muon and tau decays.

Weaker bound are derived from the non-standard neutrino interactions described by the Lagrangian $\mathcal{L}_{NSI}$ in eq. (5.21). These interactions are usually described in terms of a perturbation of the weak effective Lagrangian,

$$\mathcal{L}_{NSI} = -2\sqrt{2}G_F[\epsilon_{\alpha\beta}^{lL,R}(\overline{\nu_\alpha}\gamma^\mu\nu_\beta)(\bar{l}_{L,R}\gamma_\mu l_{L,R})], \tag{5.39}$$

where $\epsilon_{\alpha\beta}^{lL,R}$ is a small parameter measuring the size of the deviation and $l = e, \mu, \tau$. The strongest bounds are those on neutrino-electron interactions, $\epsilon_{\alpha\beta}^{eL,R}$. When $\alpha = \beta = e, \mu$ they are derived from neutrino-electron elastic scattering [82]

$$\begin{aligned} -0.07 < \epsilon_{ee}^{eL} < 0.11 \qquad & -1.0 < \epsilon_{ee}^{eR} < 0.5 \qquad [90\% \quad CL] \\ -0.025 < \epsilon_{\mu\mu}^{eL} < 0.03 \qquad & -0.027 < \epsilon_{\mu\mu}^{eR} < 0.03 \qquad [90\% \quad CL] \end{aligned} \tag{5.40}$$

For $\alpha = \beta = \tau$ the limit comes from the $e^+e^- \to \bar{\nu}\nu\gamma$ cross-section measured at LEP II [83, 84]

$$-0.6 < \epsilon_{\tau\tau}^{eL} < 0.4 \qquad -0.4 < \epsilon_{\tau\tau}^{eR} < 0.6 \qquad [90\% \quad CL] \tag{5.41}$$

Similar bounds can be derived on flavor-changing terms $\alpha \neq \beta$ from matter effects in neutrino oscillations, but they are not relevant for the present analysis. Indeed, by comparing eqs. (5.21) and (5.39), we see that in our model, only flavor conserving terms are allowed ($\alpha = \beta$) and we have

$$\epsilon_{ee}^{eL} = 2(\alpha_1 + \alpha_3) \qquad \epsilon_{\mu\mu}^{eL} = 4(\gamma_1 - \gamma_3) \qquad \epsilon_{\tau\tau}^{eL} = 4(\beta_1 - \beta_3) \quad , \tag{5.42}$$

while right-handed couplings are vanishing. From eqs. (5.40) and (5.41) we get the 90% CL bounds

$$-0.04 < (\alpha_1+\alpha_3) < 0.06 \qquad -0.006 < (\gamma_1-\gamma_3) < 0.007 \qquad -0.15 < (\beta_1-\beta_3) < 0.1 \quad . \tag{5.43}$$

With the exception of the limit on $(\gamma_1 - \gamma_3)$, at present these bounds are not competitive with those derived previously from muon and tau decays. A future improvement is expected from further analysis of data from KamLAND, SNO, SuperKamiokande and neutrino factories.

5.2.3 Charged Lepton Interactions

New interactions among charged leptons are induced by the Lagrangian (5.22). We have seen that LFV transitions obey the selection rule $\Delta L_e \Delta L_\mu \Delta L_\tau = \pm 2$. This is a very interesting feature of the model under discussion. Usually SM extensions allowing for low-energy flavor changing four-lepton interactions are severely constrained by the experimental limits on the branching ratio $\mu \to eee$: $BR(\mu \to eee) < 1.0 \times 10^{-12}$. In our model this transition is forbidden at the lowest order by the selection rule imposed by A_4 symmetry. For the same reason also the transitions $\tau \to eee$ and $\tau \to \mu\mu\mu$ are forbidden at the lowest order. The above selection rule allows the flavor changing decays [¶] $\tau^- \to \mu^+ e^- e^-$ and $\tau^- \to e^+ \mu^- \mu^-$, whose branching ratios have the following upper limits at 90% CL [19]:

$$BR(\tau^- \to \mu^+ e^- e^-) < 2.0 \times 10^{-8} \qquad BR(\tau^- \to e^+ \mu^- \mu^-) < 2.3 \times 10^{-8} \quad . \tag{5.44}$$

From (5.22), we compute the corresponding decay rates

$$\begin{aligned} \Gamma(\tau^- \to \mu^+ e^- e^-) &= \frac{G_F^2 m_\tau^5}{96\pi^3}(\alpha_1 + \alpha_3)^2 \\ \Gamma(\tau^- \to e^+ \mu^- \mu^-) &= \frac{G_F^2 m_\tau^5}{96\pi^3}\left[(\beta_1 + \beta_3)^2 + \frac{\alpha^2}{4}\right]. \end{aligned} \tag{5.45}$$

The total τ width is approximately given by:

$$\Gamma = \frac{G_F^2 m_\tau^5}{192\pi^3} \times \frac{1}{BR(\tau^- \to \mu^- \nu_\tau \bar{\nu}_\mu)} \approx \frac{G_F^2 m_\tau^5}{192\pi^3} \times \frac{1}{0.18} \quad , \tag{5.46}$$

[¶] In the context of models with an A_4 flavor symmetry, these decays were first considered in ref. [91].

and we get the 90% CL bounds

$$\begin{aligned} |\alpha_1 + \alpha_3| &< 2.4 \times 10^{-4} \\ \sqrt{(\beta_1+\beta_3)^2 + \frac{\alpha^2}{4}} &< 2.5 \times 10^{-4} \quad . \end{aligned} \tag{5.47}$$

These bounds are the most restrictive ones among those discussed so far. The effective Lagrangian (5.22) also describes flavour-conserving four-lepton interactions, such as $e^+e^- \to f\bar{f}$ ($f = e, \mu, \tau$), which have been constrained by the LEP data [85]. For instance, in terms of the effective operator $-2\sqrt{2}G_F[\epsilon_{LL}(\bar{e}\gamma^\rho e)(\ \bar{f}\gamma_\rho f)]$, ref. [85] quotes

$$\epsilon_{LL}^{f\neq e} = 0.0168 \pm 0.0133 \qquad\qquad \epsilon_{LL}^{f=e} = -0.0187 \pm 0.0320 \tag{5.48}$$

Using (5.22), we obtain the bounds at 3σ

$$-0.006 < (\gamma_1+\gamma_3) + (\beta_1+\beta_3) < 0.014 \qquad -0.124 < (\alpha_1+\alpha_3) < 0.086 \tag{5.49}$$

Similar bounds exist on four-lepton flavour-conserving operators with different chirality structure.

5.3 A Specific Realization

So far we have analyzed the consequences of the A_4 flavor symmetry in a general effective Lagrangian approach, without making reference to any particular model. The only model-dependent ingredient that we have used is the assignment of the lepton multiplets to representations of the full flavor group $A_4 \times Z_3 \times U(1)_{FN}$ given in Table 5.1. It is interesting to investigate some concrete realizations of the flavor symmetry in a specific model, to see if the expectations based on the effective Lagrangian approach are fulfilled or not. Perhaps the most significant feature of the effective Lagrangian approach is the prediction of the leading order selection rule $\Delta L_e \Delta L_\mu \Delta L_\tau = \pm 2$, which implies the dominance of the channels $\tau^- \to \mu^+ e^- e^-$ and $\tau^- \to e^+ \mu^- \mu^-$ among the flavor-changing transitions. In this section we consider the supersymmetric realization of $A_4 \times Z_3 \times U(1)_{FN}$ discussed in ref. [6]. The fields in Table 5.1 are promoted to chiral supermultiplets and a $U(1)_R$ symmetry, eventually broken down to the R-parity , is introduced to restrict the superpotential. This realization of $A_4 \times Z_3 \times U(1)_{FN}$ is particularly relevant since it offers a complete and natural solution of the vacuum alignment problem. Namely the specific pattern of VEVs given in eq. (5.2) can be reproduced from the minimization of the scalar potential of the theory in a finite portion of the parameter space, without any fine-tuning of the parameters. After SUSY breaking four-lepton operators are expected to arise at one-loop from the exchange of sleptons, charginos and neutralinos. They are naturally depleted by the effective SUSY breaking scale m_{SUSY}, so that, in the absence of other suppressions, our parameters ε are expected to be of order

$$\varepsilon \approx \frac{1}{16\pi^2}\frac{m_Z^2}{m_{SUSY}^2} \tag{5.50}$$

If $m_{SUSY} \approx 1$ TeV we have $\varepsilon \approx 10^{-4}$ which, as we have seen, is close to the experimental upper bounds on the branching ratios for $\tau^- \to \mu^+ e^- e^-$ and $\tau^- \to e^+ \mu^- \mu^-$, see eq. (5.47). For this reason it is important to proceed to a direct estimate of the rates for lepton flavor violating processes in the SUSY model in order to establish their strength and their relative hierarchy. We first focus on the potentially most dangerous transitions: $\tau^- \to \mu^+ e^- e^-$ and $\tau^- \to e^+ \mu^- \mu^-$. At one-loop these transitions are described by box diagrams alone, since penguin diagrams always require a particle-antiparticle pair in the final state. It is useful to analyze these diagrams in the so-called super-CKM basis, where gaugino-lepton-slepton vertices are flavor diagonal. Neglecting Higgsino exchange, whose contributions are suppressed by lepton masses, the only sources of flavor change are the off-diagonal terms of slepton mass matrices $(\tilde{m}^2)_{MN}$, which can be analyzed in the mass insertion approximation, expressed through the parameters

$$(\delta_{ij})_{MN} = \frac{(\tilde{m}^2_{ij})_{MN}}{m^2_{SUSY}} \tag{5.51}$$

where $M, N = (L, R)$ are the chiralities. A quick inspection of the relevant box diagrams reveals that both transitions require at least two mass insertions: $\delta_{\tau e}$ and $\delta_{\mu e}$ for $\tau^- \to \mu^+ e^- e^-$ and $\delta_{\tau\mu}$ and $\delta_{\mu e}$ for $\tau^- \to e^+ \mu^- \mu^-$ and the corresponding amplitudes scale as:

$$\mathcal{M}(\tau^- \to \mu^+ e^- e^-) \propto \frac{1}{16\pi^2} \frac{m_Z^2}{m^2_{SUSY}} \times \delta_{\tau e}\delta_{\mu e} \tag{5.52}$$

$$\mathcal{M}(\tau^- \to e^+ \mu^- \mu^-) \propto \frac{1}{16\pi^2} \frac{m_Z^2}{m^2_{SUSY}} \times \delta_{\tau\mu}\delta_{\mu e} \tag{5.53}$$

The most general slepton mass matrices compatible with the $A_4 \times Z_3 \times U(1)_{FN}$ flavor symmetry in the super-CKM basis have the following leading order structure [67, 68]:

$$\tilde{m}^2_{eLL} = \tilde{m}^2_{\nu LL} = \begin{pmatrix} 1 + O(u) & O(u^2) & O(u^2) \\ O(u^2) & 1 + O(u) & O(u^2) \\ O(u^2) & O(u^2) & 1 + O(u) \end{pmatrix} m^2_{SUSY} \tag{5.54}$$

$$\tilde{m}^2_{eRR} = \begin{pmatrix} O(1) & O(tu) & O(t^2u) \\ O(tu) & O(1) & O(tu) \\ O(t^2u) & O(tu) & O(1) \end{pmatrix} m^2_{SUSY} \tag{5.55}$$

$$\tilde{m}^2_{eRL} = k \begin{pmatrix} m_e & c\ m_e u & c\ m_e u \\ c\ m_\mu u & m_\mu & c\ m_\mu u \\ c\ m_\tau u & c\ m_\tau u & m_\tau \end{pmatrix} m_{SUSY} \tag{5.56}$$

where k and c are model dependent coefficients. Depending on the chirality structure of the four-lepton operator we can have different type of suppression:

$$\begin{aligned} \mathcal{M}(\tau^- \to \mu^+ e^- e^-) &\propto \frac{1}{16\pi^2} \frac{m_Z^2}{m^2_{SUSY}} \times u^4 \qquad (LLLL) \\ &\propto \frac{1}{16\pi^2} \frac{m_Z^2}{m^2_{SUSY}} \times t^3 u^2 \qquad (RRRR) \\ &\propto \frac{1}{16\pi^2} \frac{m_Z^2}{m^2_{SUSY}} \times t u^3 \qquad (LLRR) \end{aligned} \tag{5.57}$$

$$\begin{aligned}\mathcal{M}(\tau^- \to e^+\mu^-\mu^-) &\propto \frac{1}{16\pi^2}\frac{m_Z^2}{m_{SUSY}^2} \times u^4 \qquad (LLLL)\\ &\propto \frac{1}{16\pi^2}\frac{m_Z^2}{m_{SUSY}^2} \times t^2u^2 \qquad (RRRR)\\ &\propto \frac{1}{16\pi^2}\frac{m_Z^2}{m_{SUSY}^2} \times tu^3 \qquad (LLRR) \end{aligned} \tag{5.58}$$

The chirality structure (LRLR) is not included because it is strongly suppressed by the ratio m_i/m_{SUSY}. We see that both amplitudes vanish in the limit of exact flavor symmetry, contrary to the expectation based on our effective Lagrangian approach. In principle the flavor symmetry allows for non-vanishing amplitudes, but the specific SUSY realization considered here prevents non-vanishing contributions in the exact symmetry limit. Such a result can be justified by analyzing the specific symmetry properties of the SUSY model. Indeed, it is easy to recognize that, in the limit of exact flavor symmetry lepton masses vanish, and so does the block $\tilde{m}^2_{eRL}$, whereas $\tilde{m}^2_{eLL}$ is proportional to the unit matrix and $\tilde{m}^2_{eRR}$ is diagonal. The flavor symmetry in this limit is larger than $A_4 \times Z_3 \times U(1)_{FN}$: it contains $SU(3)_L \times U(1)_{eR} \times U(1)_{\mu R} \times U(1)_{\tau R}$, which forbids any flavor-violating transition in the lepton sector. Since both u and t symmetry breaking parameters lies in the percent range, the predicted rates for $\tau^- \to \mu^+e^-e^-$ and $\tau^- \to e^+\mu^-\mu^-$ drop by more than ten order of magnitudes below the present experimental sensitivity. Indeed in the SUSY model all the operators of $\mathcal{L}_{decay}$, eq. (5.20), originate from similar box diagrams and they get the same suppression, thus relaxing also the bounds coming from universality in leptonic muon and tau decays, and from the agreement between the Fermi constant measured in the muon decay and that extracted from the m_W/m_Z ratio.

Given this strong suppression of the a priori favored channels $\tau^- \to \mu^+e^-e^-$ and $\tau^- \to e^+\mu^-\mu^-$, we would like to establish which is the leading flavor violating process in this SUSY realization of $A_4 \times Z_3 \times U(1)_{FN}$. We should look for transitions where a single mass insertion occurs. In ref. [67,68] a detailed analysis of the dipole transitions $\mu \to e\gamma$, $\tau \to \mu\gamma$ and $\tau \to e\gamma$ was presented. In terms of the normalized branching ratios

$$R_{ij} = \frac{BR(l_i \to l_j\gamma)}{BR(l_i \to l_j\nu_i\bar{\nu}_j)} \quad . \tag{5.59}$$

the generic expectation in the SUSY model is

$$R_{ij} = \frac{6}{\pi}\frac{m_W^4}{m_{SUSY}^4}\alpha_{em}|w_{ij}\ u|^2 \tag{5.60}$$

where α_{em} is the fine structure constant and w_{ij} are dimensionless parameters of order one. Such behavior is due to the dominance of the mass insertion of RL type, leading to an amplitude linear in the symmetry breaking parameter u. As apparent from eq. (5.56) the amplitude is proportional to the model-dependent coefficient c. There is a class of SUSY model where c actually vanishes [67]. In this case the ratios R_{ij} are of the form:

$$R_{ij} = \frac{6}{\pi}\frac{m_W^4}{m_{SUSY}^4}\alpha_{em}\left[|w_{ij}^{(1)}u^2|^2 + \frac{m_j^2}{m_i^2}|w_{ij}^{(2)}u|^2\right] \tag{5.61}$$

where $w_{ij}^{(1,2)}$ are order one parameters. Even in the case $c = 0$ the dipole transitions appear much more favored with respect to $\tau^- \to \mu^+ e^- e^-$ and $\tau^- \to e^+ \mu^- \mu^-$. The best present (and future aimed for) limit is for $\mu \to e\gamma$:

$$BR(\mu \to e\gamma) < 1.2 \times 10^{-11} \ (10^{-13}) \tag{5.62}$$

which implies the following bounds (setting $w_{\mu e}^{(1,2)} \equiv 1$)

$$\begin{aligned} m_{SUSY} &> 255 \ (820) \ \text{GeV} \quad (u = 0.005) \\ m_{SUSY} &> 0.7 \ (2.5) \ \text{TeV} \quad (u = 0.05) \quad . \end{aligned} \tag{5.63}$$

Process	Suppression
$\mu^- \to e^- \gamma$	$t^2 u^2$
$\tau^- \to \mu^- \gamma$	$t^2 u^2$
$\tau^- \to e^- \gamma$	u^4
$\mu^- \to e^- e^+ e^-$	$t^2 u^2$
$\tau^- \to \mu^- \mu^+ \mu^-$	$t^2 u^2$
$\tau^- \to \mu^- e^+ e^-$	$t^2 u^2$
$\tau^- \to e^- \mu^+ \mu^-$	u^4
$\tau^- \to e^- e^+ e^-$	u^4
$\tau^- \to \mu^+ e^- e^-$	$u^6 t^2$
$\tau^- \to e^+ \mu^- \mu^-$	$u^4 t^4$

Table 5.2: Parametric suppression of the rates for lepton flavor violating processes, assuming the behavior of eq. (5.61) for the dipole transitions and of eqs. (5.57) and (5.58) for the last two processes.

A related process is the decay $\mu^- \to e^- e^+ e^-$. Within our SUSY model, at one loop there are contributions both from γ- and Z-penguin diagrams and from box diagrams, dominated by a single flavor changing mass insertion in a slepton propagator. The dominant contribution comes from the γ penguin diagrams, and we can relate the BR of this process to the $\mu \to e\gamma$ one [86]

$$\text{Br}(\mu^- \to e^- e^+ e^-) \approx 7 \cdot 10^{-3} \ \text{Br}(\mu \to e\gamma). \tag{5.64}$$

From the current upper bound $Br(\mu^- \to e^- e^+ e^-) < 1.0 \times 10^{-12}$, using the estimate for $BR(\mu \to e\gamma)$ of eq. (5.61), we find

$$m_{SUSY} > 140 \ (225) \ \text{GeV} \qquad (u = 0.005) \tag{5.65}$$

$$m_{SUSY} > 400 \ (700) \ \text{GeV} \qquad (u = 0.05) \quad , \tag{5.66}$$

where in parenthesis we have shown the results assuming an improvement of the limit by one order of magnitude. Other τ decays such as $\tau^- \to e^- e^+ e^-$,$\tau^- \to \mu^- \mu^+ \mu^-$,

$\tau^- \to \mu^- e^+ e^-$, $\tau^- \to e^- \mu^+ \mu^-$, have a relationship with $\tau \to \mu\gamma$ analogous to that between $\mu^- \to e^- e^- e^+$ and $\mu \to e\gamma$. We summarize the suppression of the rates for these processes in Table 5.2. In this SUSY model there are no LFV transitions that are non-vanishing in the limit of exact flavor symmetry. Flavor violating τ decays have rates comparable to those of μ decays, but the present and future experimental sensitivities are much worse compare to $\mu \to e\gamma$, for which the prospect of detection are the best.

Finally we comment on μ to e conversion in nuclei. Although quarks go beyond the description provided by the flavor symmetry $A_4 \times Z_3 \times U(1)_{FN}$, μ to e conversion in nuclei can be included in our discussion, since in the SUSY model considered here it is driven by a γ penguin graph similar to that entering the decay $\mu^- \to e^- e^+ e^-$. The conversion rate CR($\mu \to e$ in nuclei) is then related directly to the branching ratio of $\mu \to e\gamma$, through the relation (the range spans the nuclei used as target in real experiment)

$$1.5 \times 10^{-3} \leq \frac{CR(\mu \to e)}{BR(\mu \to e\gamma)} \leq 3 \times 10^{-2} \tag{5.67}$$

Given the current experimental limit from SINDRUMII [87] with a gold target, $CR^{Au} \leq 6.1 \times 10^{-13}$, this channel is not competitive with $\mu \to e\gamma$. However, if Mu2e [88] and PRIME [89] experiments will reach the sensitivity of $CR^{Al} \leq 6 \times 10^{-17}$ and $CR^{Ti} \leq 10^{-18}$, they could realistically set the most stringent constraint on lepton flavor violation. For a titanium target $CR^{Ti} = 0.5 \times 10^{-2}\, BR(\mu \to e\gamma)$ [90]. Setting $u = 0.05$ we get $m_{SUSY} \gtrsim 6.6$ TeV, while for $u = 0.005$, $m_{SUSY} \gtrsim 2.3$ TeV.

5.4 Conclusion of the Chapter

Violation of individual lepton numbers has been established in neutrino oscillations and might be confirmed in rare transitions involving charged leptons. Discovering LFV in charged lepton decays would represent a major step towards the solution of the flavor puzzle. First of all LFV in tau or muon decays at an observable rate requires new physics at an energy scale M not too far from the TeV scale, opening the exciting possibility of producing and detecting the new particles responsible for LFV at the LHC. Moreover, in many models the same parameters that describe neutrino masses and mixing angles are also responsible for LFV, and testable predictions can be obtained. In a previous set of papers, radiative decays of charged leptons have been studied, both in a general effective Lagrangian approach and in a specific SUSY realization of $A_4 \times Z_3 \times U(1)_{FN}$. The three decays $\mu \to e\gamma$, $\tau \to \mu\gamma$ and $\tau \to e\gamma$ have similar rates in these models, but the rates derived from the effective Lagrangian scale as u^2 and require rather large values for the scale M, while in the SUSY realization the rates can be much more suppressed and can allow for a more accessible scale of new physics M.

In the present chapter we have extended the analysis to cover all LVF transitions. We have analyzed the most general four-lepton effective Lagrangian invariant under $A_4 \times Z_3 \times U(1)_{FN}$. Such a Lagrangian describes several transitions that violate lepton flavor and that are not suppressed by any powers of t and/or u. All these unsuppressed transitions

satisfy the selection rule $\Delta L_e \Delta L_\mu \Delta L_\tau = \pm 2$, which would provide a nice signature of the assumed flavor symmetry. For instance the decays $\tau^- \to \mu^+ e^- e^-$ and $\tau^- \to e^+ \mu^- \mu^-$ would be favored over all the other decays with three charged leptons in the final state. Indeed, calling ε the strength of the generic four-lepton interaction in units of the Fermi constant, the non-observation of these tau decays provide the strongest bound on ε from the existing data: $|\varepsilon| < (2 \div 3) \times 10^{-4}$. If interpreted as a bound on the scale of new physics M, this requires M above approximately 10 TeV. Slightly milder bounds comes from the observed universality of leptonic muon and tau decays and from the agreement between the Fermi constant measured in the muon decay and that extracted from the m_W/m_Z ratio.

Then we have analyzed LFV in the specific SUSY realization of $A_4 \times Z_3 \times U(1)_{FN}$. In this model, LFV proceeds through one-loop diagrams where sleptons, charginos and neutralinos are exchanged. Working in the super CKM basis, LFV is due to off-diagonal entries in the slepton mass matrices and can be analyzed in the mass-insertion approximation. Contrary to the expectation based on the general effective Lagrangian, a different hierarchy among the rates of LFV transitions is predicted. Processes where the individual lepton number is violated by a single unit, like $\mu^- \to e^- e^+ e^-$, $\tau^- \to e^- e^+ e^-$, $\tau^- \to \mu^- \mu^+ \mu^-$, $\tau^- \to \mu^- e^+ e^-$, $\tau^- \to e^- \mu^+ \mu^-$ are favored, with the corresponding rates being suppressed by $u^4 \div t^2 u^2$, while $\tau^- \to \mu^+ e^- e^-$ and $\tau^- \to e^+ \mu^- \mu^-$ are more suppressed, their rates scaling as $u^6 t^2$ and $u^4 t^4$, respectively. We have traced back this "anomalous" behavior to the fact that, in the limit of vanishing u and t, the low-energy SUSY Lagrangian acquires a much larger flavor symmetry: $SU(3)_L \times U(1)_{eR} \times U(1)_{\mu R} \times U(1)_{\tau R}$, which forbids any flavor-violating transition in the lepton sector. We can also understand the predictions of the SUSY case by inspecting the relevant interaction terms. Once we go in the super CKM basis, neglecting Higgsino interactions that are suppressed by small lepton masses, all the relevant interaction terms are flavor-diagonal. The only source of flavor violations are the off-diagonal terms of slepton masses. But slepton masses are diagonal when t and u vanish and in this limit lepton flavor is conserved. The crucial point is that in the SUSY model lepton flavor violation proceeds through bilinear terms of the low-energy Lagrangian. The symmetry group $A_4 \times Z_3 \times U(1)_{FN}$ allows for quartic invariant operators which violate lepton flavor, such as the effective Lagrangian we have discussed in the first part of this work, but it forbids any LFV at the level of bilinear terms. Our SUSY model does not represent the most general realization of the flavor symmetry $A_4 \times Z_3 \times U(1)_{FN}$ and leads to more restrictive conclusion about LFV processes. One the one hand this feature might allow to discriminate the SUSY realization of $A_4 \times Z_3 \times U(1)_{FN}$ from other models possessing the same flavor symmetry, but having a more general structure of interaction terms. On the other hand, as we have seen, in the SUSY model there are several characteristic correlations among LFV transitions, which could hopefully allow to test $A_4 \times Z_3 \times U(1)_{FN}$ against other possible underlying flavor symmetries. At the moment, given the present experimental sensitivity, $\mu \to e\gamma$ appear as the favorite channel. In the future, with improved experimental facilities, μ to e conversion in nuclei could provide the most stringent test of the model.

Chapter 6

Multi-Higgs Models

In the models analyzed in the previous chapters, one introduces flavons, heavy scalar fields charged in the flavor space. Once the flavons develop specific vacuum expectation values (VEVs), this translates to structures in the masses and mixing of the fermions. However, imposing the correct symmetry breaking patterns on the flavons is highly non-trivial. This holds in particular if two or more flavons are used, breaking in different directions in flavor space. So far, only a few techniques have been developed, all of which need a supersymmetric context or the existence of extra dimensions [42]. Alternatively, one can look at models that require only one flavor symmetry breaking direction. In this case the scalar potential that implements the breaking can be non supersymmetric and does not require extra dimensions. Of particular interest is the possibility that one set of fields simultaneously takes the role of the flavons and the Standard Model (SM) Higgs fields, identifying the breaking scales of the electroweak and the flavor symmetries. In this chapter, we will consider the discrete flavor symmetry A_4 and we will assume that there are three copies of the Standard Model Higgs field, that transform among each other as a triplet of A_4 [91–96]. The presence of this extended Higgs sector has a deep impact on the high energy phenomenology: indeed new contributions to the oblique corrections as well as new sources of CP and flavor violation usually appear in this context. We will analyze the constraints coming from these observables for all the vacuum configurations allowed by the scalar potential and will discuss on the viability of each of them. After the analysis of that part of Higgs phenomenology which is independent from the fermion content of the theory, we will discuss flavor violation processes, first in a general way and the focusing on three models taken from the literature: two models for lepton mixing by Ma and Morisi-Peinado, and a model for quark mixing by Lavoura-Kuhbock. In the text they are labeled Model 1,2, and 3.

6.1 The A_4 Scalar Potential

We consider the Standard Model gauge group $SU(3)_c \times SU(2)_L \times U(1)_Y$ with the addition of a global flavor symmetry A_4. We consider three copies Φ_a, $a = 1, 2, 3$, of

the conventional SM Higgs field (i.e. a singlet of $SU(3)_c$, doublet of $SU(2)_L$ and with hypercharge $Y = 1/2$) such that the three Higgses are in a triplet of the flavor group A_4. Once the flavor structure of the quarks and leptons is specified, each Φ_a will couple to the three fermion families according to the group theory rules in a model dependent way.

Below, we will write down the most general scalar potential for the three Higgses that is invariant under the flavor and gauge symmetries of the model. After the fields occupy one of the minima of the potential, electroweak symmetry gets broken (while electromagnetism is conserved) and we can develop the fields around their vacuum expectation values as

$$\Phi_a = \frac{1}{\sqrt{2}} \begin{pmatrix} \text{Re}\ \Phi_a^1 + i\,\text{Im}\ \Phi_a^1 \\ \text{Re}\ \Phi_a^0 + i\,\text{Im}\ \Phi_a^0 \end{pmatrix} \to \frac{1}{\sqrt{2}} \begin{pmatrix} \text{Re}\ \phi_a^1 + i\,\text{Im}\ \phi_a^1 \\ v_a e^{i\omega_a} + \text{Re}\ \phi_a^0 + i\,\text{Im}\ \phi_a^0 \end{pmatrix}. \tag{6.1}$$

Here $v_a e^{i\omega_a}$ is the vacuum expectation value of the a^{th} Higgs field. One or two of the v_a can be zero, implying that the corresponding Higgs field does not develop a VEV. Furthermore, if all VEVs are real (so if all ω_a are zero) CP is conserved, while if one or more ω_as are nonzero, CP is broken. Note that in general, there is the freedom to put one of the phases to zero by a global rotation.

The most general potential $V[\Phi_a]$ can be written as

$$\begin{aligned} V[\Phi_a] &= \mu^2(\Phi_1^\dagger\Phi_1 + \Phi_2^\dagger\Phi_2 + \Phi_3^\dagger\Phi_3) + \lambda_1(\Phi_1^\dagger\Phi_1 + \Phi_2^\dagger\Phi_2 + \Phi_3^\dagger\Phi_3)^2 \\ &+ \lambda_3(\Phi_1^\dagger\Phi_1\Phi_2^\dagger\Phi_2 + \Phi_1^\dagger\Phi_1\Phi_3^\dagger\Phi_3 + \Phi_2^\dagger\Phi_2\Phi_3^\dagger\Phi_3) \\ &+ \lambda_4(\Phi_1^\dagger\Phi_2\Phi_2^\dagger\Phi_1 + \Phi_1^\dagger\Phi_3\Phi_3^\dagger\Phi_1 + \Phi_2^\dagger\Phi_3\Phi_3^\dagger\Phi_2) \\ &+ \frac{\lambda_5}{2}\left[e^{i\epsilon}[(\Phi_1^\dagger\Phi_2)^2 + (\Phi_2^\dagger\Phi_3)^2 + (\Phi_3^\dagger\Phi_1)^2] + e^{-i\epsilon}[(\Phi_2^\dagger\Phi_1)^2 + (\Phi_3^\dagger\Phi_2)^2 + (\Phi_1^\dagger\Phi_3)^2]\right], \end{aligned} \tag{6.2}$$

in agreement with the usual notation adopted in the two Higgs Doublet Models (2HDM) (for a review on this topic see [97]). The parameter μ^2 is typically negative in order to have a stable minimum away from the origin. All the other parameters, λ_i, are real parameters which must undergo to the condition for a potential bounded from below: this forces λ_1 and the combination $\lambda_1 + \lambda_3 + \lambda_4 + \lambda_5 \cos\epsilon$ to be positive.

It is interesting to notice that, contrary to other multi Higgs (MH) scenarios, here we can not recover the SM limit, with one light scalar and all the others decoupled and very heavy. The flavor symmetry constrains the potential parameters in such a way that the scalar masses are never independent from each other. This can be easily understood by a parameter counting: the scalar potential in eq. (6.2) presents 6 independent parameters and the number of the physical quantities is 8, i.e. the electroweak (EW) VEV and the seven masses for the massive scalar fields.

We will study the minima of the potential in eq. (6.2) under electromagnetism conserving VEVs as specified in eq. (6.1) by studying the first derivative system

$$\frac{\partial V[\Phi]}{\partial \Phi_{\mathcal{I}}} = 0\,, \tag{6.3}$$

where $\Phi_{\mathcal{I}}$ is of the fields Re Φ_a^1, Re Φ_a^0, Im Φ_a^1 or Im Φ_a^0 and by requiring that the Hessian

$$\frac{\partial^2 V[\Phi]}{\partial \Phi_{\mathcal{I}} \partial \Phi_{\mathcal{J}}} \tag{6.4}$$

has non negative eigenvalues, or in other words that all the physical masses are positive except those ones corresponding to the Goldstone bosons (GBs) that vanish.

In Sections 6.3 and 6.4 we will verify that this potential presents a number of solutions. Some of them are natural in the sense that they do not require *ad hoc* values of the potential parameters; these are only constrained by requiring the boundedness at infinity and the positivity of all the physical scalar masses. The only potential parameter constrained is the bare mass term μ^2 which is related to the physical Electroweak (EW) VEV, $v_w^2 = v_1^2 + v_2^2 + v_3^2$. Others require specific relations between the adimensional scalar potential parameters and may have extra Goldstone bosons.

6.2 The Physical Higgs Fields

The symmetry breaking of the Higgs fields of equation eq. (6.1) leads to a large number of charged and neutral Higgs bosons as well as the known Goldstone bosons of the Standard Model.

In the most general case, where CP is not conserved, the neutral real and imaginary components of eq. (6.1) mix to five CP non-definite states and a GB:

$$\begin{aligned} h_\alpha &= U_{\alpha a} \mathrm{Re}\, \phi_a^0 + U_{\alpha(a+3)} \mathrm{Im}\, \phi_a^0 \,, \\ \pi^0 &= U_{6a} \mathrm{Re}\, \phi_a^0 + U_{6(a+3)} \mathrm{Im}\, \phi_a^0 \,. \end{aligned} \tag{6.5}$$

Here $a = 1, 2, 3$ and $\alpha = 1 - 5$, while $\alpha = 6$ represents the GB π^0. In matrix form this reads

$$\begin{pmatrix} h_1 \\ \vdots \\ h_5 \\ \pi^0 \end{pmatrix} = U \begin{pmatrix} \mathrm{Re}\, \phi_1^0 \\ \vdots \\ \mathrm{Re}\, \phi_3^0 \\ \mathrm{Im}\, \phi_1^0 \\ \vdots \\ \mathrm{Im}\, \phi_3^0 \end{pmatrix} \tag{6.6}$$

Clearly eq. (6.5) holds also in the CP conserved case: in that case the 6 by 6 scalar mass matrix reduces to a block diagonal matrix with two 3 by 3 mass matrices leading to three CP even states and 2 CP odd states and the GB π^0.

The three charged scalars mix into two new charged massive states and a charged GB.

$$\begin{pmatrix} H_1^+ \\ H_2^+ \\ \pi^+ \end{pmatrix} = S \begin{pmatrix} \phi_1^1 \\ \phi_2^1 \\ \phi_3^1 \end{pmatrix} \,, \tag{6.7}$$

where π^+ is the Goldstone boson eaten by the gauge bosons W^+. In general, the S is a complex unitary matrix. In the special case where CP is conserved, its entries are real (and it is thus an orthogonal matrix).

6.3 CP Conserved Solutions

In this section, we will study minima of the potential in eq. (6.2) in which only $\mathrm{Re}\,\phi_a^0$ develops a VEV, i.e. the CP symmetry is conserved. In this case we expect having 3 neutral scalar CP-even states, 2 CP-odd states and 2 charged scalars as well as a real and a complex GBs originating from respectively the CP-odd states and the charged states.

In the CP-conserved case all the ω_a vanish and the first derivative system in eq. (6.3) reduces to

$$\begin{aligned}
v_1[2(v_1^2+v_2^2+v_3^2)\lambda_1+(v_2^2+v_3^2)(\lambda_3+\lambda_4+\lambda_5\cos\epsilon)+2\mu^2] &= 0\,,\\
v_2[2(v_1^2+v_2^2+v_3^2)\lambda_1+(v_1^2+v_3^2)(\lambda_3+\lambda_4+\lambda_5\cos\epsilon)+2\mu^2] &= 0\,,\\
v_3[2(v_1^2+v_2^2+v_3^2)\lambda_1+(v_1^2+v_2^2)(\lambda_3+\lambda_4+\lambda_5\cos\epsilon)+2\mu^2] &= 0\,,\\
v_1(v_2^2-v_3^2)\lambda_5\sin\epsilon &= 0\,,\\
v_2(v_1^2-v_3^2)\lambda_5\sin\epsilon &= 0\,,\\
v_3(v_2^2-v_1^2)\lambda_5\sin\epsilon &= 0\,,
\end{aligned} \tag{6.8}$$

where the first three derivatives refer to the real components Φ_a^0 and the second ones to the imaginary parts. In the most general case, when neither ϵ nor λ_5 is zero, the last three equations allow two different solutions

1) $v_1 = v_2 = v_3 = v = v_w/\sqrt{3}$;

2) $v_1 \neq 0$ and $v_2 = v_3 = 0$ (and permutations of the indices); in this case $v_1 = v_w$.

Both these solutions are solutions of the first three equations as well, provided that

$$\begin{cases}
\mu^2 = -(3\lambda_1+\lambda_3+\lambda_4+\lambda_5\cos\epsilon)v_w^2/3 & \text{for the first case}\\
\mu^2 = -\lambda_1 v_w^2 & \text{for the second case.}
\end{cases} \tag{6.9}$$

In this cases λ_5 can be chosen positive, as a sign can be absorbed in a redefinition of ϵ.

Next, we consider the case where $\sin\epsilon$ is 0. This implies $\epsilon = 0$ or π. We may however absorb the minus sign corresponding to the second case in a redefinition of λ_5 that is now allowed to span over both positive and negative values.

Assuming $v_1 \neq 0$, we may solve the first equation in eq. (6.8) with respect to μ^2. Then by substituting μ^2 in the other two equations we get

$$\begin{aligned}
v_2(v_1^2-v_2^2)(\lambda_3+\lambda_4+\lambda_5) &= 0\,,\\
v_3(v_1^2-v_3^2)(\lambda_3+\lambda_4+\lambda_5) &= 0\,.
\end{aligned} \tag{6.10}$$

Next to the two solutions present in the general case, this system has two further possible solutions

3) $v_3 = 0, v_2 = v_1 = v_w/\sqrt{2}$ and permutations. This requires

$$\mu^2 = -\left(4\lambda_1 + \lambda_3 + \lambda_4 + \lambda_5\right) v_w^2/4\,. \tag{6.11}$$

4) $(\lambda_3 + \lambda_4 + \lambda_5) = 0$. This condition implies that in the real neutral direction there is a enlarged–$O(3)$ accidental symmetry that is spontaneously broken by the vacuum configuration, thus we expect extra GBs. Indeed in this case v_1, v_2 and v_3 are only restricted to satisfy $v_1^2 + v_2^2 + v_3^2 = v_w^2$ and the parameter μ^2 is given by $\mu^2 = -\lambda_1 v_w^2$.

Finally, the case $\lambda_5 = 0$ allows special cases of the solutions 1) to 4), but does not give rise to new solutions. For this reason, we will discuss only the general cases and the case $\epsilon = 0$ in the remainder of this section and comment what happens for $\lambda_5 = 0$.

6.3.1 $\epsilon \neq 0$: The Alignment (v, v, v)

In the basis chosen, the vacuum alignment (v, v, v) preserves the Z_3 subgroup of A_4. It is convenient to perform a basis transformation into the Z_3 eigenstate basis, $1, 1' \sim \omega, 1'' \sim \omega^2$ according to

$$\begin{aligned} \varphi &= (\Phi_1 + \Phi_2 + \Phi_3)/\sqrt{3} \sim 1 \\ \varphi' &= (\Phi_1 + \omega\Phi_2 + \omega^2\Phi_3)/\sqrt{3} \sim \omega \\ \varphi'' &= (\Phi_1 + \omega^2\Phi_2 + \omega\Phi_3)/\sqrt{3} \sim \omega^2\,. \end{aligned} \tag{6.12}$$

When A_4 is broken to Z_3 in the Z_3 eigenstate basis, $\varphi \sim 1$ behaves like the standard Higgs doublets: its neutral real component develops a vacuum expectation values

$$m_{h_1}^2 = \frac{2}{3} v_w^2 (3\lambda_1 + \lambda_3 + \lambda_4 + \lambda_5 \cos\epsilon). \tag{6.13}$$

The neutral components of the other two doublets φ' and φ'' mix into two complex neutral states and their masses are given by

$$m_n^{\prime,\prime\prime\,2} = \frac{v_w^2}{6}\left(-\lambda_3 - \lambda_4 - 4\lambda_5\cos\epsilon \pm \sqrt{(\lambda_3+\lambda_4)^2 + 4\lambda_5^2(1+2\sin^2\epsilon) - 4(\lambda_3+\lambda_4)\lambda_5\cos\epsilon}\right). \tag{6.14}$$

The charged components of φ', φ'' do not mix, their masses being

$$m_{ch}^{\prime,\prime\prime\,2} = -\frac{v_w^2}{6}\left(3\lambda_4 + 3\lambda_5\cos\epsilon \pm \sqrt{3}\lambda_5\sin\epsilon\right). \tag{6.15}$$

6.3.2 $\epsilon \neq 0$: The Alignment $(v, 0, 0)$

In the chosen A_4 basis, the vacuum alignments $(v, 0, 0)$ preserves the Z_2 subgroup of A_4. As we did with the vacuum alignment that conserved the Z_3 subgroup, in this case

it is useful to rewrite the scalar potential by performing the following Z_2 conserving basis transformation

$$\begin{aligned} \Phi_1 &\to \Phi_1\,, \\ \Phi_2 &\to e^{-i\epsilon/2}\Phi_2\,, \\ \Phi_3 &\to e^{i\epsilon/2}\Phi_3\,. \end{aligned} \tag{6.16}$$

Φ_1 is even under Z_2 and behaves like the standard Higgs doublet, while Φ_2 and Φ_3 are odd. For what concerns the neutral states, the 6×6 mass matrix is diagonal in this basis and with some degenerated entries: using a notation similar to the 2DHM, we have

$$\begin{aligned} &m^2_{h_1} \equiv 2\lambda_1 v_w^2\,, && m^2_{h_2} = m^2_{h_3} = \frac{1}{2}(\lambda_3+\lambda_4-\lambda_5)v_w^2\,, \\ &m^2_{h_4} = m^2_{h_5} = \frac{1}{2}(\lambda_3+\lambda_4+\lambda_5)v_w^2\,, && m^2_{\pi^0} = 0\,, \end{aligned} \tag{6.17}$$

where the last state corresponds to the GB. The charged scalar mass matrix is also diagonal with

$$m^2_{C_1} = m^2_{C_2} = \frac{1}{2}\lambda_3 v_w^2\,, \qquad m^2_{\pi^+} = 0\,, \tag{6.18}$$

where the last state corresponds to the GB. The degeneracy in the mass matrices are imposed by the residual Z_2 symmetry. Contrary to the previous case the neutral scalar mass eigenstates are real and not complex.

6.3.3 $\epsilon = 0$: The Alignment $(v, v, 0)$

This vacuum alignment does not preserve any subgroup of A_4 and it holds that $v = v_w/\sqrt{2}$. From the minimum equations we have that

$$\mu^2 = -\frac{1}{4}v_w^2(4\lambda_1+\lambda_3+\lambda_4+\lambda_5)\,. \tag{6.19}$$

The scalar and pseudoscalar mass eigenvalues are given by

$$\begin{aligned} &m^2_{h_1} = -\frac{v_w^2}{2}(\lambda_3+\lambda_4+\lambda_5)\,, && m^2_{h_2} = \frac{v_w^2}{2}(4\lambda_1+\lambda_3+\lambda_4+\lambda_5)\,, \\ &m^2_{h_3} = \frac{v_w^2}{4}(\lambda_3+\lambda_4+\lambda_5)\,, && m^2_{h_4} = -\lambda_5 v_w^2\,, \\ &m^2_{h_5} = \frac{v_w^2}{4}(\lambda_3+\lambda_4-3\lambda_5)\,, && m^2_{\pi^0} = 0\,. \end{aligned} \tag{6.20}$$

For the charged sector we have

$$m^2_{C_1} = \frac{v_w^2}{4}(\lambda_3-\lambda_4-\lambda_5)\,, \qquad m^2_{C_2} = -\frac{v_w^2}{2}(\lambda_4+\lambda_5) \qquad m^2_{C_3} = 0\,. \tag{6.21}$$

For $\lambda_5 \neq 0$ the alignment $(v, v, 0)$ has the correct number of GBs, while for $\lambda_5 = 0$ we have an extra massless pesudoscalar. However in both cases, $\lambda_5 \neq 0$ or $\lambda_5 = 0$, the conditions $m^2_{h_1} > 0$ and $m^2_{h_3} > 0$ can not be simultaneously satisfied. This alignment is therefore a saddle point of the A_4 scalar potential we are studying.

6.3.4 $\epsilon = 0$: The Alignment (v_1, v_2, v_3)

This vacuum alignment, as the previous one, does not preserve any subgroup of A_4. A part from the condition $\epsilon = 0$, we recall that in this case there is the further constraint $\lambda_3 + \lambda_4 + \lambda_5 = 0$ and λ_5 may assume both positive and negative values since we have reabsorbed in the λ_5 sign the case $\epsilon = \pi$.

Let us define $v_w^2 = v_1^2 + v_2^2 + v_3^2 = (1 + s^2 + r^2)v_1^2$ with $s = v_2/v_1$ and $r = v_3/v_1$ respectively. The mass matrix for the neutral scalar states presents two null eigenvalues– as we expected since the condition $\lambda_3 + \lambda_4 + \lambda_5 = 0$ enlarges the potential symmetry– and a massive one

$$m{h_1}^2 = 2\lambda_1 v_w^2 \,. \tag{6.22}$$

At the same time the mass matrix for the CP-odd states has one null eigenvalue–the GB π^0 and two degenerate eigenvalues of mass

$$m_{h_2}^2 = m_{h_3}^2 = (\lambda_3 + \lambda_4)v_w^2 \,. \tag{6.23}$$

. Notice that for the special case $\lambda_5 = 0$ we have the constraint $\lambda_3 = -\lambda_4$ that implies two extra massless pseudoscalars. Finally for the charged scalars we have

$$m_{C_1}^2 = m_{C_2}^2 = \frac{1}{2}\lambda_3 v_w^2 \,, \qquad\qquad m_{C3}^2 = 0 \tag{6.24}$$

The total amount of GBs is 5 (7) for the case $\lambda_5 \neq 0$ ($\lambda_5 = 0$), so we have 2 (4) extra unwanted GBs: this situation is really problematic. We note that the introduction of terms in the potential that softly break A_4 can ameliorate the situation with the Goldstone bosons.

6.4 CP Non-Conserved Solutions

In this section, we consider vacua that exhibit spontaneous CP violation. This occurs if the VEV of at least one of the Higgses is inherently complex. A global rotation can always absorb one of the three phases of the VEVs.

We note that that the two natural vacua of the previous section (v, v, v) and $(v, 0, 0)$ do not have CP violating analogues as they have only one phase that can be reabsorbed to make all VEVs real.

6.4.1 The Alignment $(v_1 e^{i\omega_1}, v_2, 0)$

In this case the third doublet is inert and therefore we are left only with two doublets that develop a complex VEV and after the redefinition, there is only one phase ω_1. Taking the generic solution $(v_1 e^{i\omega_1}, v_2, 0)$ the minimum equations are solved if $\epsilon = -2\omega_1$ or $\epsilon = -2\omega_1 + \pi$, $v_1 = v_2 = v_w/\sqrt{2}$ and

$$\mu^2 = -\frac{v_w^2}{4}(4\lambda_1 + \lambda_3 + \lambda_4 + \lambda_5) \,. \tag{6.25}$$

The neutral and charged 6×6 mass matrices are quite simple and it is possible having analytical expression for the mass eigenvalues. For the neutral sector we have

$$\begin{aligned} m^2_{h_1} &= \frac{1}{2}v_w^2(-\lambda_3 - \lambda_4 - \lambda_5)\,, & m^2_{h_2} &= \frac{1}{2}v_w^2(4\lambda_1 + \lambda_3 + \lambda_4 + \lambda_5)\,, \\ m^2_{h_3} &= \frac{1}{4}v_w^2(\lambda_3 + \lambda_4 - \lambda_5 + 2\lambda_5\cos 3\omega_1)\,, & m^2_{h_4} &= -\lambda_5 v_w^2\,, \\ m^2_{h_5} &= \frac{1}{4}v_w^2(\lambda_3 + \lambda_4 - \lambda_5 - 2\lambda_5\cos 3\omega_1)\,, & m^2_{\pi^0} &= 0\,, \end{aligned} \tag{6.26}$$

and for the charged one we have

$$m^2_{C_1} = \frac{v_w^2}{4}(\lambda_3 - \lambda_4 - \lambda_5)\,, \qquad m^2_{C_2} = \frac{v_w^2}{2}(-\lambda_4 - \lambda_5)\,, \qquad m^2_{C_3} = 0\,. \tag{6.27}$$

We see that the mass of the fourth neutral boson selects negative values for λ_5, i.e. the second solution $\epsilon = -2\omega_1 + \pi$. It is interesting to see that in the CP conserved limits $\omega_1 \to 0$ (or π), it is not possible to have both $m^2_{h_1}$ and $m^2_{h_3}$ (respectively $m^2_{h_5}$) positive, but that in the general case, there are points in parameter space where indeed all masses are positive. This is in particular clear in the region around $\cos 3\omega_1 = 0$.

Finally, as for the CP conserved case, for $\lambda_5 = 0$ we have two problems: an extra GB and we cannot have all positive massive eigenstates.

6.4.2 The Alignment $(v_1 e^{i\omega_1}, v_2 e^{i\omega_2}, v_3)$

In this case all the doublets develop a VEV $v_i \neq 0$, so we may have two physical CP violating phases. We have the freedom to take $\omega_3 = 0$. Minima are obtained for $\omega_2 = -\omega_1$ and $v_2 = v_1 = v$. Defining $v_3 = rv$ and $v_1^2 + v_2^2 + v_3^2 = v_w^2$ We can also get

$$\begin{aligned} \mu^2 &= -\tfrac{v_w^2}{2+r^2}[(2+r^2)\lambda_1 + \lambda_3 + \lambda_4 + \lambda_5\cos(\epsilon - 2\omega_1)]\,, \\ \lambda_5 &= \frac{(r^2-1)(\lambda_3+\lambda_4)\sin\omega_1}{(r^2-1)\sin(\epsilon-\omega_1) - 2\cos\epsilon\sin(3\omega_1)}\,. \end{aligned} \tag{6.28}$$

and one of the following two conditions

$$\begin{aligned} &i) \quad \lambda_4 = -\lambda_3\,, \\ &ii) \quad \tan\epsilon = \frac{r^2\sin 2\omega_1 + \sin 4\omega_1}{r^2\cos 2\omega_1 - \cos 4\omega_1}\,. \end{aligned} \tag{6.29}$$

To test the validity of the solution so far sketched it is necessary to check to be in a true minimum of the potential and not to have extra GBs a part from those eaten by the gauge bosons.

Case i)

In this case the constraints $\lambda_4 = -\lambda_3$ puts λ_5 to zero and enlarge substantially the symmetries of the potential: we have an accidental $O(3)$ in the neutral real direction and

two accidental $U(1)$s due to $\lambda_5 = 0$. For this reason the neutral spectrum has 5 massless particles, the GB π^0 and 4 other GBs, and only one massive state

$$m_{h_1}^2 = 2\lambda_1 v_w^2 \,. \tag{6.30}$$

The charged scalars are

$$m_{C_1}^2 = m_{C_2}^2 = \frac{1}{2}\lambda_3 v_w^2 \,, \qquad\qquad m_{C3}^2 = 0 \tag{6.31}$$

The massive states are degenerate as in the CP conserving minima studied in

Case *ii*)

As it is not possible to find analytical solutions, here we will study the limit with r very large. This particular choice is justified by the fact that models present in literature [92,93] fall in this case.

We may then perform an expansion in term of $1/r$ and neglect terms of order $1/r^2$. From eq. (6.29) we have that

$$\epsilon \sim 2\omega_1 + N\pi \,, \tag{6.32}$$

and then eq. (6.28) reduces to

$$\begin{aligned} \mu^2 &\sim -\lambda_1 v_w^2 \,, \\ \lambda_5 &\sim -(\lambda_3 + \lambda_4) \,, \end{aligned} \tag{6.33}$$

Under these approximations we find a massless neutral scalar state, $m_{\pi^0}^2 = 0$, and the other 5 neutral masses are given at leading order by

$$\begin{aligned} &m_{h_1}^2 \sim m_{h_2}^2 \sim f[\lambda_i]\mathcal{O}(1/r^2) v_w^2 \,, \\ &m_{h_3}^2 \sim 2\lambda_1 v_w^2 \,, \\ &m_{h_4}^2 \sim m_{h_5}^2 \sim (\lambda_3 + \lambda_4) v_w^2 \,, \end{aligned} \tag{6.34}$$

where once more $f[\lambda_i]$ stays for a linear combination of the λ's potential parameters. The charged scalar mass matrix is diagonal up to terms of order $\mathcal{O}(1/r^2)$ with two massive degenerate states

$$m_{C_1}^2 = m_{C_2}^2 = \lambda_3 v_w^2/2 \,, \tag{6.35}$$

and the correct number of GBs.

We see that the expressions for $m_{h_{1,2}}^2$ say that we may have two very light neutral scalars. Taking as reference values for r the range $50 \div 200$ we find

$$m_{h_{1,2}}^2 \sim \sqrt{f[\lambda_i]}\, 5\,\text{GeV}(1\,\text{GeV}) \,, \tag{6.36}$$

giving

$$\begin{aligned} m_{1,2}^2 &\leq 50^2 \quad \text{GeV}^2 \quad \text{for} \quad r \sim 50 \,, \\ m_{1,2}^2 &\leq 10^2 \quad \text{GeV}^2 \quad \text{for} \quad r \sim 200 \,, \end{aligned} \tag{6.37}$$

where 50(10) GeV may be obtained only for very peculiar combination of the potential parameters. In other words we expect that also in the majority of the cases for r in the range $50 - 200$ we will have $m^2_{1,2}$ very light.

Of course, this does not mean that these states will be light for any value of r but it is a quite strong hint that it is possible that this could be what indeed happens. As mentioned before, the addition of soft A_4 breaking terms to the potential may help in the cases of Goldstone bosons or very light bosons.

6.5 Bounds From The Higgs Phenomenology

In this section we analyse the phenomenology corresponding to the different vacua discussed above: unitarity, Z and $W^\pm$ decays and oblique parameters. In this way we manage to constrain the parameter space and, in some cases, to rule out the studied vacuum configuration.

6.5.1 Unitarity

In this section we account for the tree level unitarity constraints coming from the additional scalars present in the theory. We examine the partial wave unitarity for the neutral two-particle amplitudes for $s \gg M_W^2, M_Z^2$. We can use the equivalence theorem, so that we can compute the amplitudes using only the scalar potential described in eq. (6.2). In the regime of large energies, the only relevant contributions are the quartic couplings in the scalar potential [98–101] and then we can write the $J = 0$ partial wave amplitude a_0 in terms of the tree level amplitude T as

$$a_0(s) \equiv \frac{1}{32\pi} \int_{-1}^{1} \mathrm{d}\cos\theta \; T(s) = \frac{1}{16\pi} F(\lambda_i) \,, \tag{6.38}$$

where F represents a function of the λ_i couplings. Using for simplicity the notation

$$\Phi_a = \begin{pmatrix} w_a^+ \\ \dfrac{v_a e^{i\omega_a} + h_a^0 + i z_a}{\sqrt{2}} \end{pmatrix} \,, \tag{6.39}$$

we can write the 30 neutral two-particle channels as follows:

$$w_a^+ w_b^- \,, \; \frac{z_a z_b}{\sqrt{2}} \,, \; \frac{h_a^0 h_b^0}{\sqrt{2}} \,, \; h_a^0 z_b \,. \tag{6.40}$$

Once written down the full scattering matrix a_0, we find a block diagonal structure. The first 12×12 block concerns the channels

$$w_1^+ w_1^- \,, \; w_2^+ w_2^- \,, \; w_3^+ w_3^- \,, \; \frac{z_1 z_1}{\sqrt{2}} \,, \; \frac{z_2 z_2}{\sqrt{2}} \,, \; \frac{z_3 z_3}{\sqrt{2}} \,, \; \frac{h_1^0 h_1^0}{\sqrt{2}} \,, ; \frac{h_2^0, h_2^0}{\sqrt{2}} \,, \; \frac{h_3^0, h_3^0}{\sqrt{2}} \,, \; h_1^0 z_1 \,, \; h_2^0 z_2 \,, \; h_3^0 z_3 \,,$$

while the other three 6×6 blocks are related to the channels

$$w_a^+ w_b^- \,,\; w_b^+ w_a^- \,,\; h_a^0 z_b \,,\; h_b^0 z_a \,,\; z_a z_b \,,\; h_a^0 h_b^0 \,,$$

once we specify the labels $(a,\, b)$ as (1, 2), (1, 3) and (2, 3). Notice that up this point the analysis is completely general and is valid for all the vacua presented. We specify the vacuum configuration, expressing the quartic couplings λ_i in terms of the masses of the scalars. Afterwards, putting the constraint that the largest eigenvalues of the scattering matrix a_0 is in modulus less than 1, we find upper bounds on the scalar masses which we use in our numerical analysis.

6.5.2 Z And $W^\pm$ Decays

From an experimental point of view gauge bosons decays into scalar particles are detected by looking at fermionic channels, such as for example $Z \to hA \to 4f$ in the 2HDM, or Z decays into partial or total missing energy in a generic new physics scenario. From this point of view gauge bosons decays bound the Higgs sector in an extremely model dependent way. However since in the SM the Z and the $W^\pm$ decays into 2 fermions, 4 fermions or *all* have been precisely been calculated and measured, we may focus on the decays $Z, W^\pm \to all$. Doing this we overestimate the allowed regions in the parameter space, but we have a first and model independent cut arising by the gauge bosons decay. Once we will pass to a model dependent analysis the region may only be restricted, not enlarged. Furthermore, defining the contribution from new physics as $\Delta\Gamma$, since

$$\Delta\Gamma^{2f}_{Z,W^\pm} \sim \Delta\Gamma^{4f}_{Z,W^\pm} \sim \Delta\Gamma^{all}_{Z,W^\pm} \ll \Gamma_{Z,W^\pm} \,, \tag{6.41}$$

we expect the error we commit being quite small.

From LEP data we have

$$\Gamma^{\rm exp}_{Z,W^\pm} = \Gamma^{\rm SM}_{Z,W^\pm} + \Delta\Gamma_{Z,W^\pm} \tag{6.42}$$

with $\Delta\Gamma_Z \sim 0.0023$ GeV and $\Delta\Gamma_{W^\pm} \sim 0.042$ GeV [19]. Therefore we may calculate the width

$$\begin{aligned} Z &\to h_i h_j \,, \\ W^+ &\to H_i^+ h_j \,. \end{aligned} \tag{6.43}$$

for the different multi Higgs (MH) vacuum configuration studied and select the points that satisfy

$$\Gamma^{MH}_{Z,W^\pm} \leq \Delta\Gamma_{Z,W^\pm} \,. \tag{6.44}$$

Here we have indicated the generic $Z \to h_i h_j$ referring to our notation introduced in Section 6.1. Clearly when CP is conserved the h_i have defined CP and only couplings to CP odd states are allowed. Of course this is not true for the configuration when CP is spontaneously broken.

In the vacuum analysis we did we have seen that in few situations we have extra massless or very light particles. For those cases the gauge bosons decays put strong bounds. For what concerns the Z decays we have

$$\begin{cases} k_Z \leq \Delta\Gamma_Z \dfrac{16\pi}{m_Z}\dfrac{4c_W^2}{g^2} & \text{if both particles } h_i \text{ and } h_j \text{ are massless}\,, \\ k_Z \left(1-\dfrac{m_{h_i}^2}{m_Z^2}\right)^3 \leq \Delta\Gamma_Z \dfrac{16\pi}{m_Z}\dfrac{4c_W^2}{g^2} & \text{if } h_j \text{ is massless and } 0 < m_{h_i}^2 < m_Z^2\,, \\ k_Z \left(1-\dfrac{m_{h_i}^2+m_{h_j}^2}{m_Z^2}\right)^3 \leq \Delta\Gamma_Z \dfrac{16\pi}{m_Z}\dfrac{4c_W^2}{g^2} & \text{if } h_i, h_j \neq 0 \text{ and } 0 < m_{h_i}^2 + m_{h_j}^2 < m_Z^2\,. \end{cases} \tag{6.45}$$

where g is the $SU(2)$ gauge coupling, c_W the cosine of the Weinberg angle θ_W and the parameter k_Z is given by

$$k_Z = \left(-U_{ab}^T U_{(a+3)c}^T + U_{(a+3)b}^T U_{ac}^T\right)^2\,, \tag{6.46}$$

with U defined in eq. (6.6).

Similarly for the $W^\pm$ decays we have

$$k_W \left(1-\frac{m_{C_i}^2}{m_W^2}\right)^3 \leq \Delta\Gamma_W \frac{16\pi}{m_W}\frac{4c}{g^2} \qquad \text{if } h_j \text{ is massless and } m_{C_i}^2 < m_W^2 \tag{6.47}$$

where, in analogy to the Z decay, the parameter k_W is given by

$$k_W = \left|S_{ab}^\dagger U_{ac}^T\right|^2 + \left|S_{(a+3)b}^\dagger U_{(a+3)c}^T\right|^2\,, \tag{6.48}$$

with S defined in eq. (6.7).

6.5.3 Large Mass Higgs Decay

Electroweak data analysis considering the data from LEP2 [102] and Tevatron [103] put an upper bound on the mass of the SM Higgs of 194 GeV at 99% CL [19]. In a MH scenario this bound may be roughly translated in the upper bound for the lightest scalar mass, m_{h_1}. For large values of the SM Higgs mass, $m_h \geq 2m_W$, the main channel decay is $h \to W^+W^-$ and the upper bound is completely model independent. Let us indicate as $\Gamma_{WW}^{SM}(194)$ the branching ratio of the SM Higgs into two $W^\pm$ at a mass of 194 GeV.

In a MH model the lightest Higgs boson couples to the gauge bosons with a coupling that is

$$\begin{aligned} g_{h_1 ZZ} &= \beta\, g_{hZZ}^{SM}\,, \\ g_{h_1 WW} &= \beta\, g_{hWW}^{SM}\,, \end{aligned} \tag{6.49}$$

with $\beta \leq 1$. In our case for example β is given by

$$f_a(\cos\omega_a\, U_{a1}^T + \sin\omega_j\, U_{(a+3)1}^T)\,, \tag{6.50}$$

with $f_a = v_a/v_w$ and ω_a the corresponding CP phase. Taking into account that h_1 is less produced then the SM Higgs and that its $\Gamma^{MH}_{WW}(m_{h_1})$ is reduced with respect to the SM one,

$$\Gamma^{MH}_{WW}(m_{h_1}) \sim |\beta|^4 \Gamma^{SM}_{WW}(m_{h_1}) \leq \Gamma^{SM}_{WW}(194)\,, \tag{6.51}$$

we can roughly constrain the upper bound for masses $m_{h_1} \geq 194$ GeV.

6.5.4 Constraints By Oblique Corrections

The consistence of a MH model has to be checked also by means of the oblique corrections. These corrections can be classified [104–108] by means of three parameters, namely TSU, that maybe written in terms of the physical gauge boson vacuum polarizations as [109]

$$\begin{aligned}
T &= \frac{4\pi}{e^2 c_W^2 m_Z^2}\left[A_{WW}(0) - c_W^2 A_{ZZ}(0)\right]\,,\\
S &= 16\pi \frac{s_W^2 c_W^2}{e^2}\left[\frac{A_{ZZ}(m_Z^2) - A_{ZZ}(0)}{m_Z^2} - A'_{\gamma\gamma}(0) - \frac{(c_W^2 - s_W^2)}{c_W s_W} A'_{\gamma Z}(0)\right]\,,\\
U &= -16\pi \frac{s_W^2}{e^2}\left[\frac{A_{WW}(m_W^2) - A_{WW}(0)}{m_W^2} - c_W^2 \frac{A_{ZZ}(m_Z^2) - A_{ZZ}(0)}{m_Z^2} - s_W^2 A'_{\gamma\gamma}(0) - 2 s_W c_W A'_{\gamma Z}(0)\right]\,,
\end{aligned} \tag{6.52}$$

where s_W, c_W are sine and cosine of θ_W and e is the electric charge. EW precision measurements severely constrain the possible values of the three parameters T, S and U. In the SM assuming $m_h^2 > m_Z^2$ we have

$$\begin{aligned}
T_h^{SM} &\sim -\frac{3}{16\pi c_W^2}\log\frac{m_h^2}{m_Z^2}\,,\\
S_h^{SM} &\sim \frac{1}{12\pi}\log\frac{m_h^2}{m_Z^2}\,,\\
U_h^{SM} &\sim 0\,.
\end{aligned} \tag{6.53}$$

For a Higgs boson mass of $m_h = 117$ GeV (and in brackets the difference assuming instead $m_h = 300$ GeV), the data allow [19]

$$\begin{aligned}
S^{exp} &= 0.10 \pm 0.10(-0.08)\\
T^{exp} &= 0.03 \pm 0.11(+0.09)\\
U^{exp} &= 0.06 \pm 0.10(+0.01)\,.
\end{aligned} \tag{6.54}$$

The constraints in eq. (6.54) must be rescaled not only for the different values of the Higgs boson mass but also for a different scalar or fermion field content: for example, if we assume to have a MH scenario this gives a contribution $T^{\rm MH}$ to the T-parameter and we need

$$T^{\rm NSS} - T_h^{\rm SM} = T^{exp}\,. \tag{6.55}$$

A detailed analysis on the TSU in a MH model has been presented in [110, 111] where all the details are carefully explained. However the resulting formulae are valid only for

scalar masses larger or comparable to m_Z. Since this is not the case for a generic MH model and particularly for the configurations studied so far, where we have a redundant number of massless or extremely light particles, we improved their results, getting full formulae valid for any value of the scalar masses (see the appendix C for details).

6.6 Results from Higgs Phenomenology

We have performed a numerical analysis for all vacuum configurations considered, neglecting the alignment $(v, v, 0)$ since in this case there are tachyonic states. Our aim was to find a region in the parameter space where all the Higgs constraints were satisfied for each configuration considered. We have analyzed the points generated through subsequent constraints, from the weaker one to the stronger according to

- points Y: true minima –all the squared masses positive– (yellow points in the figures);
- points B: unitarity bound (blue points);
- points G: Z and $W^{\pm}$ decays (green points);
- points R: TSU parameters (red points).

The ratios B/Y, G/B, R/G may be used to indicate which is the stronger constraint for each allowed minima. For almost each case we have compared the masses of the two lightest neutral states –except for the alignment studied in sec. 6.4.2 where we have only one massive neutral state– and the mass of the lightest neutral scalar versus the mass of the lightest charged one. Then we have plotted the TS oblique parameters for all the green points to check that T is the most constrained one –for this reason we have not inserted the plots concerning U.

On the contrary for the CP breaking alignment $(ve^{i\omega_1}, ve^{-i\omega_1}, rv)$ we have personalized the plots for reasons that will be clear in the following.

Notice that in all the following discussion, we refer as m_1 (m_2) to the (next-to-the-) lightest neutral state and as m_{ch_1} as the lightest charged mass state.

6.6.1 CP Conserved Solutions

The Alignment (v, v, v)

In sec. 6.3.1 we have redefined the initial 3 doublets in term of the Z_3 surviving symmetry representation: $\mathbf{1}$, $\mathbf{1}'$, $\mathbf{1}''$. One combination corresponds to a Z_3 singlet doublet, that behaves like the SM Higgs: it develops a non-vanishing VEV, gives rise to a CP even state which we call h_1 and to the three GBs eaten by the gauge bosons. The others two doublets, φ' and φ'', are inert. From these informations we may already figure out what we expect by the numerical scan:

1) when m_{h_1} is the smallest mass, h_1 is the lightest state and corresponds to the SM-like Higgs. As a result, the usual SM mass upper bound applies. On the contrary as long as we do not consider its coupling with the fermions we do not have a model independent lower mass bound. This is due to a combined effect of the CP and Z_3 symmetries: h_1 is CP even and singlet under Z_3, but couplings like $Zh_1\varphi'^0$, $Zh_1\varphi''^0$, $W^-h_1\varphi'^1$ or $W^-h_1\varphi''^1$ are forbidden because of Z_3 and then gauge boson decays cannot constrain the lower mass of h_1.

2) When φ'^0 (φ''^0) is the lightest state, we do not have an upper bound on this state because the couplings $\varphi'^0W^+W^-$ ($\varphi''^0W^+W^-$) is absent. On the contrary we may have a lower bound because couplings like $Z\varphi'^0\varphi''^0$ and $W^-\varphi'^0\varphi''^1$ are allowed.

Combining the two situations sketched in points 1) and 2), we expect neither lower nor upper bounds for the lightest Higgs mass: according to which of the two cases is most favored, we may expect a denser vertical region around $m_1 \sim m_Z/\sqrt{2}$ when the Z decay channel closes according to eq. (6.45) –case 2) more favored– or a denser vertical line around $m_1 \sim 194$ GeV, if the large Higgs mass decay constrain applies –case 1) more favored. Indeed by looking at fig. 6.1 we see that we may find R (allowed) points for very tiny m_1 masses and up to ~ 500 GeV when the unitarity bound starts to show its effect. However by looking at the crowded points in fig. 6.1 it seems that case 2) is slightly preferred with respect to case 1). Finally for the G points –those that satisfy the minimum, unitarity and decays conditions– we have compared the contributions to the oblique parameters T and S to see which of the two is more constraining. It turns out to be T, while we have not reported U because its behavior is very similar to S.

The Alignment $(v, 0, 0)$

For what concerns the second natural A_4 minimum, the Z_2 preserving one, things slightly change with respect to the Z_3 surviving case. By sec. 6.3.2 we know that as for the Z_3 case we have a SM-like doublet, Z_2 even, that develops the VEV, gives rise to a CP even neutral state, h_1, and to the GBs eaten by the gauge bosons. However contrary to the Z_3 case, in the Z_2 minima we have 4 Z_2 odd states, 2 CP even labeled $h_{2,3}$ and 2 CP odd labeled $h_{4,5}$. Moreover the 2 CP even (odd) are degenerate. As done in sec. 6.6.1 we may sketch what we expect from the numerical analysis:

1) when h_1, the Z_2 even SM-like Higgs, is the lightest we expect the SM Higgs upper bound but no lower bound because the interactions $Zh_1h_{4,5}$ are forbidden by the Z_2 symmetry;

2) when the two lightest are the Z_2 odd degenerate states $h_{2,3}$ –CP even– or $h_{4,5}$ –CP odd– we expect no upper bound. Moreover since they are degenerate we do not expect lower bound too. On the contrary we expect that Z and W decays constrain the third lightest neutral Higgs mass and that of the charged ones.

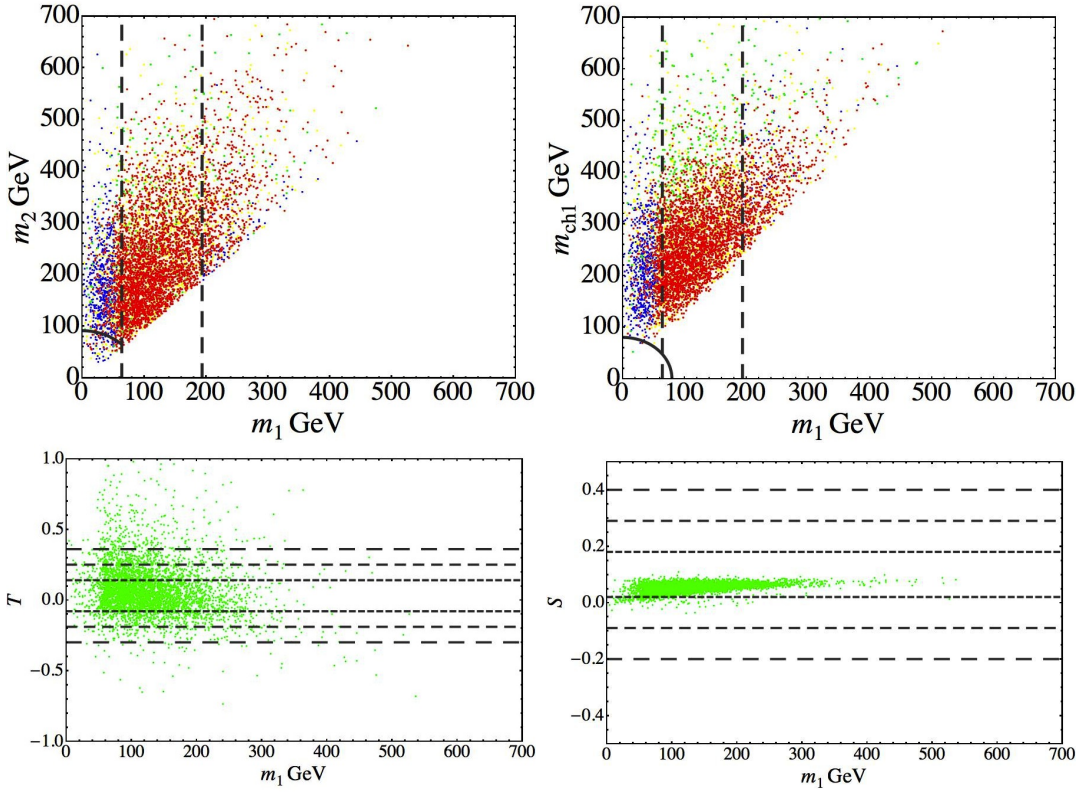

Figure 6.1: CP conserving alignment (v, v, v): *the upper panels show the lightest neutral mass* m_1 *versus the second lightest neutral mass* m_2 *and the lightest charged one* m_{ch_1} *respectively. The gray arc delimits the region below which the* Z *(* W*) decay channel opens. On the left plot the arc is only of* $45°$ *because* $m_2 \geq m_1$*. For points below the arc the* Z *(* W*) decay may happens. The points allowed stretch in the region close to the border because of the conditions of eq. (6.45). The dashed vertical lines indicates the approximated cuts that occur at* $m_1 \sim m_Z/\sqrt{2}$ *and* $m_1 \sim 194$ *GeV according to case* 2) *and case* 1) *respectively as explained in the text. The down panels show the contributions to* T *and* S *for the* G *points. The gray dashed lines indicate the experimental values at* 3, 2, 1σ *level –long,normal,short dashing respectively. The* T *parameter turns out to be the most constraining one.*

By looking at fig. 6.2 we see that indeed we have a large amount of points for which $m_1 = m_2$ for values from 0 up to 700 GeV, thus reflecting case 2). Then the points corresponding to case 1) have a sharp cut at $m_1 = 194$ GeV, that rejects many blue points, i.e. those satisfying the unitarity constrain but not the decays one. We have reported also m_1 versus m_3 to check that indeed, when $m_1 \to 0$, m_3 is bounded by m_Z as we expected. Our intuitions are also confirmed by the plot $m_1 - m_{ch_1}$. As for the Z_3 preserving case the most constraining oblique parameter is T.

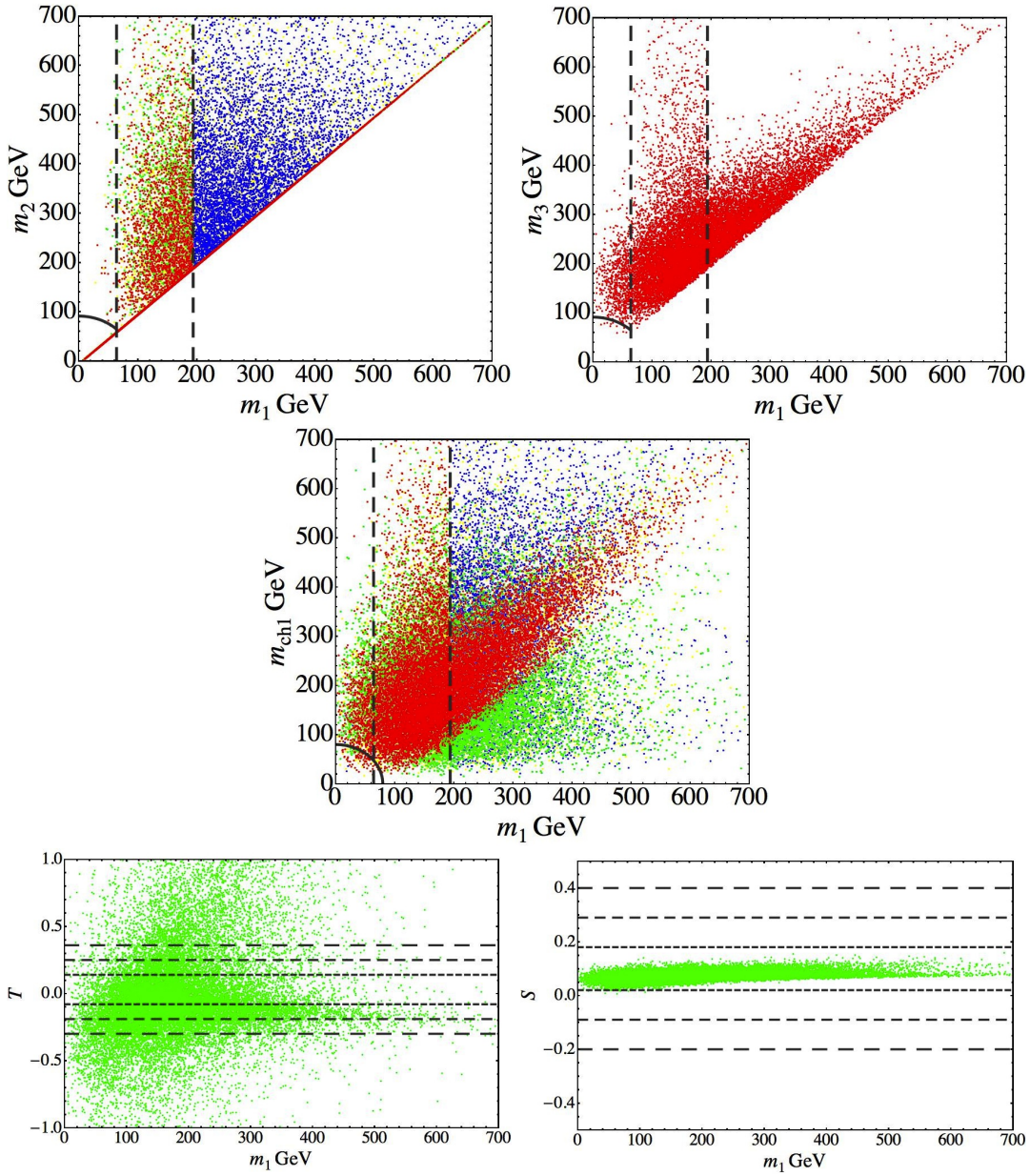

Figure 6.2: CP conserving alignment $(v, 0, 0)$: *the upper panels show* m_1 *versus* m_2 *(on the left) and third lightest* m_3 *(on the right). For the latter we reported only the R points. The central panel shows* m_1 *versus* m_{ch_1}*. The gray arc delimits the region below which the* Z *(*W*) decay channel opens while the second dashed vertical one the SM-Higgs mass upper bound at* 194 *GeV. The first dashed vertical line at* $m_1 = m_Z/\sqrt{2}$ *is reported to help a comparison with the* Z_3 *preserving case. On the first two plots the arc is only of 45 degrees because* $m_{2,3} \geq m_1$*. The down panels show the contributions to* T *and* S *for the G points. The* T *parameter turns out to be the most constraining one.*

The Alignment (v_1, v_2, v_3) with $\epsilon = 0$, $\lambda_3 + \lambda_4 + \lambda_5 = 0$

In this case we do not have any surviving symmetry which forbid some couplings. However from sec. 6.3.3 we know that the conditions $\epsilon = 0$, $\lambda_3 + \lambda_4 + \lambda_5 = 0$ give rise to

two extra massless CP even particles. Therefore we expect that

1) when the lightest massive state is CP odd, then its mass is bounded by the Z decay through eq. (6.45);

2) when the lightest massive state is CP even, then its mass could reach smaller values since the Z decay bound would constrain the combination of its mass with the lightest CP odd state mass.

Moreover in both cases we expect the mass of the lightest charged scalar bounded by W decay, according to eq. (6.47), due to its coupling with W and the massless particles.

By fig. 6.3 we see that it seems that case 2) happens very rarely because the cut at $m_1 \sim m_Z$ is in evidence. As for the Z_3 and Z_2 preserving minima the T parameter is the most constraining one.

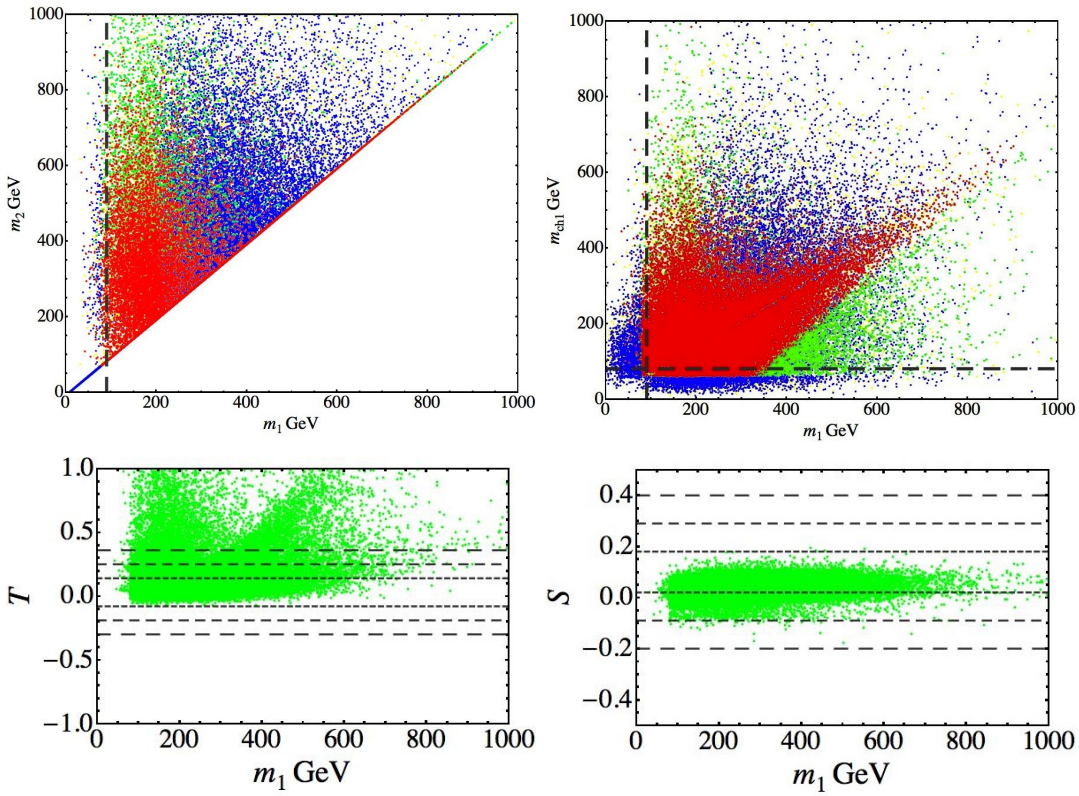

Figure 6.3: CP conserving alignment (v_1, v_2, v_3): *the upper panels show* m_1 *versus* m_2 *and* m_{ch_1} *respectively. The dashed lines at* $m_1 = m_Z$ *(vertical) and* $m_{ch1} = m_W$ *(horizontal) delimit the region below which the* Z *and* W *decay channels open respectively. The allowed points concentrate close to the borders according to eqs. 6.45-6.47. The down panels show the contributions to* T *and* S *for the G points. The* T *parameter turns out to be the most constraining one.*

6.6.2 CP Non-Conserved Solutions

The Alignment $(ve^{i\omega_1}, v, 0)$

As for the vacuum alignment (v_1, v_2, v_3) commented in sec 6.6.1 the alignment $(ve^{i\omega_1}, v, 0)$ does not preserve any A_4 subgroup. Moreover since even CP is broken any symmetry cannot help us in sketching the behavior we expect. In general any state, having a CP even and a CP odd component, may couple to Z and to another neutral state. However we expect limit situations in which for example CP is almost conserved and the 2 lightest states have almost the same CP parity. Thus for those cases we do not expect any lower bound on m_1 and m_2. On the contrary the coupling between the W with the lightest neutral and the lightest charged scalars does not go to zero when CP is almost restored. Then we expect that the quantity $m_1^2 + m_{ch_1}^2$ is bounded by the W decay (fig. 6.4). For what concerns the upper bound on the lighetst neutral mass state we do not expect any clear cut because we may not identify a SM-like Higgs.

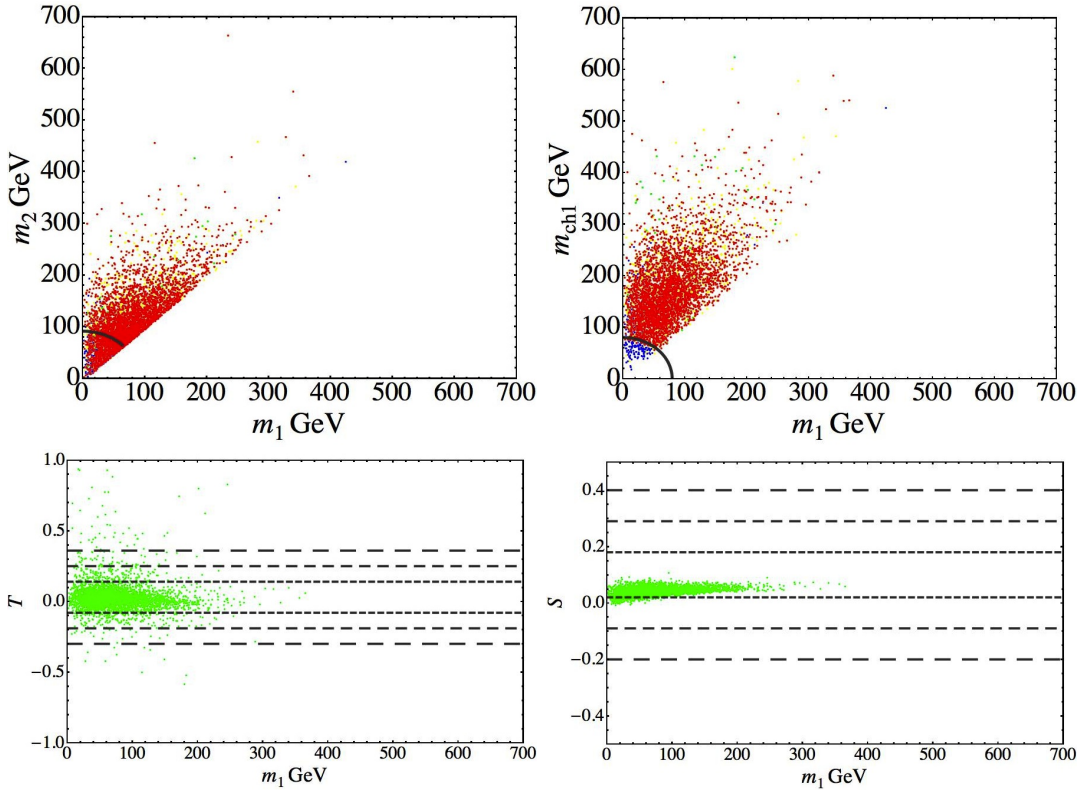

Figure 6.4: CP no conserving alignment $(ve^{i\omega_1}, v, 0)$: *as in the previous figure the upper panels show m_1 versus m_2 and m_{ch_1} respectively. In the plot on the right, the effect of the W decay constraint on $m_1^2 + m_{ch_1}^2$ is clear by looking at the B points. The down panels show the contributions to T and S for the G points. The T parameter turns out to be the most constraining one.*

The Alignment $(ve^{i\omega_1}, ve^{-i\omega_1}, rv)$ case $i)$

In sec. 6.4.2 we have seen that the alignment $(ve^{i\omega_1}, ve^{-i\omega_1}, rv)$ with the constrains $\lambda_5 = 0$, $\lambda_4 = -\lambda_3$, gives rise to 4 extra GBs and only to one neutral state. The simplicity of the analytical expressions for the three no vanishing masses ensures that the boundedness constrain $\lambda_1 > 0$ in addition to $\lambda_3 > 0$ give positive masses. Thus in this case the Y points are superfluous. As in the previous cases, we expect the B points to be similar to the Y ones, because we choose our parameters centered in 1 in order not to have problems with unitarity. In conclusion, for this case only the G and R points are interesting. Moreover we expect that the most stringent bound is given by the decay constrains and not by TSU: massless particles give a small contribution to the oblique parameters and due to the limited number of new particles (2 charged degenerate scalars) TSU should not deviate too much by the SM values. Indeed in fig. 6.5 it is shown that the oblique parameters at 3 σ level do not constrain at all the G points. For this reason we reported only the R points in the upper panel of fig. 6.5. By looking at the plot $m_1 - m_{ch_1}$ in fig. 6.5 we see that with respect to the minima so far analyzed we have much less points and that as expected there are cuts in correspondence of m_Z and m_W.

In conclusion, the solutions for the alignment $(ve^{i\omega_1}, ve^{-i\omega_1}, rv)$ with $\lambda_5 = 0$, $\lambda_4 = -\lambda_3$ are not easy to find, but the Higgs phenomenology does not completely rule out this vacuum configuration. We could introduce a weight to estimate how much a solution is stable or fine-tuned but this goes over the purposes of this work. We expect that this situation with 4 extra massless particles could be very problematic when considering the model dependent constraints [11].

$(ve^{i\omega_1}, ve^{-i\omega_1}, rv)$ case $ii)$

In the discussion of sec. 6.4.2 we have seen that in the limit $r >> 1$ we expect the presence of two very light particles. From all the numerical scans we performed we found out that solutions for the vacuum alignment $(ve^{i\omega_1}, ve^{-i\omega_1}, rv)$ with the constraints of case $ii)$ are very difficult to be found. Moreover from fig. 6.6 we see that for any value of r the two lightest states are always very light, thus confirming our rough analytical approximations and indicating that some cancellations have to occur to give all the masses greater then 0. This supports the difficulty to find solutions, difficulty that cannot to be ascribed to any constrain we imposed, because even in presence of 4 additional GBs as in sec. 6.6.2 we found out a significant larger number of solutions.

The presence of a single R point in fig. 6.6 is not statistically relevant, but more interesting is the order of magnitude of $m_{1,2}$: even in case $ii)$ we expect that the alignment $(ve^{i\omega_1}, ve^{-i\omega_1}, rv)$ may present serious problems once we add model dependent constraints [11].

Regarding the last VEV, in our previous paper we also stressed that some very light Higgs masses are expected. To avoid this feature, which is potentially in contrast with

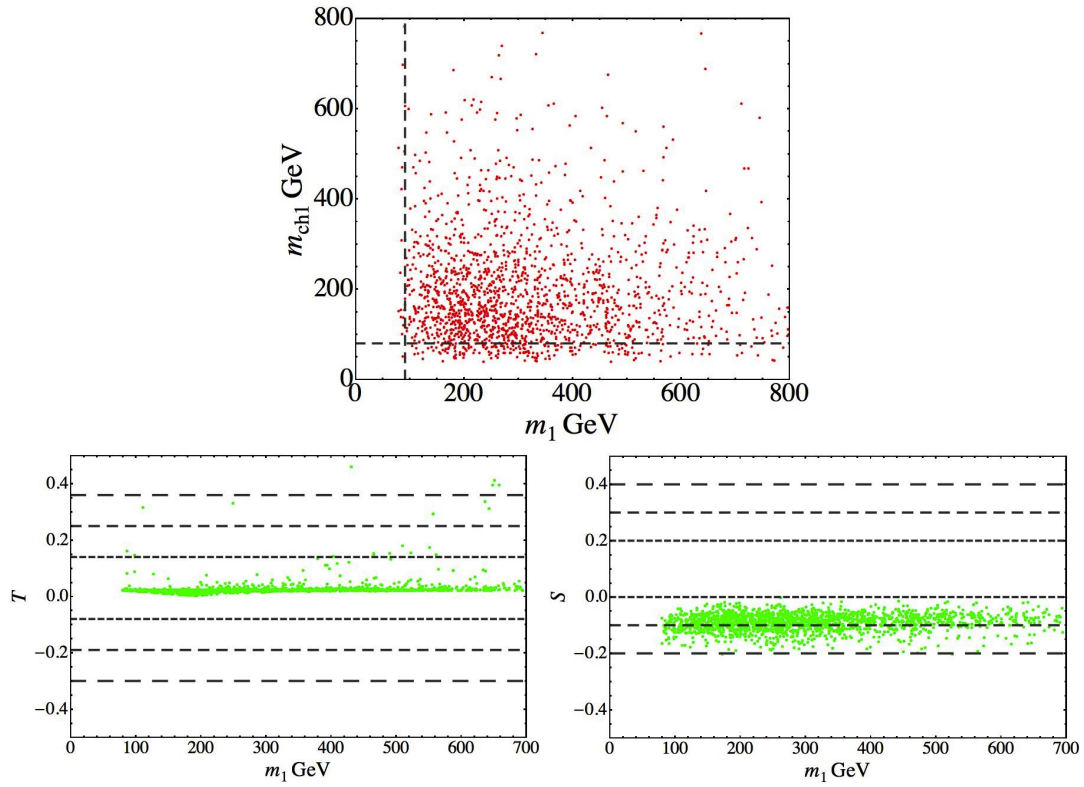

Figure 6.5: CP no conserving alignment $(ve^{i\omega_1}, ve^{-i\omega_1}, rv)$ case i): *the upper panel show* m_1 *versus* m_{ch_1}. *Only the R points are reported. The down panels show the contributions to T and S for the G points. For this specific case the TSU oblique parameter constrain is irrelevant compared to the decay one.*

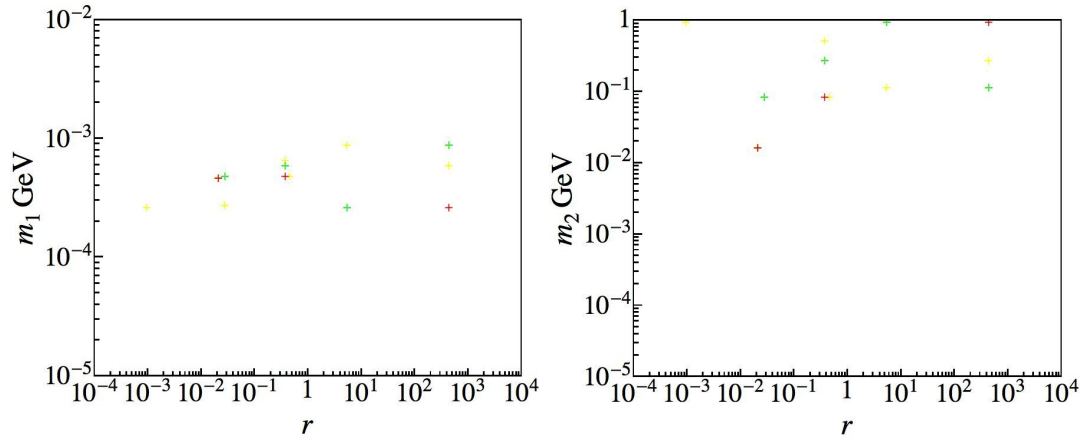

Figure 6.6: CP no conserving alignment $(ve^{i\omega_1}, ve^{-i\omega_1}, rv)$, case ii): *the panels show* m_1 *(on the left) and* m_2 *(on the right) versus* r. *The number of points is small, but the interesting information is the order of magnitude of the masses.*

the current limits on flavor violation, we add soft breaking terms to eq. (6.2) in the form

$$V_{A_4 soft} = v_w^2 \frac{m}{2}(\phi_1^\dagger \phi_2 + \phi_2^\dagger \phi_1) + v_w^2 \frac{n}{2}(\phi_2^\dagger \phi_3 + \phi_3^\dagger \phi_2) + v_w^2 \frac{k}{2}(\phi_1^\dagger \phi_3 + \phi_3^\dagger \phi_1)\,, \tag{6.56}$$

where m, n, k are adimensional parameters that should presumably be smaller than one. Notice that the chosen $V_{A_4 soft}$ is not the most general one but it prevents accidental extra $U(1)$ factor to appear.

6.7 General Analysis Of The Higgs-Fermion Interactions

We explicitly introduce the interaction of the Higgs triplets with fermions and deduce the phenomenological consequences. Without specifying the flavor group G_f and the fermion representations under it, in general Φ_a will couple to fermions through a given Y^a_{ij},

$$\mathcal{L}_Y = \left(Y^d_{ija}\overline{Q}_{Li}d_{Rj}\Phi_a + Y^u_{ija}\overline{Q}_{Li}u_{Rj}\Phi^\dagger_a\right) + (d \leftrightarrow e) + h.c. \tag{6.57}$$

where i and j are fermion family indices and a is the Higgs triplet index. Notice that, in order to keep the formulae compact, we simply use $d \leftrightarrow e$ to indicate that similar Yukawa terms are present in which down quarks are substituted by charged leptons. Without specifying any high-energy explanation for the neutrino masses, we consider the low-energy effective Weinberg operator: this term generates the neutrino masses and it has been already discussed in the models we will analyze in the next sections. After EW symmetry breaking according to eq. (6.1), the part of the Lagrangian including neutral Higgs fields becomes

$$\begin{aligned}\mathcal{L}_{Y,n} \;=\; & \left(Y^d_{ija}\overline{Q}^d_{Li}d_{Rj}\frac{v_a e^{i\omega_a}}{\sqrt{2}} + Y^d_{ija}\overline{Q}^d_{Li}d_{Rj}\frac{1}{\sqrt{2}}(\text{Re }\phi^0_a + i\,\text{Im}\,\phi^0_a) + \right. \\ & \left. + Y^u_{ija}\overline{Q}^u_{Li}u_{Rj}\frac{v_a e^{-i\omega_a}}{\sqrt{2}} + Y^u_{ija}\overline{Q}^u_{Li}u_{Rj}\frac{1}{\sqrt{2}}(\text{Re }\phi^0_a - i\,\text{Im}\,\phi^0_a)\right) + \\ & + (d \leftrightarrow e) + h.c.,\end{aligned} \tag{6.58}$$

while the part with the charged Higgs is

$$\mathcal{L}_{Y,ch} = \left(Y^d_{ija}\overline{Q}^u_{Li}d_{Rj}\Phi^1_a - Y^u_{ija}\overline{Q}^d_{Li}u_{Rj}(\Phi^1_a)^*\right) + (d \leftrightarrow e) + h.c. \tag{6.59}$$

Now we move to the mass basis of fermions through the transformations:

$$\overline{Q}^d_{Li} = \overline{\hat{Q}}^d_{Lr}V^{d\dagger}_{Lri}\,, \qquad\qquad d_{Rj} = V^d_{Rjs}\hat{d}_{Rs}\,, \tag{6.60}$$

and in analogous way for all the other particles. The neutral and the charged Higgs fields are also rotated into the mass basis, according to eqs. (6.6) and (6.7).

In the mass basis the part of the Lagrangian which includes the neutral Higgs becomes

$$\begin{aligned}\mathcal{L}_{Y,n} = & \left(\overline{\hat{d}}_r M^d_{(r)}\frac{1+\gamma_5}{2}\hat{d}_r + \overline{\hat{d}}_r(R^d)^\alpha_{rs}h_\alpha\frac{1+\gamma_5}{2}\hat{d}_s + \overline{\hat{u}}_r M^u_{(r)}\frac{1+\gamma_5}{2}\hat{u}_r + \overline{\hat{u}}_r(R^u)^\alpha_{rs}h_\alpha\frac{1+\gamma_5}{2}\hat{u}_s\right) + \\ & + (d \leftrightarrow e) + h.c.\end{aligned} \tag{6.61}$$

with

$$\begin{aligned} M^{d,u}_{ij} &= V^{d,u\dagger}_{Lri}\left(\sum_a \frac{v_a}{\sqrt{2}} Y^{d,u}_{ija}\right) V^{d,u}_{Rjs}\,, \\ (R^d)^\alpha_{rs} &= \left[V^{d\dagger}_{Lri}\frac{1}{\sqrt{2}}(iU^{\dagger(a+3)\alpha} + U^{\dagger a\alpha})Y^d_{ija}V^d_{Rjs}\right]\,, \\ (R^u)^\alpha_{rs} &= \left[V^{u\dagger}_{Lri}\frac{1}{\sqrt{2}}(-iU^{\dagger(a+3)\alpha} + U^{\dagger a\alpha})Y^u_{ija}V^u_{Rjs}\right]\,, \end{aligned} \tag{6.62}$$

and similarly for the leptons. The interaction with the charged Higgs becomes

$$\mathcal{L}_{Y,ch} = \left(\overline{\hat{u}}_r (T^d)^\beta_{rs}\hat{H}^+_\beta \frac{1+\gamma_5}{2}\hat{d}_s - \overline{\hat{d}}_r (T^u)^\beta_{rs}\hat{H}^-_\beta \frac{1+\gamma_5}{2}\hat{u}_s\right) + (d \leftrightarrow e) + h.c. \tag{6.63}$$

where

$$(T^{d,u})^\beta_{rs} = \left[V^{d,u\dagger}_{Lri} S^{\dagger b\beta} Y^{d,u}_{ijb} V^{d,u}_{Rjs}\right] \tag{6.64}$$

and similarly for the leptons. Expanding the hermitian conjugate, the Lagrangian can be written in a more compact form

$$\begin{aligned} \mathcal{L}_Y &= \Big(\overline{\hat{d}}_r M^d_{(r)}\hat{d}_r + \overline{\hat{d}}_r\big((I^d)^\alpha_{r,s} + \gamma_5 (J^d)^\alpha_{r,s}\big)h_\alpha \hat{d}_s \\ &\quad + \overline{\hat{u}}_r M^u_{(r)}\hat{u}_r + \overline{\hat{u}}_r\big((I^u)^\alpha_{r,s} + \gamma_5 (J^u)^\alpha_{r,s}\big)h_\alpha \hat{u}_s \\ &\quad + \overline{\hat{u}}_r\big(F^\beta_{r,s} + \gamma_5 G^\beta_{r,s}\big)\hat{H}^+_\beta \hat{d}_s + \overline{\hat{d}}_r\big(F^{\beta *}_{r,s} - \gamma_5 G^{\beta *}_{r,s}\big)\hat{H}^-_\beta \hat{u}_s\Big) + (d \leftrightarrow e)\,, \end{aligned} \tag{6.65}$$

with the new coefficients defined in the following way:

$$(I^{d,u})^\alpha_{r,s} = \frac{1}{2}\Big((R^{d,u})^\alpha_{rs} + ((R^{d,u})^\alpha_{sr})^*\Big)\,, \tag{6.66}$$

$$(J^{d,u})^\alpha_{r,s} = \frac{1}{2}\Big((R^{d,u})^\alpha_{rs} - ((R^{d,u})^\alpha_{sr})^*\Big)\,, \tag{6.67}$$

$$F^\beta_{r,s} = \frac{1}{2}\Big((T^d)^\beta_{rs})^* - ((T^u)^\beta_{sr})^*\Big)\,, \tag{6.68}$$

$$G^\beta_{r,s} = \frac{1}{2}\Big((T^d)^\beta_{rs})^* + ((T^u)^\beta_{sr})^*\Big)\,, \tag{6.69}$$

and similarly for leptons.

6.7.1 Flavor Changing Interactions

The interaction of fermions with the Higgs particles induces flavor violating processes in the lepton and quark sectors. In the former, rare decays of muon and tau particles into three leptons are allowed at tree-level, while processes as $l_i \to l_j\gamma$ take place through one-loop graphs. For the latter the possibility of $\Delta F = 2$ meson-antimeson oscillations is considered.

The Processes $\mu^- \to e^- e^- e^+$ and $\tau^- \to \mu^- \mu^- e^+$

We consider the decay of a muon into a positron and two electrons (fig. 6.7 on the left). In the approximation of massless final states, the decay amplitude is written as

$$\Gamma(\mu \to ee\overline{e}) = \frac{m_\mu^5}{(4\pi)^3 \times 24} I_{\mu eee}, \tag{6.70}$$

where the coefficient $I_{\mu eee}$ is a combination of I_{ij} and J_{ij}, that were defined in the previous section:

$$I_{\mu eee} = \left| \sum_\alpha \frac{I^\alpha_{\mu e} I^\alpha_{ee}}{m^{\alpha\,2}_H} \right|^2 + \left| \sum_\alpha \frac{J^\alpha_{\mu e} J^\alpha_{ee}}{m^{\alpha\,2}_H} \right|^2 + \left| \sum_\alpha \frac{I^\alpha_{\mu e} J^\alpha_{ee}}{m^{\alpha\,2}_H} \right|^2 + \left| \sum_\alpha \frac{J^\alpha_{\mu e} I^\alpha_{ee}}{m^{\alpha\,2}_H} \right|^2. \tag{6.71}$$

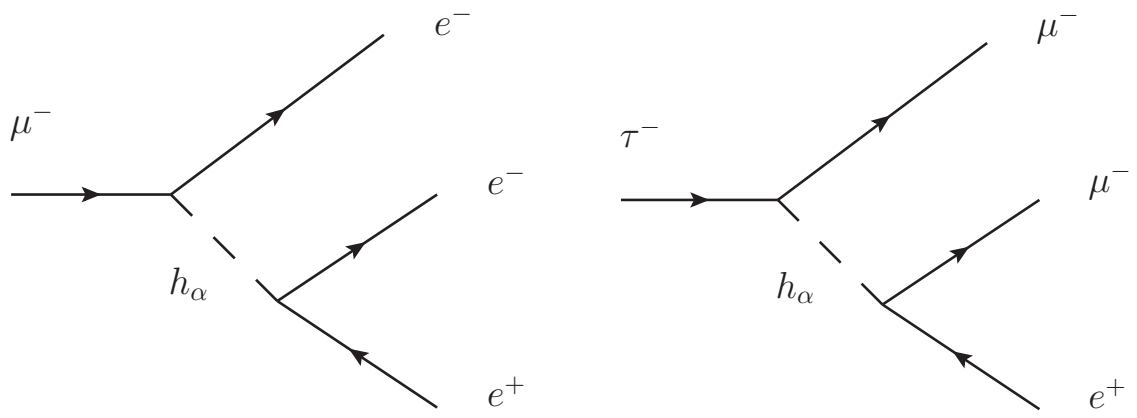

Figure 6.7: *The decays $\mu^- \to e^+ e^- e^-$ (left) and $\tau^- \to e^+ \mu^- \mu^-$ (right) can occur at tree level in our models.*

The prediction for the corresponding branching ratio is then

$$\mathrm{Br}(\mu \to ee\overline{e}) \approx \frac{\Gamma(\mu \to ee\overline{e})}{\Gamma(\mu \to e\overline{\nu}_e \nu_\mu)} = \frac{I_{\mu eee}}{8G_F^2}, \tag{6.72}$$

to be compared with the experimental value [19] of $\mathrm{Br}(\mu \to ee\overline{e})_{exp} = 1.0 \times 10^{-12}$.

The decay of a τ into two muons and a positron (fig. 6.7 on the right) is generally less constrained than the decay of the muon in two electrons and a positron, but it is of interest in models where the latter process is prohibited by the symmetries. The calculation proceeds in an analogous way. In fact, the decay amplitude is now

$$\Gamma(\tau \to \overline{e}\mu\mu) = \frac{m_\tau^5}{(4\pi)^3 \times 24} I_{\tau\mu\mu e}, \tag{6.73}$$

where the coefficient is now given by the following expression:

$$I_{\tau\mu\mu e} = \left| \sum_\alpha \frac{I^\alpha_{\tau\mu} I^\alpha_{e\mu}}{m^{\alpha\,2}_H} \right|^2 + \left| \sum_\alpha \frac{J^\alpha_{\tau\mu} J^\alpha_{e\mu}}{m^{\alpha\,2}_H} \right|^2 + \left| \sum_\alpha \frac{I^\alpha_{\tau\mu} J^\alpha_{e\mu}}{m^{\alpha\,2}_H} \right|^2 + \left| \sum_\alpha \frac{J^\alpha_{\tau\mu} I^\alpha_{e\mu}}{m^{\alpha\,2}_H} \right|^2. \tag{6.74}$$

while the branching ratio becomes

$$\mathrm{Br}(\tau \to \bar{e}\mu\mu) = 0.17 \times \frac{\Gamma(\tau \to \bar{e}\mu\mu)}{\Gamma(\tau \to \mu\bar{\nu}_\mu\nu_\tau)} = 0.17 \times \frac{I_{\tau\mu\mu e}}{8G_F^2}, \tag{6.75}$$

to be compared with the experimental limit $\mathrm{Br}(\tau \to \bar{e}\mu\mu)_{exp} = 2.3 \times 10^{-8}$ [19].

The process $\mu^- \to e^-\gamma$

The relevant diagram for this process has one loop with a charged fermion and a neutral Higgs (see fig. 6.8). We consider the limit in which the Higgs is much heavier than the virtual fermion and the final electron is massless. Under this assumption the decay amplitude becomes [113]

$$\Gamma(\mu \to e\gamma) = \frac{e^2 m_\mu^5}{6 \times (16)^3 \pi^5} \left| \sum_{\alpha,f} \frac{(R^\alpha_{fe})^* R^\alpha_{f\mu}}{{m^\alpha_H}^2} \right|^2 \tag{6.76}$$

and the branching ratio is

$$\mathrm{Br}(\mu \to e\gamma) = \frac{\Gamma(\mu \to e\gamma)}{\Gamma(\mu \to e\nu\bar{\nu})} = \frac{\alpha_{em}}{32\pi G_F^2} \left| \sum_{\alpha,f} \frac{(R^\alpha_{fe})^* R^\alpha_{f\mu}}{{m^\alpha_H}^2} \right|^2 \tag{6.77}$$

to be compared with the current [114] (future [115]) experimental bound $\mathrm{Br}(\mu \to e\gamma)_{exp} = 10^{-11}$ (10^{-13}).

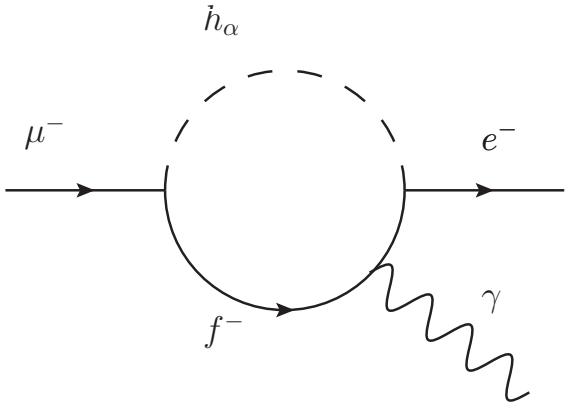

Figure 6.8: *The decays $\mu^- \to e^-\gamma$ proceeds at one loop in our models, but can be much larger than in the Standard Model, where a GIM-like cancellation occurs.*

Meson oscillations

Meson-antimeson oscillations are constrained to be generated by box processes in the SM (fig. 6.9 on the left left), but in the presence of flavor violating Higgs couplings, they can also proceed via tree-level Higgs exchange.

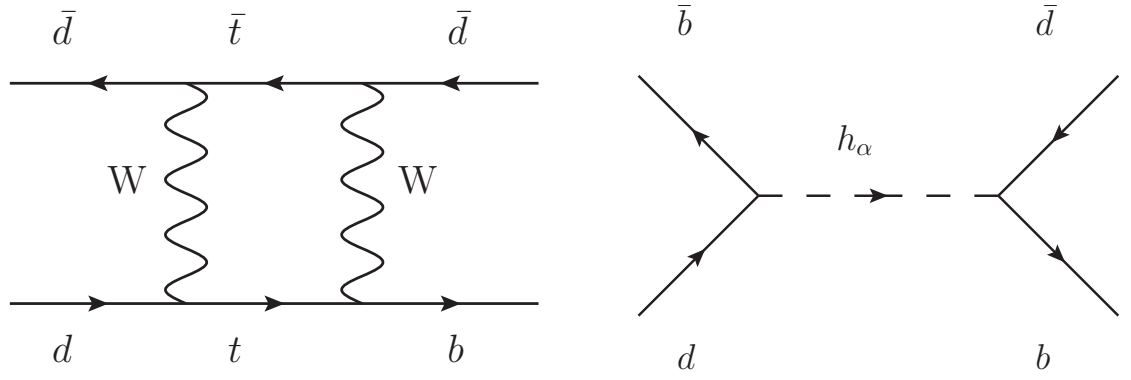

Figure 6.9: *B_d-$\overline{B}_d$ oscillations take place via box diagrams in the Standard Model, but can proceed via tree-level Higgs exchange in our model.*

For the mass splitting connected to $F^0 - \overline{F}^0$ oscillations [116, 117], we find

$$\Delta M_F = B_F^2 \, f_F^2 \, M_F \sum_\alpha \left[\frac{1}{m_H^{\alpha\,2}} \Big(|I_{rs}^\alpha|^2 \Big(\frac{1}{6} + \frac{1}{6} \frac{M_F^2}{(m_r + m_s)^2} \Big) + |J_{rs}^\alpha|^2 \Big(\frac{1}{6} + \frac{11}{6} \frac{M_F^2}{(m_r + m_s)^2} \Big) \Big) \right]. \tag{6.78}$$

Here, M_F is the mass of the meson, f_F is its decay constant and B_F are recalibration constants of order 1, related to vacuum insertion formalism. Lastly, m_r and m_s are the masses of the quarks of which the meson is build, i.e. $rs = bd$, bs, ds stands for B_d, B_s and K^0 respectively. Recent experimental values for the meson parameters, including ΔM_F that should be reproduced by the model, are given in Table 6.1

Meson	M_F (GeV)	f_F (GeV)	B_F	ΔM_F (GeV)
B_d ($\bar{b}d$)	5.2795	0.1928 ± 0.0099	1.26 ± 0.11	$(3.337 \pm 0.006) \times 10^{-13}$
B_s ($\bar{b}s$)	5.3664	0.2388 ± 0.0095	1.33 ± 0.06	$(1.170 \pm 0.008) \times 10^{-11}$
K ($\bar{s}d$)	0.497614	0.1558 ± 0.0017	0.725 ± 0.026	$(3.500 \pm 0.006) \times 10^{-11}$

Table 6.1: *Properties of neutral mesons [118].*

6.8 A_4 models for quark and/or lepton masses

In this section we will apply the general results about flavor violation to three specific models. After describing the main features of each model, plots of relevant flavor violating processes are reported. The points belonging to the plots are not chosen casually, but instead represent parts of the parameter space that fulfill the tests in the Higgs sector, as performed in Section 6.6 (positiveness of mass eigenstates, perturbative unitary constraints, bounds from Z and W decays and oblique corrections).

6.8.1 Model 1

The aim of the Model 1 [91] is to reproduce the lepton mixing parameters in the Tri-Bimaximal frame, although it is not possible without introducing hierarchies among the parameters. Quarks are briefly mentioned in the paper, but the bulk of the analysis is about the lepton sector. The triplet Φ_a couples only to charged leptons and the chosen vacuum alignment falls in the class (v, v, v), with v real. The Yukawa matrices in this sector are

$$Y_{ij1} = \begin{pmatrix} y_1 & y_2 & y_3 \\ 0 & 0 & 0 \\ 0 & 0 & 0 \end{pmatrix}, \quad Y_{ij2} = \begin{pmatrix} 0 & 0 & 0 \\ y_1 & \omega y_2 & \omega^2 y_3 \\ 0 & 0 & 0 \end{pmatrix}, \quad Y_{ij3} = \begin{pmatrix} 0 & 0 & 0 \\ 0 & 0 & 0 \\ y_1 & \omega^2 y_2 & \omega y_3 \end{pmatrix} \tag{6.79}$$

After the diagonalization of the charged lepton mass matrix, it is straightforward to relate the coefficient y_i to the mass eigenvalues:

$$y_1 = \frac{m_e}{\sqrt{3}v}, \quad y_2 = \frac{m_\mu}{\sqrt{3}v}, \quad y_3 = \frac{m_\tau}{\sqrt{3}v}. \tag{6.80}$$

Since the VEVs of the scalar potential are real, and consequently CP conserving, the U matrix that rotates the Higgs fields into the mass basis (see eq. 6.7) is block diagonal. Neutrino masses are given through a low scale ($\sim$ TeV) type I See-Saw implemented by 3 right handed neutrinos that transform as an A_4 triplet and by an $SU(2)_L$ doublet Higgs, η, singlet of A_4

$$\eta^1\eta^0 \frac{1}{\sqrt{2}} \text{Re}\, \eta^1 + i\text{Im}\, \eta^1 \text{Re}\, \eta^0 + i\text{Im}\, \eta^0 \tag{6.81}$$

Clearly η participates to the scalar potential, thus the Model 1 presents a scalar sector less minimal of that studied in the first part of the chapter. In this specific case the new scalar potential added to eq. (6.2) is given by

$$\begin{aligned} V_\eta &= \mu_\eta^2(\eta^\dagger\eta) + \lambda_\eta(\eta^\dagger\eta)^2 + \lambda_{\eta\Phi}(\eta^\dagger\eta)(\phi_1^\dagger\phi_1 + \phi_2^\dagger\phi_2 + \phi_3^\dagger\phi_3)\,, \\ V_{\eta\,soft} &= \mu_{\eta\Phi}^2 \left[\eta^\dagger(\phi_1 + \phi_2 + \phi_3) + (\phi_1^\dagger + \phi_2^\dagger + \phi_3^\dagger)\eta\right]\,, \end{aligned}$$

where the A_4 soft breaking part $V_{\eta\,soft}$ is needed in order to avoid additional GBs. $V_{\eta\,soft}$ breaks A_4 but preserves its Z_3 subgroup[§], thus the full potential may naturally realize the vacuum configuration Notice that u is responsible for neutrino masses and in the original model [91] it has been assumed to be tiny, $u \ll v \sim v_w/\sqrt{3}$. This may be easily realized if $\mu_{\eta\Phi}^2 \sim \mathcal{O}(u\, v_w)$.

We have already argued that it is not necessary to set ϵ to zero in eq. (6.2) to get this particular VEV, as is assumed in [91]. Moreover, since Z_3 is preserved, the mass eigenstates of the triplet Φ_a, 5 neutral and 2 charged, can be arranged in Z_3 representations, as discussed for the case (v, v, v): moving to this Z_3 basis, we denote the states

[§]Notice that in the original model [91], η is carrying lepton number and therefore it is broken once η develops VEV. Here, we are breaking the lepton number also by the soft terms and this prevents the appearance of further GBs.

as φ, φ' and φ'', transforming as 1, $1' \sim \omega$ and $1'' \sim \omega^2$ of Z_3, respectively. This setup has been discussed in the context of lepton triality in [119]. Notice that only the state φ develops a non-vanishing VEV in the neutral direction, while the other two are inert scalars. Moreover, φ behaves as the SM-Higgs and acquires the mass m_{h_1} defined in Section 6.3.1. Furthermore, the transformation properties of the additional scalar η allow a mixing between φ^0 (φ^1) and η^0 (η^1), both behaving as the SM-Higgs. However, this mixing interaction, $iZ\eta^0\varphi^0 + h.c.$, is irrelevant for the scalar spectrum discussion, because the coupling is extremely small being suppressed by $\sim u$. As a result, the conclusions for the case (v, v, v) apply also in this context.

The coupling of the Higgses φ'^0, φ''^0 to fermions is purely flavor violating. This setup has striking effects on the lepton processes. In fact it was shown in [9] that, when the A_4 symmetry is unbroken, only a limited number of processes is allowed and these either conserve flavor or satisfy the constraint $\Delta L_e \times \Delta L_\mu \times \Delta L_\tau = \pm 2$. The only source of symmetry breaking is the VEV of the SM-like Higgs φ^0, which is flavor-conserving and thus not involved in the processes we are looking at. We conclude that all flavor violating processes should satisfy the selection rule. In particular this implies that the decays $\mu^- \to e^- e^- e^+$ and $\mu \to e\gamma$ are not allowed, in the latter case in contrast with what was reported in [91], but in agreement with a more recent paper [120].

Of the allowed processes, the less suppressed is $\tau^- \to \mu^- \mu^- e^+$, since its branching ratio is proportional to $m_\tau^2 m_\mu^2$. However, even this decay is very rare and below the experimental limit for most values of the Higgs masses. In the upper part of fig. 6.10, we plot the branching ratio for the decay against an effective mass defined as $m_0^{-2} = m_{h_A}^{-2} + m_{h_B}^{-2}$, where A and B are the two pairs of degenerate bosons. In the lower part, the same branching ratio against the mass of the lightest state, m_1. In both the plots, the parameter ϵ is set to zero, corresponding to the real Higgs potential discussed in [91]. For the first picture, we reproduce the result of [91] that the branching ratio is proportional to m_0^{-4}. In the second one, this dependence is lost, even if we can see a similar behavior. Once we take ϵ over the full range $[0, 2\pi]$, we verified that the points cover a larger parameter space, but still concentrating around the previous points with $\epsilon = 0$.

In Figure 6.11, we show the masses of the SM-Higgs φ^0, m_{h_1}, against the mass of the lightest state m_1. A plot with the mass of the SM-Higgs η^0 against m_1 looks very similar to fig. 6.11. All the points are above the diagonal and this corresponds to the fact that the SM-Higgses are always heavier than the lightest state. As already stated before, in this situation, the standard upper bound of 194 GeV at 99% CL [19] cannot apply due to the combined effect of the CP and Z_3 symmetries and the smallness of the $iZ\eta^0\varphi^0 + h.c.$ coupling.

Finally, we can comment on the magnetic dipole moments, which could give interesting hints in this model. The discrepancy between the experimental measurement and the SM theoretical prediction of the magnetic dipole moment of the muon is usually a good test of flavor models, which could in principle provide new contributions. However, in this particular model it has already been discussed in [91] that the non-SM contributions are negligible.

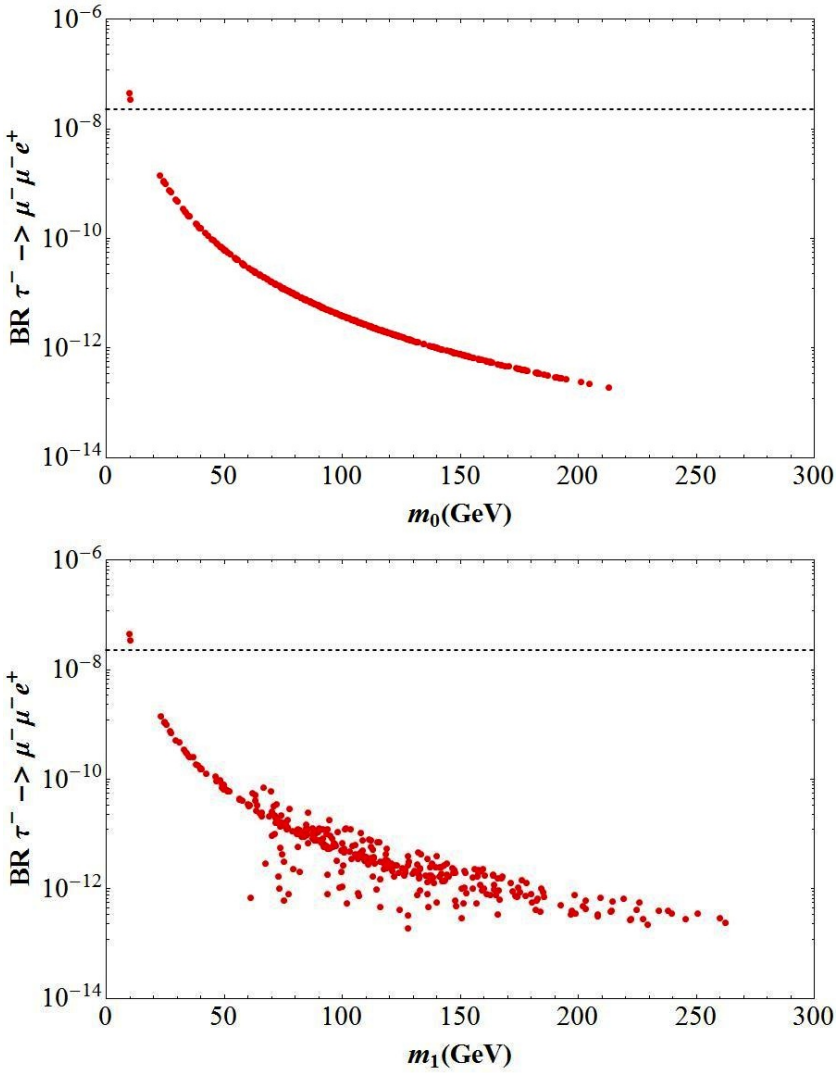

Figure 6.10: *On the upper (lower) side, the branching ratio for the decay* $\tau^- \to \mu^-\mu^-e^+$ *as a function of the effective mass* m_0 *(the smallest mass* m_1*) in the situation where the parameter* ϵ *is zero. The horizontal line corresponds to the experimental upper bound.*

6.8.2 Model 2

As in the previous section, the Model 2 [93] deals only with the lepton sector, but the vacuum configuration used is different: here $(r, e^{i\omega}, e^{-i\omega})v_w/\sqrt{2+r^2}$ is assumed, where r is an adimensional quantity. The Yukawa texture in the charged lepton sector depends on two parameters:

$$Y_{ij1} = \begin{pmatrix} 0 & 0 & 0 \\ 0 & 0 & y_1 \\ 0 & y_2 & 0 \end{pmatrix}, \quad Y_{ij2} = \begin{pmatrix} 0 & 0 & y_2 \\ 0 & 0 & 0 \\ y_1 & 0 & 0 \end{pmatrix}, \quad Y_{ij3} = \begin{pmatrix} 0 & y_1 & 0 \\ y_2 & 0 & 0 \\ 0 & 0 & 0 \end{pmatrix}. \tag{6.82}$$

In order to reproduce the masses of the leptons, $r \simeq 240$ is set and as a result the minimum of the scalar potential falls in the large r scenario, as discussed before. The final number

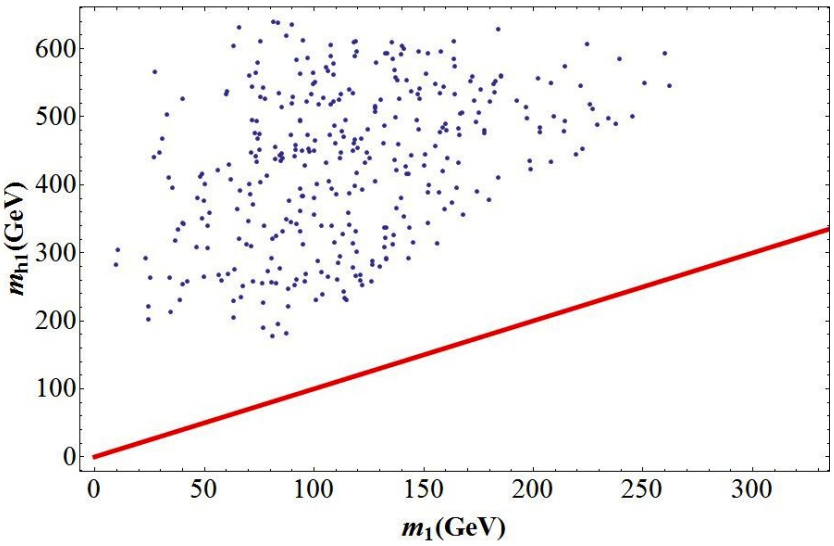

Figure 6.11: *The mass of the SM-Higgs m_{h_1} against the smallest Higgs mass.*

of the parameters in this model is four, two coming from the Yukawas and two from the vacuum configuration.

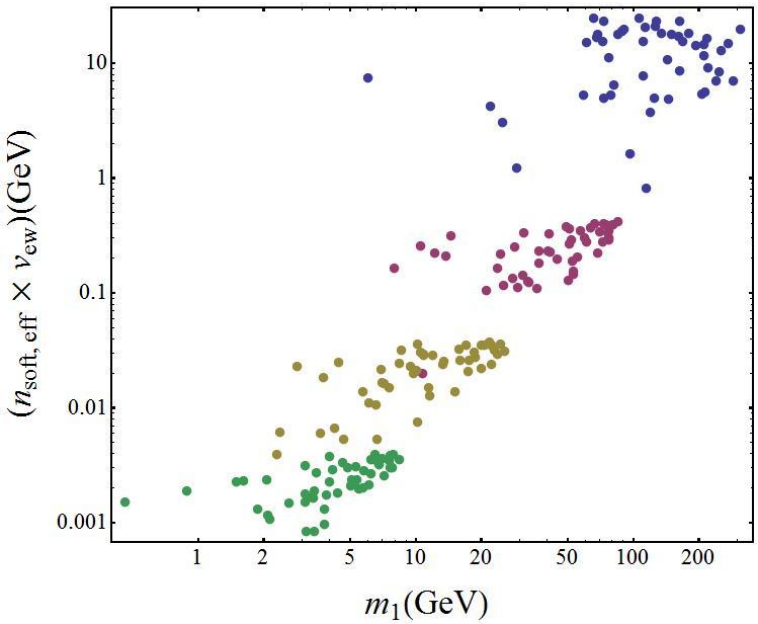

Figure 6.12: *Correlation among the lightest Higgs mass and the soft breaking parameters. The different colors correspond to the ranges that the individual parameters m, n and k are in, respectively $(0 - 10^{-4})$, $(0 - 10^{-3})$, $(0 - 10^{-2})$ and $(0 - 10^{-1})$*

We have shown that it is not possible to obtain a realistic Higgs spectrum without including soft A_4-breaking terms. Indeed if we introduce a soft breaking part, eq. (6.56),

to the potential with adimensional parameters m, n, k we can find five Higgses of mixed CP nature, all of which have masses in the LHC sensitive range between 100 GeV and 1 TeV. It is interesting to underline that such large Higgs masses have been recovered by using soft terms at most of order of 5% of the EW VEV. This underlines a non-linear dependence, as can be seen in fig. 6.12.

In contrast with the Model 1, A_4 is completely broken by the VEV of the Higgs triplet. Therefore the processes $\mu^- \to e^-e^-e^+$ and $\mu^- \to e^-\gamma$ are allowed. The first process, fig. 6.13 occurs at tree level and produces a strong bounds on the Higgs sector, where the lightest Higgs mass is expected to be above about 300 GeV. On the other hand, the radiative muon decay to an electron, fig. 6.13, is loop suppressed and the new physics leads to a branching ratio below the observed experimental bound.

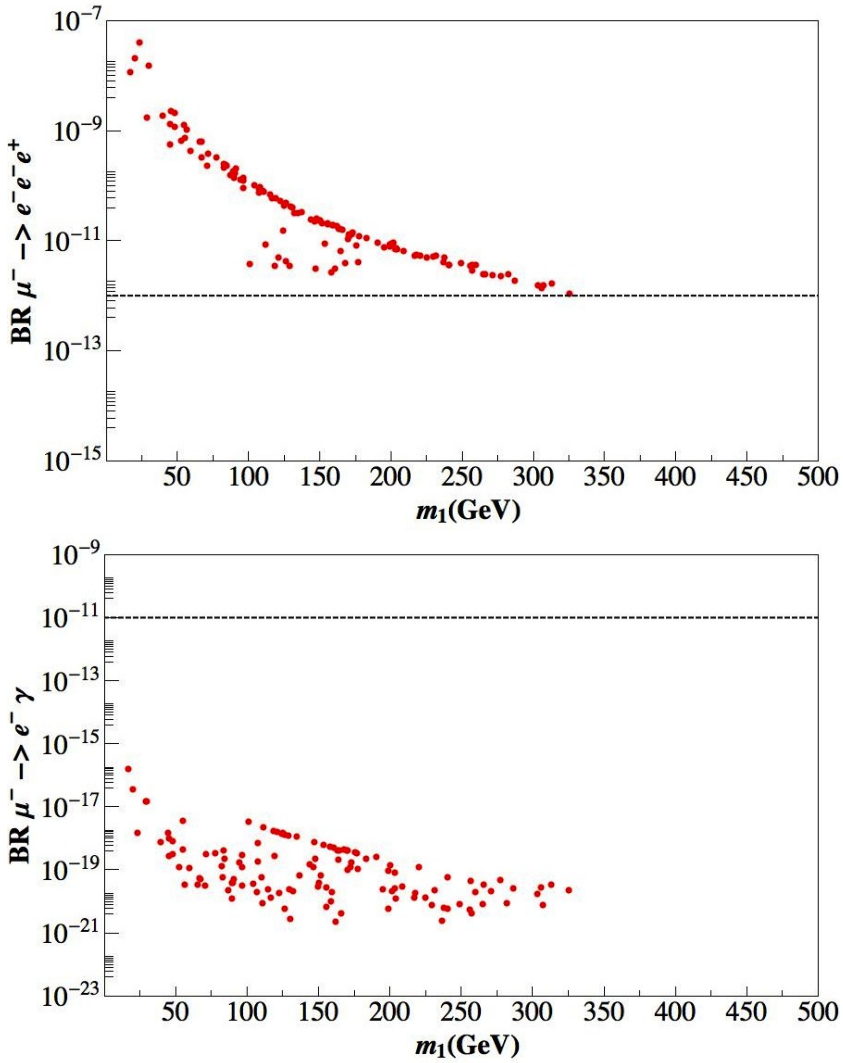

Figure 6.13: *On the upper (lower) side, the branching ratio of the decay of a $\mu^- \to e^-e^-e^+$ ($\mu^- \to e^-\gamma$) versus the lightest Higgs mass. The horizontal band is the experimental limit [19].*

6.8.3 Model 3

The Model 3 is built as an A_4 model for quarks [92], where both up- and down-type quarks couple to the Higgs triplet. There are eight parameters in their model whose values are unpredicted by the model itself, but are instead determined in order to reproduce the masses of quarks and their mixing angles. The Yukawa matrices for both up and down quarks has the same form as that of charged leptons of the Model 1, given in eq. (6.79). They provide then six parameters out of eight. The remaining two come from the VEV of the triplet in the form $(e^{i\omega}, e^{-i\omega}, r)v_w/\sqrt{2+r^2}$, where r is an adimensional quantity. Apart from a permutation in the three entries, this is the same vacuum used in Model 2.

The Higgs spectrum can only be realistic in the situation where A_4 is (softly) broken. Although ω is not absolutely constrained, the need of reproducing the neutrino mixing pattern suggests that the phase is small. In Model 2 we commented on the dependence of the Higgs masses on the soft parameters and the same applies in this case: the dependence is not linear and for even small soft parameters we get large Higgs masses. The plot in fig. 6.12 is representative also of this model.

Experimentally, in the quark sector two features have been explored: flavor changing interactions and CP violation. Remarkably, the CKM matrix obtained in the model under inspection is completely real. It seems then of scarce value to explore CP violating effects coming from the complex VEVs of the Higgs triplet, not having the dominant contribution from the Standard Model CKM matrix to compare them with. We will consequently focus only on flavor changing processes. As discussed in Section 6.7.1 meson oscillations are in these models mediated by tree level diagrams instead of box diagrams. We therefore expect strong bounds from the mass splittings in the neutral B-meson and Kaon systems. In fig. 6.14, we plot ΔM_F versus the lightest Higgs mass for these systems. Indeed ΔM_F is large, up to several orders of magnitude above the experimental value for the B_d meson and the Kaon.

6.9 Conclusions of the Chapter

Flavor models based on non-Abelian discrete symmetries under which the SM scalar doublet (and its replicas) transforms non trivially are quite appealing for many reasons. First of all there are no new physics scales, since the flavor and the EW symmetries are simultaneously broken. Furthermore this kind of models are typically more minimal with respect to the ones in which the flavor scale is higher than the EW one: in particular the vacuum configuration is simpler and the number of parameters is lower. We then expect an high predictive power and clear phenomenological signatures in processes involving both fermions and scalars. Due to the restricted number of parameters and the abundance of sensitive observables in these models, there are many constraints to analyze: the most stringent ones arise by FCNC and LFV processes [11] but even Higgs phenomenology put several constraints on this class of models.

In our work we focused on the A_4 discrete group, but this analysis can be safely gener-

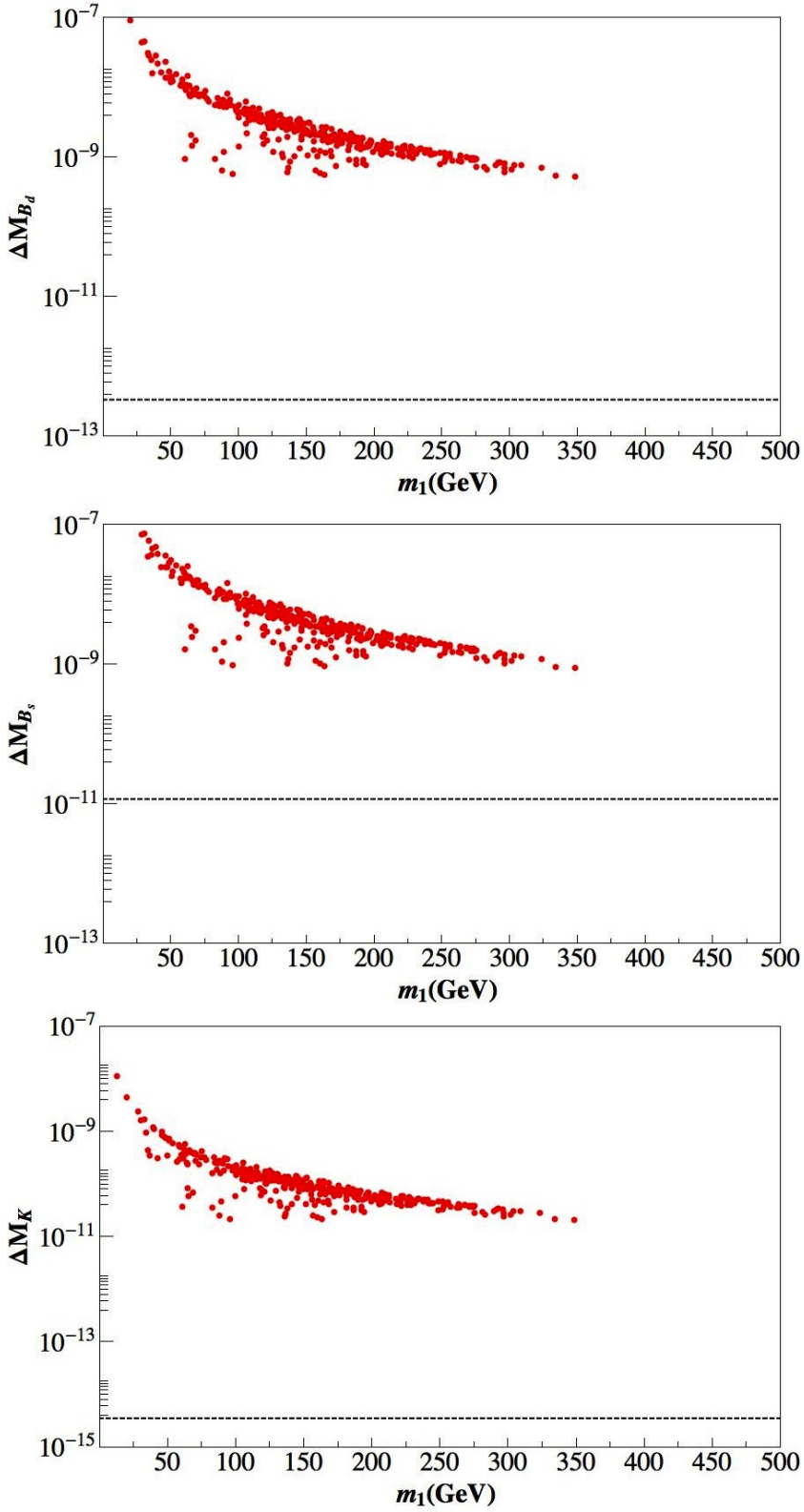

Figure 6.14: *ΔM_F for B_d, B_s and K mass splittings versus the lightest Higgs mass in the Model 3. The horizontal lines correspond to the experimental values as reported in [118].*

alized for any non-Abelian discrete symmetry. We consider three copies of the SM Higgs fields, that transform as a triplet of A_4. This setting has already been chosen in several papers [91–94] due to the simple vacuum alignment mechanism. We have considered all the possible vacuum configurations allowed by the $A_4 \times SM$ scalar potential. These configurations can either conserve or violate CP. For all of them we have first considered only model independent constraints, related to the Higgs-gauge boson Lagrangian. We have shown that the Higgs-gauge boson model independent analysis can be used to study the parameter space of the difference vacuum configurations. Among the possible solutions which minimize the scalar potential, only one is ruled out due to the presence of tachyonic states. Furthermore, some other configurations may be obtained only by tuning the potential parameters, giving rise to scalar spectra characterized by very light or even massless particles. Finally, for the remaining ones, we find that they may share common features and this increases the difficulty in discriminating among them.

As a second step we developed a very general formalism to describe the interaction of charged and neutral Higgs and of fermions. In the mass basis of both Higgs bosons and fermions the interaction depends on the Yukawa matrices that appear in the Lagrangian and the unitary matrices that rotate the flavor basis into the mass basis.

We applied the formalism to three specific models that implement the symmetry A_4. These models differ in the representations to which the fermions are assigned and in the choice of the vacuum expectation values of the scalar fields. The Model 1 [91] of lepton mixing has a CP-conserving VEV in the direction (v, v, v). In this setup, some transitions are forbidden by the symmetry and the decay $\tau^- \to \mu^-\mu^- e^+$ becomes then the most relevant process. We studied its dependence on the mass of the lightest Higgs and recognized that for the largest part of the assumed values the branching ratio is below the current experimental limit. Apart from a permutation of the components, both the Model 2 [93] and Model 3 [92] select the complex VEV $(e^{i\omega}, e^{-i\omega}, r)v_w/\sqrt{2+r^2}$. The purpose of the two approaches is to reproduce lepton and quark masses and mixing, respectively. The benchmark process in the lepton sector is the decay $\mu^- \to e^-e^-e^+$. Given the experimental bound, our analysis showed that the Model 2 is disfavored for values of the Higgs mass below 300 GeV. In the quark sector, B and K mesons oscillations mediated by Higgs exchange were considered and their predictions are largely above the current experimental limit and strongly disproves the setup of Model 3.

In conclusion, we have shown that a deep and careful analysis of the phenomenology of flavor models is fundamental to test their validity beyond the prediction of the mixing patterns and is a powerful tool to discriminate among them.

Summary and Final Remarks

We briefly summarize here the results of this work. For more details we refer to the conclusions of each chapter. This thesis tried to answer to three specific questions about neutrino physics: how do we build a model based on discrete symmetry groups, to reproduce correctly the features of neutrino oscillation in a natural way? What are the consequence of a particular model beyond the neutrino sector? Is the model still valid if we implement it in a larger theory?

To answer to the first question, we explicitly built a supersymmetric model based on the group A_5, which leads to the Golden Ratio texture. After showing the LO prediction for the mixing angles and the neutrino spectrum, we demonstrated that the vacuum alignment that produces that prediction rises in natural way from the minimization of the superpotential. It is remarkable that we achieved this result without adding driving fields to our theory. We also showed that NLO corrections are under control and could shift the predicted solar angle closer to the experimental value, while the reactor angle remains far from the prospected experimental sensitivity.

To the second question we answered at two different stages. First, we considered rare decays of μ and τ particles in an effective theory ruled by the symmetry $A_4 \times Z_3 \times U(1)$. The allowed decays satisfy the following selection rules $\Delta L_e \Delta L_\mu \Delta L_\tau = \pm 2$. From this rule it follows that radiative decays are forbidden, while the constraints to the parameters of the model come mainly from $\tau^- \to \mu^+ e^- e^-$ and $\tau^- \to e^+ \mu^- \mu^-$. Moving to a supersymmetric realization of the model, the picture is completely changed: the selection rule is not valid anymore and the previously allowed processes are strongly suppressed. Given the current and future experimental results, $\mu \to e\gamma$ and the conversion of μ in nuclei become the most interesting decays. Then, we analyzed the viability of multi-Higgs models. We recognized that only few choices of the VEVs are possible and not problematic. For all this cases, we analyzed the effects in the Higgs sector (unitarity, gauge bosons decay, corrections to S,T and U parameters) and constrained the space of the parameters of the Lagrangian. In a second step, we discussed flavor violation mediated by Higgs exchange in three models and found two of them to predict results already ruled out by experiments.

The answer to the third question materialized in the study of the running of angles and phases in models with Type I Seesaw. We were able to find a general behavior common to all mass-independent textures and studied it for the Altarelli-Feruglio model. We discovered that the predicted solar angle with inverted hierarchy is carried out of the 3σ range if $\tan\beta \gtrsim 9$, while the model is stable with normal hierarchy.

Acknowledgments

I warmly thank Ferruccio Feruglio for his guidance, his help and for having taught me how to do research with seriousness and passion.

I also thank Reinier de Adelhart Toorop, Federica Bazzocchi, Yin Lin and Luca Merlo for our profitable collaborations.

I would like to remember my office mate, Michele Gambaccini. I also remember Stefano Rizzato, whose enthusiasm about science, and cosmology in particular, has always stimulated me.

Finally, I thank my family and Anna, who have never stopped supporting me.

Appendix A

Group Theory Details

In this appendix we report the character tables and the Clebsch-Gordan coefficients of the discrete groups A_4 and A_5. Moreover, representations of A_5 different from the one used in Chapter 3 are reported, along with the transformations that allows to pass from one to the others. In the character tables, C_i are the classes of the group, $^\circ C_i$ is the order of the i^{th} class, i.e. the number of distinct elements contained in this class, $^\circ h_{C_i}$ is the order of the elements A in the class C_i, i.e. the smallest integer (> 0) for which the equation $A^{^\circ h_{C_i}} = 1$ holds. Furthermore the tables contain one representative G for each class C_i given as product of the generators S and T of the group.

A.1 The Group A_4

	classes			
	C_1	C_2	C_3	C_4
G	1	S	T^2	T
$^\circ C_i$	1	3	4	4
$^\circ h_{C_i}$	1	2	3	3
1	1	1	1	1
1′	1	1	ω	ω^2
1″	1	1	ω^2	ω
3	3	-1	0	0

Table A.1: *Character table of the group A_4. ω is the third root of unity, i.e. $\omega = e^{\frac{2\pi i}{3}} = -\frac{1}{2} + i\frac{\sqrt{3}}{2}$.*

The group A_4 is generated by two elements S and T obeying the relations [50]:

$$S^2 = (ST)^3 = T^3 = 1 \; . \tag{A. 1}$$

It has three independent one-dimensional representations, $\mathbf{1}$, $\mathbf{1}'$ and $\mathbf{1}''$ and one three-dimensional representation $\mathbf{3}$. The one-dimensional representations are given by:

$$\begin{array}{lll} \mathbf{1} & S=1 & T=1 \\ \mathbf{1}' & S=1 & T=e^{i4\pi/3}\equiv\omega^2 \\ \mathbf{1}'' & S=1 & T=e^{i2\pi/3}\equiv\omega \end{array} \tag{A. 2}$$

The three-dimensional representation, in a basis where the generator T is diagonal, is given by:

$$T=\begin{pmatrix} 1 & 0 & 0 \\ 0 & \omega^2 & 0 \\ 0 & 0 & \omega \end{pmatrix}, \qquad S=\frac{1}{3}\begin{pmatrix} -1 & 2 & 2 \\ 2 & -1 & 2 \\ 2 & 2 & -1 \end{pmatrix}. \tag{A. 3}$$

We now report the multiplication rules between the various representations. In the following $a=(a_1,\,a_2,\,a_3)^T$ and $b=(b_1,\,b_2,\,b_3)^T$ are triplets. c, c' and c'' belong to $\mathbf{1}$, $\mathbf{1}'$ and $\mathbf{1}''$ respectively.

We start with all the multiplication rules which include the one-dimensional representations:

$$\begin{aligned} &\mathbf{1}\times\mathbf{r}=\mathbf{r}\times\mathbf{1}=\mathbf{r} \qquad \text{with } \mathbf{r} \text{ any representation}\,, \\ &\mathbf{1}'\times\mathbf{1}''=\mathbf{1}''\times\mathbf{1}'\sim c'\,c''\,, \\ &\mathbf{1}'\times\mathbf{3}=\mathbf{3}\sim c'\begin{pmatrix} a_3 \\ a_1 \\ a_2 \end{pmatrix}, \qquad \mathbf{1}''\times\mathbf{3}=\mathbf{3}\sim c''\begin{pmatrix} a_2 \\ a_3 \\ a_1 \end{pmatrix}. \end{aligned} \tag{A. 4}$$

The multiplication rule with the three-dimensional representation is

$$\mathbf{3}\times\mathbf{3}=\mathbf{3}_S+\mathbf{3}_A+\mathbf{1}+\mathbf{1}'+\mathbf{1}'' \quad \text{with} \quad \begin{cases} \mathbf{1} \sim a_1b_1+a_2b_3+a_3b_2\,, \\ \mathbf{1}' \sim a_3b_3+a_1b_2+a_2b_1\,, \\ \mathbf{1}'' \sim a_2b_2+a_1b_3+a_3b_1\,, \\ \mathbf{3}_S \sim \dfrac{1}{3}\begin{pmatrix} 2a_1b_1-a_2b_3-a_3b_2 \\ 2a_3b_3-a_1b_2-a_2b_1 \\ 2a_2b_2-a_1b_3-a_3b_1 \end{pmatrix} \\ \mathbf{3}_A \sim \dfrac{1}{2}\begin{pmatrix} a_2b_3-a_3b_2 \\ a_1b_2-a_2b_1 \\ a_3b_1-a_1b_3 \end{pmatrix} \end{cases} \tag{A. 5}$$

Note that due to the choice of complex representation matrices for the real representation $\mathbf{3}$ the conjugate a^* of $a\sim\mathbf{3}$ does not transform as $\mathbf{3}$, but rather $(a_1^\star,\,a_3^*,\,a_2^*)$ transforms as triplet under A_4. The reason for this is that $T^*=U_{23}^T\,T\,U_{23}$ and $S^*=U_{23}^T\,S\,U_{23}=S$ where U_{23} is the matrix which exchanges the 2nd and 3rd row and column.

A.2 Kronecker products of the group A_5

We report here the complete list of the Kronecker products for the group A_5. We assigne $a = (a_1, a_2, a_3)^T$ and $b = (b_1, b_2, b_3)^T$ to the **3** representation, while $a' = (a'_1, a'_2, a'_3)^T$ and $b' = (b'_1, b'_2, b'_3)^T$ belong to the **3′** representation. $c = (c_1, c_2, c_3, c_4, c_5)^T$ and $d = (d_1, d_2, d_3, d_4, d_5)^T$ are pentaplets; $f = (f_1, f_2, f_3, f_4)^T$ and $g = (g_1, g_2, g_3, g_4)^T$ are tetraplets.

$\mathbf{3} \otimes \mathbf{3} = \mathbf{3}_a + (\mathbf{1} + \mathbf{5})_s$

$$
\begin{aligned}
\mathbf{1} &= a_1b_1 + a_2b_3 + a_3b_2 \\
\mathbf{3} &= (a_2b_3 - a_3b_2,\ a_1b_2 - a_2b_1,\ a_3b_1 - a_1b_3)^T \\
\mathbf{5} &= (a_1b_1 - \frac{a_2b_3}{2} - \frac{a_3b_2}{2}, \frac{\sqrt{3}}{2}(a_1b_2 + a_2b_1), -\sqrt{\frac{3}{2}}a_2b_2, -\sqrt{\frac{3}{2}}a_3b_3, -\frac{\sqrt{3}}{2}(a_1b_3 + a_3b_1))^T
\end{aligned}
$$

$\mathbf{3'} \otimes \mathbf{3'} = \mathbf{3'}_a + (\mathbf{1} + \mathbf{5})_s$

$$
\begin{aligned}
\mathbf{1} &= a'_1b'_1 + a'_2b'_3 + a'_3b'_2 \\
\mathbf{3'} &= (a'_2b'_3 - a'_3b'_2,\ a'_1b'_2 - a'_2b'_1,\ a'_3b'_1 - a'_1b'_3)^T \\
\mathbf{5} &= (a'_1b'_1 - \frac{a'_2b'_3}{2} - \frac{a'_3b'_2}{2}, \sqrt{\frac{3}{2}}a'_3b'_3, -\frac{\sqrt{3}}{2}(a'_1b'_2 + a'_2b'_1), -\frac{\sqrt{3}}{2}(a'_1b'_3 + a'_3b'_1), -\sqrt{\frac{3}{2}}a'_2b'_2)^T
\end{aligned}
$$

$\mathbf{3} \otimes \mathbf{3'} = \mathbf{4} + \mathbf{5}$

$$
\begin{aligned}
\mathbf{4} &= (a_2b'_1 - \frac{a_3b'_2}{\sqrt{2}}, -a_1b'_2 + \frac{a_3b'_3}{\sqrt{2}}, a_1b'_3 - \frac{a_2b'_2}{\sqrt{2}}, -a_3b'_1 + \frac{a_2b'_3}{\sqrt{2}})^T \\
\mathbf{5} &= (a_1b'_1, -\frac{a_2b'_1 + \sqrt{2}a_3b'_2}{\sqrt{3}}, \frac{a_1b'_2 + \sqrt{2}a_3b'_3}{\sqrt{3}}, \frac{a_1b'_3 + \sqrt{2}a_2b'_2}{\sqrt{3}}, \frac{a_3b'_1 + \sqrt{2}a_2b'_3}{\sqrt{3}}))^T
\end{aligned}
$$

$\mathbf{3} \otimes \mathbf{4} = \mathbf{3'} + \mathbf{4} + \mathbf{5}$

$$
\begin{aligned}
\mathbf{3'} &= (a_2g_4 - a_3g_1, \frac{1}{\sqrt{2}}(\sqrt{2}a_1g_2 + a_2g_1 + a_3g_3), -\frac{1}{\sqrt{2}}(\sqrt{2}a_1g_3 + a_2g_2 + a_3g_4))^T \\
\mathbf{4} &= (a_1g_1 + \sqrt{2}a_3g_2, -a_1g_2 + \sqrt{2}a_2g_1, a_1g_3 - \sqrt{2}a_3g_4, -a_1g_4 - \sqrt{2}a_2g_3)^T \\
\mathbf{5} &= (a_3g_1 + a_2g_4, \sqrt{\frac{2}{3}}(\sqrt{2}a_1g_1 - a_3g_2), \frac{1}{\sqrt{6}}(\sqrt{2}a_1g_2 - 3a_3g_3 + a_2g_1), \\
&\quad \frac{1}{\sqrt{6}}(\sqrt{2}a_1g_3 - 3a_2g_2 + a_3g_4), \sqrt{\frac{2}{3}}(-\sqrt{2}a_1g_4 + a_2g_3))^T
\end{aligned}
$$

$\mathbf{3'} \otimes \mathbf{4} = \mathbf{3} + \mathbf{4} + \mathbf{5}$

$$
\begin{aligned}
\mathbf{3} &= (a'_2 g_3 - a'_3 g_2, \frac{1}{\sqrt{2}}(\sqrt{2}a'_1 g_1 + a'_2 g_4 - a'_3 g_3), \frac{1}{\sqrt{2}}(-\sqrt{2}a'_1 g_4 + a'_2 g_2 - a'_3 g_1))^T \\
\mathbf{4} &= (a'_1 g_1 + \sqrt{2}a'_3 g_3, a'_1 g_2 - \sqrt{2}a'_3 g_4, -a'_1 g_3 + \sqrt{2}a'_2 g_1, -a'_1 g_4 - \sqrt{2}a'_2 g_2)^T \\
\mathbf{5} &= (a'_3 g_2 + a'_2 g_3, \frac{1}{\sqrt{6}}(\sqrt{2}a'_1 g_1 - 3a'_2 g_4 - a'_3 g_3), -\sqrt{\frac{2}{3}}(\sqrt{2}a'_1 g_2 + a'_3 g_4), \\
&\quad -\sqrt{\frac{2}{3}}(\sqrt{2}a'_1 g_3 + a'_2 g_1), \frac{1}{\sqrt{6}}(-\sqrt{2}a'_1 g_4 + 3a'_3 g_1 + a'_2 g_2))^T
\end{aligned}
$$

$\mathbf{3} \otimes \mathbf{5} = \mathbf{3} + \mathbf{3'} + \mathbf{4} + \mathbf{5}$

$$
\begin{aligned}
\mathbf{3} &= (\frac{2a_1 c_1}{\sqrt{3}} + a_3 c_2 - a_2 c_5, -\frac{a_2 c_1}{\sqrt{3}} + a_1 c_2 - \sqrt{2}a_3 c_3, -\frac{a_3 c_1}{\sqrt{3}} - a_1 c_5 - \sqrt{2}a_2 c_4)^T \\
\mathbf{3'} &= (a_1 c_1 + \frac{a_2 c_5 - a_3 c_2}{\sqrt{3}}, \frac{a_1 c_3 + \sqrt{2}(a_3 c_4 - a_2 c_2)}{\sqrt{3}}, \frac{a_1 c_4 + \sqrt{2}(a_2 c_3 + a_3 c_5)}{\sqrt{3}})^T \\
\mathbf{4} &= (4a_1 c_2 + 2\sqrt{3}a_2 c_1 + \sqrt{2}a_3 c_3, 2a_1 c_3 - 2\sqrt{2}a_2 c_2 - 3\sqrt{2}a_3 c_4, \\
&\quad 2a_1 c_4 - 3\sqrt{2}a_2 c_3 + 2\sqrt{2}a_3 c_5, -4a_1 c_5 + \sqrt{2}a_2 c_4 + 2\sqrt{3}a_3 c_1)^T \\
\mathbf{5} &= (a_2 c_5 + a_3 c_2, a_2 c_1 - \frac{a_1 c_2 + \sqrt{2}a_3 c_3}{\sqrt{3}}, -\frac{2a_1 c_3 + \sqrt{2}a_2 c_2}{\sqrt{3}}, \\
&\quad \frac{2a_1 c_4 - \sqrt{2}a_3 c_5}{\sqrt{3}}, a_3 c_1 + \frac{a_1 c_5 - \sqrt{2}a_2 c_4}{\sqrt{3}})^T
\end{aligned}
$$

$\mathbf{3'} \otimes \mathbf{5} = \mathbf{3} + \mathbf{3'} + \mathbf{4} + \mathbf{5}$

$$
\begin{aligned}
\mathbf{3} &= (a'_1 c_1 + \frac{a'_3 c_3 + a'_2 c_4}{\sqrt{3}}, \frac{-a'_1 c_2 + \sqrt{2}(a'_3 c_4 + a'_2 c_5)}{\sqrt{3}}, \frac{a'_1 c_5 + \sqrt{2}(a'_2 c_3 - a'_3 c_2)}{\sqrt{3}})^T \\
\mathbf{3'} &= (\frac{2a'_1 c_1}{\sqrt{3}} - a'_3 c_3 - a'_2 c_4, -\frac{a'_2 c_1}{\sqrt{3}} - a'_1 c_3 - \sqrt{2}a'_3 c_5, -\frac{a'_3 c_1}{\sqrt{3}} - a'_1 c_4 + \sqrt{2}a'_2 c_2)^T \\
\mathbf{4} &= (2a'_1 c_2 + 3\sqrt{2}a'_2 c_5 - 2\sqrt{2}a'_3 c_4, -4a'_1 c_3 + 2\sqrt{3}a'_2 c_1 + \sqrt{2}a'_3 c_5, \\
&\quad -4a'_1 c_4 - \sqrt{2}a'_2 c_2 + 2\sqrt{3}a'_3 c_1, -2a'_1 c_5 - 2\sqrt{2}a'_2 c_3 - 3\sqrt{2}a'_3 c_2)^T \\
\mathbf{5} &= (a'_2 c_4 - a'_3 c_3, \frac{2a'_1 c_2 + \sqrt{2}a'_3 c_4}{\sqrt{3}}, -a'_2 c_1 - \frac{a'_1 c_3 - \sqrt{2}a'_3 c_5}{\sqrt{3}}, \\
&\quad a'_3 c_1 + \frac{a'_1 c_4 + \sqrt{2}a'_2 c_2}{\sqrt{3}}, \frac{-2a'_1 c_5 + \sqrt{2}a'_2 c_3}{\sqrt{3}})^T
\end{aligned}
$$

$$\mathbf{4} \otimes \mathbf{4} \;=\; (\mathbf{3} \;+\; \mathbf{3'})_a \;+\; (\mathbf{1} \;+\; \mathbf{4} \;+\; \mathbf{5})_s$$

$$\begin{aligned}
\mathbf{1} &= f_1g_4 + f_2g_3 + f_3g_2 + f_4g_1 \\
\mathbf{3} &= (f_1g_4 - f_4g_1 + f_3g_2 - f_2g_3, \sqrt{2}(f_2g_4 - f_4g_2), \sqrt{2}(f_1g_3 - f_3g_1))^T \\
\mathbf{3'} &= (f_1g_4 - f_4g_1 + f_2g_3 - f_3g_2, \sqrt{2}(f_3g_4 - f_4g_3), \sqrt{2}(f_1g_2 - f_2g_1))^T \\
\mathbf{4} &= (f_3g_3 - f_4g_2 - f_2g_4, f_1g_1 + f_3g_4 + f_4g_3, -f_4g_4 - f_1g_2 - f_2g_1, -f_2g_2 + f_1g_3 + f_3g_1)^T \\
\mathbf{5} &= (f_1g_4 + f_4g_1 - f_3g_2 - f_2g_3, -\sqrt{\frac{2}{3}}(2f_3g_3 + f_2g_4 + f_4g_2), \sqrt{\frac{2}{3}}(-2f_1g_1 + f_3g_4 + f_4g_3), \\
&\quad \sqrt{\frac{2}{3}}(-2f_4g_4 + f_2g_1 + f_1g_2), \sqrt{\frac{2}{3}}(2f_2g_2 + f_1g_3 + f_3g_1))^T
\end{aligned}$$

$$\mathbf{4} \otimes \mathbf{5} \;=\; \mathbf{3} \;+\; \mathbf{3'} \;+\; \mathbf{4} \;+\; \mathbf{5} \;+\; \mathbf{5}$$

$$\begin{aligned}
\mathbf{3} &= (4f_1c_5 - 4f_4c_2 - 2f_3c_3 - 2f_2c_4, -2\sqrt{3}f_1c_1 - \sqrt{2}(2f_2c_5 - 3f_3c_4 + f_4c_3), \\
&\quad \sqrt{2}(-f_1c_4 + 3f_2c_3 + 2f_3c_2) - 2\sqrt{3}f_4c_1)^T \\
\mathbf{3'} &= (2f_1c_5 - 2f_4c_2 + 4f_3c_3 + 4f_2c_4, -2\sqrt{3}f_2c_1 + \sqrt{2}(2f_4c_4 + 3f_1c_2 - f_3c_5), \\
&\quad \sqrt{2}(f_2c_2 - 3f_4c_5 + 2f_1c_3) - 2\sqrt{3}f_3c_1)^T \\
\mathbf{4} &= (3f_1c_1 + \sqrt{6}(f_2c_5 + f_3c_4 - 2f_4c_3), -3f_2c_1 + \sqrt{6}(f_4c_4 - f_1c_2 + 2f_3c_5), \\
&\quad -3f_3c_1 + \sqrt{6}(f_1c_3 + f_4c_5 - 2f_2c_2), 3f_4c_1 + \sqrt{6}(f_2c_3 - f_3c_2 - 2f_1c_4))^T \\
\mathbf{5_1} &= (f_1c_5 + 2f_2c_4 - 2f_3c_3 + f_4c_2, -2f_1c_1 + \sqrt{6}f_2c_5, f_2c_1 + \sqrt{\frac{3}{2}}(-f_1c_2 - f_3c_5 + 2f_4c_4), \\
&\quad -f_3c_1 - \sqrt{\frac{3}{2}}(f_2c_2 + f_4c_5 + 2f_1c_3), -2f_4c_1 - \sqrt{6}f_3c_2)^T \\
\mathbf{5_2} &= (f_2c_4 - f_3c_3, -f_1c_1 + \frac{2f_2c_5 - f_3c_4 - f_4c_3}{\sqrt{6}}, -\sqrt{\frac{2}{3}}(f_1c_2 + f_3c_5 - f_4c_4), \\
&\quad -\sqrt{\frac{2}{3}}(f_1c_3 + f_2c_2 + f_4c_5), -f_4c_1 - \frac{2f_3c_2 + f_1c_4 + f_2c_3}{\sqrt{6}})^T
\end{aligned}$$

$$\mathbf{5} \otimes \mathbf{5} \;=\; (\mathbf{3} \;+\; \mathbf{3'} \;+\; \mathbf{4})_a \;+\; (\mathbf{1} \;+\; \mathbf{4} \;+\; \mathbf{5} \;+\; \mathbf{5})_s$$

$$\begin{aligned}
\mathbf{3} &= (2(c_4d_3 - c_3d_4) + c_2d_5 - c_5d_2, \sqrt{3}(c_2d_1 - c_1d_2) + \sqrt{2}(c_3d_5 - c_5d_3),\\
&\quad \sqrt{3}(c_5d_1 - c_1d_5) + \sqrt{2}(c_4d_2 - c_2d_4))^T\\
\mathbf{3'} &= (2(c_2d_5 - c_5d_2) + c_3d_4 - c_4d_3, \sqrt{3}(c_3d_1 - c_1d_3) + \sqrt{2}(c_4d_5 - c_5d_4),\\
&\quad \sqrt{3}(c_1d_4 - c_4d_1) + \sqrt{2}(c_3d_2 - c_2d_3))^T\\
\mathbf{4_s} &= ((c_1d_2 + c_2d_1) - \frac{(c_3d_5 + c_5d_3) - 4c_4d_4}{\sqrt{6}}, -(c_1d_3 + c_3d_1) - \frac{(c_4d_5 + c_5d_4) - 4c_2d_2}{\sqrt{6}},\\
&\quad (c_1d_4 + c_4d_1) - \frac{(c_2d_3 + c_3d_2) + 4c_5d_5}{\sqrt{6}}, (c_1d_5 + c_5d_1) - \frac{(c_2d_4 + c_4d_2) + 4c_3d_3}{\sqrt{6}})^T\\
\mathbf{4_a} &= ((c_1d_2 - c_2d_1) + \sqrt{\frac{3}{2}}(c_3d_5 - c_5d_3), (c_1d_3 - c_3d_1) + \sqrt{\frac{3}{2}}(c_4d_5 - c_5d_4),\\
&\quad (c_4d_1 - c_1d_4) + \sqrt{\frac{3}{2}}(c_3d_2 - c_2d_3), (c_1d_5 - c_5d_1) + \sqrt{\frac{3}{2}}(c_4d_2 - c_2d_4))^T\\
\mathbf{5_1} &= (c_1d_1 + c_2d_5 + c_5d_2 + \frac{c_3d_4 + c_4d_3}{2}, -(c_1d_2 + c_2d_1) + \sqrt{\frac{3}{2}}c_4d_4, \frac{1}{2}(c_1d_3 + c_3d_1 - \sqrt{6}(c_4d_5 + c_5d_4)),\\
&\quad \frac{1}{2}(c_1d_4 + c_4d_1 + \sqrt{6}(c_2d_3 + c_3d_2)), -(c_1d_5 + c_5d_1) - \sqrt{\frac{3}{2}}c_3d_3)^T\\
\mathbf{5_2} &= (\frac{2c_1d_1 + c_2d_5 + c_5d_2}{2}, \frac{-3(c_1d_2 + c_2d_1) + \sqrt{6}(2c_4d_4 + c_3d_5 + c_5d_3)}{6}, -\frac{2c_4d_5 + 2c_5d_4 + c_2d_2}{\sqrt{6}},\\
&\quad \frac{2c_2d_3 + 2c_3d_2 - c_5d_5}{\sqrt{6}}, \frac{-3(c_1d_5 + c_5d_1) + \sqrt{6}(-2c_3d_3 + c_2d_4 + c_4d_2)}{6})^T\\
\mathbf{1} &= c_1d_1 + c_3d_4 + c_4d_3 - c_2d_5 - c_5d_2
\end{aligned}$$

A.3 Different Representations of A_5

Shirai's basis. In this section we show how the basis chosen in this work is related to the representations given in previous articles on the group A_5. In [45, 121] the Shirai base was used, in which the presentation of the group is given in terms of two matrices S_{Sh} and T_{Sh} satisfying the following algebra:

$$S_{Sh}^2 = T_{Sh}^5 = (T_{Sh}^2 S_{Sh} T_{Sh}^3 S_{Sh} T_{Sh}^{-1} S_{Sh} T_{Sh} S_{Sh} T_{Sh}^{-1})^3 = 1 \tag{A. 6}$$

In order to connect them to the matrix S and T satisfying

$$S^2 = T^5 = (ST)^3 = 1 \tag{A. 7}$$

with T diagonal, we take an intermediate step and define first

$$S' = S_{Sh} \tag{A. 8}$$

and a matrix T' such that $(S'T')^3 = 1$ Then, we define $T_{Sh}^2 S_{Sh} T_{Sh}^3 S_{Sh} T_{Sh}^{-1} S_{Sh} T_{Sh} S_{Sh} T_{Sh}^{-1} = A_{Sh}$. Since $S'T' = A_{Sh}$ we obtain

$$T' = S'^{-1} A_{Sh} = S' A_{Sh} = S_{Sh} A_{Sh} \tag{A. 9}$$

Note that T' is not diagonal. To make it diagonal, we let an unitary matrix U act on it, such that

$$S = U^\dagger S' U, \qquad T = U^\dagger T' U. \tag{A. 10}$$

and finally

$$S = U^\dagger S_{Sh} U, \qquad T = U^\dagger S_{Sh} A_{Sh} U. \tag{A. 11}$$

Cummins-Patera's basis. The Cummins-Patera's basis [59, 60] is generated by two elements with presentation

$$A^2 = B^3 = (AB)^5 = 1, \tag{A. 12}$$

and the quintic representation are explicitly given by

$$A = \begin{pmatrix} 1 & 0 & 0 & 0 & 0 \\ 0 & -1 & 0 & 0 & 0 \\ 0 & 0 & -1 & 0 & 0 \\ 0 & 0 & 0 & 1 & 0 \\ 0 & 0 & 0 & 0 & 1 \end{pmatrix}; \quad B = -\frac{1}{2} \begin{pmatrix} 1 & 0 & 1 & -\omega^2 & -\omega \\ 0 & 1 & 1 & -1 & -1 \\ -1 & -1 & 0 & \omega & \omega^2 \\ \omega & 1 & \omega^2 & 0 & -\omega \\ \omega^2 & 1 & \omega & -\omega^2 & 0 \end{pmatrix}, \tag{A. 13}$$

where $\omega = e^{\frac{2i\pi}{3}}$ is the cubic root of unity, We can define a unitary transformation U_{CP} that relates the elements of the Cummins-Patera basis to the one introduced in Section 3 as follows:

$$S = U_{CP}^\dagger A U_{CP}, \quad (ST) = U_{CP}^\dagger B U_{CP}, \quad T = U_{CP}^\dagger (AB) U_{CP}. \tag{A. 14}$$

The unitary matrix is

$$U_{CP} = \frac{1}{\sqrt{5}} \begin{pmatrix} 0 & \omega^{-\frac{1}{2}}\sqrt{\frac{\sqrt{5}}{2\phi}} & \sqrt{\frac{\sqrt{5}\phi}{2}} & -\omega^{-\frac{1}{2}}\sqrt{\frac{\sqrt{5}\phi}{2}} & \omega^{-\frac{1}{2}}\sqrt{\frac{\sqrt{5}}{2\phi}} \\ -\sqrt{3}\omega^{\frac{1}{4}} & \frac{\omega^{\frac{1}{4}}}{\sqrt{2}} & -\frac{\omega^{\frac{1}{4}}}{\sqrt{2}} & -\frac{\omega^{\frac{1}{4}}}{\sqrt{2}} & -\frac{\omega^{\frac{1}{4}}}{\sqrt{2}} \\ 0 & \omega^{-\frac{1}{2}}\sqrt{\frac{\sqrt{5}\phi}{2}} & \omega^{-\frac{1}{2}}\sqrt{\frac{\sqrt{5}}{2\phi}} & \omega^{-\frac{1}{2}}\sqrt{\frac{\sqrt{5}}{2\phi}} & -\omega^{-\frac{1}{2}}\sqrt{\frac{\sqrt{5}\phi}{2}} \\ -\omega^2 & -e^{i\alpha} & -e^{i\beta} & -e^{i\alpha} & e^{i\alpha} \\ 1 & e^{-i\gamma} & -e^{i\gamma} & -e^{i\gamma} & -e^{-i\gamma} \end{pmatrix}, \quad \text{(A. 15)}$$

where $\alpha = \arctan\left(-\frac{2+\sqrt{5}}{\sqrt{3}}\right)$, $\beta = \arctan\left(\sqrt{3-\frac{4\sqrt{5}}{3}}\right)$ and $\gamma = \arctan\left(\sqrt{\frac{5}{3}}\right)$. It is straightforward to verify that acting with $U_{CP}^{\dagger}$ on the vector $(0,0,0,Z,\overline{Z})^T$ gives a new vector with the form given in eq. (3.38).

Appendix B

Renormalisation Group Equations

In order to calculate the evolution of the fermion mass matrix from the cutoff of the low-energy theory down to the electroweak energy scale, the renormalisation group equations for all the parameters have to be solved simultaneously. We use the notation defined in Chapter 4, where a superscript (n) denotes a quantity between the nth and the $(n+1)$th mass threshold. When all the right-handed neutrinos are integrated out, the renormalisation group equations can be recovered by setting the neutrino Yukawa coupling Y_ν to zero, while in the full theory above the highest See-Saw scale, the superscript (n) has to be omitted.

In the following, $t := \ln(\mu/\mu_0)$ and $Y_{u(d)}$ is the Yukawa coupling for the up- (down-) quarks, in the GUT normalisation, such that $g_2 = g$ and $g_1 = \sqrt{5/3}g'$.

In the MSSM context the 1-loop renormalisation group equations for the renormalisation group equations for $\overset{(n)}{Y_e}$, $\overset{(n)}{Y_\nu}$, $\overset{(n)}{M}$, $\overset{(n)}{\kappa}$, $\overset{(n)}{Y_d}$, and $\overset{(n)}{Y_u}$ are given by

$$
\begin{aligned}
16\pi^2\frac{\mathrm{d}}{\mathrm{d}t}\overset{(n)}{Y_e} &= Y_e\left\{3Y_e^\dagger Y_e + \overset{(n)}{Y_\nu^\dagger}\overset{(n)}{Y_\nu} + \mathrm{Tr}\left[3Y_d^\dagger Y_d + Y_e^\dagger Y_e\right] - \frac{9}{5}g_1^2 - 3g_2^2\right\}\,,\\
16\pi^2\frac{\mathrm{d}}{\mathrm{d}t}\overset{(n)}{Y_\nu} &= \overset{(n)}{Y_\nu}\left\{3\overset{(n)}{Y_\nu^\dagger}\overset{(n)}{Y_\nu} + Y_e^\dagger Y_e + \mathrm{Tr}\left[3Y_u^\dagger Y_u + \overset{(n)}{Y_\nu^\dagger}\overset{(n)}{Y_\nu}\right] - \frac{3}{5}g_1^2 - 3g_2^2\right\}\,,\\
16\pi^2\frac{\mathrm{d}}{\mathrm{d}t}\overset{(n)}{M_R} &= 2\left(\overset{(n)}{Y_\nu}\overset{(n)}{Y_\nu^\dagger}\right)\overset{(n)}{M_R} + 2\overset{(n)}{M_R}\left(\overset{(n)}{Y_\nu}\overset{(n)}{Y_\nu^\dagger}\right)^T\,,\\
16\pi^2\frac{\mathrm{d}}{\mathrm{d}t}\overset{(n)}{\kappa} &= \left[\overset{(n)}{Y_\nu^\dagger}\overset{(n)}{Y_\nu} + Y_e^\dagger Y_e\right]^T\overset{(n)}{\kappa} + \overset{(n)}{\kappa}\left[\overset{(n)}{Y_\nu^\dagger}\overset{(n)}{Y_\nu} + Y_e^\dagger Y_e\right] + 2\,\mathrm{Tr}\left[3Y_u^\dagger Y_u + \overset{(n)}{Y_\nu^\dagger}\overset{(n)}{Y_\nu}\right]\overset{(n)}{\kappa} +\\
&\quad -\frac{6}{5}g_1^2\overset{(n)}{\kappa} - 6g_2^2\overset{(n)}{\kappa}\,,\\
16\pi^2\frac{\mathrm{d}}{\mathrm{d}t}\overset{(n)}{Y_d} &= Y_d\left\{3Y_d^\dagger Y_d + Y_u^\dagger Y_u + \mathrm{Tr}\left[3Y_d^\dagger Y_d + Y_e^\dagger Y_e\right] - \frac{7}{15}g_1^2 - 3g_2^2 - \frac{16}{3}g_3^2\right\}\,,\\
16\pi^2\frac{\mathrm{d}}{\mathrm{d}t}\overset{(n)}{Y_u} &= Y_u\left\{Y_d^\dagger Y_d + 3Y_u^\dagger Y_u + \mathrm{Tr}\left[3Y_u^\dagger Y_u + \overset{(n)}{Y_\nu^\dagger}\overset{(n)}{Y_\nu}\right] - \frac{13}{15}g_1^2 - 3g_2^2 - \frac{16}{3}g_3^2\right\}\,.
\end{aligned}
\tag{B. 1}
$$

In the Standard Model extended by singlet neutrinos, the renormalisation group equa-

tions for the same quantities are given by

$$
\begin{aligned}
16\pi^2\frac{\mathrm{d}}{\mathrm{d}t}\overset{(n)}{Y_e} &= Y_e\left\{\frac{3}{2}Y_e^\dagger Y_e - \frac{3}{2}\overset{(n)}{Y_\nu}{}^\dagger\overset{(n)}{Y_\nu} + \mathrm{Tr}\left[3\,Y_u^\dagger Y_u + 3\,Y_d^\dagger Y_d + \overset{(n)}{Y_\nu}{}^\dagger\overset{(n)}{Y_\nu} + Y_e^\dagger Y_e\right] - \frac{9}{4}g_1^2 - \frac{9}{4}g_2^2\right\}\,,\\
16\pi^2\frac{\mathrm{d}}{\mathrm{d}t}\overset{(n)}{Y_\nu} &= \overset{(n)}{Y_\nu}\left\{\frac{3}{2}\overset{(n)}{Y_\nu}{}^\dagger\overset{(n)}{Y_\nu} - \frac{3}{2}Y_e^\dagger Y_e + \mathrm{Tr}\left[3\,Y_u^\dagger Y_u + 3\,Y_d^\dagger Y_d + \overset{(n)}{Y_\nu}{}^\dagger\overset{(n)}{Y_\nu} + Y_e^\dagger Y_e\right] - \frac{9}{20}g_1^2 - \frac{9}{4}g_2^2\right\}\,,\\
16\pi^2\frac{\mathrm{d}}{\mathrm{d}t}\overset{(n)}{M} &= \left(\overset{(n)}{Y_\nu}\overset{(n)}{Y_\nu^\dagger}\right)\overset{(n)}{M} + \overset{(n)}{M}\left(\overset{(n)}{Y_\nu}\overset{(n)}{Y_\nu^\dagger}\right)^T\,,\\
16\pi^2\frac{\mathrm{d}}{\mathrm{d}t}\overset{(n)}{\kappa} &= \frac{1}{2}\left[\overset{(n)}{Y_\nu}{}^\dagger\overset{(n)}{Y_\nu} - 3Y_e^\dagger Y_e\right]^T\overset{(n)}{\kappa} + \frac{1}{2}\overset{(n)}{\kappa}\left[\overset{(n)}{Y_\nu}{}^\dagger\overset{(n)}{Y_\nu} - 3Y_e^\dagger Y_e\right] +\\
&\quad +2\,\mathrm{Tr}\left[3\,Y_u^\dagger Y_u + 3\,Y_d^\dagger Y_d + \overset{(n)}{Y_\nu}{}^\dagger\overset{(n)}{Y_\nu} + Y_e^\dagger Y_e\right] - 3g_2^2\overset{(n)}{\kappa} + \lambda_H\overset{(n)}{\kappa}\,,\\
16\pi^2\frac{\mathrm{d}}{\mathrm{d}t}\overset{(n)}{Y_d} &= Y_d\left\{\frac{3}{2}Y_d^\dagger Y_d - \frac{3}{2}Y_u^\dagger Y_u + \mathrm{Tr}\left[3\,Y_u^\dagger Y_u + 3\,Y_d^\dagger Y_d + \overset{(n)}{Y_\nu}{}^\dagger\overset{(n)}{Y_\nu} + Y_e^\dagger Y_e\right] +\right.\\
&\quad \left. -\frac{1}{4}g_1^2 - \frac{9}{4}g_2^2 - 8g_3^2\right\}\,,\\
16\pi^2\frac{\mathrm{d}}{\mathrm{d}t}\overset{(n)}{Y_u} &= Y_u\left\{\frac{3}{2}Y_u^\dagger Y_u - \frac{3}{2}Y_d^\dagger Y_d + \mathrm{Tr}\left[3\,Y_u^\dagger Y_u + 3\,Y_d^\dagger Y_d + \overset{(n)}{Y_\nu}{}^\dagger\overset{(n)}{Y_\nu} + Y_e^\dagger Y_e\right] +\right.\\
&\quad \left. -\frac{17}{20}g_1^2 - \frac{9}{4}g_2^2 - 8g_3^2\right\}\,,\\
16\pi^2\frac{\mathrm{d}}{\mathrm{d}t}\overset{(n)}{\lambda_H} &= 6\lambda_H^2 - 3\lambda_H\left(3g_2^2 + \frac{3}{5}g_1^2\right) + 3g_2^4 + \frac{3}{2}\left(\frac{3}{5}g_1^2 + g_2^2\right)^2 +\\
&\quad +4\lambda_H\,\mathrm{Tr}\left[3\,Y_u^\dagger Y_u + 3\,Y_d^\dagger Y_d + \overset{(n)}{Y_\nu}{}^\dagger\overset{(n)}{Y_\nu} + Y_e^\dagger Y_e\right] +\\
&\quad -8\,\mathrm{Tr}\left[3\,Y_u^\dagger Y_u\,Y_u^\dagger Y_u + 3\,Y_d^\dagger Y_d\,Y_d^\dagger Y_d + \overset{(n)}{Y_\nu}{}^\dagger\overset{(n)}{Y_\nu}\overset{(n)}{Y_\nu}{}^\dagger\overset{(n)}{Y_\nu} + Y_e^\dagger Y_e\,Y_e^\dagger Y_e\right]\,.
\end{aligned}
\tag{B. 2}
$$

We use the convention that the Higgs self-interaction term in the Lagrangian is $-\lambda_H(H^\dagger H)^2/4$.

Appendix C

Analytical Formulae for the Parameters S, T and U

In this Appendix we provide a sort of *translator* from the papers [105, 108] to our notations and furnish the formulae we have used when different from their.

Reminding their notation we are in the case in which $n_d = 3$ and $n_n, n_c = 0$ so we do not have the matrices $\mathcal{T}$ and $\mathcal{R}$. Then we have

$$\begin{aligned} \mathcal{U} &\to S \\ \mathrm{Re}\mathcal{V}_{ki} &\to U_{ki}\,, \\ \mathrm{Im}\mathcal{V}_{ki} &\to U_{k+3i}\,, \\ \omega_k &\to f_k e^{i\omega_k}\,. \end{aligned} \tag{C. 1}$$

Moreover they put the GBs as first mass eigenstates while we put them as the last ones and contrary to them we use the standard definition for the photon.

We have rewritten they expression for

$$\frac{A(I,J,Q) - A(I,J,0)}{Q} = \begin{cases} dA(I,J) & \text{for } I \neq 0 \text{ and/or } J \neq 0\,, \\ \dfrac{QF(Q)}{Q} \sim \dfrac{1}{48\pi^2}\log Q & \text{for } I = J = 0 \text{ since } A(0,0,0) = 0\,. \end{cases} \tag{C. 2}$$

For the first row of eq. (C. 2) we have used

$$A(I,J,Q) \simeq A(I,J,0) + Q\frac{\partial A(I,J,Q)}{\partial Q}\bigg|_{Q=0} = A(I,J,0) + Q\,dA(I,J) \tag{C. 3}$$

with

$$dA(I,J) = \begin{cases} \dfrac{1}{288(I-J)^3\pi^2}\left[I^3+9JI^2+6(I-3J)\log(I)I^2-9J^2I-J^3+6(3I-J)J^2\log(J)\right] \\ \qquad\qquad \text{for } I,J\neq 0, I\neq J\,, \\ \dfrac{1}{288\pi^2}(1+6Log[I]) \qquad \text{for } J=0\,, \\ \dfrac{1}{48\pi^2}(1+\log[I]) \qquad \text{for } I=J\,. \end{cases} \tag{C. 4}$$

The function $\bar{A}(I,J,Q)$ enters only in the loops in which a gauge boson and a scalar run, so we have always $J=Q$ when computing the quantity

$$\frac{\bar{A}(I,J,Q)-\bar{A}(I,J,0)}{Q} \;=\; d\bar{A}(I,J)\,. \tag{C. 5}$$

As a result, for this function, it does not make sense considering the case $I=J=0$ being $J=Q=m_V^2$ the gauge boson mass. We found

$$d\bar{A}(I,Q) = \begin{cases} \dfrac{1}{8(I-Q)^3\pi^2}\left[Q\left(-I^2+2Q\log(I)I-2Q\log(Q)I+Q^2\right)\right] \quad \text{for } I\neq Q, I\neq 0\,, \\ \sim 0 \qquad \text{for } I=0\,, \\ \sim 0 \qquad \text{for } I=Q\,. \end{cases} \tag{C. 6}$$

Bibliography

[1] A. Strumia and F. Vissani, *Neutrino masses and mixings and...*, arXiv:hep-ph/0606054;

G. L. Fogli *et al.*, *Neutrino mass and mixing: 2006 status*, Nucl. Phys. Proc. Suppl. **168** (2007) 341;

M. C. Gonzalez-Garcia and M. Maltoni, *Phenomenology with Massive Neutrinos*, Phys. Rept. **460** (2008) 1 [arXiv:0704.1800 [hep-ph]];

T. Schwetz, *Neutrino oscillations: present status and outlook*, AIP Conf. Proc. **981** (2008) 8 [arXiv:0710.5027 [hep-ph]];

M. C. Gonzalez-Garcia and M. Maltoni, *Status of Oscillation plus Decay of Atmospheric and Long-Baseline Neutrinos*, Phys. Lett. B **663** (2008) 405 [arXiv:0802.3699 [hep-ph]];

A. Bandyopadhyay, S. Choubey, S. Goswami, S. T. Petcov and D. P. Roy, *Neutrino Oscillation Parameters After High Statistics KamLAND Results*, arXiv:0804.4857 [hep-ph].

[2] G. L. Fogli, E. Lisi, A. Marrone, A. Palazzo and A. M. Rotunno, *Hints of $\theta_{13} > 0$ from global neutrino data analysis*, Phys. Rev. Lett. **101** (2008) 141801 [arXiv:0806.2649 [hep-ph]];

G. L. Fogli, E. Lisi, A. Marrone, A. Palazzo and A. M. Rotunno, *What we (would like to) know about the neutrino mass*, arXiv:0809.2936 [hep-ph].

[3] T. Schwetz, M. Tortola and J. W. F. Valle, *Three-flavour neutrino oscillation update*, New J. Phys. **10** (2008) 113011 [arXiv:0808.2016 [hep-ph]];

M. Maltoni and T. Schwetz, *Three-flavour neutrino oscillation update and comments on possible hints for a non-zero θ_{13}*, arXiv:0812.3161 [hep-ph].

[4] F.Feruglio and A.Paris, *The Golden Ratio Prediction for the Solar Angle from a Natural Model with A_5 Flavour Symmetry*, arxiv:1101.0393 [hep-ph].

[5] Y. Lin, L. Merlo and A. Paris, *Running Effects on Lepton Mixing Angles in Flavour Models with Type I Seesaw*, Nucl. Phys. B **835** (2010) 238, [arXiv:0911.3037].

[6] G. Altarelli and F. Feruglio, *Tri-Bimaximal Neutrino Mixing, A4 and the Modular Symmetry*, Nucl. Phys. B **741** (2006) 215 [arXiv:hep-ph/0512103].

[7] G. Altarelli and F. Feruglio, *Tri-bimaximal neutrino mixing from discrete symmetry in extra dimensions*, Nucl. Phys. B **720** (2005) 64 [arXiv:hep-ph/0504165];

[8] G. Altarelli, F. Feruglio and Y. Lin, *Tri-bimaximal neutrino mixing from orbifolding*, Nucl. Phys. B **775** (2007) 31 [arXiv:hep-ph/0610165];

[9] F. Feruglio and A. Paris, *Rare muon and tau decays in A4 Models*, Nucl. Phys. **B840** (2010) 405 [arXiv: 1005.5526].

[10] R. d. A. Toorop, F. Bazzocchi, L. Merlo, and A. Paris, *Constraining Flavour Symmetries At The EW Scale I: The A4 Higgs Potential*, arxiv: 1012.1791.

[11] R. d. A. Toorop, F. Bazzocchi, L. Merlo, and A. Paris, *Constraining Flavour Symmetries At The EW Scale II: The Fermion Processes*, arxiv:1012.2091.

[12] S. L. Glashow, *Partial Symmetries Of Weak Interactions*, Nucl. Phys. **22** (1961) 579;

S. Weinberg, *A Model Of Leptons*, Phys. Rev. Lett. **19** (1967) 1264;

A. Salam, *Weak And Electromagnetic Interactions*, Originally printed in "Svartholm: Elementary Particle Theory, Proceedings Of The Nobel Symposium Held 1968 At Lerum, Sweden", Stockholm 1968, 367-377;

S. L. Glashow, J. Iliopoulos and L. Maiani, *Weak Interactions with Lepton-Hadron Symmetry*, Phys. Rev. D **2** (1970) 1285.

[13] S. Weinberg, *Baryon And Lepton Nonconserving Processes*, Phys. Rev. Lett. **43** (1979) 1566.

[14] P. Minkowski, *Phys. Lett.* B **67** 421 (1977);

T. Yanagida, in *Proc. of Workshop on Unified Theory and Baryon number in the Universe*, eds. O. Sawada and A. Sugamoto, KEK, Tsukuba, (1979) p.95;

M. Gell-Mann, P. Ramond and R. Slansky, in *Supergravity*, eds P. van Niewenhuizen and D. Z. Freedman (North Holland, Amsterdam 1980) p.315;

P. Ramond, *Sanibel talk*, retroprinted as hep-ph/9809459;

S. L. Glashow, in *Quarks and Leptons*, Cargèse lectures, eds M. Lévy, (Plenum, 1980, New York) p. 707;

R. N. Mohapatra and G. Senjanović, *Phys. Rev. Lett.* **44**, 912 (1980);

J. Schechter and J. W. F. Valle, *Neutrino Masses In SU(2) X U(1) Theories*, Phys. Rev. D **22** (1980) 2227; *Neutrino Decay And Spontaneous Violation Of Lepton Number*, Phys. Rev. D **25** (1982) 774.

[15] B. Pontecorvo, *Neutrino experiments and the question of leptonic-charge conservation*, Sov. Phys. JETP **26** (1968) 984 [Zh. Eksp. Teor. Fiz. **53** (1967) 1717];

Z. Maki, M. Nakagawa and S. Sakata, *Remarks On The Unified Model Of Elementary Particles*, Prog. Theor. Phys. **28** (1962) 870.

[16] N. Cabibbo, *Unitary Symmetry And Leptonic Decays*, Phys. Rev. Lett. **10** (1963) 531.

[17] M. Kobayashi and T. Maskawa, *CP Violation In The Renormalizable Theory Of Weak Interaction*, Prog. Theor. Phys. **49** (1973) 652.

[18] C. Jarlskog, *Commutator Of The Quark Mass Matrices In The Standard Electroweak Model And A Measure Of Maximal CP Violation*, Phys. Rev. Lett. **55** (1985) 1039.

[19] K. Nakamura *et al.*, *Particle Data Group*, J. Phys. **G 37** (2010) 075021.

[20] M. C. Gonzalez-Garcia, *Global analysis of neutrino data*, Phys. Scripta **T121** (2005) 72 [arXiv:hep-ph/0410030].

[21] C. Athanassopoulos *et al.* [LSND Collaboration], *Evidence for nu/mu –¿ nu/e neutrino oscillations from LSND*, Phys. Rev. Lett. **81** (1998) 1774 [arXiv:nucl-ex/9709006];

A. Aguilar *et al.* [LSND Collaboration], *Evidence for neutrino oscillations from the observation of anti-nu/e appearance in a anti-nu/mu beam*, Phys. Rev. D **64** (2001) 112007 [arXiv:hep-ex/0104049].

[22] A. Aguilar *et al.* [MiniBoone Collaboration] *Unexplained Excess of Electron-Like Events From a 1-GeV Neutrino Beam*, Phys. Rev. Lett.**102** (2009) 101802, [arxiv:hep-ex/0812.2243].

[23] A. Aguilar *et al.* [MiniBoone Collaboration], *Event Excess in the MiniBooNE Search for $\bar{\nu} \to \bar{\nu}_e$ Oscillations*, Phys. Rev. Lett. **105** (2010) 181801, [arxiv:hep-ex/1007.1150].

[24] I. Danko [MINOS Collaboration], *First Observation of Accelerator Muon Antineutrinos in MINOS*, arXiv:0910.3439.

[25] F. Ardellier *et al.* [Double Chooz Collaboration], *Double Chooz: A search for the neutrino mixing angle theta$_{13}$*, arXiv:hep-ex/0606025.

[26] Y. f. Wang, *Measuring $sin^2(2\theta_{13})$ with the Daya Bay nuclear reactors*, arxiv:hep-ex/0610024.

[27] A. B. Pereira e Sousa, *Studies of $\nu_\mu \to \nu_e$ oscillation appearance in the MINOS experiment*, FERMILAB-THESIS-2005-67.

[28] S. B. Kim [RENO Collaboration], *RENO: Reactor experiment for neutrino oscillation at Yonggwang*, AIP Conf. Proc. **981**, 205 (2008) [J. Phys. Conf. Ser. **120**, 052025 (2008)].

[29] Y. Itow *et al.* [The T2K Collaboration], *The JHF-Kamioka neutrino project*, arXiv:hep-ex/0106019.

[30] D. S. Ayres *et al.* [NOvA Collaboration], *NOvA proposal to build a 30-kiloton off-axis detector to study neutrino oscillations in the Fermilab NuMI beamline*, arXiv:hep-ex/0503053.

[31] M. Mezzetto and T. Schwetz, θ_{13}*: phenomenology, present status and prospect*, arXiv:1003.5800.

[32] C. Kraus *et al.*, *Final Results From Phase Ii Of The Mainz Neutrino Mass Search In Tritium Beta Decay*, Eur. Phys. J. C **40** (2005) 447 [arXiv:hep-ex/0412056].

[33] A. Osipowicz *et al.* [KATRIN Collaboration], *KATRIN: A next generation tritium beta decay experiment with sub-eV sensitivity for the electron neutrino mass*, arXiv:hep-ex/0109033; see also: `http://www-ik.fzk.de/~katrin/index.html` .

[34] O. Host, O. Lahav, F. B. Abdalla and K. Eitel, *Forecasting neutrino masses from combining KATRIN and the CMB: Frequentist and Bayesian analyses*, Phys. Rev. D **76** (2007) 113005 [arXiv:0709.1317 [hep-ph]].

G. L. Fogli *et al.*, *Observables sensitive to absolute neutrino masses (Addendum)*, Phys. Rev. D **78** (2008) 033010 [arXiv:0805.2517 [hep-ph]].

[35] L. Baudis *et al.*, *Limits on the Majorana neutrino mass in the 0.1 eV range*, Phys. Rev. Lett. **83** (1999) 41 [arXiv:hep-ex/9902014].

[36] A. A. Smolnikov and f. t. G. Collaboration, *Status of the GERDA experiment aimed to search for neutrinoless double beta decay of 76Ge*, arXiv:0812.4194 [nucl-ex].

[37] Majorana Collaboration, *The Majorana Neutrinoless Double-Beta Decay Experiment*, arXiv:0811.2446 [nucl-ex].

[38] H. Ohsumi [NEMO and SuperNEMO Collaborations], *SuperNEMO project*, J. Phys. Conf. Ser. **120** (2008) 052054.

[39] A. Giuliani [CUORE Collaboration], *From Cuoricino to CUORE: Investigating the inverted hierarchy region of neutrino mass*, J. Phys. Conf. Ser. **120** (2008) 052051.

[40] M. Danilov *et al.*, *Detection of very small neutrino masses in double-beta decay using laser tagging*, Phys. Lett. B **480** (2000) 12 [arXiv:hep-ex/0002003].

[41] S. P. Martin, *A Supersymmetry Primer*, arXiv:hep-ph/9709356.

[42] G. Altarelli and F. Feruglio, *Discrete Flavor Symmetries and Models of Neutrino Mixing*, arXiv:1002.0211.

[43] F. Bazzocchi and S. Morisi, *S4 as a natural flavor symmetry for lepton mixing*, arXiv:0811.0345 [hep-ph];

H. Ishimori, Y. Shimizu and M. Tanimoto, *S4 Flavor Symmetry of Quarks and Leptons in SU(5) GUT*, arXiv:0812.5031 [hep-ph].

F. Bazzocchi, L. Merlo and S. Morisi, *Fermion Masses and Mixings in a S4 Based Model*, arXiv:0901.2086 [hep-ph];

G. J. Ding, *Fermion Masses and Flavor Mixings in a Model with S_4 Flavor Symmetry*, arXiv:0909.2210 [hep-ph];

H. Ishimori, K. Saga, Y. Shimizu and M Tanimoto, *Tri-bimaximal Mixing and Cabibbo Angle in S4 Flavor Model with SUSY*, arXiv:hep-ph/1004.5004;

H. Ishimori, Y. Shimizu, M. Tanimoto and A. Watanabe, *Neutrino masses and mixing from S4 flavor twisting*, arXiv:hep-ph/1010.3805;

H. Ishimori, M. Tanimoto, *Slepton Mass Matrices, mu -¿ e gamma Decay and EDM in SUSY S4 Flavor Model*, arXiv:hep-ph/1012.2232;

F. Bazzocchi, L. Merlo and S. Morisi, *Phenomenological Consequences of See-Saw in S4 Based Models*, Phys. Rev. D **80** (2009) 053003 [arXiv:0902.2849 [hep-ph]];

G. Altarelli, F. Feruglio and L. Merlo, *Revisiting Bimaximal Neutrino Mixing in a Model with S4 Discrete Symmetry*, JHEP **0905** (2009) 020 [arXiv:0903.1940 [hep-ph]];

R. de Adelhart Toorop, F. Bazzocchi and L. Merlo, *The Interplay Between GUT and Flavour Symmetries in a Pati-Salam x S4 Model*, JHEP **1008** (2010) 001, [arXiv:1003.4502].

[44] E. Ma, *Quark mass matrices in the A(4) model*, Mod. Phys. Lett. A **17** (2002) 627 [arXiv:hep-ph/0203238];

K. S. Babu, E. Ma and J. W. F. Valle, *Underlying A(4) symmetry for the neutrino mass matrix and the quark mixing matrix*, Phys. Lett. B **552** (2003) 207 [arXiv:hep-ph/0206292];

M. Hirsch, J. C. Romao, S. Skadhauge, J. W. F. Valle and A. Villanova del Moral, *Degenerate neutrinos from a supersymmetric A(4) model*, arXiv:hep-ph/0312244; *Phenomenological tests of supersymmetric A(4) family symmetry model of neutrino mass*, Phys. Rev. D **69** (2004) 093006 [arXiv:hep-ph/0312265];

E. Ma, *A_4 symmetry and neutrinos with very different masses*, Phys. Rev. D **70** (2004) 031901;

Non-Abelian discrete symmetries and neutrino masses: Two examples, New J. Phys. **6** (2004) 104 [arXiv:hep-ph/0405152];

Non-Abelian discrete family symmetries of leptons and quarks, arXiv:hep-ph/0409075;

S. L. Chen, M. Frigerio and E. Ma, *Hybrid seesaw neutrino masses with A(4) family symmetry*, Nucl. Phys. B **724** (2005) 423 [arXiv:hep-ph/0504181];

E. Ma, *Aspects of the tetrahedral neutrino mass matrix*, Phys. Rev. D **72** (2005) 037301 [arXiv:hep-ph/0505209];

M. Hirsch, A. Villanova del Moral, J. W. F. Valle and E. Ma, *Predicting neutrinoless double beta decay*, Phys. Rev. D **72** (2005) 091301 [Erratum-ibid. D **72** (2005) 119904] [arXiv:hep-ph/0507148];

K. S. Babu and X. G. He, *Model of geometric neutrino mixing*, arXiv:hep-ph/0507217;

E. Ma, *Tetrahedral family symmetry and the neutrino mixing matrix*, Mod. Phys. Lett. A **20** (2005) 2601 [arXiv:hep-ph/0508099];

A. Zee, *Obtaining the neutrino mixing matrix with the tetrahedral group*, Phys. Lett. B **630** (2005) 58 [arXiv:hep-ph/0508278];

E. Ma, *Tribimaximal neutrino mixing from a supersymmetric model with A4 family symmetry*, Phys. Rev. D **73** (2006) 057304 [arXiv:hep-ph/0511133];

X. G. He, Y. Y. Keum and R. R. Volkas, *A(4) flavour symmetry breaking scheme for understanding quark and neutrino*, JHEP **0604**, 039 (2006) [arXiv:hep-ph/0601001];

B. Adhikary, B. Brahmachari, A. Ghosal, E. Ma and M. K. Parida, *A(4) symmetry and prediction of U(e3) in a modified Altarelli-Feruglio model*, Phys. Lett. B **638** (2006) 345 [arXiv:hep-ph/0603059];

E. Ma, *Suitability of A(4) as a family symmetry in grand unification*, Mod. Phys. Lett. A **21** (2006) 2931 [arXiv:hep-ph/0607190];

Supersymmetric A(4) x Z(3) and A(4) realizations of neutrino tribimaximal mixing without and with corrections, Mod. Phys. Lett. A **22** (2007) 101 [arXiv:hep-ph/0610342];

L. Lavoura and H. Kuhbock, *Predictions of an A(4) model with a five-parameter neutrino mass matrix*, Mod. Phys. Lett. A **22** (2007) 181 [arXiv:hep-ph/0610050];

S. F. King and M. Malinsky, *A(4) family symmetry and quark-lepton unification*, Phys. Lett. B **645** (2007) 351 [arXiv:hep-ph/0610250];

X. G. He, *A(4) group and tri-bimaximal neutrino mixing: A renormalizable model*, Nucl. Phys. Proc. Suppl. **168**, 350 (2007) [arXiv:hep-ph/0612080];

Y. Koide, *A(4) symmetry and lepton masses and mixing*, Eur. Phys. J. C **52** (2007) 617 [arXiv:hep-ph/0701018];

S. Morisi, M. Picariello and E. Torrente-Lujan, *A model for fermion masses and lepton mixing in SO(10) x A(4)*, Phys. Rev. D **75** (2007) 075015 [arXiv:hep-ph/0702034];

M. Hirsch, A. S. Joshipura, S. Kaneko and J. W. F. Valle, *Predictive flavour symmetries of the neutrino mass matrix*, Phys. Rev. Lett. **99**, 151802 (2007) [arXiv:hep-ph/0703046].

F. Yin, *Neutrino mixing matrix in the 3-3-1 model with heavy leptons and A(4) symmetry*, Phys. Rev. D **75** (2007) 073010 [arXiv:0704.3827 [hep-ph]];

F. Bazzocchi, S. Kaneko and S. Morisi, *A SUSY A4 model for fermion masses and mixings*, JHEP **0803** (2008) 063 [arXiv:0707.3032 [hep-ph]];

A. C. B. Machado and V. Pleitez, *The flavor problem and discrete symmetries*, Phys. Lett. B **674**, 223 (2009) [arXiv:0712.0781 [hep-ph]];

M. Honda and M. Tanimoto, *Deviation from tri-bimaximal neutrino mixing in A(4) flavor symmetry*, Prog. Theor. Phys. **119** (2008) 583 [arXiv:0801.0181 [hep-ph]];

B. Brahmachari, S. Choubey and M. Mitra, *The A(4) flavor symmetry and neutrino phenomenology*, Phys. Rev. D **77** (2008) 073008 [Erratum-ibid. D **77** (2008) 119901] [arXiv:0801.3554 [hep-ph]];

F. Bazzocchi, S. Morisi, M. Picariello and E. Torrente-Lujan, *Embedding A4 into SU(3)xU(1) flavor symmetry: Large neutrino mixing and fermion mass hierarchy in SO(10) GUT*, J. Phys. G **36** (2009) 015002 [arXiv:0802.1693 [hep-ph]];

B. Adhikary and A. Ghosal, *Nonzero U_{e3}, CP violation and leptogenesis in a See-Saw type softly broken A_4 symmetric model*, Phys. Rev. D **78**, 073007 (2008) [arXiv:0803.3582 [hep-ph]];

M. Hirsch, S. Morisi and J. W. F. Valle, *Tri-bimaximal neutrino mixing and neutrinoless double beta decay*, Phys. Rev. D **78** (2008) 093007 [arXiv:0804.1521 [hep-ph]];

C. Csaki, C. Delaunay, C. Grojean and Y. Grossman, *A Model of Lepton Masses from a Warped Extra Dimension*, JHEP **0810**, 055 (2008) [arXiv:0806.0356 [hep-ph]];

P. H. Frampton and S. Matsuzaki, *Renormalizable A_4 Model for Lepton Sector*, arXiv:0806.4592 [hep-ph];

E. E. Jenkins and A. V. Manohar, *Tribimaximal Mixing, Leptogenesis, and theta13*, Phys. Lett. B **668**, 210 (2008) [arXiv:0807.4176 [hep-ph]];

F. Bazzocchi, M. Frigerio and S. Morisi, *Fermion masses and mixing in models with $SO(10)xA_4$ symmetry*, Phys. Rev. D **78**, 116018 (2008) [arXiv:0809.3573 [hep-ph]];

Riazuddin, *Tribimaximal mixing and leptogenesis in a seesaw model*, arXiv:0809.3648 [hep-ph];

W. Grimus and L. Lavoura, *Tri-bimaximal lepton mixing from symmetry only*, JHEP **0904**, 013 (2009) [arXiv:0811.4766 [hep-ph]];

S. Morisi, *Tri-Bimaximal lepton mixing with A4 semidirect product Z2 x Z2 x Z2*, arXiv:0901.1080 [hep-ph];

P. Ciafaloni, M. Picariello, E. Torrente-Lujan and A. Urbano, *Neutrino masses and tribimaximal mixing in Minimal renormalizable SUSY SU(5) Grand Unified Model with A4 Flavor symmetry*, Phys. Rev. D **79**, 116010 (2009) [arXiv:0901.2236 [hep-ph]];

M. C. Chen and S. F. King, *A4 See-Saw Models and Form Dominance*, JHEP **0906**, 072 (2009) [arXiv:0903.0125 [hep-ph]];

G. C. Branco, R. G. Felipe, M. N. Rebelo and H. Serodio, *Resonant leptogenesis and tribimaximal leptonic mixing with A4 symmetry*, arXiv:0904.3076 [hep-ph];

G. Altarelli and D. Meloni, *A Simplest A4 Model for Tri-Bimaximal Neutrino Mixing*, J. Phys. G **36**, 085005 (2009) [arXiv:0905.0620 [hep-ph]];

M. Hirsch, S. Morisi and J. W. F. Valle, *A4-based tri-bimaximal mixing within inverse and linear seesaw schemes*, arXiv:0905.3056 [hep-ph];

[45] L. Everett and A. Stuart, *Icosahedral (A(5)) Family Symmetry and the Golden Ratio Prediction for Solar Neutrino Mixing*, Phys. Rev. D **79** (2009) 085005 [arXiv:0812.1057].

[46] C. Chen, T. Kephart and T. Yuan, *An A_5 Model of four Lepton Generations*, arXiv:hep-ph/1011.3199.

[47] L. Everett and A. Stuart, *The Double Cover of the Icosahedral Symmetry Group and Quark Mass Textures*, arXiv:hep-ph/1011.4928.

[48] V. D. Barger, S. Pakvasa, T. J. Weiler and K. Whisnant, *Bi-Maximal Mixing of Three Neutrinos*, Phys. Lett. B **437** (1998) 107 [arXiv:hep-ph/9806387];

Y. Nomura and T. Yanagida, *Bi-Maximal Neutrino Mixing in $SO(10)_{GUT}$*, Phys. Rev. D **59** (1999) 017303 [arXiv:hep-ph/9807325];

G. Altarelli and F. Feruglio, *Neutrino Mass Textures from Oscillations with Maximal Mixing*, Phys. Lett. B **439** (1998) 112 [arXiv:hep-ph/9807353].

[49] P. F. Harrison, D. H. Perkins and W. G. Scott, *Tri-bimaximal mixing and the neutrino oscillation data*, Phys. Lett. B **530** (2002) 167 [arXiv:hep-ph/0202074];

P. F. Harrison and W. G. Scott, *Symmetries and generalisations of tri-bimaximal neutrino mixing*, Phys. Lett. B **535** (2002) 163 [arXiv:hep-ph/0203209];

Z. z. Xing, *Nearly tri-bimaximal neutrino mixing and CP violation*, Phys. Lett. B **533** (2002) 85 [arXiv:hep-ph/0204049];

P. F. Harrison and W. G. Scott, *mu - tau reflection symmetry in lepton mixing and neutrino oscillations*, Phys. Lett. B **547** (2002) 219 [arXiv:hep-ph/0210197];
P. F. Harrison and W. G. Scott, *Permutation symmetry, tri-bimaximal neutrino mixing and the S3 group characters*, Phys. Lett. B **557** (2003) 76 [arXiv:hep-ph/0302025];

P. F. Harrison and W. G. Scott, *Status of tri- / bi-maximal neutrino mixing*, arXiv:hep-ph/0402006;

P. F. Harrison and W. G. Scott, *The simplest neutrino mass matrix*, Phys. Lett. B **594** (2004) 324 [arXiv:hep-ph/0403278].

[50] M. Hamermesh, *Group Theory and Its Application to Physical Problems*, Reading, Mass.:Addison- Wesley (1962) 509 p;

[51] Y. Kajiyama, M. Raidal and A. Strumia, *The golden ratio prediction for the solar neutrino mixing*, Phys. Rev. D **76** (2007) 117301 [arXiv:0705.4559 [hep-ph]].

[52] A. Datta, F. S. Ling and P. Ramond, *Correlated hierarchy, Dirac masses and large mixing angles*, Nucl. Phys. B **671**, 383 (2003) [arXiv:hep-ph/0306002].

[53] C. D. Froggatt and H. B. Nielsen, *Hierarchy Of Quark Masses, Cabibbo Angles And CP Violation*, Nucl. Phys. B **147** (1979) 277.

[54] C. I. Low and R. R. Volkas, *Tri-bimaximal mixing, discrete family symmetries, and a conjecture connecting the quark and lepton mixing matrices*, Phys. Rev. D **68** (2003) 033007 [arXiv:hep-ph/0305243].

[55] F. Feruglio, *Models of neutrino masses and mixings*, Nucl. Phys. Proc. Suppl. **143** (2005) 184 [Nucl. Phys. Proc. Suppl. **145** (2005) 225] [arXiv:hep-ph/0410131].

[56] W. Rodejohann, *Unified Parametrization for Quark and Lepton Mixing Angles*, Phys. Lett. B **671** (2009) 267 [arXiv:0810.5239 [hep-ph]].

[57] A. Adulpravitchai, A. Blum and W. Rodejohann, *Golden Ratio Prediction for Solar Neutrino Mixing*, New J. Phys. **11** (2009) 063026 [arXiv:0903.0531].

[58] C. Luhn, S. Nasri and P. Ramond, *Simple Finite Non-Abelian Flavor Groups*, J. Math. Phys. **48** (2007) 123519 [arXiv:0709.1447];

[59] C. Cummins and J. Patera, *Polynomial Icosahedral Invariants*, J. Math. Phys. **29** (1988) 1736-1745.

[60] C. Luhn and P. Ramond, *Quintics with Finite Simple Symmetries*, J. Math. Phys. **49** (2008) 053525 [arXiv:0803.0526].

[61] S. Antusch, J. Kersten, M. Lindner and M. Ratz, *Running neutrino masses, mixings and CP phases: Analytical results and phenomenological consequences*, Nucl. Phys. B **674** (2003) 401 [arXiv:hep-ph/0305273].

A. Dighe, S. Goswami and P. Roy, *Radiatively broken symmetries of nonhierarchical neutrinos*, Phys. Rev. D **76** (2007) 096005 [arXiv:0704.3735 [hep-ph]].

[62] A. Dighe, S. Goswami and W. Rodejohann, *Corrections to Tri-bimaximal Neutrino Mixing: Renormalization and Planck Scale Effects*, Phys. Rev. D **75** (2007) 073023 [arXiv:hep-ph/0612328];

S. Boudjemaa and S. F. King, *Deviations from Tri-bimaximal Mixing: Charged Lepton Corrections and Renormalization Group Running*, Phys. Rev. D **79** (2009) 033001 [arXiv:0808.2782 [hep-ph]].

[63] T. Miura, T. Shindou and E. Takasugi, *The renormalization group effect to the bi-maximal mixing*, Phys. Rev. D **68** (2003) 093009 [arXiv:hep-ph/0308109];

S. Antusch, P. Huber, J. Kersten, T. Schwetz and W. Winter, *Is there maximal mixing in the lepton sector?*, Phys. Rev. D **70** (2004) 097302 [arXiv:hep-ph/0404268].

A. Dighe, S. Goswami and P. Roy, *Quark-lepton complementarity with quasidegenerate Majorana neutrinos*, Phys. Rev. D **73**, 071301 (2006) [arXiv:hep-ph/0602062].

[64] S. Antusch, J. Kersten, M. Lindner, M. Ratz and M. A. Schmidt, *Running neutrino mass parameters in See-Saw scenarios*, JHEP **0503** (2005) 024 [arXiv:hep-ph/0501272];

J. W. Mei, *Running neutrino masses, leptonic mixing angles and CP-violating phases: From M(Z) to Lambda(GUT)*, Phys. Rev. D **71** (2005) 073012 [arXiv:hep-ph/0502015];

J. R. Ellis, A. Hektor, M. Kadastik, K. Kannike and M. Raidal, *Running of low-energy neutrino masses, mixing angles and CP violation*, Phys. Lett. B **631**, 32 (2005) [arXiv:hep-ph/0506122].

[65] E. Bertuzzo, P. Di Bari, F. Feruglio and E. Nardi, *Flavor symmetries, leptogenesis and the absolute neutrino mass scale*, arXiv:0908.0161 [hep-ph].

[66] F. Feruglio, C. Hagedorn, Y. Lin and L. Merlo, *Lepton Flavour Violation in Models with A4 Flavour Symmetry*, Nucl. Phys. B **809** (2009) 218 [arXiv:0807.3160 [hep-ph]];

F. Feruglio, C. Hagedorn, Y. Lin and L. Merlo, *Theory of the Neutrino Mass*, arXiv:0808.0812 [hep-ph].

F. Feruglio, C. Hagedorn, Y. Lin and L. Merlo, *Lepton Flavour Violation in a Supersymmetric Model with A_4 Flavour Symmetry*, arXiv:0911.3874 [hep-ph].

[67] F. Feruglio, C. Hagedorn and L. Merlo, *Vacuum Alignment in SUSY A4 Models*, JHEP **1003** (2010) 084 [arXiv:0910.4058 [hep-ph]].

[68] H. Ishimori, T. Kobayashi, Y. Omura and M. Tanimoto, *Soft supersymmetry breaking terms from A4 lepton flavor symmetry*, JHEP **0812** (2008) 082 [arXiv:0807.4625 [hep-ph]];

A. Hayakawa, H. Ishimori, Y. Shimizu and M. Tanimoto, *Deviation from tri-bimaximal mixing and flavor symmetry breaking in a seesaw type A4 model*, Phys. Lett. B **680** (2009) 334 [arXiv:0904.3820 [hep-ph]];

[69] I. de Medeiros Varzielas, S. F. King and G. G. Ross, *Tri-bimaximal neutrino mixing from discrete subgroups of SU(3) and SO(3) family symmetry*, Phys. Lett. B **644** (2007) 153 [arXiv:hep-ph/0512313].

[70] R. G. Felipe and H. Serodio, *Constraints on leptogenesis from a symmetry viewpoint*, arXiv:0908.2947 [hep-ph];

[71] W. Buchmuller and D. Wyler, *Effective Lagrangian Analysis Of New Interactions And Flavor Conservation*, Nucl. Phys. B **268** (1986) 621.

[72] A. Broncano, M. B. Gavela and E. E. Jenkins, *The effective Lagrangian for the seesaw model of neutrino mass and leptogenesis*, Phys. Lett. B **552** (2003) 177 [Erratum-ibid. B **636** (2006) 330] [arXiv:hep-ph/0210271].

[73] A. Broncano, M. B. Gavela and E. E. Jenkins, *Neutrino Physics in the Seesaw Model*, Nucl. Phys. B **672** (2003) 163 [arXiv:hep-ph/0307058].

[74] A. Abada, C. Biggio, F. Bonnet, M. B. Gavela and T. Hambye, *Low energy effects of neutrino masses*, JHEP **0712** (2007) 061 [arXiv:0707.4058 [hep-ph]].

[75] M. S. Bilenky and A. Santamaria, *'Secret' neutrino interactions*, arXiv:hep-ph/9908272.

[76] E. W. Kolb and M. S. Turner, *Supernova SN 1987a and the Secret Interactions of Neutrinos*, Phys. Rev. D **36** (1987) 2895.

[77] M. S. Bilenky, S. M. Bilenky and A. Santamaria, *Invisible width of the Z boson and 'secret' neutrino-neutrino interactions*, Phys. Lett. B **301** (1993) 287.

[78] M. S. Bilenky and A. Santamaria, *Bounding effective operators at the one loop level: The Case of four fermion neutrino interactions*, Phys. Lett. B **336** (1994) 91 [arXiv:hep-ph/9405427].

[79] W. J. Marciano and A. Sirlin, *Electroweak Radiative Corrections to tau Decay*, Phys. Rev. Lett. **61** (1988) 1815.

[80] B. Aubert *et al.* [BABAR Collaboration], *Measurements of Charged Current Lepton Universality and $|V_{us}|$ using Tau Lepton Decays to $e^-\bar{\nu}_e\nu_\tau$, $\mu^-\bar{\nu}_\mu\nu_\tau$, $\pi^-\nu_\tau$ and $K^-\nu_\tau$*, BABAR-PUB-09/018, [arXiv:0912.0242 [hep-ex]].

[81] A. Ferroglia, G. Ossola, M. Passera and A. Sirlin, *Simple formulae for sin**2(theta(lept)(eff)), M(W), Gamma(l), and their physical applications*, Phys. Rev. D **65** (2002) 113002 [arXiv:hep-ph/0203224].

[82] S. Davidson , C. Peña-Garay , N. Rius , A. Santamaria *Present and Future Bounds on Non-Standard Neutrino Interactions*, JHEP **0303** (2003) 011.

[83] Z. Berezhiani and A. Rossi, *Limits on the non-standard interactions of neutrinos from e+ e- colliders*, Phys. Lett. B **535** (2002) 207 [arXiv:hep-ph/0111137].

[84] J. Abdallah *et al.* [DELPHI Collaboration], *Photon events with missing energy in e+ e- collisions at s**(1/2) = 130-GeV to 209-GeV*, Eur. Phys. J. C **38** (2005) 395 [arXiv:hep-ex/0406019].

[85] See the LEP Electroweak Working Group webpage, http:/www.cern.ch/LEPEWWG/ *Combination of the LEP II ff Results.*

[86] J. Hisano, T. Moroi, K. Tobe and M. Yamaguchi, *Lepton-Flavor Violation via Right-Handed Neutrino Yukawa Couplings in Supersymmetric Standard Model*, Phys. Rev. D **53** (1996) 2442 [arXiv:hep-ph/9510309].

[87] W. Bertl *et al.* (SINDRUM II Collaboration), *A search for $\mu - e$ conversion in muonic gold*, Eur. Phys J. C **47** (2006) 337.

[88] Mu2e Collaboration, http://mu2e.fnal.gov

[89] Y. Kuno (PRISM/PRIME Collaboration), *PRISM/PRIME*, Nucl. Phys. B-Proceeding Supplements **149** (2005) 376-378.

[90] R. Barbieri, L. Hall, A. Strumia, *Violations of lepton flavour and CP in supersymmetric unified theories*, Nucl. Phys. B **445** (1995) 219.

[91] E. Ma and G. Rajasekaran, *Softly broken A(4) symmetry for nearly degenerate neutrino masses*, Phys. Rev. D **64** (2001) 113012 [arXiv:hep-ph/0106291];

[92] L. Lavoura and H. Kuhbock, *A_4 model for the quark mass matrices*, Eur. Phys. J. **C55** (2008) 303–308 [arXiv:0711.0670].

[93] S. Morisi and E. Peinado, *An A4 model for lepton masses and mixings*, Phys. Rev. **D80** (2009) 113011 [arXiv: 0910.4389].

[94] E. Ma, *Quark and Lepton Flavor Triality*, Phys. Rev. **D82** (2010) 037301 [arXiv: 1006.3524].

[95] M. Hirsch, S. Morisi, E. Peinado, and J. W. F. Valle, *Discrete dark matter*, (2010) [arXiv: 1007.0871].

[96] D. Meloni, S. Morisi, and E. Peinado, *Neutrino phenomenology and stable dark matter with A4*, (2010) [arXiv: 1011.1371].

[97] J. F. Gunion and H. E. Haber, *Conditions for CP-Violation in the General Two-Higgs-Doublet Model* , Phys. Rev. **D72** (2005) 095002 [arXiv: hep-ph/0506227].

[98] M. J. G. Veltman, *Second Threshold in Weak Interactions*, Acta Phys. Polon. **B8** (1977) 475.

[99] B. W. Lee, C. Quigg, and H. B. Thacker, *Weak interactions at very high energies: The role of the Higgs-boson mass*, Phys. Rev. **D16** (1977) 1519.

[100] B. W. Lee, C. Quigg, and H. B. Thacker, *Strength of Weak Interactions at Very High Energies and the Higgs Boson Mass*, Phys. Rev. Lett. **38** (1977) 883–885.

[101] R. Casalbuoni, D. Dominici, F. Feruglio, and R. Gatto, *Tree-level unitarity violation for large scalar mass in multi-Higgs extensions of the standard model*, Nucl. Phys. **B299** (1988) 117.

[102] R. Barate *et al.*, *Search for the Standard Model Higgs Boson at LEP*, Phys. Lett. **B565** (2003) 61 [arXiv: hep-ex/0306033].

[103] CDF and D0 Collaborations, *Combined CDF and DZero Upper Limits on Standard Model Higgs-Boson Production with up to 4.2 fb-1 of Data*, arXiv: 0903.4001.

[104] B. Holdom and J. Terning, *Large corrections to electroweak parameters in technicolor theories*, Phys. Lett. **B247** (1990) 88.

[105] M. E. Peskin and T. Takeuchi, *New constraint on a strongly interacting Higgs sector*, Phys. Rev. Lett. **65** (1990) 964.

[106] M. Golden and L. Randall, *Radiative corrections to electroweak parameters in technicolor theories*, Nucl. Phys. **B361** (1991) 3.

[107] A. Dobado, D. Espriu, and M. J. Herrero, *Chiral lagrangians as a tool to probe the symmetry breaking sector of the SM at LEP*, Phys. Lett. **B255** (1991) 405.

[108] M. E. Peskin and T. Takeuchi, *Estimation of oblique electroweak corrections*, Phys. Rev. **D46** (1992) 381.

[109] I. Maksymyk, C. P. Burgess, and D. London, *Beyond S, T and U*, Phys. Rev. **D50** (1994) 529–535 [arXiv: hep-ph/9306267].

[110] W. Grimus, L. Lavoura, O. M. Ogreid, and P. Osland, *The oblique parameters in multi-Higgs-doublet models*, Nucl. Phys. **B801** (2008) 81–96 [arXiv: 0802.4353].

[111] W. Grimus, L. Lavoura, O. M. Ogreid, and P. Osland, *A precision constraint on multi-Higgs-doublet models*, J. Phys. **G35** (2008) 075001 [arXiv: 0711.4022].

[112] A. C. B. Machado, J. C. Montero, and V. Pleitez, *Three-Higgs-doublet model with A_4 symmetry*, arXiv: 1011.5855.

[113] L. Lavoura, *General formulae for f1 $\to$ f2 gamma*, Eur. Phys. J. **C29** (2003) 191 [arXiv: hep-ph/0302221].

[114] M. L. Brooks *et al.*, *New Limit for the Family-Number Non-conserving Decay μ^+ to $e^+\gamma$*, Phys. Rev. Lett. **83** (1999) 1521 [arXiv: hep-ex/9905013].

[115] A. Maki, *Status of the MEG Experiment*, AIP Conf. Proc. **981** (2008) 363.

[116] D. Atwood, L. Reina and A. Soni, *Phenomenology of Two Higgs Doublet Models with Flavor Changing Neutral Currents*, Phys. Rev. D **55** (1997) 3156, [arXiv:hep-ph/9609279].

[117] J. D. Wells, *Lectures on Higgs Boson Physics in the Standard Model and Beyond*, arxiv: 0909.4541.

[118] A. J. Buras, M. V. Carlucci, S. Gori, and G. Isidori, *Higgs-mediated FCNCs: Natural Flavour Conservation vs. Minimal Flavour Violation*, JHEP **10** (2010) 009 [arXiv: 1005.5310].

[119] E. Ma, *Quark and Lepton Flavor Triality*, Phys. Rev. D **82** (2010) 037301, [arXiv: 1006.3524].

[120] E. Ma, *Dark Scalar Doublets and Neutrino Tribimaximal Mixing from A_4 Symmetry*, Phys. Lett. B **671** (2009) 366, [arXiv: 0808.1729].

[121] K. Shirai, *The Basis Functions and the Matrix Representations of the Single and Double Icosahedral Point Group*, J. Phys. Soc. Jpn. **61** (1992) 2735.